REPORT NO
UC SESM 72-2

STRUCTURES AND MATERIALS RESEARCH
DEPARTMENT OF CIVIL ENGINEERING

EFFECTS OF HUMIDITY ON THE TIME-DEPENDENT BEHAVIOR OF CONCRETE UNDER SUSTAINED LOADING

by

HESHAM R. AL-ALUSI
VITELMO V. BERTERO
MILOS POLIVKA

Report to:

National Science Foundation
Grant GK-3901

JANUARY 1972

STRUCTURAL ENGINEERING LABORATORY
UNIVERSITY OF CALIFORNIA
BERKELEY CALIFORNIA

Structures and Materials Research
Department of Civil Engineering
Division of Structural Engineering
and
Structural Mechanics

Report No. UC SESM-72-2

EFFECTS OF HUMIDITY ON THE TIME-DEPENDENT BEHAVIOR OF CONCRETE UNDER SUSTAINED LOADING

by

Hesham R. Al-Alusi, Ph.D.
Research Assistant

Vitelmo V. Bertero
Professor of Civil Engineering

Milos Polivka
Professor of Civil Engineering

Prepared under the sponsorship of
National Science Foundation
Grant GK-3901

Structural Engineering Materials Laboratory
University of California
Berkeley, California

January, 1972

TABLE OF CONTENTS

TABLE OF CONTENTS, Continued

TABLE OF CONTENTS, Continued

TABLE OF CONTENTS, Continued

ACKNOWLEDGEMENTS

The study reported herein was carried out by H. R. Al-Alusi in partial fulfillment of his Ph.D. degree in Civil Engineering at the University of California, Berkeley, under the direct supervision of Professors V. V. Bertero and Milos Polivka. The authors are indebted to Professor F. Hauser for his valuable comments and support of this study. The helpful discussions and assistance given by Mr. H. M. Fahmi, graduate student at the University of California, Berkeley, are also acknowledged. The assistance given by the staff of the Structural Engineering Materials Laboratory and that of the engineering students, Messrs. H. Franco and M. Wong, are gratefully appreciated.

While a graduate student, Dr. Al-Alusi was sponsored by a Gulbenkian scholarship through the University of Baghdad, Baghdad, Iraq.

This research would not have been possible without the generous financial support of the National Science Foundation, under grant No. GK-3901.

ABSTRACT

The work included in this study is concerned with the effects of humidity on the time-dependent behavior of concrete. The study is divided into two phases; experimental and analytical. In the experimental phase, tests were carried out on specimens which were in the form of hollow cylinders of micro-concrete having the following dimensions: 5-in. I.D., 6-in. O.D. and 40-in. long. The 1/2-in wall thickness (1/4-in. diffusion path) of the micro-concrete tubes was selected to minimize moisture gradients and to reduce the time required to reach stabilization of the internal humidity of the concrete. It was found that a reasonably uniform humidity of the 1/2-in. thickness of micro-concrete is reached in 14 days of exposure to a changed level of humidity (either 50 or 100 percent R.H.).

Specimens which were loaded in compression or torsion at 73°F were exposed to three different humidity environments. Some of the specimens were subjected to a humidity cycle consisting of changes in relative humidity (R.H.) from 100 to 50 to 100 percent R.H. Other specimens were exposed to a constant 100 percent R.H. and a third group of specimens were kept at a constant 50 percent R.H. Unloaded control companion specimens were also exposed to these three kinds of humidity environments. Deformations of the micro-concrete were measured by means of electrical strain gages as well as by dial gages.

In the analytical phase, the experimental results were analyzed according to the thermodynamic theory of adsorbed load-bearing water layers. Also, Bazant's constitutive equations were applied. The use of Bazant's constitutive equations requires the evaluation of the parameters and functions which characterize the material. This evaluation was conducted in accordance with findings of the experimental phase.

From the experimental phase, it was concluded that the first drying is the most important to the creep of concrete. The creep of a specimen undergoing a drying process from 100 to 50 percent R.H. was several times that of a specimen under a constant humidity.

The use of a numerical analysis together with the use of a digital computer, facilitated the application of Bazant's constitutive equations. A presentation is

given to show how to apply these constitutive equations on the results of an experimental program. The predicted creep from the application of these constitutive equations showed good agreement with creep results of specimens kept at a constant humidity, but, due to the high rate of humidity changes, the predicted creep of specimens undergoing humidity changes (100 to 50 to 100 percent R.H.) was not in as good agreement with the experimental results of the same specimen.

LIST OF NOTATIONS

A_c = Area of concrete

A_g = Gross cross-sectional area

A_s = Area of steel

A_t = Total area

C = Coefficient of hygral diffusivity

D = Supplementary constant specific to the type of concrete used

D_{oh}, D_{1h} = Equivalent surface thickness for hygral effects

E = Modulus of elasticity

E_c = Modulus of elasticity of concrete

E_{eff} = Effective modulus of elasticity (Appendix B)

E_s = Modulus of elasticity of steel

F = Force

G_b, G_c, G_d, G = Shear moduli of elasticity for elements b, c, d and Rheological model in Fig. 2, respectively

G_h = A factor which accounts for shear creep increase due to drying

K_b, K_c, K_d, K = Bulk moduli of elasticity for elements b, c, d and Rheological model in Fig. 2, respectively

K_h = A factor which accounts for volumetric creep increase due to drying

K_i = Value determined experimentally for given concrete

M = Molecular weight of water

Q = Constant dependent on the concrete

R_A = Ultimate strength of concrete

R = Ratio of the axial strain in a cylinder under triaxial stress to the axial strain in a cylinder under uniaxial stress

R_c = Measured strain by a strain gage positioned in the direction of the compression component in a torsion specimen

LIST OF NOTATIONS, Continued

R_t = Measured strain by a strain gage positioned in the direction of the tension component in a torsion specimen

S = Surface area of a member

S_h = A factor which accounts for the excessive pressure in the diffusible load-bearing layer as a result of simultaneous compressive loading and drying

S_{ij} = Total stress deviator (macroscopic)

T' = Temperature in Kelvin degrees

T = Temperature in Fehrenhite or centigrade

V = Volume of a member

----

b_T = A function (of temperature only), see equation A.1

c = Creep deformation in the strain gage in the direction of the compressive component in a torsion specimen

c_h = A function (of humidity only), see equation A.1

e_{ij} = Total strain deviator (macroscopic)

e''_{ij} = Inelastic strain deviator

f_a = Effective area factor for non-loading-bearing diffusible water layers

f_d = Effective area factor for loading-bearing diffusible water layers

h = Humidity

h_{eq} = Equivalent humidity, equation (1.4.8)

h_s = Humidity at self-desiccation, Appendix A

k = Sorption resistance, equation A.1

t = Time, or creep deformation in the strain gage in the direction of the tensile component in a torsion specimen

t_{eq} = Equivalent curing time, equation (1.4.9)

LIST OF NOTATIONS, Continued

β = A function, equation (1.4.9)

β_h = Relative hydration rates, equation (1.4.9)

β_T = A function, equation (1.4.9)

Δ_m = Creep under different hygrometric conditions

Δ_{mi} = Creep in absence of shrinkage

Δ_r = Shrinkage with the corresponding relative humidity

Δ_{ro} = Theoretical shrinkage for a non-existent relative humidity

ϕ = Rate of volumetric creep deformation

ψ = Rate of deviatoric creep deformation

κ = Hygrothermic coefficient, equation (A.1)

θ = Angle, degrees

σ = Total volumetric stress (macroscopic)

σ_A = Axial stress in a cylinder under simple load

σ_a = Pressure in fluid in diffusion element

σ_{ad} = Equilibrium value of σ_d

σ_d = Stress resultant over a unit cross-section due to disjoining pressure in the diffusible load-bearing layers in the macroscopic sense

σ_{ao} = Pressure in fluid (macroscopic)

σ_i, σ_j, σ_k or σ_1, σ_2, σ_3 = Principal stresses (macroscopic)

σ_u = Uniaxial stress

σ_{ah} = Parameter, a function of humidity only, Fig. 3-b

σ_{aQ} = Parameter, a function of temperature only

σ_{ij} = Total stress tensor (macroscopic)

ε = Total volumetric strain (macroscopic)

ε'' = Inelastic volumetric strain

ε_c = Strain in concrete, Appendix B

ε_s = Strain in steel, Appendix B

LIST OF NOTATIONS, Continued

ε_u = Strain in a uniaxially loaded specimen

μ = Poisson's ratio

μ_{iu} = Uniaxial creep Poisson's ratio

τ = Shear stress

∇^2 = Laplace operator

CHAPTER 1

INTRODUCTION

1.1 CREEP OF CONCRETE

It is a recognized fact that time-dependent deformations take place in concrete structures under stress. Tests have shown that, although the rate of deformation decreases with time, this deformation continues for several years and may reach a considerable magnitude. This time-dependent deformation (or strain) is conventionally called "creep." Creep is an inherent property of concrete, and no concrete structure subjected to a sustained load is free from the effects of creep, yet it is probably the least well known property of concrete.

In this investigation, we are concerned with creep under a magnitude of sustained stress which is within the linear range of creep strain and applied stress relationship. A stress level below 50 percent of ultimate strength is usually considered to be within this linear range.

Most attempts during the last sixty years to predict the magnitude of creep for any type of concrete, were in the form of empirical relationships between creep and some variables in the concrete mix proportions. This approach, probably due to the scarce theoretical background material on creep, was unlikely to produce more than a fragmentary picture since it is generally difficult to alter only one variable in the properties of a concrete mix. Thus, the true cause of creep variations may often have been obscured.

More recently, the attempts in the last twenty years to treat the creep of concrete according to the viscoelastic theory have succeeded in greatly improving the techniques of predicting the creep of concrete. However, the causes of creep variations are beyond the reach of the viscoelastic theory.

The Powers-Bazant theory predicts the creep of concrete according to the changes in the thermodynamic equilibrium of the diffusible load-bearing water in the cement gel of concrete. This theory predicts the creep of concrete directly--i.e., it uses material constants and environmental and loading conditions to predict creep rather than transposing the material constants and environmental and loading conditions to phenomenological actions from which creep is predicted. This theory also explains the causes behind the creep variations. (Discussion and applications of this theory are presented in Section 1.4 and in Chapter 3.)

1.2 CREEP SIGNIFICANCE

The creep of structural concrete has advantages and disadvantages: a reinforced concrete beam under sustained bending will deflect more and more with time. On the other hand, creep is very advantageous in relieving shrinkage stresses, induced thermal stresses, or stress concentrations.

In shells and two-way slabs, creep, under sustained two-dimensional stresses, has a profound effect on displacements and on the stresses developed in the reinforcement. Furthermore, prestressed concrete has stimulated interest in creep since this deformation contributes to the loss of prestress which occurs with the lapse of time.

In a statically indeterminate structure, creep, shrinkage, and relaxation of concrete play a significant role in the stress and strain distribution throughout the structure. One of these structures is the pressure vessel for nuclear power reactors. Creep of concrete is one of the most difficult factors to assess in its design because of the thermal effects and the expected state of stress.

1.3 HISTORICAL PERSPECTIVE

Available literature on the creep of concrete is extensive and, at times, contradictory. Some investigators studied the problem in general (1-8) while others concentrated on one or few aspects of the creep of concrete (9,10,11,12). The parameters which effect the creep of concrete and, consequently, the structural behavior of concrete are many, and most of them are interrelated.

The available literature provides some knowledge (though not complete) about the effect of some of the parameters such as effect of age, stress-strain relationship, effect of aggregates, and effect of water-cement ratio. On the other hand, there are still other parameters whose effects are still uncertain. Some of these are: the multiaxial loading (state of stress), constant and cyclic relative humidities, and constant and cyclic temperatures.

Excellent reviews have been prepared by Fluck and Washa (1), Wallo and Kesler (2), Sackman (3), and L'Hermite (4).

Most experimental work has been done with concentration on the concrete constituents. This, however, gave rise to questions about the results which one may expect using different types of cement, sand, gravel or water-cement ratio. In order to study the mechanism of creep of concrete and formulate a theory which points out the causes behind creep, the investigators moved to study the effect of different parameters on one type of concrete (9,10,11,12).

Many theories have been introduced to predict the creep of concrete, but none appears to be general. Neville (13) summarized most of the theories of creep in concrete and presented their weak and strong aspects. None of the theories discussed by Neville were based on a systematic study of the causes of creep in concrete, rather they were all based on action and response observations.

Powers introduced evidence proving that the adsorbed water layers in the cement gel behave as a structural element in the concrete body. He presented a theoretical interpretation on the thermodynamics of the adsorbed water layers in the cement gel which cause the creep of concrete (8,14,15,16).

Bazant (17) formulated a new theory, based on the findings of Powers and others, about the thermodynamics of the adsorbed water layers in the cement gel.

For the purpose of this study, it is more convenient to summarize all the conclusions about time-dependent behavior of concrete under a uniaxial state of stress and constant humidity, than to present the different investigators' conclusions separately, since there is a generally accepted body of knowledge concluded from the various investigations. This knowledge is presented below in Section 1.3.1.

If a concrete member is subjected to variable humidity while it is under a sustained loading, or if the concrete member is under a sustained state of stress other than a uniaxial state of stress, the problem of time-dependent behavior of concrete under such conditions is more complicated than that of a concrete member which is under uniaxial sustained loading and constant humidity. For the purpose of this study, literature concerning the effect of relative humidity and the effect of a multiaxial state of stress on the time-dependent behavior of concrete is reviewed in Sections 1.3.2 and 1.3.3 below. In Section 1.4, the Powers-Bazant theory is presented.

1.3.1 Summary of Present-Day Knowledge about Time-Dependent Behavior of Concrete under Uniaxial State of Stress.--In present day terminology, concrete is generally accepted as a time-variable linear viscoelastic material for stress levels below about 50% of ultimate strength.

Creep deformation has two main components, namely, recoverable and irrecoverable creep. It is generally believed that the behavior of concrete under uniaxial tension is the same as that under uniaxial compression except that the initial rate of creep is higher in tension than in compression, but this position may be reversed later--i.e., a later time after loading (10).

1.3.2 Literature Concerning the Effect of Relative Humidity on the Time-Dependent Behavior of Concrete.--The effect of relative humidity on the time-dependent behavior of concrete is a very important factor in studying the creep mechanism of concrete. It has been known for some time that the creep of concrete is profoundly linked to the hygrometric conditions inside and surrounding the specimen.

One of the pioneering experimental programs investigating this relationship was carried out by Davis and Davis (18) in 1931. The test program was carried out on 4 by 10-in. and 12 by 24-in. cylinders which were stored in water for 28 days after casting, then loaded between 200 and 1200 psi in axial compression. The loaded specimens were stored at relative humidities of 0, 10, 50 and 100% R.H.

Some of the tests lasted for one year, others for two or four years. They concluded that under conditions of dry storage, the flow is substantially greater than for the same quality of concrete kept continuously wet.

Davis, Davis, and Hamilton (5), in 1934, reported the results of tests carried out on cylindrical specimens having diameters between 4-18 in. and lengths between 8-48 in. The load intensity was between 300 to 1200 psi. The test specimens were moist cured after casting until time of loading (28 or 90 days) and then loaded and subjected to a certain relative humidity. Relative humidities of 50, 70 and 100% (submerged in water or placed in a fog room) were used. From the results of these tests, they concluded that for plain concrete cylinders stored under moist conditions, the total deformation due to flow and expansion may be in the order of 1/2 - 1/4 of the total deformation of similar concretes stored in dry air.

In 1934, Lynam (19) studying the role of water in portland cement, stated in his book that "shrinkage and creep are two aspects of the same phenomenon; it is impossible to separate them and no good end is served by trying to do so." At that time, the mechanism of this relationship between creep and shrinkage was unknown but this statement proved to be extremely important because it showed a deep insight into the phenomenological facts present at that time.

Later, it was Powers (8,14,15,16) who assembled the elements of the mechanism of this relationship under the theory of the thermodynamics of the adsorbed water in the cement gel.

In 1937, Dutron (20) represented data comparing creep of concrete specimens drying under 45 and 70% R.H. with those stored at 100% R.H. The following table was presented:

Storage before Loading % R.H.	Storage after Loading % R.H.	Creep as Compared with Creep under Continuous Water Storage
100	45	4.0 - 4.5
45	45	3.1 - 3.4
70	70	2.1 - 2.7
45	100	1.7 - 2.2
100	100	1.0

Lorman (22) in 1940, stated that "shrinkage or swelling due to loss or gain of moisture and creep due to seepage are interrelated phenomena." Lorman, however, considered the effect of the two separately.

Maney (22,23) in 1940 and 1941 found that non-uniform shrinkage is the "source of all time-yield in loaded concrete members" and that this time-yield is not plastic flow but is merely an elastic distribution of stress, increasing with time.

Out of this apparent confusion and disagreement, and observing the lack of adequate theoretical analysis of the state of stress and strain in a body such as concrete, Pickett (9) in 1942 published his famous paper, "The Effect of Change of Moisture-Content on the Creep of Concrete under a Sustained Load." His paper contained theoretical as well as experimental analyses. In his theoretical analysis, Pickett considered stress, strain, shrinkage, creep, etc., each as a function of the coordinates of the specimen as well as of the usually considered variables of time, loading, storage conditions, mix, etc.

He proposed that the apparent effect of drying upon creep is not to increase the stress-creep coefficient but to cause non-uniform volume changes that produce transient stresses which combine with the load stresses and give rise to a distribution and magnitude of stress far different from those in a companion specimen undergoing less drying shrinkage. He also proposed that the assumption that concrete has a non-linear stress-creep relation is sufficient to explain the observed difference in creep under different storage conditions. He considered two hypothetical materials assumed to be homogenous, isotropic, and of such nature that after having been subjected to sustained stress, one would show a linear relationship between stress and accumulated strain and the other, a non-linear relationship. He analyzed rectangular prisms of these hypothetical materials after subjecting them to various loading conditions with some of the prisms shrinking and others not.

The experimental work included tests on loaded concrete beams simulating the analyzed prisms. He concluded that an increase in creep accompanying non-uniform shrinkage or swelling is a natural consequence of the fact that the sustained-stress vs. strain curve for concrete is not linear. He also found that the increase, due to wetting or drying cycle under sustained load, was irreversible.

Duke and Davis (24), presented results of exploratory experiments carried out on tubular concrete specimens having an outside diameter of 9 in., a wall thickness of 1 1/2 in., and a length of 29 1/2 in. The load was applied in such a way as to induce primary or pure shear (torsion). The applied torques caused extreme fiber stresses in shear of 50 and 100 psi. Three tubes were tested in air at 95% R.H. and four in air at 50% R.H. Load was applied at age 7 days and continued for 50 days. The results show that shear creep was greater in drier specimens and decreased with stress, water-cement ratio, or aggregate-cement ratio.

In 1958, Troxell, Raphael and Davis (25) presented a paper with data for specimens loaded up to 28 years. Some of the tests were carried out on 4 by 14-in. cylinders. After moist curing at 70°F for 28 days, these specimens were loaded axially with 800 psi. Storage after loading was at 70°F and either 50, 70 or 100% relative humidity. They found that the creep in air at 50% R.H. was about 1.4 times that in air at 70% R.H. and about 3 times that for storage in water.

L'Hermite (4) proposed a formula for predicting creep under different hygrometric conditions:

$$\Delta_m = \Delta_{mi}(1 + Q \frac{\Delta_r}{\Delta_{ro}})$$

where: Δ_{mi} = creep in the absence of shrinkage

Q = constant dependent on the concrete

Δ_{ro} = theoretical shrinkage for a non-existent relative humidity

Δ_r = shrinkage with the corresponding relative humidity

The prediction of creep according to this formula was reported for concrete tests carried out by Davis. The correlation is excellent. Realizing the effect of initial curing, L'Hermite modified his formula to:

$$\Delta = \frac{D}{R} \cdot \Delta_{mi}\left(1 + Q \frac{\Delta_r}{\Delta_{ro}}\right)$$

where: D = supplementary constant specific to the type of concrete considered

R = ultimate strength of concrete

It may be better to replace $\frac{D}{R}$ by a function of R to be determined or by a function of the curing time in a medium of a given relative humidity.

Mamillan (26), from tests on 1.6 by 1.6 by 5.0-in. cement paste prisms, found that for the same sustained stress, the creep is three to four times as great for the dry-stored specimens as for the water-stored ones.

De la Pena (27) presented some data on tests carried out on very thin-walled cylindrical specimens. The wall thickness of the specimen was 2 mm. The inside diameter of the cylinder was 45 mm and had a length of 100 mm. The material tested was cement mortar with three mixes, 8:2. 6:4, and 4:6 cement to sand ratio by weight. The water/cement ratio was 0.31, 0.35, and 0.48, respectively. The required relative humidity was insured by means of mixes of water and glycerine. He used relative humidities of 10, 50, and 100%. The test program reported was continuing at that time; thus, only partial conclusions were drawn. From the presented data, it is clear that creep under high relative humidities is only a fraction of the creep at low relative humidities.

Hansen (6) according to a series of tests carried out on 2 by 5 by 25-cm beams which were loaded at 28 and 128 days, states that the results confirm that a simultaneous shrinkage or water diffusion during the time of sustained loading greatly increases creep. The more the relative humidity of the surroundings differs from the level of moisture equilibrium of the concrete, the more the concrete creeps, while the difference levels out by drying or wetting.

Based on tests carried out on beams which were dried in an atmosphere of 5-10% R.H. before sealing, and loaded in liquid paraffin, Hansen states that wet concrete creeps more than dry concrete when no moisture diffusion takes place during the time of sustained loading.

Hansen, in 1958 (28), concluded that any internal diffusion of water within the cement gel, whether positive or negative, should accelerate creep. This conclusion was based on results of tests carried out on concrete beams. Later, in 1960, based on the same type of tests, he concluded (6) that only the first period of drying has an accelerating influence upon creep. Hansen also stated that it is more reasonable to believe that the "strong" creep during the first period of drying is due to an irreversible modification of the cement gel and that this effect is not repeated during any subsequent period of drying. He reported that there are several evidences of such a modification of the cement gel.

Hansen also noticed that with quicker variations in humidity, the total creep will end towards the value obtained when concrete is constantly exposed to the average humidity during the time of sustained loading.

Tomes, Hunt and Blaine (29,30) in 1957, and 1960, found that the surface area of cement gel is greatly reduced during the first period of drying. This substantiates the theory that the irreversible modification of the cement paste is a collapse or irreversible compression of the gel structure.

Glucklich (31), according to a series of tests with 2 by 22-in. mortar cylinders, which were loaded in pure shear (torsion) and subjected to severe drying (110^{o}C for one week), found that creep is nearly nonexistent in mortar deprived of almost all of its evaporable water. His results showed that the creep rate approaches zero for an evaporable water content of 0.07. It then increases linearly with an increase in the evaporable water content, up to a value of evaporable water content of 0.45, after which it becomes nonlinear, and continues to be nonlinear up to the saturation point - i.e., point at which evaporable water content = 1.0.

For an evaporable water content of zero, he reported that no creep was observed after three days. Also, deformations up to three days were described as erratic and, therefore, not reported.

Ishai (32), basing his conclusions on tests carried out on 2 by 22-in. mortar cylinders loaded in pure shear (torsion) and subjected to 80 - 100% R.H., or which were sealed, observed that total and residual creep become similar to creep at 50-60 days after loading and that reversible creep increases rapidly during the first few days under all hygrometric conditions, reaching a maximum after 50 to 60 days from time of loading.

Mullen and Dolch (33) conducted tests on hollow cylindrical specimens of cement paste, 7-in. long and 1.1-in. outer diameter with 0.1-in. wall thickness. They observed that oven-dried (110^{o}C) portland cement paste does not creep under sustained loading and that water is the dominant intrinsic factor in the group of concrete. They concluded that "The most important mechanism of creep is seepage."

Hansen and Mattock (34), presented results on the influence of size and shape of member on the shrinkage and creep of concrete. They derived a relationship between creep, shrinkage, volume to surface ratio, and time, which could serve as a guide for predicting the effect of volume to surface ratio on creep and shrinkage of concrete. This relationship is represented in this report in Fig. 1. Finally, they concluded that changes in size and shape of member affect, at all ages, both the shrinkage and creep of concrete stored under drying conditions. Both the rate and the final values of shrinkage and creep decrease as the member becomes larger. For very large members, the creep approaches the value of basic creep, corresponding to a sealed specimen.

Sackman (3) in 1963, suggested the idea of "humidity compensated time", similar in nature to temperature compensated time. To check this, Sackman replotted the data presented by Hansen (6) against log time. He then attempted to shift all the curves to a single base curve. The results obtained were not in good agreement but he suggested that it might be used as a crude approximation.

Ali and Kesler (35) concluded that drying creep has time-variation characteristics closely resembling free shrinkage and appears to be influenced in practically the same manner by the same organismic and environmental factors.

Illston (10), based on limited tests carried out on concrete cylinders with 3 1/2-in. diameter, noticed that the creep of a specimen under sustained uniaxial tensile stress is the same both for a specimen which is kept wet throughout loading and for a specimen which is drying.

Bertero (36) in a recent paper, 1969, presented results of tests carried out on solid cylindrical specimens with 3 3/4-in. diameter and hollow cylindrical specimens with outside diameter of 3 3/4-in. and inside diameter of 2 1/4-in. which were loaded in pure shear (torsion). Based on his results, and others, Bertero concluded that "changes in environmental conditions produce an increase in creep, even in cases where the concrete is subjected to a level of sustained loading stress below its plastic limit" and that most of the increase in creep due to changes in relative humidity is of an irrecoverable nature.

Bertero's work is the most reliable and significant work published concerning the effect of cyclic relative humidity. This has been emphasized by the choice of specimens and the testing program. The conclusion that he drew regarding the effect of cyclic relative humidity on creep of concrete was that "Although new increases in creep occur during the successive cycles of similar changes in hygrometric conditions, these increases are of considerably smaller magnitude than those induced by the first cycle and die out as the number of cycles increases, becoming practically negligible after 3 or 4 cycles."

Upon reviewing the above literature, it is obvious that the effect of relative humidity on the creep of concrete was realized at an early stage. The complex state of strain and stress, which will exist in a member subjected to a varying relative humidity, added to the lack of understanding of the effect of varying relative humidity on creep. It is true that the transient stresses in a concrete member due to differential drying will increase the amount of creep of a concrete member, but the effect of transient stresses on creep was found to be incapable of producing the <u>amount</u> of creep which was observed experimentally. Therefore, the effect of varying humidity on the creep of concrete contains other factors aside from merely producing transient stresses.

With more refined experimental procedures, it was observed by Hansen (28) and Bertero (36) that the first drying produces the greatest amount of the increase in creep during humidity cycling and that this creep increase is largely irreversible. Irreversible changes in the structure of the cement gel are also expected to take place in the first drying of a concrete specimen.

The observations of Tomes, Hunt and Blaine (29, 30) substantiated this assumption of irreversible changes in the structure of the cement gel by noting irreversible changes in the surface area of the cement gel.

This review of available literature has by no means attempted to be exhaustive, but has merely presented the pertinent studies which affect the present investigation, with an emphasis on presenting their various conclusions.

1.3.3 <u>Literature Concerning Time-Dependent Behavior of Concrete Under Multiaxial State of Stress</u>.--It should be realized that the experimental studies done on the time-dependent behavior of concrete under multiaxial state of stress are limited; this is due to the fact that the instrumentation for the application of load and strain measurements in the multiaxial state is elaborate and time-consuming. Nevertheless, data on lateral measurements have been obtained as early as 1931.

Published work is summarized herein in order to indicate some of the historical background and the present day knowledge of the problem.

On observations of lateral deformations of columns which are reinforced laterally, Davis (18) reported that there was no evidence of an appreciable lateral "flow". It is noted, however, that the level of stressing of these columns was quite low to be measured by the instruments he was using. Also, the columns were under drying shrinkage, and it is probable that the lateral "flow" was confused with drying shrinkage.

In 1934 Davis, Davis, and Hamilton (5) observed the lateral "flow" of two 18 by 36-in. cylinders which were loaded at age of two months. The stress was 1200 psi and the cylinders were stored in the open air after loading. Strain measurements were taken by Carlson strain meters which were embedded in the cylinders while Whittemore gages were used for surface measurements.

They reported a Poisson's ratio of 1/5, using internal measurements. In the same report (5), results of triaxial loading were presented. The test was carried out on two similar specimens at ages of 28 and 57 days. The specimens were 12 by 48-in. cylinders. The specimens were sealed inside copper containers. While applying the longitudinal load, the lateral dimension was maintained constant by lateral pressure applied radially against the circumferential surface of the cylinders.

It was found that the lateral pressures required to maintain constant lateral dimension decreased rapidly in the first day or two after loading and more slowly at later ages. From these tests it was observed that the initial Poisson's ratio for the specimen loaded at age 28 days was 0.20, and it became 0.16 after 19 days under 1090 psi. The lateral pressure for these specimens is given for the start of the test and for the end of the test. For the specimen loaded at 57 days, initial Poisson's ratio was 0.16 and became 0.12 after 28 days of loading (same axial loading as of specimen loaded at age 28 days, but different lateral pressures). No data were reported concerning the effect of age on the modulus of elasticity or Poisson's ratio. The investigators noted that the axial "flow" occurring when the lateral dimension is maintained constant is of the same order of magnitude as the flow observed in similar concretes under no lateral restraint.

Duke and Davis (24) reported in 1944 the results of tests carried out on 8 by 16-in. concrete cylinders. The loads were applied 7 or 10 days after casting the concrete and were sustained for 2 or 3 months. Whittemore strain gages as well as Carlson embedded gages were used. The investigators used more than one method to seal the specimens but they reported that all covering proved ineffective in preventing passage of moisture over the period of testing. Based on total strains, Poisson's ratio under sustained load is found to be 1/6 for cylinders under triaxial loading. They reported that the creep characteristics under triaxial loading were not appreciably influenced by whatever differences may have existed in the composition of the cement. For the concrete cylinders subjected to the same axial load, existence of lateral pressure caused a marked decrease in longitudinal strain and caused lateral compressive strains exceeding the lateral dimensions due to the Poisson's ratio effect under axial load only. Also, it was found that under equal triaxial pressures (hydrostatic loading), the total strains ceased increasing and began to decrease after about three weeks under load.

In their paper, Duke and Davis (24) presented the formula for the prediction of the strain-time relationship for triaxial stress as:

$$R_A = \frac{\sigma_1}{\sigma_A} - \mu \frac{\sigma_2}{\sigma_A} - \mu \frac{\sigma_3}{\sigma_A}$$

where R_A = Ratio of the axial strain in a cylinder under triaxial stress to the axial strain in a cylinder under uniaxial stress;

$\sigma_1, \sigma_2, \sigma_3$ = Major, intermediate, and minor principal stresses, respectively (in the tests on cylindrical specimens, σ_1 was the axial stress);

σ_A = Axial stress in a cylinder under simple load; and

μ = Poisson's ratio.

In order to apply the above formula, the following assumptions were made:

(1) The total strains (elastic + creep) are proportional to the magnitude of the sustained stresses.

(2) The Poisson's ratio effect is constant.

It is reported that estimates according to the above formula are resonably close to the observed strains for the first month or so under load, and in consideration of the errors involved in analysis where data of this sort are used, the estimated values would probably be good enough for practical purposes in a number of situations. But, it should be mentioned here, that in addition to the assumptions asserted by the investigators, the formula implies that concrete under sustained triaxial stressing behaves as an isotropic material.

The results of exploratory experiments on tubular concrete specimens were also reported (24). Specimens of 9-in. outer diameter and a wall thickness of 1 1/2 in. were loaded at age 7 days by applying equal torques at the ends of the tube. Stresses induced at the extreme fibres were 50-100 psi. The load was applied at age 7 days; and the shear creep strains are presented after 50 days under sustained torsional loading. The numerical value of shear creep was in the order of twice the compressive creep that would have occurred under a compressive stress of the same magnitude as the applied shear stress. The investigators proposed the estimation of approximate magnitude of creep under triaxial stress for a state of pure shear which is created by equal, perpendicular direct stresses as:

$$R_s = \frac{\text{Creep due to shear}}{\text{Creep due to axial compression}}$$

$$R_s = 2(1 + \mu)\frac{\tau}{\sigma_A}$$

where τ = shear stress

σ = axial compressive stress

μ = Poisson's ratio.

Ross (11) in 1954, reported experiments on slabs 6 by 6 by 2-in. which were loaded biaxially under two compressive stresses and on tubes with 6-in. O.D. and 3/4-in. wall thickness which were under hoop tensile stress and axial compressive stress. All specimens were under drying shrinkage on the surface where no load was applied. Ross concluded that concrete as a material, when loaded initially, behaves elastically with a normal low value of Poisson's ratio. Shrinkage proceeds with lapse of time and, under sustained two-dimensional stressing, creep also develops in the principal directions with magnitudes generally of the same order as the corresponding creep under simple stresses--i.e., Poisson's ratio for creep is negligible or zero. He expected that creep strains in concrete may be influenced by the sequence of application of the stresses.

Gambarov (37) reported the results of tests carried out on 14 by 70-cm cylinders. Some of the specimens were triaxially loaded, others axially loaded and restrained on the cylindrical surface. Based on his results, he concluded that the general creep behavior is similar to that under uniaxial stress and that creep is reduced in the axial direction due to the lateral compression of the concrete. Poisson's ratio was found to be 1/6.

Arthanari (12) in 1967 presented creep data for 12 by 12 by 4-in. slabs which were loaded under uniaxial and equal biaxial compressive stresses. The experimental program was designed to investigate the creep of concrete under uniaxial and biaxial stresses at elevated temperatures. Some specimens were sealed, others were unsealed. He concluded that an effective Poisson's ratio of 0.2 can be assumed for design purposes. He indicated that the ratio of elastic plus creep strain under uniaxial stress to the elastic plus creep strain under equal biaxial stresses of the same intensity lies between 0.76 and 0.84.

Jordaan (38) concluded that creep Poisson's ratio is zero and that for any particular stress system--i.e., uniaxial, biaxial, or triaxial, the elastic values of Poisson's ratio on loading and unloading were approximately equal. Jordaan's conclusions were based on tests of sealed concrete cubes which were subjected to uniaxial, biaxial and triaxial loading with different levels of stressing. In analyzing the results in terms of volumetric and deviatoric components, he found that out of three deviatoric components, only two are independent.

Gopalakrishnan (39,40), basing his assumptions on experiments done on concrete cubes, concluded that uniaxial creep Poisson's ratio is approximately the same as elastic Poisson's ratio and that creep under multiaxial compression is less than under uniaxial compression of the same magnitude in a given direction. Lateral compression was observed to reduce axial creep by up to 20 percent in excess of reduction through creep Poisson's ratio. It follows that the effective creep Poisson's ratio is a function of the overall state of stress in the specimen. He further concluded that "creep under multiaxial stress cannot be simply predicted from uniaxial creep measurements. Thus, the principle of superposition does not hold for creep strain under multiaxial compression. This is supported by an analytical study (41) of aggregate-matrix interaction under sustained load." Gopalakrishnan postulated that creep under multiaxial compression can be predicted by using an equation similar to the elasticity equation for anisotropic materials with the effective creep Poisson's ratio μ_i in any direction i, taken as a function of a parameter ε_{ei} representing the state of stress. Thus:

$$\varepsilon_i = (\varepsilon_u/\sigma_u)\left[\sigma_i - \mu_i(\sigma_j + \sigma_k)\right]$$

where $\mu_i = \mu_{cu} - K_i\varepsilon_{ei}$

μ_{cu} = uniaxial creep Poisson's ratio

ε_{ei} = instantaneous strain in direction i on loading

K_i = value determined experimentally for the given mix

ε_u, σ_u = strain and stress in a uniaxial specimen, respectively

σ_i, σ_j, σ_k = stresses in three general principal directions.

In conclusion, it can be stated that in order to determine the behavior of Poisson's ratio under sustained loading, instruments of a high degree of precision should be used for measuring deformations. These instruments should also have a high degree of stability for the measuring of deformations throughout the period of testing.

Most of the above-reviewed investigations were lacking in one or both of the required properties for instruments that should be used in such an investigation. Hence, the conclusions which resulted were incomparable and many times contradictory. However, most investigators are inclined to conclude that creep Poisson's ratio is not a property of concrete material, but rather a function of state of stress, humidity conditions and other factors.

Furthermore, it can be concluded that creep of concrete under multiaxial state of stress is less than that of concrete under a uniaxial state of stress.

1.4 DIFFUSIBLE LOAD-BEARING LAYERS AND THE POWERS-BAZANT THEORY

Of all the components which effect the creep of concrete, cement gel is the most important. Cement gel generally occurs in the form of thin, rolled or crumpled sheets (42,43). Adsorption tests and microscopic observations suggest that these sheets have an average thickness of 15 Å with the possibility that the interface distances are less than this average (15). The average surface area of gel is about 500 m^2 per cm^3 of cement paste.

Based on experimental findings, Harkins (44) believed that on an open surface of saturated vapor, adsorption can build up a layer five water molecules thick (13 Å). The average thickness of the adsorbed layers decreases with the decrease of humidity. At a humidity of 50%, Powers (15) estimated the average thickness of the adsorbed water layer to be 5 Å, or about two molecules. It is expected, therefore, that a significant amount of cement gel water is in the adsorbed state, and the water molecules, which are in the adsorbed state are held there by Van der Waals forces (8).

In a narrow gap, thinner than 26 Å, above a certain humidity the total thickness of the two adsorbed layers of these opposite solid surfaces cannot be accommodated, and adsorbed water molecules fill the gap completely, in which case it becomes "hindered adsorption" (8). When adsorbed water layers are accommodated freely between two solid surfaces, they are referred to as "free adsorbed water layers".

In areas where there is hindered adsorption, the pressure between the two solid surfaces is called "disjoining pressure". Disjoining pressure is at a maximum in a saturated specimen--i.e., a specimen at 100% R.H. The hindered adsorbed water layers can thus transmit normal stress and, at the same time, diffuse into or from the free adsorbed layers. They represent a transition component between the solid and the fluid. "Hindered adsorbed water layers" are also called "diffusible load-bearing water layers", and are recognized as a structural element of hardened cement paste (8).

The thickness of a diffusible load-bearing layer is governed by humidity (h), temperature (T), and pressure applied on the layer (P), according to the first and second laws of thermodynamics.

An increase in P or a decrease in h or T will cause the adsorbed water to diffuse out to the nearest pores, thus decreasing the thickness of the load-bearing layer. A decrease in P or an increase in h or T will cause more water from the surrounding free water to diffuse in the load-bearing layer, thus increasing its thickness. The effect of drying a specimen would be the creation of a negative film stress which, added algebraically to the stress in the load-bearing water, changes the disjoining pressure which ultimately will change the thickness of the layer.

In addition to the adsorbed water, other types of water exist in the cement paste. One of these types is water chemically held in the cement gel. This water does not affect creep or shrinkage of concrete. Another type is capillary water. Capillary water is that water which exists in the capillary space. Capillary space is that which is in excess of the space required for hydrated cement in its densest form of aggregation--i.e., cement gel, which has a width of 26 Å or more. Capillary water is governed by surface tension in the spaces where it exists. Some of the capillary water is drawn up into thin and long capillaries (thicker than 26 Å). Upon application of load, this capillary water becomes hindered and the only way to move it from these thin, long capillaries is by diffusion. Therefore, it is considered a part of the diffusible load-bearing layers.

Bazant (17), derived constitutive equations for the diffusible load-bearing layers. Using these constitutive equations in which the relationship between diffusible load-bearing water and the solid part of concrete structure was considered by utilizing a rheological model, he derived constitutive equations for creep of concrete under any state of stress with varying humidity and temperature. Later, Bazant refined these constitutive equations and presented a numerical analysis (45) for them. Two assumptions were involved in the derivation of these equations:

(a) At the macroscopical level, concrete is an isotropic material.

(b) Analysis is limited to the range within which the stress-strain relationship is linear.

With the above two assumptions, the concrete's behavior can be separated into two components; Volumetric and Deviatoric. The rheological model used in deriving the constitutive equation for creep of concrete is shown in Fig. 2. This model consists of a diffusion unit (a) connected in series with an elastic spring (b). The diffusion unit consists of a diffusion element (d) and an elastic spring (c), c and d are connected in parallel. Element d represents the diffusible load-bearing layers while c and b represent the solid skeleton of the cement gel and concrete body.

For the model shown in Fig. 2, and with a change of relative humidity, Δh, while temperature T is constant, Bazant's constitutive equations are reduced to the following:

$$\dot{\varepsilon} = \frac{\dot{\sigma}}{K} + \dot{\varepsilon}''^{*} \tag{1.4.1}$$

$$\dot{e}_{ij} = \frac{\dot{S}_{ij}}{2\,G} + \dot{e}''_{ij} \tag{1.4.2}$$

where:

$$\dot{\varepsilon}'' = \dot{\varepsilon}'_{\mu}{}^{*} - \frac{\dot{\sigma}_a}{K} \tag{1.4.3}$$

$$\dot{\varepsilon}'_{\mu} = \phi_{\mu}(\sigma_{d\mu} - \sigma_{ad\mu}) - \sigma_{d\mu}\frac{\dot{h}_{eq}}{K_{h\mu}} \tag{1.4.4}$$

$$\dot{\sigma}_{d\mu} = \nu_{\mu}(\dot{\sigma} - \dot{\sigma}_{a\mu}) - K_{c\mu}\dot{\varepsilon}'_{\mu} \tag{1.4.5}$$

$$\dot{e}''_{ij} = \dot{e}'_{ij\mu}{}^{*} = S_{d_{ij\mu}}\left(\frac{1}{2}\psi_{\mu} - \frac{\dot{h}_{eq}}{2G_{h\mu}}\right) \tag{1.4.6}$$

$$\dot{S}_{d_{ij\mu}} = \nu'_{\mu}\dot{S}_{ij\mu} - 2G_{c\mu}\dot{e}'_{ij\mu} \tag{1.4.7}$$

also,

$$K = [K_b^{-1} + (K_c + K_d)^{-1}]^{-1}\,,\quad \nu_{\mu} = \frac{K_d}{K_c+K_d}$$

$$G = [G_b^{-1} + (G_c + G_d)^{-1}]^{-1}\,,\quad \nu'_{\mu} = \frac{G_d}{G_c+G_d}$$

---

* $\dot{\varepsilon}''$, $\dot{e}''_{ij}$, $\dot{\varepsilon}'_{\mu}$ and $\dot{e}'_{ij\mu}$ have been used instead of ε'', e''_{ij}, ε'_{μ} and $e'_{ij\mu}$ as they are reported (Bazant (17)) in order to maintain consistency in presenting the numerical analysis as it is discussed in Section 3.1.

$(\cdot) = \frac{\partial(\ )}{\partial t_{eq}}$, where t_{eq} is equivalent curing time.

All terms subscripted with μ belong to the Powers diffusion unit, Fig. 2. Henceforth, this subscript will be omitted for simplicity.

$\dot{\varepsilon}$, $\dot{e}_{ij}$ = rate of volumetric and deviatoric strain respectively.

σ, S_{ij} = total volumetric and deviatoric stress (macroscopic),

$\dot{\sigma}$ and $\dot{S}_{ij}$ are the rate of applied volumetric and deviatoric stresses respectively.

$\frac{\dot{\sigma}}{K}$ and $\frac{\dot{S}_{ij}}{K}$ account, therefore, for the rate of volumetric and deviatoric elastic strains.

$\dot{\varepsilon}''$, $\dot{e}''_{ij}$ = rate of inelastic volumetric and deviatoric strain respectively.

ϕ, ψ = rate of volumetric and deviatoric creep parameters.

σ_d = stress resultant over a unit cross-section due to disjoining pressure in the diffusible load-bearing layers in the macroscopic sense, σ_d has the so-called hidden variables.

σ_{ad} = equilibrium value of σ_d at a given humidity and a given temperature.

σ_{ad} is represented by:

$$\sigma_{ad} = \frac{T}{T_o}\,\sigma'_{ah} + \left(\frac{T}{T_o} - 1\right)\sigma_{aQ}$$

σ_{aQ} = a function of temperature only.

T_o = reference temperature.

If $T = T_o$, then:

$$\sigma_{ad} = \sigma'_{ah}$$

where $\sigma'_{ah} = f_d \cdot \frac{RT'}{M} \cdot S_h \cdot \sigma_{ah}$

R = universal gas constant in cc. atm/deg/mol.

T' = temperature in degrees Kelvin.

M = molecular weight of water. At a temperature of 298^{o} Kelvin or 25^{o}C, RT'/M = 1360.

σ_{ah} = a parameter, Fig. 3-b, which was assumed by Bazant (46) to have the following expression:

σ_{ah} = $(h_s - h)(1 + h_{eq})$ at a temperature of 25°C

h_{eq} = equivalent humidity defined by:

$$dh_{eq} = dh + dh_s \tag{1.4.8}$$

h_s = humidity for self-desiccation, see Appendix A.

The basis of Bazant's estimation of σ_{ah} is that $\left.\frac{\partial\sigma_{ah}}{\partial h}\right|_{h=0} = 0$ and that the value $\sigma_{ah}\big|_{h=1.0} = 0$, these values are expected to be reasonable estimations (47).

f_d = effective area factor for diffusible load-bearing layers.

S_h = a factor which accounts for the exessive pressure in the diffusible load-bearing layer as a result of simultaneous compressive loading and drying.

σ_a = volumetric stress due to fluid--i.e., capillary water which is represented by:

σ_a = $\sigma_{ad}\frac{f_a}{f_d}$, σ_a is needed for static equilibrium.

$\frac{\dot{\sigma}}{K}$ is, therefore, instantaneous shrinkage which corresponds to shrinkage due to a change in surface tension.

f_a = effective area factor for non-load-bearing layers

K_h = a modulus which accounts for delayed deformation of concrete under load due to a change in the effective area factor f_d of the load-bearing layers, occurring as a consequence of a change in humidity (or temperature). The term $(\sigma_d \frac{\dot{h}_{eq}}{K_h})$ accounts for the fact that "creep under conditions of drying is greater than creep at a constant humidity."

K_b, K_c, K_d, K = bulk moduli of elasticity of elements shown in Fig. 2. If modulus of elasticity is represented by E and Poisson's ratio by μ, then

$$K = \frac{E}{1-2\mu}, \text{ and } E = 2G(1+\mu)$$

or

$$K = \frac{2G(1+\mu)}{(1-2\mu)}$$

Where G is shear modulus of elasticity of the model shown in Fig. 2. G_b, G_c

and G_d are similar to G except for the individual elements of the model. K_d and G_d represent that part of K, G which depends on the compressibility of the diffusible load-bearing layers, hence, it is a function of humidity.

t_{eq} = equivalent curing time or, simply, equivalent time, is a function of the maturity parameter β and is defined as:

$$t_{eq} = \int_{t_o}^{t} \beta dt' \qquad (1.4.9)$$

where β = $\beta_T\beta_h$, β_T is a function of temperature only and β_h is a function of humidity only. For constant temperature, β_T = 1, thus $\beta = \beta_h$. β_h is called the relative hydration rate. Bazant (46) approximated β_h by:

$$\beta_h = [1 + (7.5-7.5h)^4]^{-1} \qquad (1.4.10)$$

This approximation is based on the observation by Powers (48) that hydration is considerably slower at $h = 0.95$ and stops at about $h = 0.80$. Also, Keeton (49) showed that the modulus of elasticity and the compressive strength cease to rise when humidity is below about 0.80. The relationship between β_h and h, equation 1.4.9, is shown in Fig. 3-a.

In Chapter 3, the discussions and significance of the various terms mentioned above as well as their effect on the prediction of creep results will be presented and discussed in detail.

1.5 STATEMENT OF PROBLEM

It has been experimentally observed (3,4,6,8,9,13,36) that when concrete is subjected to changes in humidity, there is considerable increase in creep. These observations appear to indicate that the real creep characteristics of a given concrete, depend significantly on the environmental conditions to which the concrete is subjected. Therefore, this should be taken into consideration in the interpretation of the experimental results, especially when extrapolating laboratory tests to predict behavior of structural elements subjected to alternate variation of humidity. Most of the theories and work concerning creep of concrete members (3,7,22,25,28,31,34,35,37,39,50,51) is being undertaken from an engineering standpoint which concerns itself with the creep of concrete as a particular phenomenon in each case rather than as a result of a mechanism or properties of concrete.

Accordingly, these theories failed to predict the creep of concrete members except for a limited range of environmental conditions--e.g., a constant humidity and constant temperature or a constant humidity with change in temperature such as a change from room temperature up to 200°F. In these works, no convincing theory or explanation was suggested regarding the effect of changes in the environmental conditions upon the creep of concrete members. Even the experimental data available do not give a clear picture of the real effects of these changes. This is not surprising since the nature of creep of concrete is still uncertain, and, in the strict sense of the word, there is no existing theory of creep.

An understanding of the mechanism of creep should stem from an examination of the components of the concrete structure on the microscopical and submicroscopical levels, such as the nature of the cement gel, phases in which water exists in the cement gel, interaction between water in the cement gel and elastic components of the cement gel, etc.

Powers (8,14,15,16) was the first to suggest the presence of the load-bearing adsorbed water layers in the gel structure in the study of shrinkage and creep on concrete. The basic assumption of Powers' theory is that hindered adsorbed water is "load-bearing water" and, therefore, it is one of the structural elements of hardened cement paste.

As was mentioned before, Bazant (17,46), basing his assumptions on a rheological model like the one shown in Fig. 2, formulated constitutive equations 1.4.1 and 1.4.2, composed of a set of equations (1.4.3 to 1.4.7) for predicting the creep of concrete under variable humidity and temperature. Equations 1.4.1 and 1.4.2 are presented in terms of the derivative of total strain (elastic strain + creep strain + shrinkage, if any) with equivalent time. The nature of the constitutive equations requires a numerical solution. The numerical analysis suggested by Bazant (45) was the one used for the solution of these equations. This numerical analysis is presented in Section 3.1.

A glance at equations 1.4.1 to 1.4.7 will reveal that the prediction of creep according to these equations requires the knowledge of some of the properties of concrete such as those properties represented by the moduli of elasticity, the rate of creep strain, effective area factors for load-bearing layers and non-load-bearing layers and special terms K_h and G_h.

As can be seen from equations 1.4.4 and 1.4.6, $\dot{h}_{eq}$ should be given in order to be able to solve the problem of creep of a concrete member subjected to changing humidity; therefore, one should solve, simultaneously, the moisture diffusion problem in the concrete member. The moisture diffusion problem is a boundary value problem hence, it requires the knowledge of the coefficient of hygral diffusivity of concrete as well as equivalent surface thickness, all of which are discussed in Appendix A.

This study is concerned with an investigation of the effects of humidity on the creep of concrete. Because the prediction of creep of concrete using equations 1.4.1 and 1.4.2 requires the determination of the various material parameters and functions which are discussed in Section 1.4, it was decided to carry out the following studies: (1) experimental - presented in Chapter 2, and (2) analytical - presented in Chapter 3. The analytical study was based on the results of Chapter 2.

1.6 OBJECTIVE

The objective of this investigation was to carry out a predesigned experimental program which would yield results enabling the evaluation of the following terms:

1. All bulk moduli of elasticity K'_s, and shear moduli of elasticity, G'_s.
2. Effective area factors f_d and f_a.
3. Rate of creep parameters ϕ and ψ.
4. Coefficient of hygral diffusivity C which would enable us to solve the moisture diffusion problem in the internal pores of the concrete body.
5. Humidity for self-desiccation, h_s.

Knowing the expressions of the above terms (1-5), it is possible, by the use of constitutive equations 1.4.1 and 1.4.2 to predict the creep of concrete under any type of loading and under changing humidity. Furthermore, the experimental program was designed to yield results which would promote understanding of the effect of types of loading and effect of changing humidity on the creep of concrete.

1.7 SCOPE

The change of humidity studied in this investigation ranged from 100 to 50 to 100%. The scope of the experiments and analysis was to study the effect of the variable humidity as well as the effect of constant 100 and 50% R.H. All the work of this investigation was carried out at a constant temperature of 73°F. Since the study is mainly concerned with the mechanism of the creep of concrete as well as its prediction, only one type of concrete was used. The loading types were:

uniaxial compression, biaxial compression, as well as torsional loading. The level of sustained stress was kept below the so-called limit of the linear range of creep strain-stress law.

CHAPTER 2

EXPERIMENTAL PROGRAM AND RESULTS

For simplicity in presenting the experimental program and its test results, this chapter is divided into two parts. Part 1 is concerned with the study of effects of cyclic humidity on time-dependent behavior of concrete. Part 2 is concerned with the study of effect of biaxial loading on time-dependent behavior of concrete. In this chapter, the experimental program is presented and results discussed. The main factors which affect the creep of concrete are evaluated from an engineering point of view. For clarity, the determination of terms mentioned in Section 1.6 is delayed until Chapter 3.

PART 1 - TESTS ON EFFECTS OF HUMIDITY ON TIME-DEPENDENT BEHAVIOR OF CONCRETE

2.1 OBJECTIVE

The objective of this phase of the investigation is to obtain and study results of tests on the effects of humidity on the creep characteristics of concrete members.

2.2 SCOPE

To achieve the above objective, the following experiments were conducted:

2.2.1 Pilot Experiments.--The pilot tests were intended to determine whether or not the proposed method of experimentation (Section 2.3) is in general adequate to yield the required information. Through such pilot tests any unanticipated problems which might arise could be corrected and any modifications indicated for improving the experimentation could be made.

Several aspects of the technique (Section 2.3.3) to be used were checked and tested in these pilot experiments. The first step was to check the adequacy of steel rings as a method of transferring sustained torque to and from the specimen. Several trial specimens were made. These trial specimens were cast utilizing these steel rings on both ends of the specimen. Just as the lower ring transfers torque from the specimen to the base, the upper ring was intended to transfer the sustained torque to the specimen (Fig. 7-a). Development of large cracks at the lower edge of the upper steel ring in the specimen made it obvious that the steel ring should be discarded. It is believed that the cracks resulted from differential settlement between the fresh concrete and the steel rings. Consequently, epoxy was used to attach the loading arms at the top of the specimen. This proved to be a very successful substitute for the upper steel ring. The lower steel ring was cast into the specimen.

The next technique which was evaluated was the bond between concrete and the strain gage. In testing this, three 3 by 6-in. solid cylinders were cast with two strain gages embedded in each. The embedding was done in the same manner as that proposed for the main specimens. The results proved the bond to be very satisfactory and no modifications were necessary.

To test the prototype experimental procedure itself, three specimens were cast: one torsion, one compression, and one control companion specimen. These resembled the proposed main specimens in all aspects. The results obtained from these specimens after testing them under cyclic humidity showed the method of experimentation to be satisfactory.

2.2.2 Main Experiments.--After the pilot experiments were completed and the necessary modifications made, the main experiments were started. For these, one type of specimen was used--a hollow cylinder, 5-in. I.D., 6-in. O.D., and 40-in. long. Henceforth, these hollow tube specimens will be referred to simply as "specimens".

These specimens were tested under constant R.H. of 50 and 100%, and under cyclic relative humidities, 50 to 100 to 50%. Two types of loading were employed, namely, uniaxial compression and torsion. In this report, they will be referred to as compression specimens and torsion specimens.

Also control specimens, which were not subjected to any type of loads, were made to determine volumetric changes of the concrete due to cyclic changes in humidity.

All specimens were loaded at age 21 days and then subjected to different hygral treatments. For each specimen under compressive loading, there was a companion control specimen under no load. This control specimen, however, underwent the same hygral treatment as the loaded specimen. In order to remain below the limit of the linear range, the stress level for the compression specimens was 25% of the compressive strength. For torsional loading, the small deformations occurring in the pilot tests suggested that the use of a higher stress level was preferable. Consequently, a stress level of 40% of the torsional strength was used. A total number of nine specimens were tested. From these specimens, the deformation-time curve for each was obtained.

Other tests were performed which were designed to yield an approximate relation between strength, modulus of elasticity, shear modulus of elasticity and Poisson's ratio, all versus time--i.e., instantaneous or short-time tests. These relationships are required to construct the bulk moduli of elasticity K_b, K_c, K_d and K as well as the shear moduli of elasticity G_b, G_c, G_d and G. Two types of specimens were used and tested at different ages: seventy-four solid 3 by 6-in. cylinders of the same material as the main specimens, and twelve specimens resembling the main ones--i.e., hollow cylinders.

2.2.3 Tests to Evaluate Coefficient of Hygral Diffusivity and Humidity for Self-Desiccation.--To be able to solve the problem of moisture diffusion in the concrete pores, it is necessary to have a value for the coefficient of hygral diffusivity of concrete, C. For this purpose, two concrete blocks instrumented with Monfore gage wells were used to study the coefficient of hygral diffusivity. These blocks were cast in brass boxes in a direction perpendicular to that of the expected water diffusion. Block No. 1 was 3 by 7 by 7 in. with six Monfore gage wells. This block was left open on one side; all other sides were sealed against moisture loss. Block No. 2 was 2 3/16 by 7 by 8 in. with seven Monfore gage wells and two open sides (see Appendix A).

For tests on humidity for self-desiccation, two concrete rods were cast with one Monfore gage well installed in each. These rods were sealed against moisture loss on all sides at age of 21 days.

Block No. 1, Block No. 2 and the two rods were cured for 21 days at 73°F and 100% R.H., then they were sealed as mentioned above. For details and calculations of coefficient of diffusivity see Appendix A.

2.3 FABRICATION OF SPECIMENS

2.3.1 Concrete Mix.--The concrete material used can better be described as "micro-concrete" since the aggregate used was sand only. The cement was Santa Cruz Type I portland cement having the chemical composition shown in Table 1. The aggregate was a 50-50 blend by weight of Silver sand and Felton sand. This proportioning of sand blend* was dictated by trials which showed this combination to have the least amount of air voids in the specimen, especially on its surface. Sieve analysis of this sand is given in Table 2. The cement-aggregate ratio was 1:2 by weight.

* Contained about 80% silica and 20% feldspar.

The micro-concrete had a nominal cement content of 12 scy (1128 lbs per cubic yard). The water-cement ratio was 0.58 by weight. The mix proportions are shown in Table 3.

2.3.2 Instrumentation with Embedded Electrical Strain Gages.--Microdot weldable strain gages (SG 189/6) were used in this investigation (Figs. 4 and 5). Three such strain gages were embedded in each specimen which were later loaded in compression. Likewise, three strain gages were embedded in each companion specimen: two in a longitudinal direction (180° apart) and one in the lateral direction (Fig. 6-a). The specimens subjected to torsion were intrumented with four Microdot strain gages--two pair of gages, 180° apart, were embedded. Each gage was at 45° to the axis of the specimen. All strain gages were embedded at the center of the specimen's wall thickness as well as being at the midpoint of its length (Fig. 6-b).

The lead-out wires of the strain gages (1/32-in. diameter) were taken out of the outer shell. A bridge completion unit was used with each Microdot strain gage to minimize the effect of the change of the terminals' resistance. In order to improve the bond between the concrete and the strain gage body, the flange of the gage was pin-holed with an average of 24 holes on both sides of the strain tube. Pilot tests on embedded strain gages in 3 by 6-in. solid cylinders proved that the bond between strain gage body and concrete was very good. These cylinders were tested under instantaneous loading, short-term creep (7 days), and drying-wetting cycles of about 7-day duration.

2.3.3 Casting of Specimens.--The mold used for casting the tube test specimens consisted of two concentric cylinders. The outside cylindrical shell of the mold was a 1/2-in. thick Plexiglass tube. The inner cylinder was a 1/4-in. thick steel tube (Figs. 7-a and c).

To permit demolding of the concrete specimen, the outside shell was made of two halves and the inner shell of three segments. The mold was held together by means of an upper and a lower flange, upper holding plate and rods (Figs. 7-b and d). For the torsion specimens casting molds, recesses were made on the bottom ends of the inner and outer shells to house a steel ring which was cast with the specimen (Figs. 7-a and e).

The mold was assembled by using Duxseal to fill the bottom and longitudinal joints. All joints were then covered with Mylar tape. This was done to prevent mortar from washing out at the seams when casting. A light film of bond breaker was used on the inner surfaces of the mold to help break the bond. Four wood discs were distributed along the length of the mold inside the inner steel tube to support the smallest segment of this tube. Concrete was deposited through specially designed funnels. During casting of the specimens the entire mold assembly was vibrated to insure proper consolidation of the concrete. A variable resistance unit was used to reduce the original speed of the vibrating table and control it throughout the casting of the specimen.

2.3.4 Curing.--After casting, the filled molds were moved to a fog room maintained at 73°F. The specimens were demolded 72 hours after casting, then returned to the fog room. The 72 hours were required for the concrete to develop enough strength to withstand the stress during stripping. The strain gage lead-outs and bridge completion units were wrapped in plastic bags to keep them from contact with moisture.

2.4 TESTING OF SPECIMENS

2.4.1 Testing Apparatus.--The compressive load was applied by means of restraining plates, rods, and a loading cell. Fig. 8-a shows a sketch of the compression loading frame including a specimen. The sustained pressure was kept constant by means of a hydraulic accumulator--i.e., reservoir. The stress variation of ± 2 psi per day of the hydraulic system was checked daily and corrected whenever needed. The frame was then placed in a metal pan 6-in. high. The specimen was covered by a polyethylene bag (Fig. 8-b) which was sealed on the outer side of the metal pan. Water jets then kept the inner atmosphere of the polyethylene bag at 100% R.H. Small fans were fixed near the top of the specimen to blow air inside the specimen. Perforated steel sleeves were placed between the loading cell and specimen. These sleeves have the same cross sectional area as the specimen but were only 2 in. in length. Details of the loading cells are described by Best et al (52).

The pictorial view (Fig. 9) shows a frame built to load one specimen in pure torsion. Fig. 10 depicts the principal dimensions of the frame. Each torsion creep apparatus was separately built directly on the floor with a concrete base of 30 by 2 by 6 in. The torsional strength tests also utilized this apparatus. For providing a 100% R.H. atmosphere, the same procedure as described above for the compression specimens was followed--i.e., using a polyethylene bag (10 mils) and metal pan.

2.4.2 Loading Preparations and Loading Procedures.--At age 21 days the specimens which were to be tested at a constant 100% R.H. were loaded, then placed in the fog room. Specimens which were to undergo cyclic humidity were moved to the 50% R.H. control room and were kept under the polyethylene bag where humidity was maintained at 100% R.H. Specimens which were to be tested at 50% R.H. were moved at age 18 days to the 50% R.H. control room and were kept there until the age of 32 days at which time they were loaded.

At age 14 days, the torsion specimens were moved out of the fog room. At that time, the torsional arm was attached to the specimen by means of epoxy. The specimens were kept sealed (100% R.H.) throughout this operation which took about one hour. They were later returned to the fog room.

At age 14 days, the compression specimens were moved out of the fog room in order to trim their ends. Each specimen was cut 1 to 2 in. on each end. The trimming was done in one cut without rotating or tilting the specimen in order to provide an even and smooth end surface. The cut surface was perpendicular to the axis of the specimen. The trimming was done by means of a rotary type diamond saw. Each cut took about one minute. The final trimmed specimen length was about 40 in. (Fig. 7-e).

2.4.3 Hygral Treatment.--Specimens which were to be tested at 50% R.H. were moved at age 18 days to a room with 50 $\pm$ 2% R.H. and 73°F temperature. They were loaded and kept there until the end of testing. Specimens which were to be tested at 100% R.H. were loaded at age 21 days and kept in a 100% R.H. and 73°F curing room until the end of the testing period.

Specimens which were to be subjected to cyclic humidity were moved to the 73°F control room at age 21 days. They were loaded and subjected to a 100% R.H. environment for one week. The environment of these specimens was then changed to 50% R.H. by stopping the water jets and removing the polyethylene bag. The specimens were kept at this 50% R.H. environment for two weeks. They were then subjected to 100% R.H. for two weeks. These changes were continued for two weeks each, as shown in Figs. 11 and 12. It should be noted here that the changes were not abrupt changes. For example, in order to alter the humidity from 100% to 50% R.H., the specimens were permitted to dry without accelerating this process by blowing air on them. However, in order to insure the inner surface of drying, a small fan was used to blow air down into the tubular specimen. In the case where the change of humidity from 50% to 100% R.H. took place, the specimen was covered with the polyethylene bag and the water jets were turned on. These jets did not spray water directly onto the specimen. In half an hour's time, all surfaces of the specimen were covered with free moisture.

2.4.4 Application of Load

(a) Compressive load.--The specimen was first placed in the loading frame and the upper and lower plates were stored as close as possible without restraining the specimen. The hydraulic loading system was then pressurized to the required level; the valve nearest to the loading cell was closed (Fig. 13). The hydraulic accumulator's valve was then closed, the loading cell's valve was opened quickly, and the system was pumped up to the required stress level. The valve of the pump was then closed, and the accumulator's valve was reopened in order to adjust the system. Readings were taken as soon as the valve of the accumulator was open. This took about 20 seconds from the start of stressing the specimen. This reading was considered as a zero reading for the creep data. A reading of the dial gage and of all strain gages required an additional 25 seconds.

(b) Torsional load.--The total amount of weight required to produce the desired torque was placed in the load baskets (Fig. 9) in two steps which took about 15 seconds. As soon as the weight was placed, a reading of the dial gages and strain gages was started. This reading was considered as the zero reading for the creep data. The reading of all dial gages and strain gages required an additional 30 seconds.

2.4.5 Deformation Measurements.--Two methods of deformation measurements were used, electrical and mechanical.

(a) Electrical.--As mentioned before, compression specimens had three electrical strain gages each, while torsion specimens had four strain gages each.

(b) Mechanical.--Two 1/10,000-in. dial gages were used on each torsion specimen. With a 12-in. arm, a 2.75-in. average specimen radius and a 35-in. specimen gage length, the resolution obtained was 0.69×10^{-6} radians.

For compression specimens, three aluminum rings were attached, by means of three pointed screws each on the outer surface of the specimen. A dial gage, which was connected to the aluminum ring, was in contact with a 3/8-in. dia. aluminum rod. The aluminum rod was firmly screwed to the lower ring and passed through a slightly oversized hole in the middle ring (Fig. 14). The 1/10,000-in. dial gage and the specimen gage's length of 35 in. gave a resolution of 2.86 microstrain. All dial gages used on specimens which were subjected to 100% R.H. or cyclic humidity were sealed inside plastic bags.

2.5 TEST RESULTS

The tests described in the above experimental program yielded the following results:

2.5.1 Control Specimens.--Two types of control specimens were tested.

(a) Solid cylinders, 3 by 6 in. Three or six such cylinders were tested to obtain the modulus of elasticity, Poisson's ratio and strength under uniaxial compression at age 3,4,7,14,20,21,23,27,28,30,37,45,56,80 and 102 days. These tests were carried out by means of XYY' recorders. Two LVDT's were used for measuring lateral deformations and two for measuring longitudinal deformations. Modulus of elasticity, E, as reported here is in terms of initial value of E. Results are shown in Fig. 15. Average strength of six cylinders after 21 days of 100% R.H. curing was 3800 psi. Average modulus of elasticity was 3.60×10^6 psi, and the average Poisson's ratio was 0.18.

The results of these tests Fig. 15-a can serve as a check on the behavior of modulus of elasticity, E, with time. Results shown in Fig. 15-b for Poisson's ratio vs. time indicate some inconsistencies. A constant value of 0.17 for Poisson's ratio could serve as an average for all ages.

(b) Hollow cylinders, 6-in. O.D., 5-in. I.D., and 40-in. long. Two such cylinders were tested under uniaxial compression at age 21 days. Results are given in Table 4. Average strength was 3600 psi. Average E was 3.43×10^6 psi, and average Poisson's ratio was 0.17. Four more specimens were tested at later ages. All of these cylinders were kept at 100% R.H. Results obtained from these six cylinders are shown in Figs. 16-a and b. These tests were carried out in the same way as described in (a) above. For torsional strength and shear modulus of elasticity, two hollow cylinders were tested at age 21 days. Results are given in Table 4. Average shear modulus of elasticity was 1.80×10^6 psi at 21 days. Three other cylinders were tested at later ages. All were at 100% R.H. Results are shown in Fig. 17-a and b. Beside the above tests, the compression companion specimens--i.e., specimens with no load, as well as all specimens which were maintained at a constant humidity, were loaded or unloaded instantaneously, that is, for only the period of time it took to take readings (about one minute). The results of these tests are included in the corresponding curves and in Figs. 16 and 17. Figs. 15-a and 16-a could be used to evaluate the bulk moduli of elasticity K_b and K_c while Figs. 16-a and c would be used to evaluate K_d. In the same way Fig. 17-a would be used to evaluate G_b and G_c while Fig. 17-b would be used to evaluate G_d. All these evaluations are presented in Chapter 3.

2.5.2 Creep Tests

(a) Specimens loaded under compression.--The changes in deformation, which occurred during the period of sustained loading, are summarized in Figs. 11, 18 and 19. These curves would be used in constructing the rate of volumetric creep parameter and the coefficient K_h.

(b) Companion specimens.--These specimens resemble the compression specimens in every aspect except that they are not loaded. Figs. 12 and 20 show the results obtained for deformations of concrete vs. time under cyclic humidity and under constant 50% R.H., respectively. Deformations of unloaded specimens which were kept at 100% R.H. all the time were insignificant, about 1 microstrain per week.

Creep deformations of a specimen under a humidity other than a constant 100% would be obtained by subtracting the companion specimen's deformations from deformations of loaded specimens which have the same hygral treatment.

Deformations obtained from companion specimens would enable the determination of a value for the area factor, f_a, of non-load-bearing layers in concrete, as well as checking the value of the area factor, f_d, of the load-bearing layers. These deformations (Figs. 12 and 20) also assist in establishing the coefficient of hygral diffusivity C (see Appendix A).

(c) Specimens loaded under torsion.--The deformations which occurred during the period in which these specimens were under sustained loads are summarized in Figs. 21 and 22. These curves serve the evaluation of the rate of deviatoric creep parameter ψ, and in evaluating G_h.

2.6 EVALUATION OF TEST RESULTS

2.6.1 Effect of Moisture Condition at Time of Loading.--For modulus of elasticity E and shear modulus of elasticity G, the effect of humidity level at time of loading was negligible.

The creep test results indicate that, after 54 days under the same sustained compressive loading, the amount of creep of the specimen maintained at 100 R.H. is decreased by 45 percent in comparison with the creep of a similar specimen of equal maturity (t_{eq}) maintained at a humidity of 50%. This agrees with results obtained in references (12,15,28,35) which can be explained by the fact that the area factor of the load-bearing water, "adsorbed water", is smaller for a specimen at 50% R.H. than it is for a specimen at 100% R.H. In a specimen at

100% R.H. the load has a larger area on which to be distributed, than does the load in a 50% R.H. specimen (see Bazant, reference 46). In order to obtain a true picture of the effect of humidity, it should also be noted that both specimens should have their internal humidity fairly well stabilized.

For specimens loaded under uniaxial compression and of the same maturity it was observed, after 33 days of loading, that a specimen at 50% R.H. has creep deformation equal to 1.56 times the creep deformation of a specimen at 100% R.H. For torsional loading, the ratio is 2.02. It is believed that drying accelerates microcracking due to the tensile component of the torsion loading, thus the ratio of creep in torsion is higher than that of compression. Specimens at 100% R.H. were aged for 21 days at 100% R.H. and $73^{o}F$; specimens at 50% R.H. were aged for 18 days at 100% R.H. and $73^{o}F$. Added to this is the maturity gained during the period from 100% R.H. to 50% R.H., which was accomplished in 14 days. Thus, the 50% R.H. specimens were loaded at age 32 days but were assumed to have a maturity of 21 days at 100% R.H. and $73^{o}F$--i.e., $t_{eq} = 21$ days. Fig. 3-a depicts the maturity vs. relative humidity. As is demonstrated, no significant maturity is gained at a humidity below 80%. Discussions about maturity are presented in Section 1.4.

To demonstrate how moisture conditions have a pronounced effect on shrinkage and on creep results, especially on thin-walled specimens, the following data should be noted: after 50 days of drying at 50% R.H., shrinkage ε_s was 1500 microstrain (average of two specimens). After 104 days of drying at 50% R.H., shrinkage was also 1500 microstrain (one specimen). If we assume that shrinkage at 104 days is the maximum shrinkage, $\varepsilon_{s\infty}$, that can be achieved at a relative humidity of 50% for such a specimen (1/2-in. wall thickness, 1/4-in. diffusion path), then the ratio $\varepsilon_s/\varepsilon_{s\infty}$ at 50 days is 1.0. The volume to surface ratio, V/S, of these specimens is 1/4. In comparing this with the results obtained by Hansen and Mattock (34), after extrapolating their curves which are represented in this report in Fig. 1, we see that for V/S of 1, $\varepsilon_s/\varepsilon_{s\infty}$ is 0.55 and for a hypothetical value of V/S of 1/4, $\varepsilon_s/\varepsilon_{s\infty}$ is 0.65, while for V/S of 6, $\varepsilon_s/\varepsilon_{s\infty}$ is 0.10. It is obvious that the value of $\varepsilon_s/\varepsilon_{s\infty}$ obtained in this investigation is very high. However, this discrepancy can be partially attributed to the differences in the types of concrete used--i.e., Hansen used 3/4-in. gravel and a cement content of 5.44 sacks per cubic yard, while in this investigation the maximum aggregate was that which has a dimension equal to sieve No. 4 with 12 sacks of cement per cubic yard.

For this investigation on the other hand, the ratio for creep at 50 days under 50% R.H. was 0.83, while that found by Hansen was 0.68. This difference should be attributed to the effect of shrinkage on creep as well as differences in material properties.

2.6.2 Effect of Cyclic Humidity Condition.--This study was carried out to investigate the effect of a change in relative humidity from 100 to 50 to 100%.

A study of the results presented in Figs. 11 and 22 reveals the following:

(a) On exposure to 50% R.H., the specimens which were loaded at 100% R.H. exhibit a sharp increase in creep. This observation is in agreement with results obtained by Bertero (36) even though there is a slight difference in the method of hygral treatment and specimen size. Bertero's hygral treatment was done by blowing air at 60% R.H. on the specimens for 3 hours, while in this investigation specimens were left to dry in the control room at 50% R.H. Bertero's specimens had a wall thickness of 3/4 in.; specimens of this investigation have a wall thickness of 1/2 in.

For compression specimens, creep is defined as the deformation of the loaded specimen less the deformation of the unloaded companion specimen divided by the gage length (Fig. 23). In torsion specimens, creep is the torsional deformation of the loaded specimen per unit length (Fig. 22).

(b) The largest increase in creep occurred with the first change of humidity from 100 to 50% R.H. After that, the amount of increase per change decreased with the number of changes (one cycle = 2 changes, 50 to 100 and 100 to 50% R.H.). In fact, no significant increase was observed after the third change. This observation is also in agreement with results obtained by Bertero (36), Hansen (6,28) and L'Hermite (53).

(c) As shown in Fig. 20, shrinkage at 14 days was 1360 microstrain, while shrinkage at 30 days was only 1500 microstrain, and that at 104 days was also 1500 microstrain. If we assume shrinkage to be a parameter of stability of internal humidity, then the assumption that 14 days are enough to stabilize the internal humidity is justifiable.

In the case of sorbtion--i.e., 50% to 100% R.H. change, the time required to stabilize the humidity at 100% R.H. was shorter (5-6 days), as can be seen in Fig. 12. This is due to the effect of meniscus forces in the capillary water. Therefore, the duration of humidity cycles of 28 days was enough to stabilize the internal humidity of the specimen.

2.6.3 Effect of Type of Loading.--The amount of sustained stress was kept below the so-called linear limit, which is about 50% of compressive strength in a short term test. In these tests, the amount of sustained stress was 25% of compressive strength for compression specimens (900 psi) and 50% of torsion strength for torsion specimens (95 psi at extreme outer fiber), see Section 2.2. It is believed that in case of creep under torsion, the linear limit is of a shorter range than in the case of creep under uniaxial compression (36). The reason for this is the fact that strength in torsion is controlled by the tensile strength of concrete and that fracture occurs with little plastic deformation.

When creep curves of compressive loading were compared with the corresponding curves of torsional loading, it was observed that creep per spi under torsional loading is always higher than that under compressive loading. The ratio of torsion-creep to compression-creep ranges from 1.4 to 3.15 for a specimen under cyclic relative humidity. For constant 50% R.H. specimens the ratio was 2.8, and for constant 100% R.H. specimens it was 2.0.

If we take into account the fact that torsion specimens were under 40% of torsional strength and that compression specimens were under only 25% of compressive strength, and if we divide the torsional creep by 0.40 and the compressive creep by 0.25, we will find that creep under torsion is approximately equal to creep under compression when relative humidity of the specimens is about 100%. There is no literature available which compares torsion and compression creep at 100% R.H. Therefore, whether creep under torsion is equal to creep under compression or not is still unclear, and it needs more experimental investigation to prove or disprove it. When relative humidity is about 50%, torsion-creep is 1.75 to 2.00 times compression-creep. This observation is in agreement with earlier test results by Duke (24). Duke noted that "The numerical value of shear creep was in the order of twice the compressive creep that would have occurred under a compressive stress of the same magnitude as the applied shear stress." These observations can, however, be attributed to excessive and/or non-linear deformation--i.e., microcracking due to drying, which could have taken place while the torsion specimen was under 50% R.H.

2.6.4 Effect of Method of Measuring Deformations.--The deformations observed from using a dial gage represent an average value of surface deformation for the totality of gage length--i.e., specimen gage length under test.

Deformations obtained from an embedded strain gage represent the internal deformation of the body over the length of the strain gage itself. The Microdot strain gages used had an average length of one inch. Thus, it is expected that deformations measured with a dial gage would be more representative than those measured with an embedded strain gage.

In order to determine the torsional deformation from the embedded strain gages which were positioned at 45° to the axis of the specimen, an assumption must be introduced. This assumption is that creep under compression is equal to creep under tension.

If we let c = creep in the direction of the compression component of stress which always has a negative sign, and t = creep in the direction of the tensile component of stress which is always positive, then for every strain measurement, R_c, the difference between the given reading and a zero strain reading of a strain gage positioned in the direction of the compression component of stress--i.e., 45° to the axis of the specimen, we have:

$$R_c = c + \varepsilon_s$$

R_c here is always negative if we assume ε_s, which is drying shrinkage, to be negative.

Similarly, for every strain measurement, R_t, of a strain gage positioned in the direction of the tensile component of stress, we have:

$$R_t = t + \varepsilon_s$$

R_t can be negative or positive depending on the difference between t and ε_s.

Assuming that quantity of creep in tension to be equal to the quantity of creep in compression (t = -c), we obtain:

$$R_c = c + \varepsilon_s \tag{2.6.1}$$

$$R_t = -c + \varepsilon_s \tag{2.6.2}$$

Subtracting equation 2.6.2 from 2.6.1 we get:

$$c = \frac{R_c - R_t}{2} \tag{2.6.3}$$

and

$$\varepsilon_s = R_c - \frac{R_c - R_t}{2} \tag{2.6.4}$$

If we tabulate the readings of strain gages R_c and R_t, then, using equation 2.6.3 will yield creep of specimen while use of equation 2.6.4 will yield shrinkage of specimen.

It should be noted that the assumption of equal quantities of compression creep and tensile creep is not strictly correct, but it is acceptable on the engineering level (10). Strictly speaking, tensile creep is expected to be larger than compression creep due to microcracking.

Measurements obtained from torsion specimens, which were subjected to cyclic humidity, were analyzed according to equations 2.6.3 and 2.6.4. The results of shrinkage vs. time showed fair agreement with results obtained from unloaded specimens which underwent the same treatment Figs. 12 and 24 For creep results, c vs. time, it seems that creep obtained from this analysis follows qualitatively the creep behavior obtained by dial gages. As to the reliability of the c vs. time results, we have no other results for comparison purposes. Fig. 22 shows shear strain (by converting c) vs. time.

In general, from comparison of the results obtained with dial and strain gages, the following was observed:

(a) Elastic deformation.--For all compression specimens, the deformation given by a dial gage--i.e., one dial gage supported by an aluminum ring attached to the specimen by three pointed screws, was about 1.09 times the deformation given by embedded Microdot strain gages--i.e., average of two vertically embedded strain gages. In other words, the ratio of apparent creep measured in a section with a strain gage was about 92% of that measured in a section which has no strain gage. This percentage--i.e., 92%, is an acceptable one according to the calculations and discussion in Appendix B.

For torsion tests, the dial gage deformation (an average of two dial gages per specimen) was 2.44 times that of embedded strain gages (each specimen having an average of four embedded strain gages at 45^{o} to the axis of the specimen). However, this result could be attributed to the reinforcement offered by the strain gage.

(b) Creep deformation for specimens kept at a constant humidity.--For all these specimens, the deformation given by a dial gage was 1.1 to 1.5 times the deformation given by embedded gages.

(c) Creep deformation for specimens under cyclic humidity.--For compression specimens, the information obtained from the dial gage was much more consistent than that from the embedded strain gages. Fig. 23 shows the creep deformation (dial gage) vs. time after loading. The creep deformation given by embedded strain gages declined throughout the drying cycles. As yet, there is no reasonable explanation for this phenomenon.

For torsion specimens the dial gage deformations were also consistent. The embedded strain gage deformations, however, were less consistent and were always lower than those obtained by the dial gages. The ratio of the deformation of dial gages to the deformation from the strain gages was about 2:1. This can be partially explained by the fact that the strain gages reinforce the concrete section (Appendix B), but as yet there is no complete reasonable answer.

2.6.5 Effects of Humidity and Type of Loading on the Reversibility of Concrete Deformations.--A study of Fig. 12, which represents shrinkage vs. time, reveals that humidity cycles of 100 to 50% produce shrinkage in concrete having reversible and irreversible components. The first humidity cycle has the greatest effect. The ratio of the irreversible shrinkage to the total shrinkage of this cycle was 0.24, while for the second cycle it was about 0.10 and for the third, about 0.06. Plotting these values against the number of cycles (Fig. 25), it can be clearly noted that irreversible shrinkage may diminish at the fifth or sixth cycle. These observations seem to be in agreement with results obtained by other investigations. For example, Pickett (54) observed that the shrinkage from the first cycle of moisture change is greater than any subsequent expansion or shrinkage. Hansen (6,28) and L'Hermite (53) reported that after three cycles no irreversible shrinkage was observed.

Study of Fig. 23, indicating creep deformations vs. time under compressive loading and cyclic humidity, reveals that at 83 days after applying the load, the amount of creep under cyclic humidity was 1200 microstrain. Extrapolating from Fig. 23, the amount of creep recovery at 83 days after removing the load was 120 microstrains. Thus irreversible creep is about 90% of total creep at 83 days. It is expected that the irrecoverable creep due to increase in the modulus of elasticity, E, through aging is of small magnitude or small significance only because the ratio of E at 83 days to E at 21 days is about 1.2 for specimens kept at 100% R.H. all the time. Therefore, creep due to cyclic humidity is largely of a nonrecoverable nature.

For the specimen loaded in compression at 50% R.H. (Fig. 19), the amount of irreversible creep, 66 days after unloading, was about 75% of the creep after 66 days under load. For 100% R.H., the amount of irreversible creep, 54 days after unloading, was about 80% of the creep after 54 days under load.

For the specimens loaded in torsion at cyclic humidity (Fig. 22), the amount of irreversible creep was about 90% of the total creep. For the specimens at constant 50 and 100% R.H. the irreversible creep was about 65 and 95 percent, respectively.

In the case of specimens under constant humidity, irreversible creep is believed to be due to increase of modulus of elasticity of concrete, E, and microcracking of concrete. On the other hand, for specimens under cyclic humidity, it is believed that the large amount of irreversible creep is due to irreversible changes in the internal structure of the cement gel, which take place while it is undergoing change in humidity for the first time. Powers (15) states that "when the cement paste is dried for the first time, porosity diminishes only slightly while internal surface area diminishes considerably." This change of surface area is expected to affect the adsorbed water layers, thus changing the area factor of load-bearing layers.

2.6.6 Effect of Carbonation on Creep Results.--Carbonation shrinkage in hydrated portland cement is believed to be the result of dissolution of calcium hydroxide crystals while the crystals are under pressure. When a concrete member is under drying conditions, capillary water is in a state of hydrostatic tension while the rigid, solid part of hydrated cement, which includes calcium hydroxide crystals, is under counteracting compression. Carbonation does not cause shrinkage if it occurs when there is no pressure on the calcium hydroxide crystals; carbonation of other hydration products does not involve dissolution and therefore produces no shrinkage (55).

Powers (55) concluded that "if the internal humidity of a specimen remains at the saturation point, carbonation causes no shrinkage because the calcium hydroxide crystals are not under pressure while they dissolve. Carbonation of concrete specimens, while they remain saturated, or nearly so, eliminates all or most of carbonation shrinkage. In any event, carbonation offers more resistance to shrinkage force than does the calcium hydroxide that it replaced."

Verbeck (56) noted that intentional carbonation may improve the strength and hardness and reduce the permeability of concrete products. He presented information regarding experiments done on 1 by 1 by 11-in. mortar bars which were subjected to drying and carbonation with different carbon dioxide concentrations at 50% R.H. It was found that at a carbon dioxide concentration of 0.03 percent, which is the concentration at which carbon dioxide exists normally in a rural area or in a ventilated room, the length change during subsequent carbonation was only about 0.028 percent, as compared to about 0.103 percent when the carbon dioxide concentration is 100%.

Verbeck (56) also noted that the carbonation shrinkage which results from a specimen being dried and carbonated at the same time is less than the carbonation shrinkage which results when the same specimen is first dried (in a free carbon dioxide atmosphere) and then carbonated at a later time (simultaneous vs. subsequent crying and carbonation stages).

In the tests here reported, all specimens were cured in a fog room which has a relative humidity of 99-100% and which has a normal carbon dioxide concentration of about 0.03 percent. It is expected then that some carbonation took place for about 18 days during the period from the time of demolding the specimens until time of loading. For torsion specimens, subsequent carbonation or simultaneous carbonation and shrinkage should not have any effect, since carbonation shrinkage, like drying shrinkage, has only volumetric effects. Thus, the pure deviatoric deformation of creep under sustained torsion should not be affected by carbonation.

For compression specimens it is expected that the advantages of pre-carbonation (curing specimens in a fog room) and simultaneous drying-carbonation would reduce the effect of carbonation shrinkage to a minimum. Still, however, we should expect a small factor in all compression creep results to be due to carbonation shrinkage.

Conducting tests in a free carbon dioxide atmosphere would be the best solution to avoid carbonation shrinkage. Trials were carried out to prepare free carbon dioxide environmental cells which would have controlled humidity--i.e., constant 50% R.H. or constant 100% R.H., as well as cells in which the humidity would be changed from 50 to 100 to 50 percent R.H. To obtain a constant humidity, various saturated salt solutions such as $MgCl_2$ and NaCl were tried, but because of the large space required for housing the test specimen, they were ineffective. Although these cells were later improved by blowing into the cell a mixture of 21% oxygen and 79% nitrogen by volume, simulating air, but the control of humidity was still rather poor. At this stage it was concluded that the cost of equipment and labor to obtain environmental cells with controlled humidity and free of carbon dioxide would be unjustifiable compared to the minor effect that carbonation was expected to have on the test results of this investigation.

PART 2 - TESTS ON EFFECT OF BIAXIAL LOADING

2.7 OBJECTIVE

The objective of this phase of investigation was to examine the effect of sustained biaxial loading on the time-dependent behavior of concrete. The results were to be used in improving the creep predictions of the mathematical model by refining the creep rate parameter and the Poisson's ratio behavior under such loading.

2.8 SCOPE

Four groups of two specimens each were tested. All specimens were kept in the same room at 73°F and 50% R.H. The first group has two control specimens which were tested for modulus of elasticity, Poisson's ratio, and strength at 21 days. Specimens of the second group, called Group A, were sealed at age 21 days and has,no load applied to them. Specimens of Group B were sealed at age 21 days and loaded under a uniaxial compressive load. Specimens of Group C were also sealed at age 21 days, then loaded under equal biaxial compressive load. The amount of compressive loading was 25% of compressive strength. Each specimen was cast in the form of a hollow cylinder with a 5-in. I.D., 6-in. O.D. and length of 20 in. One type of concrete was used (see "Concrete Mix" in Section 2.3.1). All specimens were cured for 21 days at 73°F and 100% R.H.

2.9 CASTING AND INSTRUMENTATION

Specimens of this phase of the study were cast in the same manner as those described in Section 2.3.3. Likewise, the mold was similar to those described in Section 2.3.3, except that they were only 20-in. long,and that the inner shell was made of Plexiglass having a thickness of only 1/2 in. Each specimen was instrumented with four Microdot strain gages--two sets of two gages at 180° apart, one positioned parallel and the other perpendicular to the axis of the specimen. The method of positioning these gages was the same as was described in Section 2.3.3. Three specimens, one in each group, were further instrumented with one Carlson strain meter. These Carlson meters were used over the entire length of the specimen. See Fig. 26 for details. The ends of all specimens were trimmed at age 14 days by means of a diamond rotary saw,as previously described for compression specimens.

2.10 SEALING AND LOADING

Each specimen was sealed in a 1/8-in. thick neoprene rubber sleeve. Lead-out wires of embedded Microdot gages penetrated through the sleeve's wall and were sealed with silicone rubber. At the ends of the specimen, the sleeves were fastened with metal clamps to 1-in. thick stainless steel discs (Fig. 26). Calculations and experimental trials proved that no significant water loss from the concrete would occur during a test period of six months. The use of neoprene rubber sleeves was preferred over other types of sealing because this method has no side effects such as restraining the specimen's movement or affecting the distribution of stresses.

Loading of specimens of Group B, which were under uniaxial compression, was accomplished in the same way as described in Section 2.4.4. However, the perforated steel sleeve was eliminated because it was not needed for sealed specimens. The top loading plate was solid--i.e., no concentric hole.

Loading of specimens of Group C which were under equal biaxial compressive stresses was accomplished by means of a pressure vessel and a loading cell. As shown in Fig. 27, the specimen was loaded uniaxially by constraining it between the top flange and the loading cell. The circumferential pressure was supplied by a separate hydraulic system through the wall of the vessel. The loading procedure was as follows: the axial pressure was applied first, all readings taken, and then the circumferential pressure was applied with oil under hydraulic pressure, and readings again taken. This last reading was considered as a zero reading for creep deformations. The loading procedure took about three minutes for a crew of three persons to complete; this included readings.

2.11 TEST RESULTS AND THEIR EVALUATION

Results of tests on control specimens are shown in Table 4. Average strength was 3650 psi, average modulus of elasticity was 3.3×10^6 psi, and average Poisson's ratio was 0.17. Results obtained from Group A, two specimens for which there was no load, showed no significant deformations (1 microstrain per week). This shows that swelling due to progressive hydration, and shrinkage due to self-desiccation of a sealed specimen, cancel each other.

Creep results are shown in Fig. 28. The lower curve in Fig. 28 gives creep deformations, average of two specimens, of Group B which was loaded under uniaxial compressive loading. The upper curve, in Fig. 28, gives creep deformations, average of two specimens, of Group C which was under equal compressive loading.

Deformations obtained by using Carlson strain meters, were slightly higher than those obtained by using Microdot embedded strain gages. This is believed to be due to the reinforcement offered by the embedded strain gage, to the section of specimen.

The specimens loaded under uniaxial compression (Group A), showed axial deformations which compare very well with those obtained on specimens which were under uniaxial compressive loading and 100% R.H. (Sections 2.6.1 and 2.6.3). The ratio of a sealed specimen's creep to that of one under 100% R.H., at 54 days after loading, was 1.05.

From lateral deformation, we observe that creep Poisson's ratio is zero. This is in agreement with the conclusion reached by Ross (11).

It can be noted from studying Fig. 28, that the equal biaxial loading produced equal deformations in both directions, which indicates isotropy of concrete at the macroscopical level.

Creep deformation of a specimen under biaxial compressive loading, after deducting elastic Poisson's ratio and assuming creep Poisson's ratio to be zero (see above), was about 0.80 of creep of a specimen under uniaxial compressive loading at 54 days after loading. Comparing these observations with results found by other investigators, it can be seen that they are in agreement with Duke's results (24), which showed that creep under uniaxial loading would be reduced if the specimen is subjected to triaxial loading. Gopolakrishnan (39) and Jordaan (38) gave nearly similar conclusions.

From Fig. 28, we note that 50 days after unloading the specimens of Group B, irreversible creep was about 75% of the total creep obtained 50 days after loading. For Group C, which was under equal biaxial compressive loading, irreversible creep was about 75% of the total creep at 50 days after loading. Considering the effect of self-desiccation of sealed specimens, we see that this result is in reasonable agreement with results found in Section 2.6.5 for specimens at 50 or 100% R.H., for which the ratio was 75 to 80%.

2.12 OBSERVATIONS BASED ON RESULTS OF EXPERIMENTAL PROGRAM

From the results presented in Section 2.5, and discussed in Section 2.6, and results of Section 2.11, the following observations can be made:

1. For concrete cured at 100% R.H., the increase in modulus of elasticity, E, in the period 21 to 160 days, is very small compared to the value of the modulus of elasticity itself at 21 days.

2. There is no appreciable difference between the modulus of elasticity of a specimen which has an internal humidity of 50% throughout its entire cross-section, and the modulus of elasticity of similar specimens but with an internal humidity of 100% throughout.

3. Results on elastic Poisson's ratio were inconsistent, but, for the purpose of this study, it will be assumed to be constant with a value of 0.17.

4. Shrinkage of concrete specimens subjected to humidity cycles of 100 to 50 to 100%, is generally of a recoverable nature. Furthermore, shrinkage and swelling become totally recoverable after three humidity cycles.

5. The creep of a specimen in compression or torsion, kept at a constant humidity of 50%, was generally higher than that of a specimen maintained at a humidity of 100%. However, since creep at 100% R.H. has a small magnitude, and, since it is expected that some shrinkage is still taking place, especially on the inner part of the cross section (i.e., the specimen surfaces may have the same humidity as the environment, namely, 50%, while the central section of the specimen's wall thickness is still asymptotically approaching a humidity of 50%), some shrinkage and effect of shrinkage on creep could have been incorporated in the creep results. Therefore, more elaborate and extensive experimentation is needed to confirm or deny this issue. For the purpose of this study, the results presented in Section 2.5 will be assumed valid--i.e., creep at 50% R.H. is higher in magnitude than creep at 100% R.H.

6. Creep increase of specimens subjected to humidity cycles of 100 to 50 to 100% is generally of an irrecoverable nature. For both types of specimens under uniaxial compression or torsional loading, creep is sharply increased by the first humidity change--i.e., 100 to 50% R.H. At the end of the first drying period, the magnitude of creep of a specimen under uniaxial compression and changing humidity was 7 times the magnitude of creep of a specimen under the same loading and 50% R.H., and it was 13 times the magnitude of creep of a specimen under the same loading but at 100% R.H.

For torsional loading, at the end of the first drying period, the creep obtained from a specimen subjected to a changing humidity, 100 to 50%, was 4 times that of a specimen under constant 50% R.H., and 6 times that of a specimen under constant 100% R.H. and same loading. Subsequent humidity changes have very little effect on creep, and after three humidity changes, they become negligible.

7. No clear observation can be drawn on the difference between creep under sustained compressive loading and creep under sustained torsional loading.

8. For sealed specimens, creep under equal sustained biaxial compressive loading was about 0.80 that of a specimen under uniaxial compressive loading. Also, it was observed that equal biaxial loading produced equal deformations in both directions. This indicates isotropy of concrete at the macroscopical level.

9. It should be recognized that the effects of humidity on the creep of concrete have been magnified in the tests of this investigation, because of the choice of specimen dimensions and because of the rate of humidity change to which these specimens were subjected. An ordinary structural member--e.g., a beam or a column, usually has a very high volume/surface ratio compared to the specimens of this investigation. Therefore, the humidity distribution patterns of an ordinary structural member is greatly different from those of the tested specimens. In a column 6 in. in diameter, for example, the humidity gradient will be much smaller than for the specimens in the same environment. Hence, the effect of humidity change on the creep of the member is expected to be less than the effect of this same change on the creep of the tested specimens as observed in 6. above.

10. In a structural element, the period required to change the humidity throughout the member is very much longer than that required to change the humidity in the tested specimens. In the tested specimen, a period of 14 days was enough to change the humidity throughout the specimen from 100 to 50 $\pm$ 3% R.H. In a structural member, for example, a column 6 in. in diameter, the period required to produce the same change is about 3 years, Hansen (57). Since typical environmental conditions do not endure for such long periods of time, it is believed that structural members will never be able to be fully dry except if the environment's humidity is always a constant low humidity. Typical environmental humidity changes every few months, and usually there is at least one change per year. Since a structural member starts drying at a certain time in the year, then, after a few months the humidity will be reversed. Hence, it starts gaining moisture until the humidity is reversed back again, after another few months, then the member starts drying again, and so forth. It appears, then, that no structural member will be strictly under constant humidity unless it is permanently under water or is extremely bulky such as in the case of a dam.

In such a case, humidity changes at the surface have negligible effects. Thus, it can be deduced that typical environments submit ordinary structural members (beams, columns, slabs, etc.) to continuous humidity changes, i.e.

continuous moisture migration in or out of the member. The effect of this continuous humidity change is to set the rate of the creep of the structural member at a value between that of the creep of the first drying and that of the creep at 100% R.H.

CHAPTER 3

MATHEMATICAL MODEL, PREDICTIONS AND COMPARISONS

3.1 INTRODUCTION

A mathematical model represents an equation or set of equations which consists of what is conventionally known as the constitutive equation, as well as parameters and functions representing the properties of material for which the mathematical model is being constructed. In this study, the constitutive equations are given by equations 1.4.1 and 1.4.2. In order to obtain a mathematical model, which will be able to obtain a solution for a given problem, it is essential to determine expressions for the terms which represent the material properties--i.e., K, G, f_d, f_a, S_h, K_h, G_h, and C.

As it was mentioned earlier in Section 1.4, the best solution for the constitutive equations 1.4.1 and 1.4.2 is a numerical solution. Bazant (45) suggested a numerical procedure which may proceed as follows:

1. Present the constitutive equations 1.4.1 and 1.4.2 in a numerical form as follows:

For a given subdivision t_o, t_1, ..., t_n of time t, introduce subintervals $t = t_r - t_{r-1}$ and examine $\Delta\varepsilon$, e_{ij}, $\Delta\sigma$, S_{ij}, $\Delta\sigma_d$, $S_{d_{ij}}$ during Δt. The finite difference form of the constitutive equations is,

$$\Delta\varepsilon = \frac{\Delta\sigma}{K} + \Delta\varepsilon'' \tag{3.1.1}$$

$$\Delta e_{ij} = \frac{\Delta S_{ij}}{2G} + \Delta e''_{ij} \qquad (i,j = 1,2,3) \tag{3.1.2}$$

where

$$\Delta\varepsilon'' = \Delta\varepsilon' - \frac{\Delta\sigma_a}{K} \tag{3.1.3}$$

$$\Delta\varepsilon' = \Delta t \cdot \phi(\sigma_d - \sigma_{ad}) - \sigma_d \frac{\Delta h_{eq}}{K_h} \tag{3.1.4}$$

$$\Delta\sigma_d = \nu(\Delta\sigma - \Delta\sigma_a) - K_c(\Delta\varepsilon') \tag{3.1.5}$$

$$\Delta e''_{ij} = \Delta e'_{ij} = \frac{1}{2} \cdot \Delta t \cdot \psi \cdot S_{d_{ij}} - S_{d_{ij}} \frac{\Delta h_{eq}}{2\ G_h} \tag{3.1.6}$$

$$\Delta S_{d_{ij}} = \nu' \cdot \Delta S_{ij} - 2G_c \cdot \Delta e'_{ij} \tag{3.1.7}$$

Here it is clear that the terms which represent material properties are K, G, ϕ, ψ, K_h, and G_h while the terms $\Delta\varepsilon$, $\Delta\sigma$, $\Delta\varepsilon''$, Δe_{ij}, ΔS_{ij}, $\Delta e''_{ij}$, $\Delta\varepsilon'$, $\Delta\sigma_a$, $\Delta\sigma_d$, ν, ν', $\Delta S_{d_{ij}}$ are parasitical terms--i.e., once the material properties are given, these terms can be determined utilizing the constitutive equation. The term Δh_{eq} will be found by solving the diffusion problem inside the concrete body for time interval Δt.

2. Given the initial values of h and T at t_o, calculate h_{eq}, t_{eq}, and h_s according to their definition in equations 1.4.8, 1.4.9 and A.7, respectively. Then calculate $\sigma_d = f_d \times 1360 \times S_h(h_s - h)(1 + h_{eq})$. (Notice that $\frac{T}{T_o} = 1$ and $(\frac{T}{T_o} - 1) = 0$ in the expression of σ_{ad} in Section 1.4, because T = T for this analysis); f_d and S_h are to be determined in Section 3.6. Then calculate $\Delta\sigma_a = \frac{f_a}{f_d} \cdot \Delta\sigma_d$ (f_a is to be determined in Section 3.5).

3. Calculate K_b, K_c, K_d, K, ν, G_b, G_c, G_d, G and ν' according to their expressions (to be determined in Section 3.4).

4. Given σ and S_{ij} which are applied stresses where $\sigma = \frac{1}{3}(\sigma_{11} + \sigma_{22} + \sigma_{33})$, volumetric stress and $\sigma_{ij} = \sigma + S_{ij}$, stress tensor determine the volumetric and deviatoric components σ_d and $S_{d_{ij}}$ of the initial values in step Δt, equation 3.1.5. ($\Delta\varepsilon'$ = as an initial value).

5. Calculate the values of ϕ and ψ according to their expressions (to be determined in Section 3.6).

6. Given changes in humidity Δh, calculate K_h and G_h according to their expressions (to be determined in Section 3.7).

Solve the moisture diffusion problem inside concrete body for step time Δt because the humidity changes are usually given at the surface of the concrete body--i.e., environmental humidity changes. This problem of diffusion is solved by a finite difference scheme for the partial differential equation governing this problem which is presented in Appendix A. This solution is carried out in the computer program Appendix C in Section 9.

7. According to equations 3.1.4, 3.1.5, 3.1.6 and 3.1.7, calculate $\Delta\varepsilon'$ and $\Delta e'_{ij}$. (Note that this process involves 2 to 4 iterations,

Bazant (45).) Calculate $\Delta\varepsilon''$ according to equation 3.1.3 and $\Delta e''_{ij} = \Delta e'_{ij}$ from equation 3.1.6.

8. Assuming that in the given problem, the values of σ_d, $S_{d_{ij}}$, σ, ε, S_{ij}, e_{ij} have already been calculated up to the time t_{r-1} (or have been given at this time if $t_{r-1} = t_o$) together with the values $\Delta\varepsilon''$ and $\Delta e''_{ij}$ as outlined above in 1 to 7, then equations 3.1.1 and 3.1.2 may be formally regarded as A FICTITIOUS INCREMENTAL ELASTIC STRESS - STRAIN LAW WITH PRESCRIBED INCREMENTAL INITIAL STRAINS $\Delta\varepsilon''$ AND $\Delta''e_{ij}$. The calculations of $\Delta\sigma$, $\Delta\varepsilon$, ΔS_{ij}, Δe_{ij} for the given load increments and given boundary displacement increments is, therefore, A Problem of Elasticity. This problem can then be solved by the finite element method for the given body. In the case of a creep test for a specimen under constant load, $\Delta\sigma = \Delta S_{ij} = 0$. In the case of a relaxation test for a specimen under a constant deformation, $\Delta\varepsilon = \Delta e_{ij} = 0$.

9. For a creep problem, at the end of one process like that above (1 to 8), the increment in creep strain $\Delta\varepsilon$ and Δe_{ij} will be determined for the given Δt--i.e., at $t_o + \Delta t = t_1$. For a relaxation problem, $\Delta\sigma$ and ΔS_{ij} will be determined, instead of $\Delta\varepsilon$ and Δe_{ij}, at t_1. For the solution of the first time step, notice that the elastic stresses and strains represent the initial values of σ, S_{ij}, ε, e_{ij}.

Suppose that the problem is a creep problem and assume that t = 2 days, for example; then creep strain after 2 days from loading will be $(\varepsilon + \Delta\varepsilon)$ for volumetric strain and $(e_{ij} + \Delta e_{ij})$ for deviatoric strain (ε and e_{ij} are given initial values). Notice that creep strain $\Delta\varepsilon_{ij}$ is $\Delta\varepsilon_{ij} = \Delta\varepsilon + \Delta e_{ij}$ where

$\Delta\varepsilon = \dfrac{\Delta\varepsilon_{11} + \Delta\varepsilon_{22} + \Delta\varepsilon_{33}}{3}$; ε_{11}, ε_{22} and ε_{33} are principal strains.

For the next time step, the values calculated in the above step will be used as initial values and the same procedure should be carried out to compute $\Delta\varepsilon$, Δe_{ij} at the end of next Δt.

The use of the bulk modulus of elasticity K is adopted rather than the use of the modulus of elasticity E. The use of K is more convenient in the calculations than the use of E, especially for the computation of stresses and strains due to shrinkage, which is a pure volumetric process. Hence the use of volumetric and deviatoric components of stresses and strains is adopted in the constitutive equations.

It can be concluded that if material properties are given as expressions of K_b, K_c, K_d, G_c, G_d, f_d, f_a, ϕ, ψ, K_h, G_h and C, the creep problem can be solved by utilizing the constitutive equations, 3.1.1 and 3.1.2, as demonstrated above for any type of loading and any environmental condition--hence, the advantages of these constitutive equations. The size effect, rate of drying, shape of concrete member, type of load, etc., are all included in the solution of any creep problem according to the above procedure because of the nature of the constitutive equations and the nature of the procedure to be followed for the solution of such equations.

All solutions of the constitutive equations according to the above procedure were carried out using a computer program which is capable of solving this problem for any axisymmetric body. This computer program is presented in Appendix C.

3.2 OBJECTIVE

As pointed out in Section 1.6, the objective of this phase of investigation is to evaluate parameters and functions which are necessary for the prediction of the time-dependent behavior of concrete. These parameters and functions are the moduli of elasticity of the rheological model shown in Fig. 2, f_d, f_a, S_h, ϕ, ψ, K_h and G_h, all of which are discussed in Section 1.4.

3.3 SCOPE

As already discussed in Section 1.7, the evaluation of different terms mentioned above is restricted to the type of concrete used in the experimental program presented in Chapter 2. Validity of these terms is, therefore, limited to the scope of the experimental program--i.e., constant temperature of 73°F, humidity range of 50 to 100% and compressive or torsional loading.

3.4 MODULI OF ELASTICITY

The definition of the bulk modulus of elasticity K, for the model shown in Fig. 2 is: the ratio of applied volumetric (hydrostatic) stress to the volumetric strain (unit volumetric change), thus

$$K = \frac{\sigma_v}{(\varepsilon_1 + \varepsilon_2 + \varepsilon_3)} \tag{3.4.1}$$

where $(\varepsilon_1 + \varepsilon_2 + \varepsilon_3) = \frac{\Delta V}{V}$, ΔV is volume change

ε_1, ε_2 and ε_3 are principal strains, and

and $$\sigma_v = \frac{\sigma_1 + \sigma_2 + \sigma_3}{3},$$ where σ_1, σ_2 and σ_3 are principal stresses.

This definition of K applies also to K_b, K_c and K_d which are the bulk moduli of elasticity of spring b, spring c and diffusion element d, respectively.

From Fig. 2:

$$K = [K_b^{-1} + (K_c + K_d)^{-1}]^{-1} . \tag{3.4.2}$$

The bulk modulus of elasticity K relates to the modulus of elasticity E as follows,

$$K = \frac{E}{1 - 2\mu}$$ where μ is Poisson's ratio,

also

$$K_b = \frac{E_b}{1 - 2\mu_b},\ K_c = \frac{E_c}{1 - 2\mu_c} \text{ and } K_d = \frac{E_d}{1 - 2\mu_d} . \tag{3.4.3}$$

The relation between modulus of elasticity E and shear modulus of elasticity G, is given by:

$$G = \frac{E}{2(1 + \mu)},$$ also

$$G_b = \frac{E_b}{2(1 + \mu_b)},\ G_c = \frac{E_c}{2(1 + \mu_c)} \text{ and } G_d = \frac{E_d}{2(1 + \mu_d)} . \tag{3.4.4}$$

From equations 3.4.3 and 3.4.4, keeping similar subscripts together; i.e., G and K, G_b and K_b, G_c and K_c, and G_d and K_d, and solving for μ's, we get:

$$\left.\begin{aligned} \mu &= \frac{K/2 - G}{K + G} \\ \mu_b &= \frac{K_b/2 - G_b}{K_b + G_b} \\ \mu_c &= \frac{K_c/2 - G_c}{K_c + G_c} \\ \text{and} \quad \mu_d &= \frac{K_d/2 - G_d}{K_d + G_d} \end{aligned}\right\} \tag{3.4.5}$$

$$\left.\begin{aligned}\frac{G_b}{K_b} &= \frac{\frac{1}{2} - \mu_b}{1 + \mu_b} \\ \frac{G_c}{K_c} &= \frac{\frac{1}{2} - \mu_c}{1 + \mu_c} \\ \frac{G_d}{K_d} &= \frac{\frac{1}{2} - \mu_d}{1 + \mu_d}\end{aligned}\right\} \qquad (3.4.6)$$

The experimental results of E and μ shown in Fig. 16 were used to evaluate K by utilizing the first of equation 3.4.3. These K values are presented in Fig. 29. Poisson's ratio, μ, was assumed to be a constant equal to 0.17 (see Section 2.12 for conclusions on Poisson's ratio).

Since K_b is the bulk modulus of elasticity of spring b in Fig. 2, and the characteristics of spring b continually change due to progressive hydration, then K_b is a function of equivalent curing time t_{eq}. The term t_{eq} is a parameter for hydration (see Section 1.4).

The characteristics of the diffusion unit; i.e., elements c and d, under isothermal conditions, is affected by both humidity and hydration. The characteristics of element d are related to the compressibility of the diffusible load-bearing water layers. The behavior of the diffusible load-bearing layers is governed by humidity (see Section 1.4). On the other hand, element c represents the elastic solid part of cement paste or concrete visualized as being connected in parallel with element d. The characteristics of element c are also dependent on hydration but do not necessarily have the same degree of dependence as K_b. Therefore, it is justified to assume K_c to be a function of t_{eq} only and K_d as a function of h_{eq} only. To summarize:

$$K_b = f_1(t_{eq})$$
$$K_c = f_2(t_{eq})$$
$$K_d = f_3(h_{eq}) .$$

K is known to decrease only slightly at drying (58,59,60). The following table was extracted from Plowman's work (60) for concrete with w/c ratio of 0.55 and using a Poisson's ratio of 0.17 for calculating K and G from given experimental E values.

Maturity* °F x hrs	E, from Table I Plowman (61)			Calculated K, by eq. 3.4.3 with $\mu = 0.17$			Calculated G, by eq. 3.4.4 with $\mu = 0.17$		
	Curing, 64°F and			Curing, 64°F and			Curing, 64°F and		
	Water	Air 90% RH	Air 65% RH	Water	Air 90% RH	Air 65% RH	Water	Air 90% RH	Air 65% RH
3,800	4.34	4.41	4.75	6.77	6.90	7.41	1.84	1.87	2.01
8,900	4.82	4.82	4.78	7.56	7.56	7.47	2.04	2.04	2.02
17,800	5.00	4.89	5.07	7.80	7.64	7.91	2.13	2.08	2.16
26,700	5.07	5.03	5.12	7.90	7.85	8.00	2.15	2.13	2.17
35,600	5.28	5.13	5.16	8.25	8.02	8.06	2.23	2.17	2.18
115,700	5.68	5.26	5.10	8.86	8.21	7.96	2.40	2.23	2.17
230,130	5.85	5.53	5.21	9.14	8.64	8.15	2.48	2.34	2.20
455,190	5.92	6.91	5.05	9.24	10.80	7.90	2.51	2.92	2.14

*Maturity = (Temperature in °F of concrete - 11°) x time in hours.

From the experimental program of this investigation, it was noticeable from Fig. 29-a and b that the effect of humidity on K is even less than that shown in the above table. At t_{eq} = 21 days, K of h = 1.00 was approximately equal to K of h = 0.50. From the above table, and for a maturity of 26,700°F x hr., which is equal to curing of 21 days at 64°F, K for h = 1.00 is 7.90 while K for h = 0.65 is 8.00.

Fig. 17-a and b show that at 21 days, G with h = 1.00 is approximately equal to, or less than, G at 21 days with h = 0.50. From the above table, at maturity of (26,700)°F x hrs., G at h = 1.00 was 2.15, and when h = 0.65, it was 2.17.

From the above observations, it can be concluded that K_d must be rather high compared to K_c in equation 3.4.2 in order to produce such minor dependence of K on K_d.

Suppose an average value of K_c of 1.0×10^6 psi is used, then K_d is expected to be $(80.0 \text{ to } 100.0) \times 10^6$ psi in order to produce such low dependence on humidity. Examination of equation 3.4.2 would reveal that such values of K_d will make the value of K highly dependent on the value of K_b; e.g., if $K_c = 1.0 \times 10^6$,

$K_d = 99.0 \times 10^6$, then equation 3.4.2 gives: $K = \frac{1}{(1/K_b) + (1/100)} \times 10^6$. Therefore, K is approximately equal to K_b. The same deductions can be made for shear modulus of elasticity (G); i.e., G is approximately equal to G_b.

At greater maturity (t_{eq} = 200 days or more), the change of K with humidity is negligible; therefore, we may assume $K_d \to \infty$, $G_d \to \infty$, and K can be safely approximated as $K = K_b$, and $G = G_b$. It is apparent that K_c and/or K_d have only a slight effect on elastic properties of concrete which are represented by K. Likewise, G_c and/or G_d have only a slight effect on elastic properties of concrete which are represented by G. However, K_c has also a significant effect on the time-dependent volumetric deformations of concrete because the change in thickness of the diffusible load-bearing layer; i.e., change in the thickness of element d (Fig. 2) affects the rate of change with time of stress in the diffusible load-bearing layer itself; that is to say, K_c affects the term $\dot{\sigma}_d$ in equation 1.4.5. However, K_b and K_d have no effect on the time-dependent deformation other than being components of K. Also, G_c has the same effect on time-dependent deviatoric deformations as K_c has on the time-dependent volumetric deformations. G_c affects the term $\dot{S}_{d_{ij}}$ in equation 1.4.6.

The derivation of K_b, K_c, K_d, G_b, G_c, and G_d then proceeded according to the following:

1. Guided by the previous discussions, a value was given to K_b and K_c at t_{eq} = 21 days (21 days was chosen because this value of K was obtained from average of six tests), and a value for K_d with h = 1.0, such that calculated K, equation 3.4.2, is equal to experimental K at 21 days with a humidity of 100% (Fig. 29), which was extracted from experimental E values (Fig. 16) with Poisson's ratio equal to 0.17.

2. With some increase in K_b and K_c, and for the same K_d, another K was calculated for t_{eq} = 150 days. This increase in K_b and K_c made calculated K equal to experimental K at 150 days for a humidity of 100% (150 days was chosen because 150 days was the highest t_{eq} value of experimental data available based on an average of three tests).

The estimated value of K_b when t_{eq} = 21 days was 6.4 and when t_{eq} = 150 days was 7.0. Values of K_c were estimated at

1.3 when $t_{eq} = 21$ days and 2.4 when $t_{eq} = 150$ days respectively. Using these two values of K_b and K_c, the curves labeled "first trial" in Fig. 30-a and b were then obtained.

Since K_c affects the time-dependent deformations directly, K_c was examined by comparing the creep predicted from "first trial" K_c with experimental creep data (see Section 3.5). From this it was found that with minor changes of K_c, better results would be obtained. K_c was then modified in such a way as to make creep predictions as close as possible to the experimental data (see Fig. 30-b for modifications.)

Using modified K_c with the experimental values of K, (Fig. 29) and assumed K_d values at 100% R.H., K_b was redetermined. This new K_b was called modified K_b (see Fig. 30-a). The modification of K_c to obtain creep results as close as possible to experimental creep data was a matter of trial and error. For each time a K_b or a K_c curve was assumed or redetermined, the curve was first fitted by the least squares method to produce a mathematical expression convenient for use in a digital computer. Then the expression was examined to check whether or not it satisfied the necessary conditions. If it satisfied the conditions, it was accepted, and if it did not, it was modified, refitted by the least squares method, and examined again for satisfaction of the conditions. The least squares method used was similar in procedure to the one explained by Conway (61), p. 44. This procedure was executed with the help of the "Symbolic Matrix Interpretive System" (SMIS), programmed by E. L. Wilson (62).

The final trial curves of K_b and K_c have the following expressions:

$$K_b = (7.2 - 20.4/t_{eq} + 59.0/t_{eq}^2) \times 10^6 \qquad (3.4.7)$$

and

$$K_c = (2.9 - 50.0/t_{eq} + 221.0/t_{eq}^2) \times 10^6 . \qquad (3.4.8)$$

3. Since K increased only slightly with a lower humidity level at the time of testing (see previous discussion), it is expected that a linear relationship between K_d and h would be sufficient for such a K change with h. Actually, even a constant value of K_d might be acceptable. However, it was found more efficient as far as calculations were concerned to represent K_d in the following form:

$$K_d = a(b + h) \times 10^6.$$

To evaluate a and b, the values of K_d at h = 1.0 and at h = 0.5 were determined from experimental values of K at t_{eq} = 21 days with h = 1.0 and h = 0.5 respectively, with values of K_b and K_c at t_{eq} = 21 days, which are independent of h. From these two values of k_d, it was found that a = 85.2 and b = 0.05; therefore,

$$K_d = 85.2(0.05 + h) \times 10^6 . \qquad (3.4.9)$$

4. For element d, whose elastic properties depend on the compressibility of diffusible water layers, no lateral deformation was expected in such layers if they were uniaxially loaded. Hence, Poisson's ratio of this element is zero, i.e., $\mu_d = 0$. This implies, according to equation 3.4.6, that $\frac{G_d}{K_d} = 0.5$.

5. Using $\mu_b = 0.17$ and $\mu_c = 0.17$, then $\frac{G_b}{K_b} = 0.28$ and $\frac{G_c}{K_c} = 0.28$. G was calculated, and it was found that slight modifications were needed to make this calculated G consistent with G values found experimentally. Since G_b affects G directly (in the same way that K_b affects K) and G_c affects G only indirectly after being combined with G_d, which has a relatively high value (G_d/G_c about 100), it was decided to change G_b rather than G_c. With the experimental values of G (Fig. 17-a) and with values of $G_c = 0.28\ K_c$ and $G_d = 0.5\ K_d$ with the expressions of K_c and K_d as given by equations 3.4.8 and 3.4.9 respectively, a G_b vs time curve was determined for h = 1.00. This curve was fitted by the least squares method to a suitable expression, then the G values were recalculated and found to be very close to the experimental values (see the solid line in Fig. 17-a). This G_b expression was,

$$G_b = (2.3 - 15.0/t_{eq} + 50.0/t_{eq}^2) \times 10^6 . \qquad (3.4.10)$$

<u>Summary of Section 3.4</u>

Guided by previous knowledge about effects of humidity on the modulus of elasticity E, and studying the relationship between E and K as well as between E and G, and studying the behavior of the rheological model (Fig. 2) it was concluded that K_d has a relatively high value compared to K_c or K_b. Using experimental values of K with Poisson's ratio equal to 0.17 and by the trial and error procedure, the expressions 3.4.7, 3.4.8 and 3.4.9 were determined. Predictions of K according to these expressions were in good agreement with the experimental results (see Fig. 29).

Using a value of $\frac{G_d}{K_d} = 0.50$ and a value of $\frac{G_c}{K_c} = 0.28$, a G_b expression was deduced, expression 3.4.10, which will make calculated values of G consistent with experimental results (see Fig. 17).

3.5 DETERMINATION OF CREEP RATE PARAMETERS, ϕ AND ψ

By definition, ϕ is the rate of volumetric creep parameter, and ψ is the rate of deviatoric creep parameter. From equation 1.4.4 it can be seen that for a constant equivalent humidity ($\dot{h}_{eq} = 0$), $\varepsilon' = \phi(\sigma_d - \sigma_{ad})$, where ε' is volumetric creep strain and $\sigma_d - \sigma_{ad}$ represents the difference between the existing stresses over a unit cross-section due to pressure in the diffusible load-bearing layers and its equilibrium value for a given humidity and temperature, i.e., thermodynamic equilibrium. This difference $(\sigma_d - \sigma_{ad})$ is the determining factor for creep at a constant humidity. Let $\sigma' = \sigma_d - \sigma_{ad}$, then:

$$\phi = \frac{\varepsilon'}{\sigma'} .$$

Also, for $\dot{h}_{eq} = 0$, equation 1.4.6 gives:

$$\psi = \frac{2e'_{ij}}{S_{d_{ij}}} .$$

Therefore, the derivation of σ and ψ will be based on experimental creep data obtained from specimens which have no moisture movement such as those results presented in Figs. 19 and 21, so that $\dot{h}_{eq} = 0$.

ϕ is expected to be a function of humidity or h_{eq} and a function of time after load application. Since the difference between creep at a constant humidity of 50% and creep at a constant humidity of 100% is only a slight one (as found by experimental results presented in Fig. 19), then for convenience ϕ should be used either as a constant or as a linear function of humidity. If ϕ is assumed to be constant with humidity change, then creep at a constant humidity of 0% will be equal to creep at a constant humidity of 100%, a case which could prove to be true later (see discussion in Section 2.12).

For this study, however, since creep at a constant humidity of 50% is observed to be higher than that at a constant humidity of 100%, a linear relationship between ϕ and humidity will be assumed rather than assuming ϕ as constant with humidity change.

After several trials, the following expressions were found suitable:

$$\phi = 21.3 \times 10^{-9}(0.9 - 0.4\ h_{eq})(\frac{t + 500.0}{t + 1.0})\ \text{psi/day} \qquad (3.5.1)$$

and

$$\psi = 14.2 \times 10^{-8}(1.5 - h_{eq})(\frac{t + 500.0}{t + 1.0})\ \text{psi/day} \qquad (3.5.2)$$

where t is time in days after application of load.

Using values of moduli of elasticity as derived in Section 3.4 and a value of $f_d = 0.0375$ (see Section 3.6 below), and following the procedure outlined in Section 3.1 by utilizing the computer program (Appendix C), creep strains were calculated for uniaxial compressive and torsional loadings. Loads used in these calculations were of the same magnitude as those used in the experiments, namely, 25% of compressive strength for uniaxial compressive loading and 40% of torsional strength for torsional loading. The calculated creep strains are in good agreement with the experimental results which were discussed in Section 2.5.2. Fig. 31 shows the experimental and calculated results, according to expressions 3.5.1 and 3.5.2 above, for a specimen loaded under uniaxial compression, while Fig. 32 shows experimental and calculated results according to the same expressions but for a specimen under torsional loading.

It should be recognized here that both ϕ and ψ affect the creep of a specimen loaded under a uniaxial compressive loading while only ψ affects the creep of a specimen under a torsional load*.

3.6 DETERMINATION OF AREA FACTORS f_d AND f_a, AND SPECIAL COEFFICIENTS K_h AND G_h

3.6.1 Determination of Area Factors f_d and f_a.--f_d is the effective area factor for load-bearing water layers. This factor represents that fraction of gross cross-sectional area over which pressure in the load-bearing layers is effective. f_a is the effective area factor for non-load-bearing water layers. It represents that fraction of gross cross-sectional area over which fluid pressure in the non-load-bearing layers is effective.

As was shown in Section 1.4, f_d affects σ_d and σ_{ad}, hence, it also affects creep characteristics of concrete. f_a affects σ_a, which in turn affects σ_a, which in turn affects shrinkage of concrete. Therefore, f_d is a function of the amount of water in the load-bearing layers, and f_a is a function of the amount of adsorbed water in the cement paste.

*Shortage of computer time prevented predicting creep under biaxial loading. However, this is believed to be a matter of a straight forward application of the terms ϕ and ψ.

Using the computer program (Appendix C) in which the moduli of elasticity have the expressions derived in Section 3.4 and the coefficient ϕ and ψ have the expressions derived in Section 3.5, solutions of creep problems showed that a value of 0.0375 for f_d will be appropriate to give creep strains corresponding to the experimental values for all specimens in a constant humidity enrivonment, namely, uniaxial compression as well as torsion at 50 or 100% R.H. The calculated and experimental shrinkage curves are shown in Fig. 33. Hence, f_d was assumed to be a constant with a value of 0.0375.

The term f_a was found by solving the problem of shrinkage of a specimen having the same characteristics as those mentioned above; a value of 0.431 will produce the same amount of shrinkage as that obtained from a specimen drying at a humidity of 50% at the age of 18 days. Calculated shrinkage values, as well as experimental shrinkage values for such a specimen are shown in Fig. 33. Therefore, it was assumed that for a specimen drying (desorption) from 100 to 50% R.H., a value of $f_a = 0.431$ would be sufficient to produce shrinkage equal to that obtained experimentally. It should be noted that the rate of shrinkage depends on C, the coefficient of hygral diffusivity, and D_{oh} and D_{1h}, the equivalent surface thicknesses. C, D_{oh} and D_{1h} are all presented in Appendix A. Their values as developed in Appendix A were used in the solution of all problems involving a moisture exchange with the outer atmosphere of the concrete specimen.

The value of $f_a = 0.431$ was also suitable for the solution of the shrinkage problem of the companion specimen which was under cyclic changes of humidity of 100 to 50 to 100%, however, it was suitable for the first humidity change only, which was a 14-day drying process from a humidity of 100 to 50% R.H. Results from the solution of this shrinkage problem as well as corresponding experimental values, are shown in Fig. 34.

For the solution of the swelling problem for the second humidity change of the same specimens--i.e., from 50 to 100% R.H., it was found that a value of f_a of 0.431 would produce greater swelling than that obtained experimentally. Thus, a decrease in f_a value is necessary for the swelling magnitude to be equal to that obtained experimentally. The low magnitude of swelling (experimental) is the result of what is known as the irreversibility of sorption and desorption. This irreversibility is greatest for the first humidity change. It has been observed that the first humidity change produces drastic changes in the cement gel. By means of visual evidence (Scanning Electron Microscope), Mills (63) observed that the structure of cement hydrates collapses upon drying. Helmuth (64) and Feldman (65) have shown experimentally that the first drying does, in fact, produce a large amount of irreversible shrinkage and that this is due to the fact that first drying is a manifestation of a major rearrangement of the layers or sheets of cement gel. This was also found to be true in the experimental phase of this study (see Section 2.6.5).

For the purpose of predicting swelling values, an abrupt change of the value of f_a at the time when the humidity is reversed will be necessary. Thus, it was found that, in order to match the swelling values obtained experimentally, the value of f_a had to be changed from 0.431 to 0.337. Calculated values are shown in Fig. 34. Values of D_{oh} and D_{1h} used were 0.0 for each (see Appendix A).

After the first cycle--i.e., second humidity, the values of f_a which were necessary to produce swelling or shrinking of the same order as obtained experimentally were as follows:

third change (desorption), $f_a = 0.337$
fourth change (sorption), $f_a = 0.300$
fifth change (desorption), $f_a = 0.337$
sixth change (sorption), $f_a = 0.300$.

Calculated and experimental deformations for all cycles are shown in Fig. 34.

3.6.2 Determination of Special Coefficients K_h and G_h.--K_h is defined as a coefficient which accounts for delayed volumetric deformation under load due to a change in f_d occurring as a consequence of a change in humidity. Similarly, G_h is a coefficient which accounts for delayed deviatoric deformations due to the same factors.

As observed in Section 3.5.1, the amount of shrinkage was greatest at the first drying. This phenomenon consequently affected the amount of creep obtained simultaneously throughout the period of the first drying. After the first drying, the increase in creep (experimental) appeared to be slight. No significant increase in creep was recorded after the third humidity change (see Section 2.6.3). This observation applies to both creep under uniaxial compression and creep under torsion. Because of the small increases in creep which occurred during the third humidity change and all other humidity changes which followed, it was assumed that creep increases significantly only during the first and second humidity changes.

After several trials of predicting the creep deformations while the specimen was being subjected to changes in humidity, it was found that the amount of computations required to predict creep for every single humidity change was not practical since (1) the work would be very long and complicated, and (2) the creep values obtained were not in such good agreement as to merit such long and complex computations.

These difficulties were believed to exist because of the severe changes in the structure of cement gel due to cyclic changes in humidity. Therefore, it was believed that predicted creep values of a specimen under cyclic humidity should be approximated. A reasonable approximation seems to result from the observations of the experiments in Section 2.6.3 which show that, for both creep under torsion and creep under compression, creep increases significantly only during the first and second humidity changes, and no increase was observed after the third humidity change. Hence, the K_h and G_h expressions were developed so as to match the large increase in creep during the first humidity change. Furthermore, so that no abrupt increases in creep would take place at the time of the humidity change, the K_h and G_h expressions were set so that the computed creep rate would be equivalent to the experimental rate for all subsequent humidity changes.

In constructing the K_h and G_h expressions, it should be noted that both K_h and G_h should be functions of humidity. Since shear deformations (torsion) are affected only by G_h, it was decided to first ascertain the expression for G_h. After a few trials using the computer program as presented in Appendix C, and utilizing all expressions developed in Sections 3.4, 3.5 and 3.6.1 as well as those in Appendix A, the following expressions were found suitable:

$$G_h = 19.0 \times 10^4 (1.0 + h) \qquad \text{for first humidity change} \qquad (3.6.1)$$

and

$$G_h = 28.4 \times 10^6 \times \Delta h \times (1.5 + h)^{-1} \qquad \text{for all humidity changes after the first} \qquad (3.6.2)$$

Calculated creep results according to these expressions are shown in Fig. 35, together with the corresponding experimental results.

Finding an expression for K_h involves deviatoric as well as volumetric creep. Also, the prediction of deformations for a specimen loaded under uniaxial compression and subjected to humidity changes is inherently linked to that for the same specimen when it is subjected to the same humidity changes but with no loading. This linkage occurs because volumetric deformation components exist in both the deformation of an unloaded specimen subjected to changing humidity and of a loaded specimen also subjected to changing humidity (except if the specimen is loaded under pure shear). Furthermore, since the shrinkage stresses and uniaxial compressive loading act in the same direction-- i.e., both are increasing the pressure in the diffusible load-bearing layers, it is expected that the value of S_h in the equation $\sigma_{ad} = f_d \frac{RT}{M} \cdot S_h \cdot \sigma_{ah}$, presented in Section 1.4,should be increased above the value of $S_h = 1.0$. Because this fact was realized, the following procedure was devised to be used in predicting creep and total (creep + shrinkage) deformations for a concrete specimen under any type of load (other than pure shear) being subjected to prescribed humidity changes:

(1) Construct a K_h and G_h expressions which will give creep deformations (after subtracting shrinkage of an unloaded specimen) as close as possible to the experimental creep results of the first drying.

(2) With these K_h and G_h expressions find the "total deformations" curve for the period under which the specimen is under load. Use K_h and G_h expression which will give a higher increase in total deformation, than the set used in (1). Use a value of S_h higher than 1.0.

(3) From the curve obtained in (2), subtract the shrinkage for the specimen, assuming that drying took place from time of first humidity change until time of unloading with no subsequent humidity changes. The resulting curve represents the creep curve under the same type of load and given humidity changes.

(4) To obtain total deformations of the specimen, solve the shrinkage problem according to the prescribed humidity history (see Section 3.5.1), and combine this solution with the curve found in (3).

A limitation should be imposed on the type of humidity changes that could take place for a member whose creep problem is to be solved according to the above procedure. This limitation is that no subsequent drying should exceed the first drying of the member while it is under sustained loading. In other words subsequent drying of a member under load should not produce a humidity distribution in which the humidity of any part of the cross-section is less than that of the same part at the end of the first drying (while the member is under loading). This limitation is required because the increase of creep due to humidity change (mainly drying) is highly dependent on the first drying as was discussed previously in this section.

If the first drying produced a certain humidity distribution, there is a certain increase in the amount of creep of a given member. If a subsequent drying exceeded the first drying (by extending the period of drying or lowering the humidity of the atmosphere in which the member is drying), it will produce another humidity distribution which has a lower value of humidity for some parts of the member's cross-section, thus increasing the amount of creep beyond that of the first cycle. This limitation also implies that no drying of the specimen should take place before application of sustained loading.

After the first drying, subsequent dryings may take place for a shorter period of time but at the same humidity environment as that of the first drying.

To demonstrate the above procedure, the experimental creep results presented in Sections 2.4.3, 2.5.2, and 2.6.2 were calculated as follows:

1. First a K_h expression was constructed (based on trials for the first drying) as,

$$K_h = 23.7 \times 10^4 \ (1.0 + h) \qquad (3.6.3)$$

with $G_h = 2K_h$ and $S_h = 10.0$.

2. With these K_h, G_h and S_h expressions the "total deformations" curve was produced as if there were only one humidity change. In this case, no change in K_h, G_h or S_h was needed to yield an increase in "total deformations," due to second humidity change.

3. The shrinkage was found for a specimen as if drying took place from the time of the first drying of the first humidity cycle until the time of unloading (as in Section 3.5.1). Subtract this shrinkage curve from the curve found in (2) above. The resulting curve represents creep value which corresponds to the experimental creep value in Fig. 23. The results calculated above are shown in Fig. 36.

4. In order to calculate the total deformations (creep + shrinkage), the shrinkage-swelling problem was solved (Fig. 34) according to Section 3.5.1. It was then combined with Fig. 36. The result is shown in Fig. 37.

Comparison of experimental creep and/or total deformation results with calculated results show a fair to poor agreement up to the end of the first cycle but fail to give the sudden increase as soon as there is a new change in humidity. However, it should be emphasized that this procedure gives only an approximation of the problem of creep of concrete as affected by cyclic humidity because the structure of the cement gel changes so drastically under a combination of humidity change and sustained loading that characteristics of the new gel structure--i.e., gel structure after first humidity change become very much different from the characteristics of the old gel structure--i.e., gel structure before any humidity change.

It is believed that the steepness of the sudden changes in the creep curve (Fig. 35) is caused by a combination of the high rate of humidity change and the smallness of the specimen's wall thickness. It is also believed that this combination caused excessive microcracking in the concrete which resulted in the steepness of the sudden changes in the creep curve (Fig. 35). It is expected, however, that for a specimen having a wall thickness ten times that of the specimen used in this investigation, the steepness of the sudden changes in the creep curve will be less than that for the creep curve of the specimens used in this investigation. Although the high rate of humidity change will produce microcracks in the specimen of large wall thickness, these cracks will have little effect on the deformation of the specimen because there will still be a large portion of the specimen's cross-section which is uncracked. However, if for the large wall thickness specimen the humidity change was such that microcracks produced throughout the cross-section of this specimen are comparable to the microcracks produced throughout the cross-section of the specimen of this investigation, then the steepness of the sudden changes in the creep curve of both specimens should be the same. Microcracks are produced on the surface of a concrete specimen for any environmental humidity change higher than 0.06% R.H. per hour, Bazant (46). The humidity change used in the experimental program was 50% R.H. over a period of about five minutes, which is the period through which free water was observed to disappear from the surface of the specimen when humidity was changed from 100 to 50% R.H. (see procedure of humidity change described in Section 2.4.3). This humidity change is far above the limit of non-crack producing humidity change--i.e., 0.06% R.H. per hour; hence, the effects of microcracking on concrete deformations was significant, as discussed above.

The Bazant theory represented by the constitutive equations 1.4.1 and 1.4.2, does not account for the effect of microcracks on the creep deformations. Therefore, the prediction of creep of concrete for a specimen subjected to changing humidity should not be expected to be in full agreement with experimental results. Therefore, the larger the amount of microcracking is, the higher the difference between experimental and predicted creep for a specimen under changing humidity is expected to be. Indeed, the predicted creep results according to Bazant's theory show a significant difference with the experimental results for a specimen under changing humidity (Figs. 35, 36 and 37). The maximum difference between predicted and experimental results occurred at the end of the first drying cycle, which was about 16% of total creep at 80 days after loading and six humidity changes, which is equivalent to about 6% of total deformation (creep plus shrinkage) at 80 days after loading and six humidity changes. On the other hand, predicted creep results according to the same theory for specimens under constant relative humidity were in good agreement with experimental results, being within the range of 1% of total creep at 80 days after loading. However, in a concrete member having a large cross-section (e.g., 24 in. by 24 in.) which is subjected to changing humidity, the difference between predicted and experimental creep results is expected to be smaller than 16% of total creep at 80 days after loading.

Although the problem of steep sudden increase of creep in a structural member is expected to be of less significance than that of the specimen of this investigation (because usually a structural member would have a wall thickness much larger than 1/2 in.), as was discussed earlier, a solution can be achieved by modifying the properties of concrete by modifying the expressions of moduli of elasticity, ϕ, ψ, K_h, G_h, a process which requires the same amount of work as that in Sections 3.5, 3.6, 3.7 and Appendix A. Generally, for more precise predictions of creep of concrete under changing humidity, a more sophisticated model with more parameters and functions representing the material properties, together with more experimental observations, is needed.

3.7 SUMMARY

Based on both the experimental results presented in Chepter 2 and on the considerations of the thermodynamics of diffusible load-bearing water layers, a mathematical model can be developed. This mathematical model consists of the constitutive equations:

$$\dot{\varepsilon} = \frac{\dot{\sigma}}{K} + \dot{\varepsilon}'' \qquad \text{and} \qquad \dot{e}_{ij} = \frac{\dot{S}_{ij}}{2\,G} + \dot{e}''_{ij}$$

where

$$\dot{\varepsilon}'' = \dot{\varepsilon}'_{\mu} - \frac{\dot{\sigma}_a}{K} \qquad \dot{e}''_{ij} = \dot{e}'_{ij\mu}$$

$$\dot{\varepsilon}' = \phi_{\mu}(\sigma_{d\mu} - \sigma_{ad\mu}) - \frac{\sigma_{d\mu}\,\dot{h}_{eq}}{K_{h\mu}} \qquad \dot{e}'_{ij\mu} = S_{d_{ij\mu}}\left(\frac{1}{2}\,\psi_{\mu} - \frac{\dot{h}_{eq}}{2G_{h\mu}}\right)$$

$$\dot{\sigma}_{d\mu} = \nu_{\mu}(\dot{\sigma} - \dot{\sigma}_{a\mu}) - K_{c\mu}\dot{\varepsilon}'_{\mu} \qquad \dot{S}_{d_{ij\mu}} = \nu'_{\mu}\dot{S}_{ij\mu} - 2G_{c\mu}\dot{e}'_{ij\mu}$$

$$K = \left[K_b^{-1} + (K_c + K_d)^{-1}\right]^{-1} \qquad G = \left[G_b^{-1} + (G_c + G_d)^{-1}\right]^{-1}$$

$$\nu = \frac{K_d}{K_c + K_d} \qquad \nu' = \frac{G_d}{G_c + G_d}$$

The different terms of the above equation set were discussed in Section 1.4. This model also consists of a set of material characteristics given by:

$\sigma_{ad} = 1360 \times \sigma_{ah} \times f_d$

$\sigma_{ad} = 1360 \times \sigma_{ah} \times f_a$

$\sigma_{ah} = S_h(1 - h^2)$

$f_d = 0.0375$

$f_a = 0.431$ For first humidity change.

$f_a = 0.337$ For second humidity change.

$f_a = 0.337$ For third humidity change.

$f_a = 0.300$ For fourth humidity change.

$f_a = 0.337$ For fifth humidity change.

$f_a = 0.300$ For any subsequent change.

$S_h = 1.0$

$\phi = 21.3 \times 10^{-9}(0.9 - 0.4\, h_{eq})(\frac{t + 500.0}{t + 1.0})$

$K_h = 23.7 \times 10^4(1.0 + h_{eq})$

with $G_h/K_h = 2.0$

$\psi = 14.2 \times 10^{-8}(1.5 - h_{eq})(\frac{t + 500.0}{t + 1.0})$

$G_h = 19.0 \times 10^4(1.0 + h_{eq})$

for first humidity change and,

$G_h = 28.4 \times 10^6 \times \Delta h(1.5 + h_{eq})^{-1}$

for all changes after the first change.

$$C = 17.8 \times 10^{-3}(0.1 + h)(\frac{t_{eq} + 4}{t_{eq}}) \qquad \text{(desorption)}$$

$$C = 15.0 \times 10^{-3}(0.76 + \frac{2.16}{h} + \frac{1}{h^2})(\frac{t_{eq} + 4}{t_{eq}}) \qquad \text{(sorption)}$$

together with

$$D_{oh} = D_{1h} = 1.0 \qquad \text{(desorption)}$$

$$D_{oh} = D_{1h} = 0.0 \qquad \text{(sorption)}$$

Together with the elastic properties of elements of the rheological model shown in Fig. 2 ,

CHAPTER 4

CONCLUSIONS AND FUTURE RESEARCH

The conclusions reached in this chapter are based on the experimental program presented in Chapter 2 and the analytical work presented in Chapter 3. Since the only type of concrete material used in this study was micro-concrete (see Section 2.3.1), the conclusions of this chapter are primarily valid for that type of concrete only. Furthermore, these conclusions are limited by the scope of this study as indicated in Section 1.7.

4.1 CONCLUSIONS REGARDING EXPERIMENTAL PROGRAM

The following conclusions can be made regarding the experimental phase of this study:

1. For a concrete member under sustained loading, any change in humidity will increase creep. As mentioned in Section 2.12, at the end of the first drying period, the magnitude of creep of a specimen under uniaxial compression and changing humidity was seven times the magnitude of creep of a specimen under the same loading and 50% R.H. It was thirteen times the magnitude of creep of a specimen under the same loading and 100% R.H. For torsional loading, at the end of the first drying period, the creep obtained from a specimen subjected to a changing humidity of 100 to 50% was four times that of a specimen under constant 50% R.H. and six times that of a specimen under constant 100% R.H. and the same loading.

   The first drying period is found to produce the greatest increase in creep. Subsequent wetting or drying produces only minor increases in creep. After the third humidity change, the increase in creep is practically negligible.

   If the first drying causes complete humidity stabilization over the entire cross-section of the member*, then it is expected that no

* A complete humidity stabilization means that, if drying is taking place in an atmosphere of 70% R.H., complete humidity stabilization will be achieved only if the entire cross-section of the member reaches a humidity of 70% R.H.

significant creep increase will take place during any drying thereafter provided that the relative humidity of the subsequent dryings is not lower than that of the first drying.

2. The increases in creep due to the conditions mentioned above are generally of a non-recoverable nature.

3. The creep of concrete in compression or torsion kept at a constant humidity of 50% was generally higher than that of a specimen maintained at a humidity of 100%.

4. Shrinkage of a concrete specimen subjected to humidity cycles of 100 to 50 to 100% is of a relatively recoverable nature. The largest non-recoverable shrinkage is that which occurs after the first drying; it was about 20% of total shrinkage at the end of the first drying. Furthermore, shrinkage and swelling become totally recoverable after the fifth or sixth humidity change.

   It is suggested, according to the above conclusions, that drying a structural member at least once before loading would aid significantly in reducing excessive creep increases under variable humidity. It would aid significantly in reducing excessive shrinkage. This suggestion can be economically adopted for precast structural members, especially those that are prestressed.

5. For sealed members loaded under equal biaxial compressive loading, the amount of creep in either direction was less in magnitude than that of a member under uniaxial compressive loading, and creep Poisson's ratio was zero.

4.2 CONCLUSIONS ON ANALYTICAL WORK

From the analytical phase, a mathematical model consisting of constitutive equations and material parameters and functions was developed. It is summarized in Section 3.7. This model was developed to reflect the experimental findings of this study, and a successful demonstration was presented regarding the creep of concrete members subjected to a constant humidity. The difference between predicted and experimental results was within 1% of total creep at 80 days after loading. However, the model was not as successful in predicting the creep of concrete members under variable humidity. The difference between predicted and experimental results was within 6% of total deformation at 80 days after loading. This is believed to be due to the excessive cracking occurring at the surface of the concrete specimens caused by the high rate of humidity change used in these tests.

Since the objective of the analytical phase of this study is to develop a mathematical model by studying the experimental results and finding expressions for the parameters and functions representing the material properties K's and G's, ϕ, ψ, f_d, f_a, S_h, K_h, and G_h, it can be concluded that such an application of the Powers-Bazant theory is possible. However, a modification of this theory is recommended so that effects of microcracking on creep can be introduced.

4.3 PRACTICAL APPLICATIONS

In an ordinary concrete structural member, the concrete material is expected to be different from the material used in this investigation. The concrete usually used in a structural member has an aggregate/cement ratio higher than the aggregate/cement ratio used in this investigation which was 2/1. The aggregate size is also expected to be larger than the maximum aggregate size used here which had a maximum size smaller than sieve No. 4 (see Table 2). The conclusions of Section 4.1 are, therefore, only qualitatively valid for a structural concrete material--i.e., a concrete which has different aggregate/cement ratio or has a different water/cement ratio from those of this study for example. It is expected [Polivka (66)] that if the concrete has a higher aggregate/cement ratio (or less cement paste content) than that of the concrete used in this investigation, the magnitude of creep would be smaller than that obtained and presented in Section 2.5.2. Effect of humidity change on creep of structural concrete is also expected to have the same qualitative effect and to be of a smaller quantity than that of the concrete of this study.

For the solution of creep problems, from a practical point of view, the theory, together with the program (Appendix C), was simple and economical to use provided that the material properties are known. On the 7090 IBM computer the solution of a problem for 100 days after load application will require about 55 seconds. What seems to be a handicap at this stage, however, is the evaluation of the material properties.

Since this theory was applied for the first time on actual experimental results in this study, the role of the different parameters and functions is still not very clear. The importance of some of them and the insignificance of others still remains to be determined.

4.4 FUTURE RESEARCH

After completing this investigation, both experimentally and analytically, it seems that the following future research is necessary to explore the possibility of a more comprehensive application of the Powers-Bazant theory to creep problems:

1. Experiments on specimens which are kept at different constant relative humidities in order to investigate in detail the effect of the level of constant relative humidity on the creep of concrete.

2. Experiments to study the effect of changing humidity (100 to 70% R.H.) on creep of specimens having a large cross-section--i.e., hollow cylinders with wall-thickness of two inches.

3. For analytical work, the experimental data of other investigators can be analyzed according to the Powers-Bazant theory. However, some of these experimental data may not provide sufficient information about loading, hygral treatment and other experimental aspects needed for the analysis.

4. In order to predict the effects of microcracking, a modification in the constitutive equations is necessary. This modification might be achieved by adding new parameters which will account for the effects of microcracks on the creep of concrete. However, it is recommended that the effect of microcracks be first investigated and evaluated, then the modification in the constitutive equations can be easily made.

APPENDIX A

EVALUATION OF COEFFICIENT OF HYGRAL DIFFUSIVITY AND SELF-DESICCATION FUNCTION

A. EVALUATION OF COEFFICIENT OF HYGRAL DIFFUSIVITY

A.1 Theory.--The objective of these tests is to investigate the factors which affect the coefficient of hygral diffusivity and provide an expression for this coefficient in terms of these factors.

It has been shown (45) that humidity h, as a function of time t and space coordinates, satisfies the following partial differential equation of the parabolic type:

$$\frac{\partial h}{\partial t} = kb_T c_h \nabla^2 h + k \text{ grad } (b_T c_h) \text{ grad } h + \frac{\partial h_s(t_{eq})}{\partial t} + \varkappa \frac{\partial T}{\partial t} \qquad (A.1)$$

where ∇^2 = Laplace operator.

$kb_T c_h$ = coefficient of hygral diffusivity, b_T is a function of temperature only, c_h is a function of humidity only and k is sorption resistance.

h_s = humidity at self-desiccation, a function of t_{eq} (see part B in this Appendix).

T = temperature.

$\varkappa$ = hygrothermic coefficient.

t_{eq} = equivalent curing time.

In these tests $\frac{\partial T}{\partial t} = 0$, therefore, the last term of equation A.1 is zero.

The self-desiccation function $h_s(t_{eq})$ as it is found in part B in this appendix, was very close to 1.00. The change $dh_s(t_{eq})$ was only about 1.5% after a period of 180 days. Examining the mathematical expression for h_s which is,

$$h_s(t_{eq}) = \frac{0.985\, t_{eq} + 20}{t_{eq} + 20}$$

for $t_{eq} = 1$, $h_s = 1.00$ and for $t_{eq} = 200$, $h_s = 0.990$.

Therefore, it can be assumed as an estimation that $\frac{\partial h_s(t_{eq})}{\partial t} = 0$, hence the third term of the right side of equation A.1 is zero.

It is believed (46) that grad $(b_T c_h)$ = gradient of $b_T c_h$ is very small and that to eliminate this term it would make calculations much easier. Therefore, equation A.1 reduces to:

$$\frac{\partial h}{\partial t} = k b_T c_h \nabla^2 h$$

or

$$\frac{\partial h}{\partial t} = C \frac{\partial^2 h}{\partial x^2} \qquad \text{(A.2)}$$

for one dimensional diffusion process. C is the coefficient of hygral diffusivity which is (kb_Tc_h).

Using a standard finite difference representation,

$$\frac{\partial h}{\partial t} = \frac{h_{i,j+1} - h_{i,j}}{a}$$

$$\frac{\partial^2 h}{\partial x^2} = \frac{h_{i+1,j} - 2h_{i,j} + h_{i-1,j}}{d^2}$$

where a,d,i and j are as shown in Fig. A-1 below.

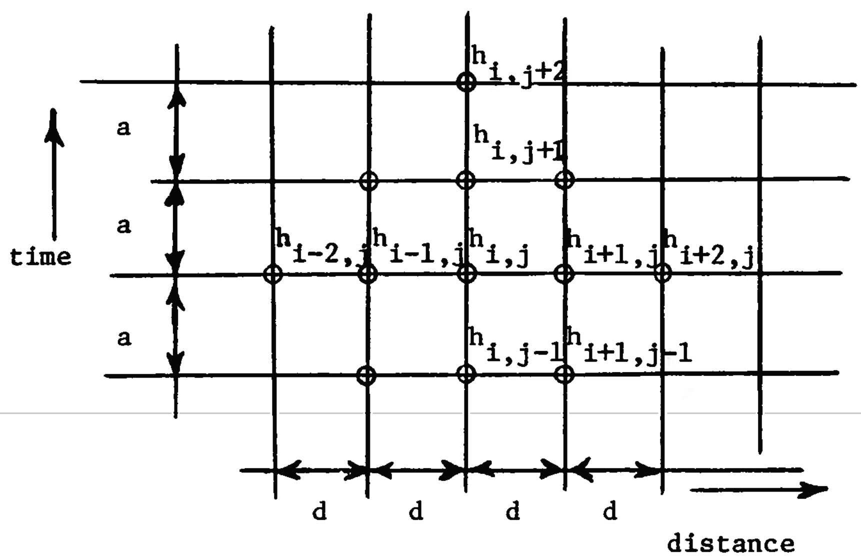

Fig. A-1. Mesh for finite difference representation.

Therefore,

$$C_{i,j} = \left(\frac{h_{i,j+1} - h_{i,j}}{a}\right) \Big/ \left(\frac{h_{i+1,j} - 2h_{i,j} + h_{i-1,j}}{d^2}\right) \qquad \text{(A.3)}$$

where i is the thickness (space) subscript and j is the time subscript.

For a boundary value problem, the formulation of boundary conditions is necessary. Suitable expressions for boundary conditions were presented by Bazant (45) as,

$$\left.\begin{aligned} D_{oh} \frac{\partial h}{\partial x} &= \ln(h/h_{ex_o}) \quad \text{for } x = x_o \\ D_{1h} \frac{\partial h}{\partial x} &= -\ln(h/h_{ex_1}) \quad \text{for } x = x_1 \end{aligned}\right\} \qquad \text{(A.4)}$$

where, h_{ex_o} = humidity at x_o

h_{ex_1} = humidity at x_1

ln ( ) = natural logarithm and

D_{oh} and D_{1h} are equivalent surface thicknesses at x_o and x_1 respectively.

These imaginary surface thicknesses characterize the rate of moisture transmission at the surface of specimen. $D_{oh} = \infty$ for a specimen sealed at the surface $x = x_o$, and $D_{1h} = 0$ for the surface at $x = x_1$ which is unsealed and has perfect ventilation.

A.2 Experiments.--As was mentioned in Section 2.2.3, two blocks were cast using the same material as that of the main specimens which was described in Section 2.3.1. Block No. 1 (Fig. 38) had all sides sealed except one. Block No. 2 (Fig. 39) had all sides sealed except two opposite ones. Block No. 1 was tested for desorption only--i.e., drying conditions, at a humidity of 50%, while Block No. 2 was tested for sorption and desorption--i.e., wetting and drying, between 50 to 100% R.H. All tests were carried out at 73°F temperature. Monfore gages, such as the one described by Monfore (67), were used.

A.3 Results.--Results obtained from the above described tests are presented in Figs. 43 and 37. Fig. 40 shows the distribution of internal relative humidity of Block No. 1 as obtained after different periods of drying times. Fig. 41 shows the distribution of internal relative humidity of Block No. 2 after different periods of drying time. Internal humidity distribution for Block No. 2 after wetting was erratic.

Calculations of C, according to equation A.3 shown in Section A.1, were done and results are presented in Fig. 42. In order to avoid the boundary effects, the values of C for wells closest to the surface were not calculated--i.e., wells at 1/4-in. from surface.

A.4 Evaluation of Results and Coefficient of Hygral Diffusivity.--The C values obtained from these tests were very scattered (Fig. 42). But with the help of observed deformations of control specimens (6 in. O.D., 5 in. I.D. and 40 in. long) which were subjected to drying and wetting, some general conclusions can be drawn regarding the behavior of C. From these conclusions, an expression for C will be determined. These observations are:

1. For drying conditions, it was found by trial that a linear relationship between C and t_{eq} of the form

$$C = 17.8 \times 10^{-3} (0.1 + h) \quad \text{in.}^2/\text{day}$$

with $D_{oh} = D_{1h} = 1.0$ (see A.1 above) will give satisfactory results in terms of amount and rate of drying deformations of control companion specimens (see Fig. 24 and pertinent discussions in Section 3.4 as well as discussions below about dependence of C on t_{eq}). This relationship is shown in Fig. 42 by the solid linear curve (desorption).

2. For sorption, it was observed that the control specimens were nearly stabilized in terms of deformation, which is a measure of humidity, after about five days (see Fig. 12). The following expression was tried and was found to satisfy the requirements of the control companion specimen, with the given factor of time (see discussion below) and with $D_{oh} = D_{1h} = 0$ (see Fig. 33).

$$C = 15.0 \times 10^{-3} \left(0.76 + \frac{2.16}{h} - \frac{1}{h^2}\right), \ \text{in.}^2/\text{day}.$$

This expression is presented by the upper solid curve in Fig. 42.

All values obtainable, for R.H. of 50 to 100%, from the above two expressions for the coefficient of hygral diffusivity fall within the limit established by experimental values of C in Fig. 42. As for the sorption values of C, there are no reliable results to depend upon. Therefore, these expressions will be assumed for C.

It is expected that C depends on t_{eq}, the equivalent curing time. However, it was not possible to verify this dependence because all control specimens and Blocks No. 1 and No. 2 were tested at the same age (21 days). It was observed while searching for an expression for C that to increase the value of C by a factor of $\frac{t_{eq} + 4}{t_{eq}}$ will make calculated deformations closer to experimental results of deformations of control specimens. Consequently the following expressions were adopted:

For desorption

$$C = 17.8 \times 10^{-3}\ (0.1 + h)\left(\frac{t_{eq} + 4}{t_{eq}}\right) \tag{A.5}$$

and for sorption

$$C = 15.0 \times 10^{-3}\ \left(0.76 + \frac{2.16}{h} - \frac{1}{h^2}\right)\left(\frac{t_{eq} + 4}{t_{eq}}\right). \tag{A.6}$$

A.5 Determination of D_{oh} and D_{1h}.--As was mentioned above, a value of $D_{oh} = D_{1h} = 1.0$ was required in order to obtain shrinkage results which have the same rate as those obtained experimentally while for the sorption phase, a value of $D_{oh} = D_{1h} = 0$ was required for the same purpose. This seems to be in agreement with the definition of D_{oh} and D_{1h} as being equivalent surface thicknesses. In a desorption phase, the rate of exchange of moisture between the specimen surface and the surrounding atmosphere is being hindered by the rate of transmission of water vapor from water surfaces to air which is a function of humidity of the surrounding atmosphere, ventilation and all other factors which may affect evaporation of water. In the sorption phase, water reaches the specimen surface directly, and it was accelerated to the inside of the specimen by means of capillary action. Hence, the thickness of equivalent surfaces is assumed to be zero, and it was indeed necessary to assume $D_{oh} = D_{1h} = 0$ in order to obtain predicted swelling rates equal to experimental swelling rates in a sorption phase. These values of D_{oh} and D_{1h} will be used accordingly in all calculations which involve moisture exchange with the surrounding atmosphere of the specimen.

B. EVALUATION OF SELF-DESICCATION FUNCTION

Self-desiccation, dh_s, represents the change of internal humidity of concrete due to hydration of unhydrated cement, with no moisture exchange with the external atmosphere--i.e., the concrete remains at a constant water content. The following tests were carried out to observe the change of internal humidity of concrete specimens under self-desiccation conditions and to provide a mathematical expression for this change as a function of equivalent curing time (t_{eq}).

Two bars, 1 by 20 in., were cast using the same material as that of the main specimens. They were cured for 21 days at 100% R.H. and 73°F. They were then enclosed in brass tubes, each having one end closed and the other instrumented with a Monfore gage's attachments. Each bar was then separately sealed except for the Monfore gage well which was filled with a brass rod (see Fig. 43).

Both bars were kept in a 73°F room throughout the testing period which was about 180 days. Readings with the Monfore gage were taken periodically. These are plotted in Fig. 44.

It was obvious (Fig. 44) that the change of internal humidity was very small, a decrease of about 1.5% after 180 days. This low decrease in internal humidity can be attributed to the high water/cement ratio of the concrete used which was 0.58 by weight.

For the results shown in Fig. 44, it was found that an expression which may yield an average value of h_s at a given equivalent time, t_{eq} is,

$$h_s = \frac{0.985\ t_{eq} + 20}{t_{eq} + 20} \tag{A.7}$$

The value of h_s vs. t_{eq} from this expression are represented in Fig. 44 by the solid line.

APPENDIX B

EFFECT OF STRAIN GAGE ON CONCRETE DEFORMATIONS

The following analysis is meant to demonstrate the reinforcing effect of an embedded strain gage on the deformations of the cross-section of a specimen under a sustained uniaxial compressive loading. Details of strain gages are shown in Figs. 5 and 45. Details of an embedded strain gage are shown in Fig. 46. Concrete properties are all taken to be similar to those cured at 100% R.H. for 21 days. Those properties used in this analysis are given below. Strain gage dimensions and properties were obtained from the manufacturer, "Microdot Inc."

The effect of the reinforcement offered by the strain gage body is most important in the region of the concrete's cross-section closest to the strain gage: the further away from the strain gage, the less the effect of the strain gage in reinforcing the concrete's cross-section.

Since the strain tube is filled with compacted powder of magnesium oxide (MgO) and since the flange of the gage is perforated, the modulus of elasticity of gage material should be replaced by the effective modulus of elasticity defined as follows:

$$E_{eff} = \frac{E_s A_s}{A_t}$$

where

E_s = the modulus of elasticity of strain gage

A_s = cross-sectional area of gage

A_t = total cross-sectional area occupied by gage.

Since information on the stiffness of MgO powder is lacking, two cases can be considered to give an upper and lower bound on the value of E_{eff}. These two cases are:

1. When the MgO powder has a very small modulus of elasticity as compared to strain gage steel, then the strain tube should be assumed empty except for the sensitive elements. See Fig. 45, Section 1.1, Scheme C.

2. When the MgO powder has a modulus of elasticity equal to the modulus of elasticity of the strain gage material, consider the tube as a solid. See Fig. 45, Section 1.1, D.

The following values are calculated according to the dimensions of the strain gage shown in Fig. 45:

$$A_t = 803 \times 10^{-6} \text{ sq. in.}$$

$$A_s \text{ (according to Scheme C)} = 329 \times 10^{-6} \text{ sq. in.}$$

$$A_s \text{ (according to Scheme D)} = 653 \times 10^{-6} \text{ sq. in.}$$

Using a modulus of elasticity equal to 30.0×10^6 psi (as given by manufacturer), the following effective moduli were determined:

$$E_{eff} \text{ (according to Scheme C)} = 12.3 \times 10^6 \text{ psi}$$

$$E_{eff} \text{ (according to Scheme D)} = 24.5 \times 10^{-6} \text{ psi.}$$

Since in both cases, E_{eff} is larger than $E_{concrete}$, it is clear then that E_{eff}, according to Scheme D, will produce a significantly larger effect in terms of reinforcement offered by strain gage to concrete than does E_{eff} according to Scheme C. Therefore, Scheme D will be considered in the analysis below.

Considering the bond between strain gage and concrete, and, considering the continuity of the cross-section of the specimen, it is obvious that the only rigorous solution is one which considers the time-dependent behavior of continuous media. Other solutions, less rigorous, could offer an excellent estimation of the amount of reinforcement offered by the strain gage to the concrete. One of these solutions is a finite element approach with time effects (68). Such a solution would consider shear between every two elements as well as considering normal stresses. For the purpose of this analysis, a segmental approach is used. This segmental approach neglects the effect of shear but considers the normal stresses and strains for one time step. Nine different segments were used for one half of the cylinder. The first segment has an angle of 2.5° between two radii; the second has 10°, and the third has 20°. Others were originated by adding 10° on each side (Fig. 47).

ASSUMPTIONS FOR ANALYSIS

1. Steel (material of strain gage) remains elastic.
2. The strain gage if fully bonded to concrete.
3. For every segment (Fig. 47) a straight section before creep remains straight and parallel to its original direction.

If creep strain, ε_c, occurs in Section 1.1, Fig. 45, then the force required to restore the specimen's original length is:

$$F = \varepsilon_c \times E_c \times A_g \tag{B.1}$$

where

E_c = modulus of elasticity of concrete

A_g = gross cross-sectional area of Section 1.1.

If creep strain, ε_c', occurs in Section 2.2, the resistance offered by the embedded strain gage, against this deformation, tends to make $\varepsilon_c' < \varepsilon_c$. The force required to restore the original length of this section is:

$$F' = \varepsilon_c' \times E_c \times A_c + \varepsilon_s \times E_{eff} \times A_s \qquad (B.2)$$

where

ε_s = strain in steel

E_{eff} = effective modulus of elasticity of strain gage material

A_s = cross-sectional area of steel

if

$F = F'$ to restore the original length, then

$$\varepsilon_c \times E_c \times Ag = \varepsilon_c' \times E_c \times A_c + \varepsilon_s \times E_s \times A_s$$

Assumptions 2 and 3 require that $\varepsilon_c' = \varepsilon_s$, then

$$\varepsilon_c \times E_c \times A_g = \varepsilon_s \times E_c \times A_c + \varepsilon_s \times E_{eff} \times A_s$$

or

$$\frac{\varepsilon_s}{\varepsilon_c} = \frac{E_c A_g}{E_c A_c + E_{eff} A_s} = \frac{\text{Creep in a reinforced section}}{\text{Creep in a section with no reinforcement}} \qquad (B.3)$$

The following table was prepared by calculating $\frac{\varepsilon_s}{\varepsilon_c}$ according to equation B.3:

θ^{o}, Angle of Segment, Fig. 46	$A_g \times 10^{-3}$ sq. in.	$E_c A_g \times 10^{-6}$ lbs.	$A_c \times 10^{-3}$ sq. in.	$E_c A_c \times 10^{-6}$ lbs.	$E_c A_c + E_{eff} A_s$ 10^{-6} lbs.	$\frac{\varepsilon_s}{\varepsilon_c}$
2.5	60.00	0.210	59.35	0.208	0.224	0.93
10	240.00	0.840	239.35	0.839	0.855	0.98
20	480.00	1.680	479.35	1.679	1.695	0.99
40	960.00	3.360	959.35	3.359	3.375	1.00
60	1,440.00	5.040	1,439.35	5.040	5.056	1.00
80	1,920.00	6.710	1,919.35	6.710	6.726	1.00
100	2,400.00	8.400	2,399.35	8.400	8.416	1.00
120	2,880.00	10.090	2,879.35	10.090	10.106	1.00
140	3,360.00	11.750	3,359.35	11.750	11.766	1.00
160	3,840.00	13.420	3,839.35	13.420	13.436	1.00
180	4,320.00	15.100	4,319.35	15.100	15.116	1.00

$E_{eff} = 24.5 \times 10^{6}$ psi, $E_c = 3.50 \times 10^{6}$ psi, $A_s = 0.653 \times 10^{-3}$ sq.in.

$E_{eff}\ A_s = 0.016 \times 10^{-6}$ lbs.

Results of $\frac{\varepsilon_s}{\varepsilon_c}$ vs. θ from the above table are plotted in Fig. 47.

DISCUSSION

For $\theta = 2.5^{o}$, the section of concrete is the one which is within the two radii that include the strain gage (see Fig. 47). The $\frac{\varepsilon_s}{\varepsilon_c}$ value of this section is clearly not representative of what is actually taking place in the creep specimen since it is expected that the concrete which is 1/8 in., or even 1/4 in. away from the strain gage boundary would share the effect of reinforcement offered by the strain gage, with the concrete contained in the section of $\theta = 2.5^{o}$. It seems reasonable, then, that the section which could be used as a representative for the effect of the strain gage's reinforcement would be one such as that of $\theta = 1.0^{o}$ (see Fig. 47). This, then, means that the ratio of the apparent creep measured in a section with a strain gage to the creep measured by a method which does not reinforce the concrete's cross-section is 98% of the creep measured by the latter section. However, unaccounted-for microcracks or bond failure may change this ratio.

The difference between the analysis of the strain gage's effect on the creep deformations and that of the elastic deformations is that, in the case of creep, it is expected that there would be no effect of hair cracks which might close up in the course of creep deformations. On the other hand, in the case of elastic loading, existing hair cracks (if any) would close up after applying a compressive load causing an additional amount of deformations. The deformations obtained from a section which does not have an embedded strain gage will consist of elastic deformations gained by the closing up of the hair crack's components which are in a direction perpendicular to the direction of applied compressive load. In a section which has an embedded strain gage, the strain gage will try to resist the closing of the hair cracks and will reinforce the section against elastic deformations. Therefore, actual deformation ratios may probably be higher in the case of elastic loading than those shown in the table.

In the case of shrinkage, the strain gage reinforces the section against shrinkage so that a section with a strain gage is expected to show less shrinkage than a section without one. As for swelling (sorption), the strain gage is expected to reinforce the section against dilatation.

APPENDIX C

COMPUTER PROGRAM AND ITS USE

The computer program used in this investigation (except for curve fitting by the least squares method) was that reported by Bazant (45). This program was slightly modified to allow for the input of new material parameters and more varying humidity behavior. All the modified and added program statements are underlined in the program listing which appears at the end of this appendix. In order not to repeat most of the material in Reference 45, the reader is referred to this reference for the main aspects of the program. However, some of the necessary details for usage of the modified program are explained here according to their appearance in the program.

DIMENSIONING

Dimensions of arrays are set at a minimum for a number of elements; NEL = 8 and number of diffusion units, NU = 3. To change these two numbers, the dimensions should be changed. RATGC (3) and RATGD (3) are added.

SECTION 1

In this section, the basic material characteristics such as functions of humidity, temperature, time, change of humidity, etc., are built.

The data statement is presented to aid in constructing the material characteristics which are represented by functions which relate to the diffusion units.

SECTION 2

Other data,which may not relate to the material characteristics but which are necessary for the program, are given. Notice that the torsional loading has been inserted in the data statement of this section. The rest of this section is mainly for reading the input cards at the end of the program listing.

SECTION 3

This section is devoted to writing the input data of the problem at the start of the expected output, to check the input.

SECTION 7

The modified program allows for loading and unloading of sustained torsional load whether or not there is an axial load, whereas the unmodified program allows for loading of sustained torsional load only if there is a compressive axial load. It does not allow for unloading in any case.

SECTION 8

In this section, the humidity and temperature of the member is changed in the event an immediate change of humidity and temperature is required. Such a change is accomplished by specifying LØPT = 77 in the input cards at the end of the program. Any value of LØPT other than 77 will not produce an immediate humidity and temperature change.

In the program reported in (45), if humidity is changed from 100 to 90%, the t_{eq} value will no longer increase--i.e., t_{eq} value will stay as a constant which has a value equal to its value at the last time step when humidity change started. The added statements will allow for the t_{eq} increase as it should be, as a function of time, humidity and temperature. This same change works if temperature is changed.

SECTION 9

A statement has been added to make the new expression of HDIFFU workable for the first time step. This statement is: IF (IT. EQ.1) DHEQ = 0.0001

The value of DHEQ in this statement is irrelevant.

SECTION 11

K_b, K_c, K_d, G_b, G_c and G_d are all made independent of each other. Hence, the new statements are needed. Notice that in Section 1, functions for G_b, G_c and G_d have been added.

SECTION 12

Because ϕ and ψ are made functions of time after loading, the following statement is added:

TEE = (IT - IL1) * DT

where TEE is time in days after loading. Other changes in the statements of this section are needed to allow the use of different G_h for a specimen under torsional loading only. For a specimen which has no humidity change or which has compressive loading it is necessary to make IH3 larger than IT.

SECTION 18 and 19

While the original program has ANGLE on the output, the modified program has SHSTN on its output. ANGLE is the relative angle in radians resulting from the sustained torsional loading and SHSTN is the shear strain due to the same loading. If ANGLE is required on the output, put ANGLE instead of SHSTN in the first WRITE statement in Section 19 and in the statement (FØRMAT 14) in Section 3.

The following is a list of modified or added variables and functions as used in the modified program:

GBB = G_b

GCC = G_c

GDD = G_d

IH3 = Time in days at which the first drying period is ended. It is to be used for torsional loading only to change G_h. Make IH3 larger than IT if there is no axial loading or if there is constant humidity.

PHHDT1 = G_h after IH3

PSI = ψ_1(ψ of diffusion unit number 1)

PSPH = G_{h_1}/K_{h_1}

RATE = ϕ_μ/ϕ_1

RATGC = G_{c_μ}/G_{c_1}

RATGD = G_{d_μ}/G_{d_1}

RATPSI = ψ_μ/ψ_1

TEE = Time after loading (for ϕ and ψ)

The input data for the program are presented in three cards for each problem to be solved. These input data are:

CARD 1

LØPT = Integer parameter to allow for immediate internal humidity and temperature change (LØPT = 77) or solve diffusion problem (LØPT ≠ 77).

NEL = Number of elements in the axisymmetric solid (member) to be used in finite element solution of strains and stresses.

NU = Number of Powers' units in the rheological model, according to Fig. 2, NU = 1.

NPRINT = For output purposes. Every NPRINT step print deformations and stresses.

MPRINT = For output purposes. Every MPRINT step print humidity, temperature, time and internal stresses.

TIMEO = Initial time.

TSTART = Temperature of member at initial time.

HSTART = Humidity of member at initial time.

AL = A parameter; for AL = 1.0, pure temperature dilatation is included; for AL = 0.0, pure temperature dilatation is omitted.

SW = A parameter; for SW = 1, thermal swelling is considered; for SW = 0.0, thermal swelling is omitted.

HY = A parameter; for HY = 1.0, the hygral deformations are included; for HY = 0.0, the hygral deformations are omitted.

TDISTO = Equivalent surface thickness for inner surface of cylinder for heat diffusion.

TDIST1 = Equivalent surface thickness for outer surface of cylinder for heat diffusion.

HDISTO = Equivalent surface thickness for inner surface of cylinder for moisture diffusion.

HDIST1 = Equivalent surface thickness for outer surface of cylinder for moisture diffusion.

CARD 2

DT = Time step to be used in the solution in days.

IT1 = Number of interval (IT) at which first temperature change occurs.

IT2 = Number of interval (IT) at which the step change of STEPT per DT is to be stopped.

TO = Temperature at the inner surface of cylinder at IT1.

T1 = Temperature at the outer surface of cylinder at IT1.

STEPT = Changes of temperature at the inner and outer surfaces of the cylinder starting at the initial time and ending at IT2.

IH1, IH2, HO, H1, STEPH — are the same as IT1, IT2, TO, T1, and STEPT, respectively but for humidity.

IP1, IP2, DPOO, DP11, STEPP — are the same as IT1, IT2, TO, T1 and STEPT, respectively but for circumferential pressure.

CARD 3

IL1 = Number of interval (IT) at which the specimen is loaded.

IL2 = Number of interval (IT) at which the specimen is unloaded.

DLD = Axial load per one radian.

DLD1 = (Unused space yet.)

PREST = Prestress of reinforcement.

RELAX = A Parameter. If Longitudinal force is prescribed, put RELAX = 0.0. If longitudinal extension is prescribed, make RELAX = 1.0.

RO = Inner radius of cylinder.

R1 = Outer radius of cylinder.

REVER = Modulus for unloading. It makes modulus of elasticity for unloading equal to modulus of elasticity before loading times REVER.

TDIFFU = Coefficient of thermal diffusivity.

EA = Young's modulus of elasticity of reinforcement.

SCALE (1), (2), (3), (4) = For plotting purposes.

CHAR = Array of characters for plotting on printer.

The data cards for solving a typical problem using the program are presented on the following page. The computer output for this problem is presented on page 103.

TYPICAL SET OF DATA CARDS FOR ONE PROBLEM

CARD 1

Col. No. 5	10	15	20	25	30	35	40	45	50	55	60	65	70	75	80
LØPT	NEL	NU	NT	NPRINT	MPRINT	TIMEO	TSTART	HSTART	AL	SW	HY	TDISTO	TDIST1	HDISTO	HDIST1
1	8	1	80	1	1	21.	25.	1.0	0.	0.	1.0	0.	0.	1.E0	1.E0

CARD 2

Col. No. 5	10	15	20	25	30	35	40	45	50	55	60	65	70	75	80
DT	IT1	IT2	TO	T1	STEPT	IH1	IH2	HO	H1	STEPH	IP1	IP2	DPOO	DP11	STEPP
1.0	999	999	0.	0.	0.	8	999	0.50	0.50	0.0	999	999	0.0	0.0	0.0

CARD 3

Col. No. 5	10	15	20	25	30	35	40	45	50	55	60	65	70	75	80
IL1	IL2	DLD	DLD1	PREST	RELAX	RO	R1	REVER	TDIFFU	EA	SCALE(1)	SCALE(2)	SCALE(3)	SCALE(4)	CHAR
19	999	560.0	0.0	0.0	0.0	6.35	7.62	1.00	0.0	0.0	2.0	2.0	2.0	2.0	xxxxx

```
            PROGRAM   MAIN  ( INPUT, OUTPUT, TAPE5 = INPUT, TAPE6 = OUTPUT )
          C ANALYSIS OF STRAINS, STRESSES, HUMIDITY AND TEMPERATURE IN A LONG THIC        K-WALLED
          C OR SOLID CONCRETE CYLINDER, REINFORCED AND PRESTRESSED, AT VARIABLE TE        MPERATU-
          C RE AND HUMIDITY - THERMODYNAMIC THEORY. (BY Z.P.BAZANT, U.C.BERKELEY,A        UG.1969)
          C     ( MODIFIED  BY  H.R.AL-ALUSI   OCTOBER, 1970  )
          C TIME IN DAYS, DIMENSIONS IN CM, TEMPERATURE IN DEG C, FORCE IN KP, HEA         T IN CAL
          C WARNING. THIS PROGRAM HAS NOT BEEN DEBUGGED FOR ALL TYPICAL SITUATIONS         WITHIN
          C ITS INTENDED SCOPE. ITS GENERAL CORRECTNESS CANNOT BE GUARANTEED.
000003        DIMENSION  HUM(10),HUMI( 9),TEM(10),TEMI( 9),TEQ( 9),TEQI( 9),HEQ(
             110),HEQI( 9),S(4, 8),SI(4, 8),SD(4, 8,3),SDI(4, 8,3),DS(4, 8),DSD(
             2 4, 8,3),SO(4, 8),SS(5),SSD(5,3),SAD(3),U(10),F(10),A(10,10),ERASE          (10)
             3(10),RKC(3),RKD(3),GC(3),GD(3), PAST(2),    RK( 8),G( 8),RALFA(3),
             4 UNIT(4),RATE(3),RATPSI(3),QU(5,3),CK(3, 8),CG(3, 8),GTOKC(3),RATK          D
             5D(3),RATKC(3),RATDH(3), RATSAD(3), B(10,2),RATSA(3),  DDHUM(9)
             6,FA(5),RIGA(5),SA(5),DSAPR(5),IA(4),HUM2(11),TEM2(11),DDTEM( 9)
             7,HEQ2(11), REINF(5)
             8,  CHAR(5),PLOT(132),SCALE(4),APLOT(3,56),IPLOT(4,56)  ,RATGC(3),
             9  RATGD(3)
          CRATGC(3)  AND RATGD(3)  ARE ADDED
          C THESE ARE THE MINIMUM POSSIBLE DIMENSIONS FOR NEL=8, NU=3 .
          C NDIM MUST BE SET SO THAT DIMENSION BE A(NDIM,NDIM),F(NDIM),B(NDIM,2)
          CK, CG ARRAYS MAY BE OMITTED AND VALUES RECALCULATED WHENEVER NEEDED (ST        ORAGE)
000003        EQUIVALENCE (U(1),F(1),B(1,1)),(HUM2(2),HUM(1)),(TEM2(2),TEM(1))
             1,(S(1,1), DS(1,1), SO(1,1)),  (SD(1,1,1), DSD(1,1,1))
             2,(DDHUM(1),RK(1)),(DDTEM(1),G(1)),(HEQ2(2),HEQ(1))
          C
          C
          C
          C1------------CHARACTERISTICS  OF  MATERIAL-----------------------------
000003        SADH(HUM,HEQ,TEM,TEQ)  =  ((( .985 *TEQ + 20. )/(TEQ + 20. ) - HUM
             1) *  (1.0  +  HEQ))  *((TEM  + 273. )   *  .00336  )
000026        SADQ(HEQ,TEM) =  HEQ**2 * ((TEM-25.)*.014 )
000035        PHI(HEQ,TEM,TEE) = 1.5E-9*(0.9-0.4*HEQ)*((TEE+500.)/(TEE+1.0))
000051        PSI(HEQ,TEM,TEE)= 1.E-8*(1.5-1.0*HEQ)*((TEE+500.)/(TEE+1.))
000065        PHIHDT(DHEQ,HEQ) = 1.5E-4*((ABS(DHEQ))/(HEQ+1.))
000074        PHHDT1(HEQ)=1.0E-6*(HEQ+1.5)
000101        ALFA0( HEQ, TEQ ) = 11.E-6  + HEQ * 23.E-6
000107        DALFA1( HEQ, TEQ ) =  HEQ * 10.E-6
000114        HDIFFU(HEQ,TEQ,DHEQ)=((0.0106+(0.0308/HEQ)-(0.014/HEQ**2))*(0.5
             1+SIGN(0.5,DHEQ))+((0.025*(0.1+HEQ))*(0.5-SIGN(0.5,DHEQ))))   *((
             2  TEQ+4.00)/TEQ)
000144        SORPTI(HEQ)=4.62
000150        DESIC(TEQ)   =(0.985   *TEQ  +  20.0)  /(TEQ  +  20.0)
000160        TKAPA( HUM ) = .009 * ((HUM*(1.003-HUM))/(1.3 - HUM))
000171        EQUIV(H,TEM)=(1./(1.+(7.5-7.5*H)**4)) * 1.000
000201        BBULK(TEQ)=(.86/14.20)*(8.39-(23.62/TEQ)+(68.52/TEQ**2))*1000000.0
000212        CBULK(TEQ)=(1.0/14.2) *(2.9+(-50.0/TEQ)+(221.0/TEQ**2))*1000000.00
000223        DBULK(HEQ) =(85.2/14.2) *(0.05 +HEQ)   * 1000000.000
000232        GBB(TEQ) = (1.0/14.2)* (2.3- 15.0/TEQ  +(50.0/(TEQ**2)))*1000000.0
000244        GCC(TEQ) = (1.0/14.2)* (0.8-14.0/TEQ +(62.0/(TEQ**2))) *1000000.00
000256        GDD(HEQ) = (42.6/14.2) *(0.05+HEQ) * 1000000.000
000265        HYHEAT( TEQ ) = 0.
000271        ADHEAT( HEQ ) = HEQ * 10.
```

```
        C SADH AND SADQ BOTH ACCOUNT FOR SHRINKAGE, SADH..HYGROTH.DILAT.,SADQ..T      H.SWELL.
        C (SADH+SADQ)/RK=INSTANTANFOUS SHRINKAGE
        C  1/(273+25) = .00336 .  (ACCOUNTS FOR CHANGE IN ADS.FILM TENSIUN WITH      TEMP.)
        C PHI IN (KP/CM2)/DAY.      1.E-6=.4/1*4.E5 ..SHORT-TIME CREEP
        C .50E-7 = 1/(1000*4.E5)    ..LONG-TIME CREEP (1 FOR 50 DAYS)
        C PHIHDT IS IN CM2/KP, (..-SIGN..)=1 FOR DHEQ.LT.0., 0 FOR DHEQ.GT.0.
        C ALFAO = INSTANT.THERMAL DEF.,DALFA1= DIFFERENCE BETWEEN HIND.LAYERS AN      D SPRING
        C HDIFFU = ( .1    CM2/DAY) / SORP,    SORP = 1 / POROSITY
        CCC    SURPTI(HEQ) = 2. + HEQ**3 + .5*(1.-HEQ)**3    WOULD BE MURE ACCURA      TE
        C TKAPA - .024 GIVES MAX.KAPPA = .006
        C         HYHEAT = ADIABATIC TEMPERATURE CHANGE DUE TO HYDRATION
        C ADHEAT = ADIABATIC TEMPER.CHANGE DUE TO ADSORPTION. USUALLY IT MAY BE      NEGLECT.
        C THERMAL DIFFUSION COEFF. = TDIFFU = 1200 CM2 / DAY.  POROSITY = 1 / SO      RP
        C EXACTLY, TDIFFU  IS ALSO A FUNCTION (OF HEQ). THEN IT MAY BE INCORPORA      TED INTO
        C THE  PROGRAM IN A SIMILAR MANNER AS  HDIFFU .
000275        DATA RATGD/1.,1.,1./,  PERCNT/.005 /, RATGC/1.,1.,1./,
             1               RATKC/1.,  .7/, RATKD/ 1., .5/, RATDH/1.,1./, RAREA/
             211.5/, IH3/ 21/,  RATE/1.,300.,0./,RATPSI/1.,1.,1./,          RALFA/
             3 1., 1. /,RATSAD/10.0,0., 0. /,RATSA/0.,0.,0./, PSPH/.5/,EB/0. /
             4,FD/.05 /, IA/3,2,1,1/,  REINF/1.,0.,0.,0.,1./, SORPIR/1.5/
        C E = K(1 - 2 MI) = 3KG/(K+G), 2G = K(1 - 2 MI)/(1 + MI), MI=(.5-G/K)/(1      .+G/K)
        C GTOKC IS GREATER FOR LONG TIME THAN FOR SHORT TIME.    RAREA =      FA      / FD1
        C RATPSI = PSI/PHI, CORRESP.TO K/G RATIO, MUST BE .GT.2.  GTOKB=GB/KB (.      LT. .5)
        C RATE = PHI(IU)/PHI(1).  PERCNT=PERCENTAGE OF REINF.(OF CROSS SECTION)      FOR FA=1
        C PSPH=2. IMPLIES THAT POISS.RATIO FOR DRYING CREEP = 0.
        CHOOSE  IU=1 ..SLOWEST CREEP, IU=NU ..FASTEST CREEP  (ARRAYS RATE,PAST,R      KC...)
        C
        C
        C
        C2--------------------------------OTHER INPUT DATA------------------------------------------
000275        DATA IEX/1/,NDIM/10/, K2/2/,KSTEP/1/,NITER/2/, PAST/1.E9,1.E9/
             1,T10,T11,H10,H11/0.,0.,0.,0./,TORQLD/2410. /,UNIT/1.,1.,1.,0./
        C FOR HIGH HUM, TENSION IN CAPILLARY WATER = 1360.*LOG.NAT.(HUM)  AT 25      DEG C
000275        FD = FD * 1360.
000277        FAO = FD * RAREA
000301        READ(5,4)  AJ
000306      4 FORMAT(   1A1    )
000306     10 READ(5,11) LOPT,NEL,NU,NT,NPRINT,MPRINT,  TIMEO,TSTART,HSTART,
             1 AL,SW,HY,  TDISTO,TDIST1,HDISTO,HDIST1
000352        IF(LOPT.EQ.99999)  STOP
000356        READ(5,13)             DT,  IT1,IT2,TO,T1,STEPT,  IH1,IH2,HO,H1,
             1STEPH,  IP1,IP2,DPOO,DP11,STEPP,  IL1,IL2,DLD,DLD1,PREST,
             2 RELAX,   RO,R1,   REVER, TDIFFU, EA
             3,(SCALE(J),J=1,4),  (CHAR(J),J=1,4), BLANK
        C IF TEMPERATURE IS TIME CONSTANT, PUT  TDIFFU = 0.
        C OPTION LOPT=77 MEANS THAT INTERNAL HUM.AND TEMP.CHANGE IS IMMEDIATE.
000466     11 FORMAT(  6I5,  6F5.1,  4F5.1  )
000466     13 FORMAT( F5.1, 3(2I5,3F5.1) / 2I5,3F5.1,  5F5.1, 5E5.1,5A1 )
        C
        C
        C
        C3----------------READ  AND  WRITE  DATA  ---------------------------
000466        WRITE(6,12)IEX, LOPT,NEL,NU,NT,NPRINT,MPRINT, TIMEO,TSTART,HSTART,
             1 AL,SW,HY,  TDISTO,TDIST1,HDISTO,HDIST1,    DT, IT1,IT2,TO,T1,
```

```
              2STEPT, IH1,IH2,HO,H1,STEPH, IP1,IP2,DP00,DP11,STEPP, IL1,IL2,DLD,
              3 DLD1,PREST,   RELAX,   RO,R1,   REVER, TDIFFU, EA
              4,(SCALE(J),J=1,4),  (CHAR(J),J=1,4), BLANK, AJ
000642      12 FORMAT( 1X /  5HOCASE  3X
              1          125HLOPT     NEL      NU      NT  NPRINT  MPRINT   TIMEO
              2 TSTART  HSTART      AL      SW      HY  TDISTO  TDIST1  HDISTO  H       DIST1
              3DIST1  /2XI2,6I8,6F8.2,        1P 4E8.0 / 10X 122HDT     IT1     IT      2
              42       TO       T1    STEPT     IH1     IH2      HO      H1   STEPH
              5    IP1     IP2     DP00    DP11   STEPP /4XOP F8.3, 3(2I8,3F8.2) /
              69X124HIL1     IL2     DLD    DLD1   PREST   RELAX      RO      R1
              7  REVER  TDIFFU     EA SCALE(1)   ..(2)   ..(3)   ..(4)   CHAR   /
              8  4X 2I8,  4F8.1,  4F8.2,  1P 5E8.1,  3X 6A1         )
         C IF DEFORMATION WITHOUT SHRINKAGE IS WANTED, PUT HY=0.,SW=0.   WITHOUT       THERMAL
         C DILATATION...PUT AL=0..  WITHOUT ALL OF THESE...PUT FD=0.
000642         IF( NEL .EQ. 1 )    STOP
000646         IF( NPRINT .LT. 200 )    WRITE(6,14)
000654      14 FORMAT(       133HO IT  TIME   DEFZ       DEFX      SHSTN     COMPLI
              1     RIGT       FORCE     SI(1,K)   SI(2,K)   SI(3,K)   SI(4,K)     T
              2EQI     TEMI    HUMI                        )
         C
         C
         C
         C4------------------DIVISION  OF  BODY  INTO FINITE  ELEMENTS-----------
000654         NNODE = NEL + 1
000656         NA = NNODE + 1
000657         THICK = R1 - RO
000661         DX = THICK / FLOAT( NEL )
000663         DX5 = DX * .5
000665         DX2 = DX * 2.
000667         DX1 =  1. / DX
000670         DX4 = DX * .25
000672         DX2IN = 1. / DX**2
000674         DX5IN =  .5 / DX
000676         NUO = NU
000677         DTIME = DT
000701         DTX2 = DT / DX**2
000703         IF( RO .EQ. 0. )    TDISTO = 1.E25
000705         IF( RO .EQ. 0. )    HDISTO = 1.E25
000710         IF( RO .EQ. 0. )    RO = 1.E-25
000712         ROO = RO - DX * .5
000715         RO1 = 1. / THICK
         C IF(2.*DX.GT.TDISTO) TDISTO=0 ASSUMED. SIMILARLY FOR HDISTO, TDIST1,HDI       ST1.
000717          IF (TDISTO .GE.  DX2)  T10= DX2/TDISTO
000723         IF (TDIST1 .GE. DX2 )  T11=DX2/TDIST1
000726         IF( HDISTO .GE. DX2 )  H10 = DX2 / HDISTO
000731           IF( HDIST1 .GE. DX2 )  H11 = DX2 / HDIST1
         C REINFORCEMENT. FA(5) = LONGITUDINAL, FA(1-4) = CIRCUMFERENTIAL IN K =       IA(J)
         C REINFORCEMENT, FA(5)..LONGITUDINAL, (FA(J),J=1,4)..HOOP(PER HEIGHT=1),      K=IA(J)
000734         DO 6  J = 1, 5
000736         SA(J) = 0.
000737         FA(J) = 0.
000740       6 RIGA(J) = 0.
000743         IF( EA .EQ. 0. )  GO TO 21
000744         FA(5) = (THICK*((RO+R1)*.5)) * (REINF(5) * PERCNT)
```

```
000753         RIGA(5) = (EA - EB) * FA(5)
000756         DO 46  J = 1, 4
000757         FA(J) = THICK * (REINF(J) * PERCNT)
000762         X = RO + DX * FLOAT( IA(J) - 1 )
000767      46 RIGA(J) =((EA - EB)*FA(J)) / X**2
        C
        C
        C
        C5----------------ASSINGING  INPUT DATA TO NODAL  POINTS---------------
000775      21 DO 29  K = 1, NNODE
000777         TEM(K) = TSTART
001001         TEMI(K) = TEM(K)
001003         HUM(K) = HSTART
001004         HUMI(K) = HUM(K)
001006         HEQ(K) = HUMI(K)
001010         HEQI(K) = HEQ(K)
001012         TEQ(K) = TIMEO
001013      29 TEQI(K) = TEQ(K)
001017         Q=FD*(HY*SADH(HSTART,HSTART,TSTART,TIMEO)+SW*SADQ(HSTART,TSTART))
001031         DO 30  K =  1, NEL
001032         DO 30  IS = 1, 4
001033         S(IS,K) = 0.
001036         SI(IS,K) = 0.
001040         DO 30  IU = 1, NU
001042         SD(IS,K,IU) =(RATSAD(IU) * Q) * UNIT(IS)
001051      30 SDI(IS,K,IU) = SD(IS,K,IU)
001066         DEFZ = 0.
001067         DEFX = 0.
001070         ANGLE = 0.
001071         EXPAN = 0.
001072         HEXTO = HSTART
001073         HEXT1 = HSTART
001074         TEXTO = TSTART
001075         TEXT1 = TSTART
001076         TIME = TIMEO
001077         IT = 0
        C
        C
        C
        C6----------------  STEP  BY  STEP  INTEGRATION  ---------------------
001100     100 IT = IT + 1
001102         DT = DTIME
001103         NU = NUO
001105         IF( TIME .GT. PAST(2) )   NU = 2
001110         IF( TIME .GT. PAST(2) )   DT = 10. * DTIME
001114         IF( TIME .GT. PAST(1) )   NU = 1
001120         IF( TIME .GT. PAST(1) )   DT = 100. * DTIME
001124         IF( TIME .GT. PAST(1) )   LOPT = 77
        C ENABLES ANALYSIS FOR WIDE RETARDATION SPECTRUM AND STEADY LOADING
        C
        C
        C
        C7----------------GENERATION  OF  LOADE  AND  BOUNDARY CONDITIONS-----
        C LOADS (AND REINFORCEMENT) MUST BE GIVEN PER RADIAN SECTION OF CYLINDER
```

```
        C DNLOAD IS POSITIVE FOR TENSION, DLD FOR COMPRESSION
001127        DNLOAD = 0.
001130        IF(IT.EQ.IL1) DNLOAD = - DLD
001134        DTLOAD = 0.
001135        IF(IT.EQ.IL1)     DTLOAD=TORQLD
001140        PRESTR = 0.
001141        IF(IT.EQ.IL1) PRESTR = PREST
001144        DPO  = 0.
001145        IF(IT.EQ.IP1) DPO = DPOO
001150        DP1 = 0.
001151        IF(IT.EQ.IP1) DP1 = DP11
001154        IF(IT.EQ.IL2)   DNLOAD = DLD
001160        IF(IT.EQ.IL2)     DTLOAD=-TORQLD
001163        IF((DNLOAD.NE.0..OR.PRESTR.NE.0.).OR.(DPO.NE.0..OR.DP1.NE.0.))
             1 DT = 1.E-38
001200        DTEXO = 0.
001201        DTEX1 = 0.
001202        IF(IT.EQ.IT1) DTEXO = TO - TEXTO
001206        IF(IT.EQ.IT1) DTEX1 = T1 - TEXT1
001211        DHEXO = 0.
001212        DHEX1 = 0.
001213        IF(IT.EQ.IH1) DHEXO = HO - HEXTO
001217        IF(IT.EQ.IH1) DHEX1 = H1 - HEXT1
001222        IF( STEPT .EQ. 0. )    GO TO 121
001223        DTEXO = 0.
001224        DTEX1 = 0.
001225        IF(IT.LT.IT2)  DTEXO = STEPT
001230        IF(IT.LT.IT2)  DTEX1 = STEPT
001233    121 IF( STEPH .EQ. 0. )    GO TO 122
001234        DHEXO = 0.
001235        DHEX1 = 0.
001236        IF(IT.LT.IH2)  DHEXO = STEPH
001241        IF(IT.LT.IH2)  DHEX1 = STEPH
001244    122 DO 118  J = 1, 5
001246    118 DSAPR(J) = PRESTR
001251        TIME = TIME + DT
001253        DT5 = DT * .5
001255        IF( DT .GE. 1.E-37 )    GO TO 119
001257        IF( IT .EQ. IH1 )    IH1 = IH1 + 1
001262        IF( IT .EQ. IT1 )    IT1 = IT1 + 1
001265        GO TO 201
        C
        C
        C
        C8----------------- IMMEDIATE  HUMIDITY  AND  TEPERATURE  CHANGE ------
001266    119 IF( LOPT .NE. 77 )     GO TO 177
        C IF THE WALL THICKNESS IS SMALL OR DT TOO LONG, TEMPERATURE AND HUMIDIT          Y CHANGE
        C MAY BE CONSIDERED TO BE IMMEDIATE.
001270        DTEQ = DT * EQUIV( HUM(1),TEM(1))
001274        IF( HDISTO .NE. 0.  .AND.  HDIST1 .NE.0. )
             1HUM(1)=HUM(1)+DESIC(TEQ(1)+DTEQ)-DESIC(TEQ(1))
001312        IF( HDIST1.EQ.0.)  HUM(1) = HUM(1) + DHEX1
001315        IF(HDISTO.EQ.0. .AND. DHEX1.EQ.0.)  HUM(1) = HUM(1) + DHEXO
001325        IF( TDISTO .EQ. 0. )  TEM(1) = TEM(1) + DTEX1
```

```
001330          HUM(1)                         = HUM(1) + DTEX1 * TKAPA( HUM(1) )
001334           DO  176  K=1,NNODE
001336          HUM(K) = HUM(1)
001340          TEQ(K)=TEQ(K)+DTEQ
001343          HEQ(K)=HUM(K)
001344      176 TEM(K) = TEM(1)
001351          GO TO 201
          C
          C
          C
          C9-----------------HUMIDITY  DIFFUSION  ,  TEAT  CONDUCTION  -----------
          C FOR CONVERGENCE IN FORWARD DIFFERENCES,DT MUST BE .LE. DX**2 /(C*2.)
          C THEREFORE DT  IS SUBDIVIDED IN SMALLER STEPS DDT.
          C ITERATION WITH MEAN VALUES IN STEP WOULD BE NUMERICALLY UNSTABLE
001351      177 IDIV = INT( DTX2 * ( TDIFFU * 4.  ) )  + 1
001355          IF(IT.EQ.  1)   DHEQ=-0.00001
001360          IDIVH = INT( DTX2 * ((SORPTI(1.)*HDIFFU(1.0,TIMEO,DHEQ))  *
               1  4.00  ))+1
001371          IF(IDIV.LE.100 .OR.(TDIST1.NE.0..AND.TDISTO.NE.0.)) GO TO 179
001403          IDIV = IDIVH
001404          TDIFFU = 1.E25
          C IN THIS CASE INSTANTANEOUS INTERNAL TEMPERATURE CHANGE IS ASSUMED
001405      179 IF( IDIVH .GT. IDIV )   IDIV = IDIVH
001410          IF(IDIV .GT. 1000)   STOP
001415          DDT = DT / FLOAT( IDIV )
001420          DDTEXO= DTEXO / FLOAT(IDIV)
001422          DDTEX1= DTEX1 / FLOAT(IDIV)
001424          DDHEXO = DHEXO / FLOAT(IDIV)
001426          DDHEX1 = DHEX1 / FLOAT(IDIV)
001430          TDIFFT = TDIFFU * DDT
001432          DO 203  ITT = 1, IDIV
001433          TEXTO = TEXTO + DDTEXO
001435          TEXT1 = TEXT1 + DDTEX1
001437          HEXTO = HEXTO + DDHEXO
001441          HEXT1 = HEXT1 + DDHEX1
          C EXTRAPOLATED VALUE OUTSIDE THE CYLINDER
001443          TEM2(1) = TEM(2) + T10 * (TEXTO - TEM(1))
001447          TEM(NA) = TEM(NEL) + T11 * (TEXT1 - TEM(NNODE))
001455          HUM2(1) = HUM(2) + H10 * (1. - HUM(1) / HEXTO)
001462          HUM(NA) = HUM(NEL) + H11 * (1. - HUM(NNODE) / HEXT1 )
001471          HEQ2(1) = 2.*HEQ(1) - HEQ(2)
001474          HEQ(NA) = 2.*HEQ(NNODE) - HEQ(NEL)
001501          XX = RO
001502          DO 200  K = 1, NNODE
001504          K1 = K + 1
          C BECAUSE OF EQUIVALENCE, HUM2(K) = HUM(K-1), TEM2(K) = TEM(K-1), K1 = K          +1
001506          DTEQ = DDT * EQUIV( HUM(K), TEM(K) )
001511          TEQQ = TEQ(K) + DTEQ
001513          DDESIC = DESIC( TEQQ ) - DESIC( TEQ(K) )
001520          SORT = SORPTI( HEQ(K) ) * DDT
001524          Q1 = ( TEM(K1) - 2.*TEM(K) + TEM2(K) )*DX2IN
001532          Q2 = ( HUM(K1) - 2.*HUM(K) + HUM2(K) )*DX2IN
001540          DERDIF=(HDIFFU(HEQ(K1),TEQ(K1),DHEQ) - HDIFFU( HEQ2(K),TEQQ,DHEQ))
               1*DX5IN
```

```
001550          DERHUM = ( HUM(K1) - HUM2(K) ) * DX5IN
001553          IF( XX .GE. DX4 )  GO TO 187
001556          DDTEM(K) = 2.*( TDIFFT * Q1 )
001561          DH=(2.*SQRT)*(HDIFFU(HEQ(K),TEQ(K),DHEQ)*Q2)
001567          GO TO 188
001570      187 DDTEM(K) = TDIFFT*( Q1 + ((TEM(K1)-TEM2(K))*DX5IN)/XX)
001600          DH=SQRT*(HDIFFU(HEQ(K),TEQ(K),DHEQ)*(Q2+DERHUM/XX)+DERDIF*DERHUM)
001612      188 DHEQ = DH + DDESIC
          C IRREVERSIBILITY OF DESORPTION ISOTHERM
001614          IF( DHEQ .GT. 0. )   DHEQ = DH * SORPIR  + DDESIC
001620          IF(K.EQ.1.AND.HDISTO.LT.DX2) DHEQ = HEXTO - HUM(1)
001634          IF(K.EQ.NNODE.AND.HDIST1.LT.DX2) DHEQ = HEXT1 - HUM(NNODE)
001650          HEQQ = HEQ(K) + DHEQ
001653          IF( TDIFFU .NE. 0. )   DDTEM(K) = DDTEM(K) +
               1   HYHEAT(TEQQ)-HYHEAT(TEQ(K))+ADHEAT(HEQQ)-ADHEAT(HEQ(K))
001671          IF( K.EQ.1.AND.TDISTO.LT.DX2) DDTEM(1) = TEXTO - TEM(1)
001705          IF(K.EQ.NNODE.AND.TDIST1.LT.DX2) DDTEM(K) = TEXT1 - TEM(NNODE)
001722          DDHUM(K) = DHEQ + DDTEM(K)*TKAPA( HUM(K) )
          C VALUES AT THE END OF THE SMALL STEP  DDT
001730          HEQ(K) = HEQQ
001732          TEQ(K) = TEQQ
001734      200 XX = XX + DX
001740          DO 202  K = 1, NNODE
001741          HUM(K) = HUM(K) + DDHUM(K)
001743      202 TEM(K) = TEM(K) + DDTEM(K)
          CONDITIONS OF UNINSULATED SURFACE (FOR TDISTO,TDIST1 THEY ARE ALREADY SA          TISFIED)
001750          IF( HDISTO .LT. DX2 )  HUM(1) = HEXTO
001754          IF( HDIST1 .LT. DX2 )  HUM(NNODE) = HEXT1
001761          IF( TDIFFU .LT. 1.E24 )    GO TO 203
001764          DO 204   K = 1, NNODE
001765      204 TEM(K) = TEXT1
001771      203 CONTINUE
          C NOW HUM(K),..= FINAL VALUES IN THE BIG STEP DT
          C
          C
          C
          C10 ----- STRESS, DEFORMATION ANALYSIS WITH FINITE ELEMENT ------------
001774      201 DO 446  K = 1, NNODE
001776      446 B(K,2) = 0.
002003          B(NA,2) = 1.
002005          ITER = 0
002006      450 ITER = ITER + 1
002010          DO 452  K = 1, NA
002011          F(K) = 0.
002012          DO 452  L = 1, NA
002014      452 A(K,L) = 0.
002025          TORQO = 0.
002026          RIGT = 0.
002027          X = ROO
002030          DO 600  K = 1, NEL
002032          X = X + DX
002034          K1 = K+1
002036          TEMI5 = ( TEMI(K) + TEMI(K1) )*.5
002041          TEMF = ( TEM(K) + TEM(K1) )*.5
```

```
002044          DTEM = TEMF - TEMI5
002046          TEM5 = TEMI5 + DTEM *.5
002050          HUMI5 = ( HUMI(K) + HUMI(K1) )*.5
002054          HUMF = ( HUM(K) + HUM(K1) )*.5
002057          DHUM = HUMF - HUMI5
002061          HUM5 = HUMI5 + DHUM*.5
002063          HEQI5 = ( HEQI(K) + HEQI(K1) )*.5
002067          HEQF = ( HEQ(K) + HEQ(K1) )*.5
002072          DHEQ = HEQF - HEQI5
002074          HEQ5 = HEQI5 + DHEQ *.5
002076          TEQI5 = ( TEQI(K) + TEQI(K1) )*.5
002102          TEQF = ( TEQ(K) + TEQ(K1) )*.5
002105          TEQ5 = ( TEQI5 + TEQF )*.5
          C
          C
          C
          C11 --------------- MATERIAL  PARAMETERS  -----------------------------
002107          SAD(1)=FD*(HY*SADH(HUM5,HEQ5,TEM5,TEQ5)+SW*SADQ(HEQ5,TEM5))
002121          DSA=FAO*(HY*(SADH(HUMF,HEQF,TEMF,TEQF)-SADH(HUMI5,HEQI5,TEMI5,
               1 TEQI5)) )
002132          DO 490  IU = 1, NU
002133          SAD(IU) = SAD(1) * RATSAD(IU)
          C FORM VOLUMETRIC AND DEVIATORIC COMPONENTS OF STRESS IN HINDERED LAYERS
002135          SSD(5, IU) = (SD(1,K,IU)+SD(2,K,IU) + SD(3,K,IU) )/3.
002150          DO 490  IS = 1, 4
002152      490 SSD(IS,IU) = SD(IS,K,IU) - SSD(5,IU) * UNIT(IS)
          C  ELASTIC (SPRING) CONSTANTS OF THE RHEOLOGICAL MODEL
002172          RKB = BBULK( TEQ5 )
002174          GB=GBB(TEQ5)
002176          GC=GCC(TEQ5)
002200          GD=GDD(HEQ5)
002202          RKC(1) = CBULK ( TEQ5 )
002204          RKD(1) = DBULK ( HEQ5 )
002206          DO 460  IU = 1, NU
002207          RKC(IU) = RKC(1) * RATKC(IU)
002211          GC(IU)=RATGC(IU)*GC
002213          GD(IU)=RATGD(IU)*GD
002215      460 RKD(IU) = RKD(1) * RATKD(IU)
          CHECK FOR UNLOADING  (RACHET SNAP-IN)
002221          IF( REVER .EQ. 1. )   GO TO 467
002223          SV = (S(1,K) + S(2,K) + S(3,K) ) / 3.
002233          SVI = (SI(1,K) + SI(2,K) + SI(3,K)) / 3.
002241          Q  = SAD(1) * RAREA
002243          DO 465  IU = 1, NU
002244          IF((SV -Q)*(SSD(5,IU)-SAD(IU)).LT.0.) RKC(IU)=RKC(IU)*REVER
002254          SUM = 0.
002255          SVSDVI = SVI - (SDI(1,K,IU)+SDI(2,K,IU)+SDI(3,K,IU))/3.
002270          DO 463  IS = 1, 4
002272          STR = S(IS,K) - SV*UNIT(IS) - SSD(IS,IU)
002301          DSTR5 = STR - SI(IS,K) + SDI(IS,K,IU) + SVSDVI * UNIT(IS)
002313      463 SUM  =  SUM + (STR*DSTR5)*(2.-UNIT(IS))
002322      465 IF( SUM .LT. 0. )  GC(IU) = GC(IU) * REVER
002331      467 SUMK = 1. / RKB
002333          SUMG = 1. / GB
```

```
002335          DO  469  IU = 1, NU
002336          Q1 = 1./( RKC(IU) + RKD(IU) )
002341          Q2 = 1./( GC(IU) + GD(IU) )
002344          CK(IU,K) = RKD(IU) * Q1
002347          CG(IU,K) = GD(IU) * Q2
002353          SUMK = SUMK + Q1
002355      469 SUMG = SUMG + Q2
002360          RK(K) = 1. / SUMK
002363          G(K) = 1. / SUMG
        C
        C
        C
        C12----------------INELASTIC STRAINS, STRESSES IN HINDERED LAYERS-------         --------
        C FORM COEEFICIENTS FOR SO AND DSD, CREEP RATE PARAMETERS
002365          TEE=(IT-IL1) * DT
002371          PHIDT1 = DT * PHI( HEQ5, TEM5, TEE)
002375          IF(IT.GE.IH3)  GO TO 222
002377          GO TO 333
002400      222 CONTINUE
002400          DTPHIH=PHHDT1(HEQ5)
002402          GO TO 444
002402      333 DTPHIH = PHIHDT( DHEQ, HEQ5 )
002405      444 DTPSIH = DTPHIH * PSPH
002407          DO 500  IU = 1, NU
002411          PHIDT = PHIDT1 * RATE(IU)
002413          PSIDT1=DT*PSI(HEQ5,TEM5,TEE)
002417          PSIDT=PSIDT1*RATPSI(IU)
        C   BECAUSE PHI IS MADE A FUNCTION OF ELAPSED TIME SINCE LOADING) TEE IS           BEEN
        C  INTRODUCED TO REPRESENT THE TIME SINCE LOADING IN DAYS .  REGARDLESS          OF  TEQ
        C DTPHIH = DHEQ/RKH(1),DTPSIH=DHEQ/GH(1)Y PHI = CK*PHID, CK = NU, CG = N          U PRIME
        C QU = (EPSILON PRIME)(VOLUMETRIC) OR(2.* E PRIME)(DEVIATORIC)
        C SAD = SD FOR THERMODYNAMIC EQUILIBRIUM
002421          QU(5,IU)= PHIDT*(SSD(5,IU)-SAD(IU))+(DTPHIH*RATDH(IU))*SSD(5,IU)
002433          DO 500  IS = 1, 4
002434      500 QU(IS,IU) = (PSIDT + DTPSIH*RATDH(IU)) * SSD(IS,IU)
        C BECAUSE OF EQUIVALENCE  S  AND DS  MAY NOT BE USED UNTIL BEFORE 623
        COMPUTE INITIAL STRAINS AND CORRESPONDING PRESTRESSES
002453          SUM = 0.
002454          DO 510  IU = 1, NU
002455      510 SUM = SUM + QU(5,IU)
        C DSA..INSTANT.SHRINKAGE, ALFAO..INSTANT,THERM.DILAT.
002463          SVO = - DSA + ((AL*ALFAO(HEQ5,TEQ5))*DTEM + SUM) * RK(K)
002473          DO 520  IS = 1, 4
002475          SUM = 0.
002476          DO 515  IU = 1, NU
002500      515 SUM = SUM + QU(IS,IU)
002506      520 SO(IS,K) =  SUM * G(K)  + SVO * UNIT(IS)
        COMPUTE AND STORE PARTS OF THE EXPRESSION FOR DSD (LATER ADD ONLY TERMS          WITH DS)
002516          DALFA = DALFA1( HEQ5, TEQ5 ) * AL
002521          DO 530  IU = 1, NU
002522          SSD(5,IU) = - RKC(IU)*(QU(5,IU)+DTEM*(DALFA*RALFA(IU)))
               1             -(DSA*RATSA(IU)) * CK(IU,K)
002537          DO 530  IS = 1, 4
002541      530 DSD(IS,K,IU) = - GC(IU)*QU(IS,IU) + SSD(5,IU)*UNIT(IS)
```

```
        C BECAUSE OF EQUIVALENCE  SD  MAY NOT BE USED UNTIL 626
        C
        C
        C
        C13--------------------FINITE ELEMENTS (RECTANGULAR RINGS)-------------         --------
        C STIFFNESS A  * NODAL DISPL.U = GIVEN NODAL LOADS - FORCES BALANCING DI         STRIBUT.
        C LOADS  - FORCES BALANCING INITIAL STRAINS
        C FORM ELEMENT STIFFNESS MATRIX AND SUPERPOSE IT ON TOTAL STIFFNESS MATR         IX
002562        Q = RK(K) + 4.*G(K)
002566        EE = Q / 3.
002570        RMII = ( RK(K) - 2.*G(K) ) / Q
002574        Q = X * DX1
002576        Q1 = DX4 / X
002577        Q2 = Q + Q1
002601        Q5 = X * DX
002602        A(K,K) = ( Q2 - RMII ) * EE  + A(K,K)
002610        A(K1, K1)  = ( Q2 + RMII ) * EE + A(K1,K1)
002616        A(NA,NA) =    Q5  * EE + A(NA,NA)
002622        A(K,K1)  = ( Q1 - Q ) * EE +A(K,K1)
002631        A(K,NA) =   -(RMII * (X - DX5)) * EE  + A(K,NA)
002640        A(K1, NA) =  ( RMII * (X+DX5)) * EE  + A(K1, NA)
002647        A(K1, K) = A(K, K1)
002654        A(NA,K) = A(K,NA)
002661        A(NA,K1) = A(K1,NA)
002665        RIGT = RIGT + (Q5 * X) * G(K)
        C
        C
        C
        C14---------------RIGHT-HAND SIDE OF EQUILIBRIUM EQUATIONS-------------         --------
        C RIGHT-HAND SIDE = (TRANSP.GEOM.MATR.) *(INITIAL STRESS)* X * DX
002672        TORQO = TORQO + Q5 * SO(4,K)
002675        Q3 = X * SO(1,K)
002700        Q4 = DX5 * SO(2,K)
002703        F(K) = Q4 - Q3 + F(K)
002706        F(K1) = Q4 + Q3 + F(K1)
002711    600 F(NA) =  Q5 * SO(3,K)    + F(NA)
        C
        C
        C
        C15-------------------------------------------------------------------         --------
        C ADD STIFFNESS DUE TO REINFORCEMENT
002720        IF( EA .EQ. O. )   GO TO 608
002721        A(NA,NA) = A(NA,NA) + RIGA(5)
002725        F(NA) = F(NA) - DSAPR(5)*FA(5)
002730        DO 606  J = 1, 4
002732        K = IA(J)
002734        X = RO + DX*FLOAT(K-1)
002740        A(K,K) = A(K,K) + RIGA(J)
002744    606 F(K) = F(K) - (DSAPR(J) * FA(J))/X
002752    608 F(NA) = F(NA) + DNLOAD
002755        TORQ = TORQO + DTLOAD
        C LATERAL EQUILIBRIUM - EXTERNAL PRESSURE CHANGES  DPO, DP1
002757        F(1) = F(1)  + RO * DPO
002762        F(NNODE) = F(NNODE) - R1 * DP1
```

```
        C IN CASE OF A SOLID CYLINDER, RO = 0.     ... U(1) = 0.
002766        IF( RO .LT. DX4 )  A(1,1) = 1.E38
002772        IF(RELAX.EQ.1. .AND. IT.NE.IL1)  A(NA,NA) = 1.E38
        C
        C
        C
        C16================SOLUTION OF A SYSTEM OF LINEAR ALGEBRAIC EQUATIONS===          ========
        C SOLVED DISPLACEMENTS U(K) ARE STORED IN F(K). FOR TORSION ONE SEPARATE           EQUAT.
        C ERA E SEROES  FOR STORAGE IN THE SUBROUTINE, DIMENSI N ERASE( NA )
003006        NDIM=NA
003010        N=NA
003011        SCALE=0.
003012        IF(ITER.EQ.NITER.AND.((IT-1)/NPRINT)*NPRINT.EQ.IT-1) GO TO 613
003027        N1=1
003030        B=F
003031        LINEQ=LNEQF(NDIM,N,N1,A,B,SCALE,ERASE)                                     AU=F
003041        GO TO 614
003041    613 N1=2
003042        LINEQ=LNEQF(NDIM,N,N1,A,B,SCALE,ERASE)
003052    614 IF( LINEQ .NE. 1 )     STOP
003056        DANGLE = TORQ  / RIGT
        C
        C
        C
        C17-----------------------------------------------------------------------         --------
        CALCU ATE S R+SSES  = ELAST.MASTR. * GEOM.MATR. * NODA  DISPL.  - PRESTR          ESS  SO
        C SO = ELASTICITY MATRIX * INITIAL STRAINS
003060        X = ROO
003062        DO 626  K = 1, NEL
003063        X = X + DX
003065        Q2 = .5 / X
003067        Q=RK(K)+4.*G(K)
003072        EE = Q / 3.
003074        RMII = ( RK(K) - 2.*G(K) ) / Q
003100        Q3 = DX1 * RMII
003102        Q4 = Q2 * RMII
003103        Q7 = RMII * U(NA)
003105        K1 = K + 1
003107        DS(1,K) = ((Q4-DX1)*U(K)+(Q4 +DX1)*U(K1)  + Q7 ) * EE  - SO(1,K)
003125        DS(2,K) =((Q2-Q3)*U(K)+(Q2+Q3)*U(K1)  + Q7 ) * EE - SO(2,K)
003140        DS(3,K) = ((Q4-Q3)*U(K)+(Q4+Q3)*U(K1)  + U(NA)) * EE - SO(3,K)
003154        DS(4,K) = (DANGLE * X) * G(K)  - SO(4,K)
        C INCREMENTS OF STRESS IN HINDERED LAYERS - VOLUMETRIC AND DEVIATORIC,TH          EN TOTAL
003162        DSV = ( DS(1,K) + DS(2,K) + DS(3,K) ) / 3.
003170        DO 623  IU = 1, NU
003171        SSD(5,IU) = CK(IU,K) * DSV
003176        DO 623  IS = 1, 4
003177        SSD(IS,IU) = CG(IU,K)*(DS(IS,K) - DSV*UNIT(IS))
003210    623 DSD(IS,K,IU) = DSD(IS,K,IU) + SSD(IS,IU) + SSD(5,IU)*UNIT(IS)
        C PART OF DSD IS CALCULATED EARLIER
        CALCULATE TOTAL STRESS VALUES IN THE MIDDLE OF STEP DT
003225        DO 626  IS = 1, 4
003227        S(IS,K) = SI(IS,K) + DS(IS,K) * .5
003236        DO 626  IU = 1, NU
```

```
003240     626 SD(IS,K,IU) = SDI(IS,K,IU) + DSD(IS,K,IU) * .5
003264         IF( ITER .LT. NITER )  GO TO 450
         C
         C
         C
         C18============================================================================   ========
         C VALUES AT THE END OF INTERVAL DT (INITIAL VALUES FOR THE NEXT STEP DT          )
003266         FORCE = 0.
003267         DO 661  K = 1, NNODE
003270         HUMI(K) = HUM(K)
003272         TEMI(K) = TEM(K)
003273         TEQI(K) = TEQ(K)
003275     661 HEQI(K) = HEQ(K)
003300         X = R00
003302         DO 664  K = 1, NEL
003303         X = X + DX
003305         DO 663  IS = 1, 4
003307         SI(IS,K) = 2.*S(IS,K) - SI(IS,K)
003315         S(IS,K) = SI(IS,K)
003320         DO 663  IU = 1, NU
003321         SDI(IS,K,IU) = 2.*SD(IS,K,IU) - SDI(IS,K,IU)
003331     663 SD(IS,K,IU) = SDI(IS,K,IU)
003342     664 FORCE = FORCE + SI(3,K) * X
         C FORCE = FORCE ACTING IN CONCRETE PART ONLY
003350         FORCE = FORCE * DX
003351         IF( EA .EQ. 0. )   GO TO 643
         C STRESSES IN REINFORCEMENT, EVENTUALLY PRESTRESSED
003352         SA(5) = SA(5) + EA * U(NA) + DSAPR(5)
003356         DO 641  J = 1, 4
003360         K = IA(J)
003362         X = R0 + DX * FLOAT(K-1)
003366     641 IF(FA(J).NE.0.) SA(J) = SA(J) + EA*(U(K)/X) + DSAPR(J)
         C DEFORMATIONS AND COMPLIANCE
003377     643 COMPLI = B(NA,2)
003401         DEFZ = DEFZ + U(NA)
003403         DEFX = DEFX + ( U(NNODE) - U(1) ) * R01
003410         ANGLE = ANGLE + DANGLE
003412         EXPAN = EXPAN + U(NNODE)
003414         SHSTN=ANGLE/(2.*3.14)
         C     ANGLE IS THE RELATIVE  SPECIFIC ANGLE   WHILE  SHSTN IS THE SHEAR            STRAIN
         C
         C
         C
         C19*****************************************************************OUTPUT*     ********
         C STRESSES ARE GIVEN IN CENTERS OF ELEMENTS, ALL OTHER VALUES IN NODAL P        OINTS
         C S(3,K)=AXIAL STRESS, S(1,K)=RADIAL, S(2,K)=HOOP, S(4,K)=SYZ=SHEAR
         C VALUE OF FORCE SERVES AS A CHECK (IN RELAXATION DEFZ IS A CHECK)
003416         IF( NPRINT .GE. 200 )   GO TO 910
003420         IF(((IT-1)/NPRINT)*NPRINT.EQ.IT-1)   WRITE(6,777) IT, TIME, DEFZ,
              1 DEFX, SHSTN, COMPLI, RIGT, FORCE, (SI(IS,1),IS=1,4), TEQI(1),TEMI
              2 (1), HUMI(1)
003466     777 FORMAT(1H  I3, F8.2, 10(1PE10.2), 0PF9.2, F7.1, F6.3 )
003466         IF(((IT-1)/MPRINT)*MPRINT.NE.IT-1)   GO TO 910
003475         DO 781  K = K2, NEL, KSTEP
```

```
003477      781 WRITE(6,778) K,HEQI(K),(SI(IS,K),IS=1,4),TEQI(K),TEMI(K),HUMI(K)
003526      778 FORMAT(47X 2HK= I2,3X6H(HEQI=F6.3,1H)3X 1P 4F10.2, 0PF9.2,F7.1,
               1  F6.3            )
003526          WRITE(6,789) EXPAN, IDIV, NNODE, HEQI(NNODE), HEQI(1),
               1 TEQI(NNODE), TEMI(NNODE), HUMI(NNODE)
003551      789 FORMAT(7X 6HEXPAN= 1P E9.2,0P 13X 5HIDIV= I3, 4X2HK= I2, 3X      6H
               1(HEQI= F6.3, 10H)(HEQI(1)= F6.3, 1H) 27X F9.2, F7.1, F6.3        )
003551          WRITE(6,785)  (U(I), I=1,NNODE)
003564      785 FORMAT( 4X  19H   INCREMENTS U(I)=      1P   11E10.2             )
003564          IF(EA.NE.0.) WRITE(6,787) (SA(J),J=1,5)
003577      787 FORMAT(  6X 7H SA(J)=    1P  5E10.2        )
003577          WRITE(6,986)
003603      986 FORMAT(     1X                           )
003603      910 IF( SCALE(1) .EQ. 0. )    GO TO 782
          C FOR PLOTTING ON PRINTER
003604          IPLOT(1,IT) = INT( .5 + HUMI(1)/SCALE(1) ) + 26
003612          IPLOT(2,IT) = INT( .5 + ABS(EXPAN)/SCALE(2) ) + 26
003620          IPLOT(3,IT) = INT( .5 + ABS(DEFX)/SCALE(3) ) + 26
003626          IPLOT(4,IT) = INT( .5 + ABS(DEFZ)/SCALE(4) ) + 26
003634          APLOT(1,IT) = DEFZ
003636          APLOT(2,IT) = HUMI(1)
003641          APLOT(3,IT) = TIME
003643      782 IF( IT .LT. NT )  GO TO 100
003646          IF( SCALE(1) .EQ. 0. )    GO TO 918
          C PLOTTING ON PRINTER
003647          WRITE(6,911)
003652      911 FORMAT( 132H1      DEFZ  HUM   TIME IT 0....5...10....5...20....5..
              1.30....5...40....5...50....5...60....5...70....5...80....5...90...
              2.5..100..                    )
003652          DO 916  IT = 1, NT
003654          DO 912  J = 25, 132
003655      912 PLOT(J) = BLANK
003660          DO 913  J = 26, 132, 20
003662      913 PLOT(J) = AJ
003665          DO 915  I = 1, 4
003667          J = IPLOT(I,IT)
003672      915 IF( J .LE. 132 )    PLOT(J) = CHAR(I)
003701          IF( NT .LE. 25 )    WRITE(6,986)
003710      916 WRITE(6,914) (APLOT(J,IT),J=1,3),IT, (PLOT(J), J=25,132)
003736      914 FORMAT(1H 1P E9.2, OP F5.3, F7.2, I3, 108A1       )
003736      918 IF( TDIFFU .GE. 1.E24 )   WRITE(6,955)   TDIFFU
003747      955 FORMAT(47H INTERNAL TEMPERATURE CHANGE IMMEDIATE, TDIFFU=1PE10.2)
003747          IEX = IEX + 1
003751          GO TO 10
003751          END
```

```
CASE  LUPT    NEL     NU     NT  NPRINT  MPRINT   TIMEO  TSTART  HSTART     AL      SW      HY  TDISTO  TDIST1  HDISTO  HDIST
 1       1      8      1      5       1       1   21.00   25.00    1.00    0.      0.     1.00  0.      0.      1.E+00  1.E+0
        DT    IT1    IT2     TO      T1   STEPT     IH1     IH2      HO     H1   STEPH     IP1     IP2    DP00    DP11   STEP
     1.000    999    999  0.      0.      0.          8     990     .50    .50   0.          0       0   0.      0.      0.
       IL1    IL2    DLD   DLD1   PKEST   RELAX      RO      R1   REVER TDIFFU      EA SCALE(1)  ..(2)   ..(3)   ..(4)   CHAR
         1  99999  560.0  0.      0.      0.       6.35    7.62    1.00   0.   0.    2.0E+00 2.0E+00 2.0E+00 2.0E+00   XXXX

 IT  TIME   DEFZ       DEFX      SHSTN      COMPLI    RIGT       FORCE     SI(1,K)   SI(2,K)   SI(3,K)   SI(4,K)     TEQI     TEMI  HU
  1  21.00 -2.33E-04  4.11E-05  5.36E-05  4.15E-07  7.16E+06 -5.60E+02  2.65E-11  3.26E-10 -6.31E+01  2.49E+02    21.00    25.0 1.
                                          K= 2      (HEQI= 1.000)       1.63E-11  3.15E-10 -6.31E+01  2.56E+02    21.00    25.0 1.00
                                          K= 3      (HEQI= 1.000)       1.22E-11  3.06E-10 -6.31E+01  2.62E+02    21.00    25.0 1.00
                                          K= 4      (HEQI= 1.000)       1.02E-11  2.96E-10 -6.31E+01  2.68E+02    21.00    25.0 1.00
                                          K= 5      (HEQI= 1.000)       4.08E-12  2.88E-10 -6.31E+01  2.74E+02    21.00    25.0 1.00
                                          K= 6      (HEQI= 1.000)       2.04E-12  2.79E-10 -6.31E+01  2.80E+02    21.00    25.0 1.00
                                          K= 7      (HEQI= 1.000)      -1.38E-38  2.73E-10 -6.31E+01  2.86E+02    21.00    25.0 1.00
                                          K= 8      (HEQI= 1.000)      -1.38E-38  2.65E-10 -6.31E+01  2.92E+02    21.00    25.0 1.00
     EXPAN= 3.13E-04              IDIV=  R        K= 9      (HEQI= 1.000)(HEQI(1)= 1.000)                          21.00    25.0 1.00
     INCREMENTS U(I)=   2.61E-04  2.68E-04  2.74E-04  2.81E-04  2.87E-04  2.94E-04  3.00E-04  3.07E-04  3.13E-04

  2  22.00 -2.63E-04  4.99E-05  6.12E-05  4.13E-07  7.21E+06 -5.60E+02 -3.16E-04 -2.56E-02 -6.32E+01  2.49E+02    22.00    25.0 1.
                                          K= 2      (HEQI= 1.000)      -6.26E-04 -7.38E-04 -6.31E+01  2.56E+02    22.00    25.0 1.00
                                          K= 3      (HEQI= 1.000)      -4.70E-04  1.27E-02 -6.31E+01  2.62E+02    22.00    25.0 1.00
                                          K= 4      (HEQI= 1.000)      -1.03E-04  1.82E-02 -6.31E+01  2.68E+02    22.00    25.0 1.00
                                          K= 5      (HEQI= 1.000)       3.00E-04  1.74E-02 -6.31E+01  2.74E+02    22.00    25.0 1.00
                                          K= 6      (HEQI= 1.000)       6.00E-04  1.05E-02 -6.31E+01  2.80E+02    22.00    25.0 1.00
                                          K= 7      (HEQI= 1.000)       6.58E-04 -3.94E-03 -6.31E+01  2.86E+02    22.00    25.0 1.00
                                          K= 8      (HEQI= 1.000)       3.01E-04 -2.86E-02 -6.32E+01  2.93E+02    22.00    25.0 1.00
     EXPAN= 3.81E-04              IDIV= 24        K= 9      (HEQI= 1.000)(HEQI(1)= 1.000)                          22.00    25.0 1.00
     INCREMENTS U(I)=   5.59E-05  5.74E-05  5.88E-05  6.01E-05  6.15E-05  6.29E-05  6.43E-05  6.57E-05  6.71E-05

  3  23.00 -2.82E-04  5.58E-05  6.62E-05  4.09E-07  7.30E+06 -5.60E+02 -6.14E-04 -4.98E-02 -6.32E+01  2.49E+02    23.00    25.0 1.
                                          K= 2      (HEQI= 1.000)      -1.23E-03 -2.24E-03 -6.31E+01  2.56E+02    23.00    25.0 1.00
                                          K= 3      (HEQI= 1.000)      -9.17E-04  2.61E-02 -6.31E+01  2.62E+02    23.00    25.0 1.00
                                          K= 4      (HEQI= 1.000)      -1.55E-04  3.83E-02 -6.31E+01  2.68E+02    23.00    25.0 1.00
                                          K= 5      (HEQI= 1.000)       6.85E-04  3.61E-02 -6.31E+01  2.74E+02    23.00    25.0 1.00
                                          K= 6      (HEQI= 1.000)       1.29E-03  2.00E-02 -6.31E+01  2.80E+02    23.00    25.0 1.00
                                          K= 7      (HEQI= 1.000)       1.36E-03 -1.07E-02 -6.31E+01  2.85E+02    23.00    25.0 1.00
                                          K= 8      (HEQI= 1.000)       6.09E-04 -5.78E-02 -6.32E+01  2.93E+02    23.00    25.0 1.00
     EXPAN= 4.25E-04              IDIV= 25        K= 9      (HEQI= 1.000)(HEQI(1)= 1.000)                          23.00    25.0 1.00
     INCREMENTS U(I)=   3.70E-05  3.80E-05  3.89E-05  3.98E-05  4.07E-05  4.16E-05  4.26E-05  4.35E-05  4.44E-05

  4  24.00 -2.97E-04  6.02E-05  6.99E-05  4.05E-07  7.38E+06 -5.60E+02 -8.33E-04 -6.75E-02 -6.32E+01  2.49E+02    24.00    25.0 1.
                                          K= 2      (HEQI= 1.000)      -1.66E-03 -3.03E-03 -6.31E+01  2.56E+02    24.00    25.0 1.00
                                          K= 3      (HEQI= 1.000)      -1.23E-03  3.64E-02 -6.31E+01  2.62E+02    24.00    25.0 1.00
                                          K= 4      (HEQI= 1.000)      -1.70E-04  5.35E-02 -6.31E+01  2.68E+02    24.00    25.0 1.00
                                          K= 5      (HEQI= 1.000)       9.97E-04  5.01E-02 -6.31E+01  2.74E+02    24.00    25.0 1.00
                                          K= 6      (HEQI= 1.000)       1.82E-03  2.69E-02 -6.31E+01  2.80E+02    24.00    25.0 1.00
                                          K= 7      (HEQI= 1.000)       1.90E-03 -1.62E-02 -6.31E+01  2.86E+02    24.00    25.0 1.00
                                          K= 8      (HEQI= 1.000)       8.43E-04 -8.01E-02 -6.32E+01  2.93E+02    24.00    25.0 1.00
     EXPAN= 4.59E-04              IDIV= 25        K= 9      (HEQI= 1.000)(HEQI(1)= 1.000)                          24.00    25.0 1.00
     INCREMENTS U(I)=   2.81E-05  2.88E-05  2.95E-05  3.02E-05  3.09E-05  3.16E-05  3.23E-05  3.30E-05  3.37E-05

  5  25.00 -3.08E-04  6.38E-05  7.28E-05  4.01E-07  7.46E+06 -5.60E+02 -9.93E-04 -8.04E-02 -6.32E+01  2.49E+02    25.00    25.0 1.
                                          K= 2      (HEQI= 1.000)      -1.98E-03 -3.52E-03 -6.31E+01  2.56E+02    25.00    25.0 1.00
```

REFERENCES

1. Fluck, P. G. and Washa, G. W., "Creep of Plain and Reinforced Concrete," ACI Journal, Proc. Vol. 54, No. 10, April 1958, pp. 879-895.

2. Wallo, E. and Kesler, C., "Prediction of Creep in Structural Concrete," T. and A. M. Report No. 670, University of Illinois, Urbana, Illinois, December 1966.

3. Sackman, J., "Creep in Concrete and Concrete Structures," Proc. Conference on Solid Mechanics, Princeton University, November 1963.

4. L'Hermite, R., "What Do We Know About the Plastic Deformation and Creep of Concrete?" RILEM Bulletin, No. 1, March 1959, pp. 21-51.

5. Davis, R., Davis, H., and Hamilton, J., "Plastic Flow of Concrete Under Sustained Stress," Proc. ASTM, Vol. 34, 1934, pp. 354-386.

6. Hansen, T. C., "Creep and Stress Relaxation of Concrete," Swedish Cement and Concrete Research Institute, Proc. No. 31, Stockholm, 1960.

7. McHenry, D., "A New Aspect of Creep in Concrete and Its Application to Design," Proc. ASTM, Vol. 43, 1943, pp. 1069-1084.

8. Powers, T. C., "Some Observations on the Interpretation of Creep Data," RILEM Bulletin, No. 33, December 1966, pp. 381-391.

9. Pickett, G., "The Effect of Change in Moisture-Content of the Creep of Concrete Under a Sustained Load," ACI Journal, Proc. Vol. 38, No. 4, February 1942, pp. 333-355.

10. Illston, J. M., "The Creep of Concrete Under Uniaxial Tension," Magazine of Concrete Research, Vol. 17, No. 51, 1965, pp. 77-85.

11. Ross, A. D., "Experiments on the Creep of Concrete Under Two-Dimensional Stressing," Magazine of Concrete Research, Vol. 6, No. 16, June 1954, pp. 3-10.

12. Arthanari, S. and Yu, C. W., "Creep of Concrete Under Uniaxial and Biaxial Stresses at Elevated Temperatures," Magazine of Concrete Research, Vol. 19, No. 60, September 1967, pp. 149-156.

13. Neville, A. M., "Theories of Creep in Concrete," ACI Journal, Proc. Vol. 52, No. 1, September 1955.

14. Powers, T. C., Discussion of "Mechanism of Creep in Concrete," by Ali, I. and Kesler, C., Symposium on Creep of Concrete, ACI Publication SP-9, 1964, pp. 57-62.

15. Powers, T. C., "Mechanisms of Shrinkage and Reversible Creep of Hardened Cement Paste," International Conference on the Structure of Concrete, Paper G1, London, 1965.

16. Powers, T. C., "The Thermodynamics of Volume Change and Creep," RILEM Bulletin, No. 6, 1968, pp. 487-507.

17. Bazant, Z. P., "Constitutive Equation for Concrete Creep and Shrinkage Based on Thermodynamics of Multiphase System," Department of Civil Engineering, University of Toronto, March 1969. Published in RILEM Bulletin, No. 13, January 1970.

18. Davis, R. E. and Davis, H. E., "Flow of Concrete Under the Action of Sustained Loads," Proc. ACI, Vol. 27, No. 7, March 1931, pp. 837-901.

19. Lynam, C. G., "Growth and Movement in Portland Cement Concrete," Oxford University Press, 1934, 139 pp.

20. Dutron, R., "Deformations Lentes du Beton et du Beton Arme Sous L'Action des Charges Permanentes," Goemaere, Bruxelles, 1937.

21. Lorman, W. R., "The Theory of Concrete Creep," Proc. ASTM, Vol. 40, 1940, pp. 1082-1102.

22. Maney, G. A. and Lagaard, M. B., "Stress Increases in Compressive Steel Under Constant Load Caused by Shrinkage," ACI Journal, Proc. Vol. 36, No. 6, June 1940, pp. 541-552.

23. Maney, G. A., "Studies in Engineering - No. 1, Warping on Non-Uniform Shrinkage Over Cross-Section Found to be Source of All Time Yield in Loading Concrete Members," Northwestern Technological Institute, 1941.

24. Duke, C. M. and Davis, H. E., "Some Properties of Concrete Under Sustained Combined Stresses," Proc. ASTM, Vol. 44, 1944, pp. 888-896.

25. Troxell, G. E., Raphael, J. M., and Davis, R. E., "Long-Time Creep and Shrinkage Tests of Plain and Reinforced Concrete," Proc. ASTM, Vol. 58, 1958, pp. 1101-1120.

26. Mamillan, "A Study of the Creep of Concrete," RILEM Bulletin, No. 3, 1959, pp. 15-31.

27. De la Pena, C., "Shrinkage and Creep of Specimens of Thin Section," RILEM Bulletin, No. 3, 1959, pp. 60-70.

28. Hansen, T. C., "Creep of Concrete. A Discussion of Some Fundamental Problems," Swedish Cement and Concrete Research Institute, Bulletin No. 33, Stockholm, September 1958.

29. Tomes, L. A., Hunt, C. M., and Blaine, R. L., "Some Factors Affecting the Surface Area of Hydrated Portland Cement as Determined by Water Vapor and Nitrogen Adsorption," Journal of Res. Nat. Bur. of Standards, Vol. 59, 1957, pp. 357-364.

30. Hunt, C. M., Tomes, L. A., and Blaine, R. L., "Some Effects of Aging on the Surface Area of Portland Cement Paste," Journal of Res. Nat. Bur. of Standards, Vol. 64, No. 2, 1960, pp. 163-169.

31. Glucklich, J. and Ishai, O., "Creep Mechanism in Cement Mortar," ACI Journal, Proc. Vol. 59, No. 7, July 1962, pp. 923-948.

32. Ishai, O., "Elastic and Inelastic Behavior of Hardened Mortar in Torsion," Symposium on Creep of Concrete, ACI Publication SP-9, 1964.

33. Mullen, W. G. and Dolch, W. L., "Creep of Portland Cement Paste," Proc. ASTM, Vol. 64, 1964, pp. 1146-1170.

34. Hansen, T. C. and Mattock, A. H., "Influence of Size and Shape of Member on the Shrinkage and Creep of Concrete," ACI Journal, Proc. Vol. 63, No. 2, February 1966, pp. 267-290.

35. Ali, I. and Kesler, C. E., "Mechanism of Creep in Concrete," Symposium on Creep of Concrete, ACI Publication SP-9, 1964.

36. Bertero, V. V., "Effect of Short-Time Variations in the Environmental Conditions Upon Creep of Concrete," Department of Civil Engineering, University of California, Berkeley, July 1969.

37. Gambarov, G. A., "Creep and Shrinkage of Triaxially Prestressed Concrete," Translation C. F. S. T. I., No. TT6419989.

38. Jordaan, I. J. and Illston, J. M., "The Creep of Sealed Concrete Under Multiaxial Compressive Stresses," Magazine of Concrete Research, Vol. 21, No. 69, December 1969, pp. 195-204.

39. Gapalakrishnan, K. S., Neville, A. M., and Ghali, A., "A Hypothesis on Mechanism of Creep of Concrete with Reference to Multiaxial Compression," ACI Journal, Proc. Vol. 67, No. 1, January 1970, pp. 29-35.

40. Ibid, "Creep Poisson's Ratio of Concrete Under Multiaxial Compression," ACI Journal, Proc. Vol. 66, No. 12, December 1969, pp. 1008-1020.

41. Gapalakrishnan, K. S., "Creep of Concrete Under Multiaxial Compressive Stresses," Ph.D. Dissertation, The University of Calgary, April 1968.

42. Brunauer, S. and Greenberg, S. A., "The Hydration of Tricalcium Silicate and Dicalcium Silicate at Room Temperature," Proc. of the Fourth International Symposium on the Chemistry of Cement, Nat. Bur. of Standards, Monograph 43, Vol. 1, Washington, 1962, pp. 135-167.

43. Brunauer, S., Kantro, D. L., and Weise, C. H., "The Surface Energy of Tobermorite," PCA Research Department Bulletin 105.

44. Harkins, W. D. and Jura, G., "Determination of the Decrease of Free Surface Energy of a Solid by an Adsorbed Film," Journal Amer. Chem. Soc., Vol. 66, 1944.

45. Bazant, Z. P., "Numerical Analysis of Long-Time Deformations of a Thick-Walled Concrete Cylinder," Structures and Materials Research Report No. 69-12, Department of Civil Engineering, University of California, Berkeley, August 1969.

46. Bazant, Z. P., "Thermodynamic Theory of Concrete Deformation at Variable Temperature and Humidity," Structures and Materials Research Report No. 69-11, Department of Civil Engineering, University of California, Berkeley, August 1969.

47. Private Communication with Dr. Z. P. Bazant.

48. Powers, T. C., "A Discussion of Cement Hydration in Relation to the Curing of Concrete," Proc. of the Highway Research Board, Vol. 27, 1947; PCA Research Department Bulletin 25.

49. Keeton, J. E., "Study of Creep in Concrete-Phase I (I-Beam)," Technical Report R333-1, U.S. Naval Civil Engineering Laboratory, Port Hueneme, California, January 1965.

50. Selna, L. G., "Time-Dependent Behavior of Reinforced Concrete Structures," Ph.D. Dissertation, Department of Civil Engineering, University of California, Berkeley, August 1967. (Structures and Materials Research Report No. 67-19.)

51. Mukaddam, A. M., "Behavior of Concrete under Variable Temperature and Loading," Ph.D. Dissertation, Department of Civil Engineering, University of California, Berkeley, August 1969.

52. Best, C. H., Pirtz, D., and Polivka, M., "Loading System for Creep Studies of Concrete," ASTM Bulletin No. 224, September 1957, pp. 44-47.

53. L'Hermite, R. G., "Volume Changes in Concrete," Proc. of the Fourth International Symposium on the Chemistry of Cement, Nat. Bur. of Standards, Monograph 43, Vol. 2, Washington, 1962, pp. 659-694.

54. Pickett, G., "Effect of Aggregate on Shrinkage of Concrete and a Hypothesis Concerning Shrinkage," ACI Journal, Proc. Vol. 52, No. 5, January 1956, pp. 581-590.

55. Powers, T. C., "A Hypothesis on Carbonation Shrinkage," PCA Research Department Bulletin 146.

56. Verbeck, G. J., "Carbonation of Hydrated Portland Cement," PCA Research Department Bulletin 87.

57. Hanson, J. A., "Effects of Curing and Drying Environments on Splitting Tensile Strength of Concrete," PCA Development Department Bulletin D141; ACI Journal, July 1968.

58. Mills, R. H., "Effect of Sorbed Water on Dimension, Compressive Strength and Swelling Pressure of Hardened Cement Paste," Symposium on Structure of Portland Cement Paste and Concrete, Highway Research Board, Special Report 90, Washington, D.C., 1966.

59. Ross, A. D., Illston, J. M., and England, G. L., "Short- and Long-Term Deformations of Concrete as Influenced by Its Physical Structure and State," International Conference on the Structure of Concrete, Paper H1, London, 1965.

60. Plowman, J. M., "Young's Modulus and Poisson's Ratio of Concrete Cured at Various Humidities," Magazine of Concrete Research, Vol. 15, No. 44, July 1963, pp. 77-82.

61. Conway, J. B., "Numerical Methods for Creep and Rupture Analysis," Gordon and Breach Science Publishers, New York, 1967.

62. Wilson, E. L., "Symbolic Matrix Interpretive Systems," (FORTRAN IV), University of California Computer Center, Berkeley, October 1967.

63. Mills, R. H., "Collapse of Structure in Cement Hydrates," Conference on Scanning Microscopy, Cambridge, England, 8-10 July 1968.

64. Helmuth, R. H. and Turk, D., "The Reversible and Irreversible Drying Shrinkage of Hydrated Portland Cement and Tricalcium Silicate Pastes," Journal of the PCA Research and Development Laboratories, Vol. 9, No. 2, May 1967, pp. 8-21.

65. Feldman, R. F. and Sereda, P. J., "A Model for Hydrated Portland Cement Paste as Deduced from Sorption-Length Change and Mechanical Properties," RILEM Bulletin, No. 6, 1968, pp. 509-519.

66. Polivka, M., Pirtz, D., and Adams, R. F., "Studies of Creep in Mass Concrete," Symposium on Mass Concrete, 1958, ACI Publication SP-6.

67. Monfore, G. E., "A Small Probe-Type Gage for Measuring Relative Humidity," PCA Research Department Bulletin 160.

68. Callahan, J. P., "Summary of Tests Conducted on Perivale Vibrating Wire Gage in Oak Ridge Laboratory," Summary of Conference on the Concrete Materials Investigation, September 11-12, 1968, at the University of Texas, Austin, Texas.

TABLE 1

Chemical Composition of Type I Santa Cruz Cement

Oxide	Percent	Compound	Percent
SiO_2	22.28	C_3S	54.7
Al_2O_3	3.94	C_2S	22.7
Fe_2O_3	2.64	C_3A	6.0
CaO	63.85	C_4Al	8.0
MgO	2.02	$CaSO_4$	3.3
SO_3	1.95	Others	5.3
Ignition loss	1.04		
Insoluble residue	0.28		

TABLE 2

Sieve Analysis of Blended Sand
(50% Silver Sand - 50% Felton Sand, by weight)

Sieve No.	Percent Retained	Cumulative Percent Retained
4	0.0	0.0
8	1.0	1.0
14	7.6	8.6
28	17.7	26.3
48	26.7	53.0
100	13.5	66.5
200	29.6	96.1
Pan	3.9	100.0

Fineness Modulus (F.M.) = 1.55.

TABLE 3

Concrete Mix Proportions

	Mix Proportions By Weight	Mix Proportions Per Cubic Yard (pcy)
Water	5.2	652
Cement	9.0	1128
Sand	18.0	2256

Cement Content, 12 sacks per cubic yard (scy).

TABLE 4

Strength and Elastic Properties of Concrete Control Specimens

(Specimens - 5-in. I.D., 6-in. O.D. at 21 days. Specimens were kept under 100% Relative Humidity after casting.)

Tests (average of two tests)	Strength, psi	Modulus of Elasticity, psi	Shear Modulus of Elasticity, psi	Poisson's Ratio
Uniaxial Compression, 40 in. long cylinder	3600	3.43×10^6	1.45×10^6*	0.17
Uniaxial Compression, 20 in. long cylinder	3650	3.30×10^6	1.40×10^6*	0.17
Torsion, 40 in. long cylinder	238	-	1.80×10^6	-

*Calculated by using Modulus of Elasticity and Poisson's Ratio.

LIST OF FIGURES

LIST OF FIGURES, Continued

LIST OF FIGURES, Continued

LIST OF FIGURES, Continued

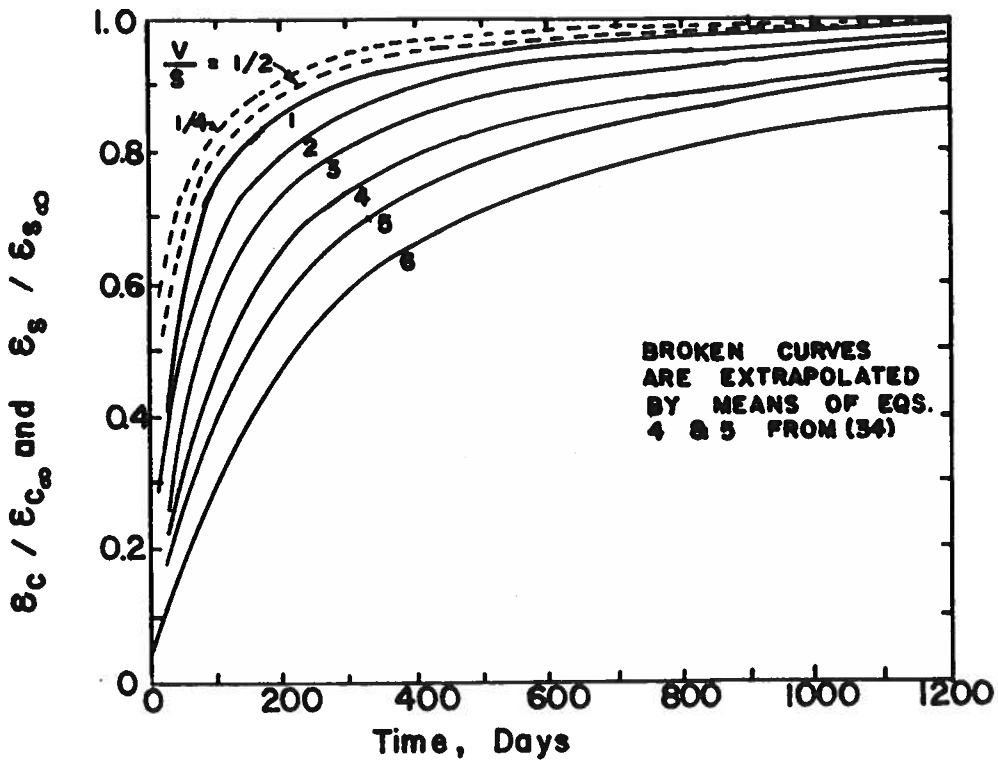

FIG. 1 CALCULATED VARIATION OF SHRINKAGE AND CREEP WITH TIME FOR GIVEN VOLUME/SURFACE RATIOS (After Hansen & Mattock, 34)

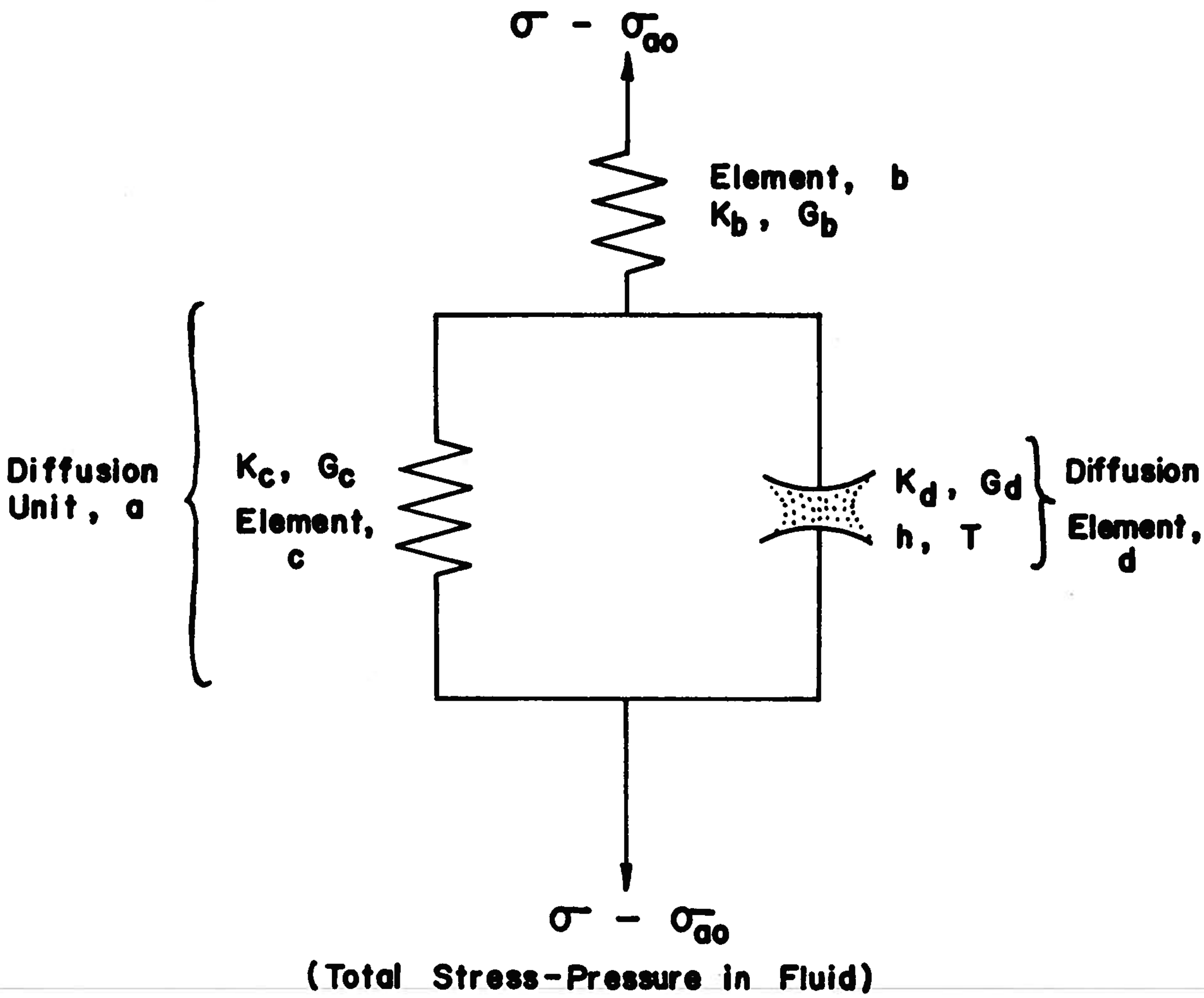

FIG. 2 RHEOLOGICAL MODEL FOR THE INTERACTION OF THE ELASTIC SOLID PART OF CEMENT PASTE OR CONCRETE WITH THE DIFFUSIBLE LOAD-BEARING LAYERS, WITH ONE DIFFUSION UNIT.

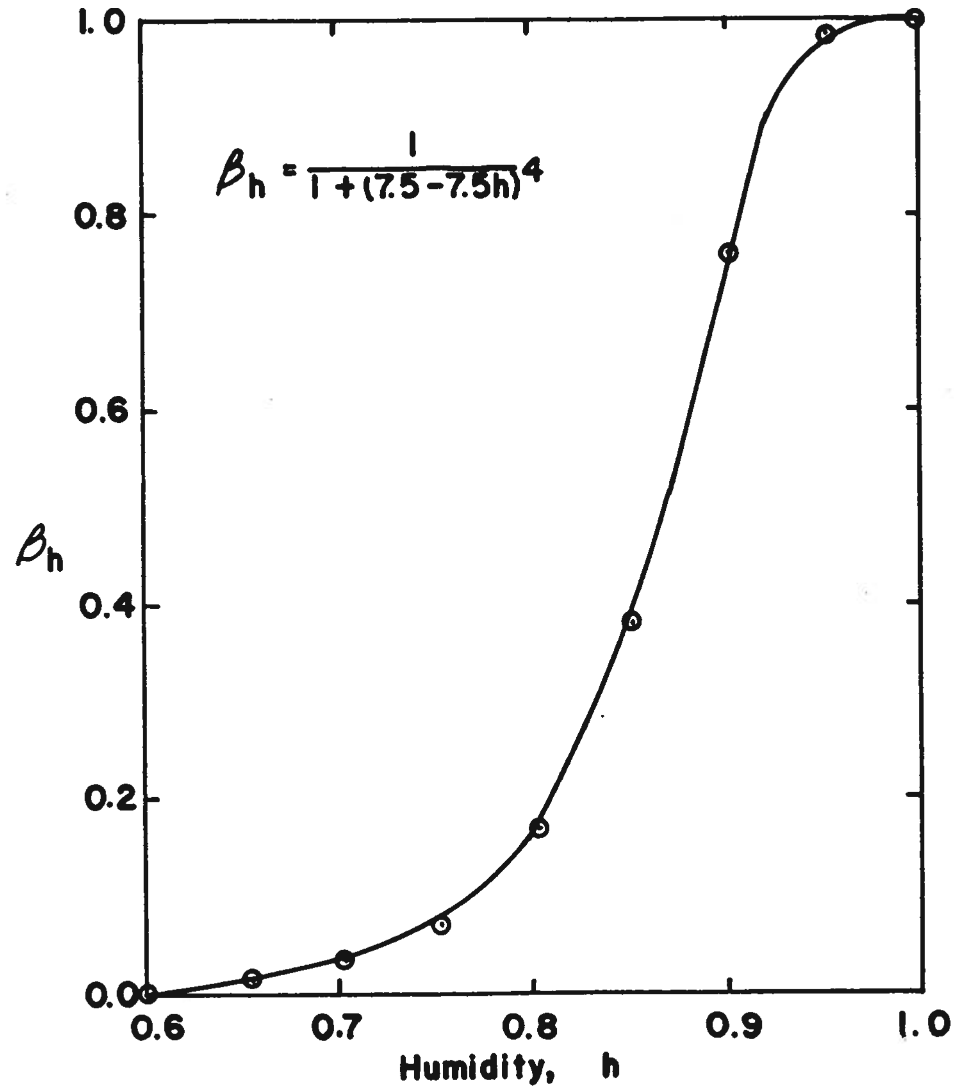

FIG. 3-a APPROXIMATE FORM OF THE VARIATION OF THE HYDRATION RATE, β_h WITH HUMIDITY, h (After Bazant)

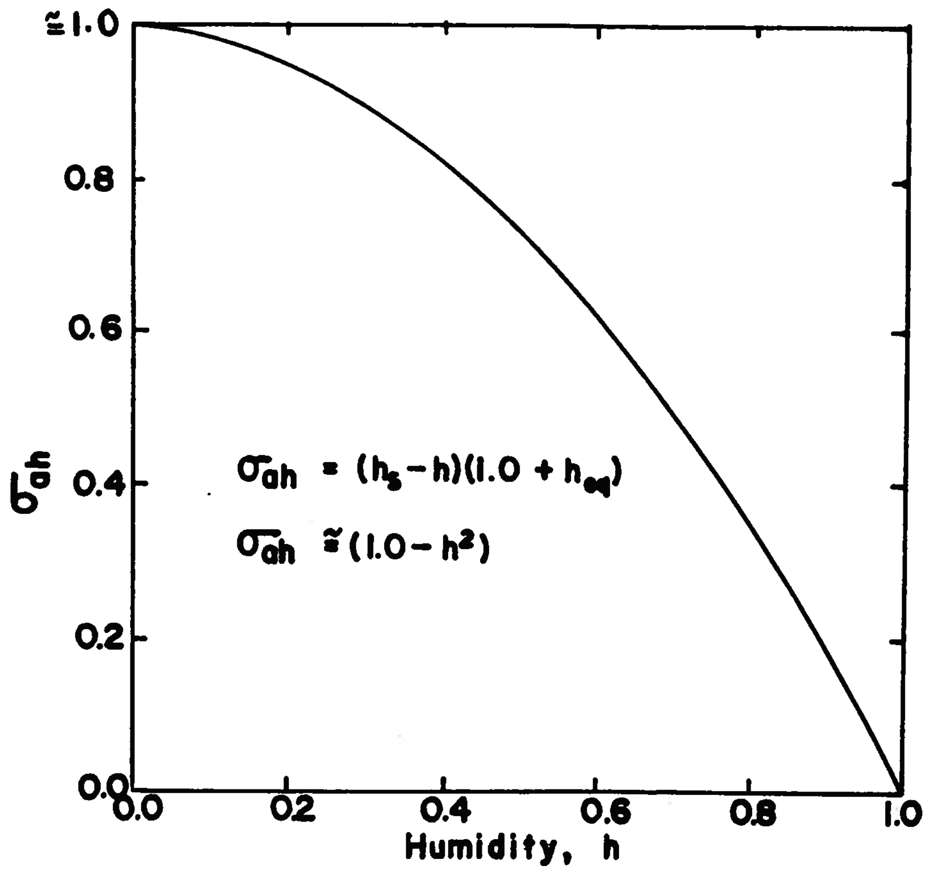

FIG. 3-b ESTIMATED VARIATION OF THE PARAMETER (σ_{ah}) IN A FLUID WITH HUMIDITY (h). (After Bazant)

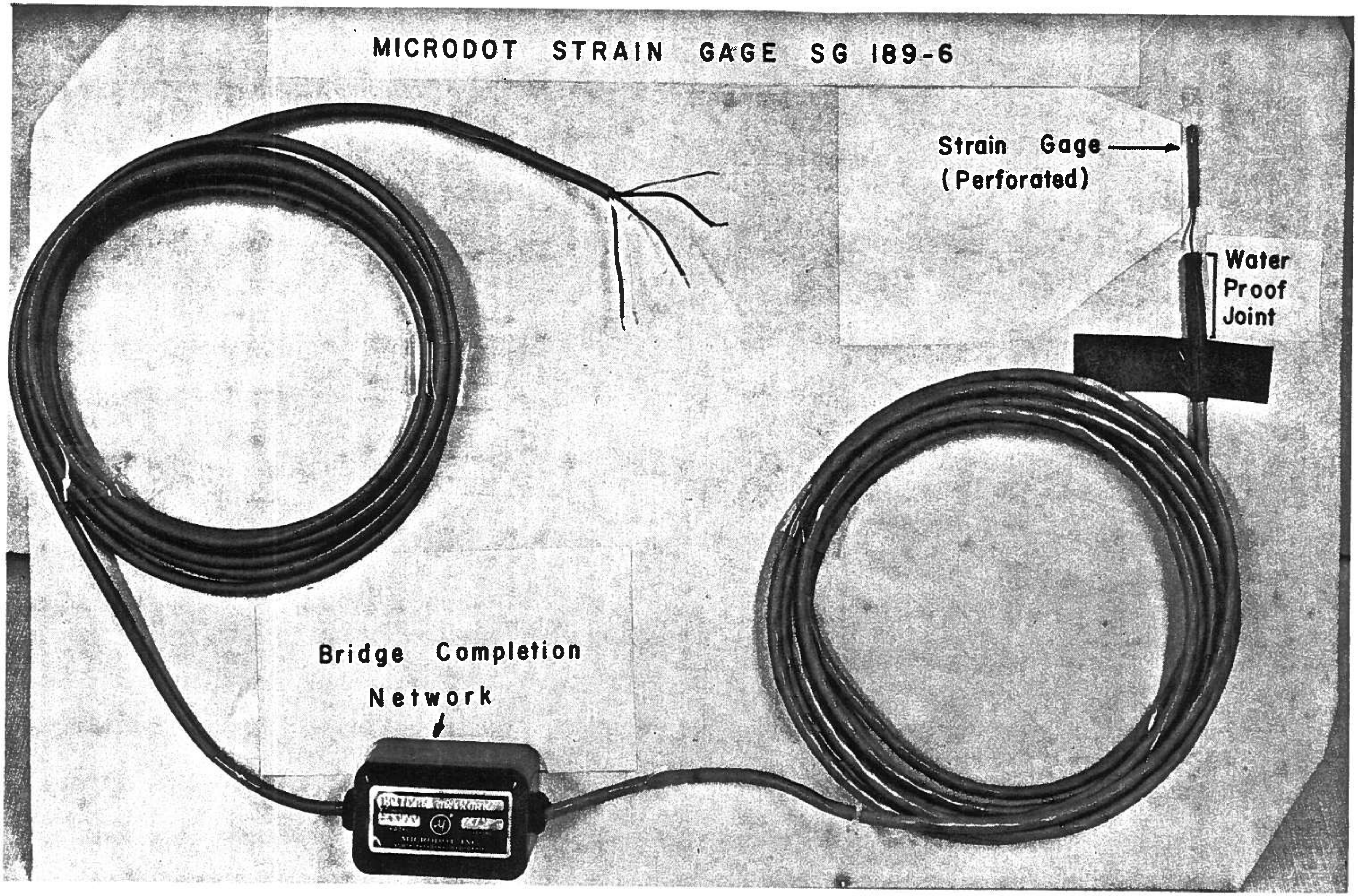

FIG. 4 MICRODOT STRAIN GAGE AND ACCESSORIES

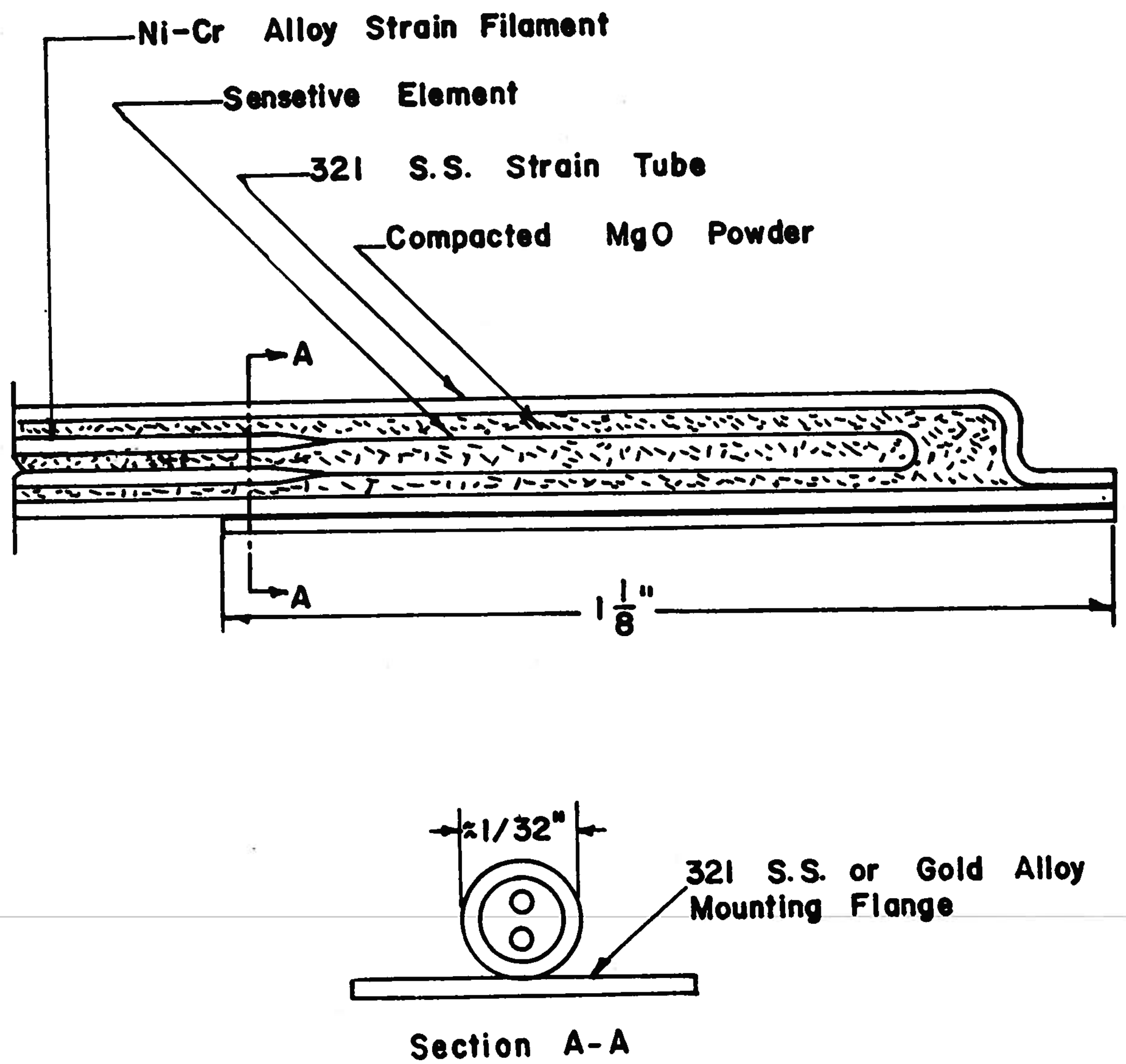

FIG. 5 DETAILS OF MICRODOT EMBEDDED STRAIN GAGE (SG 189)

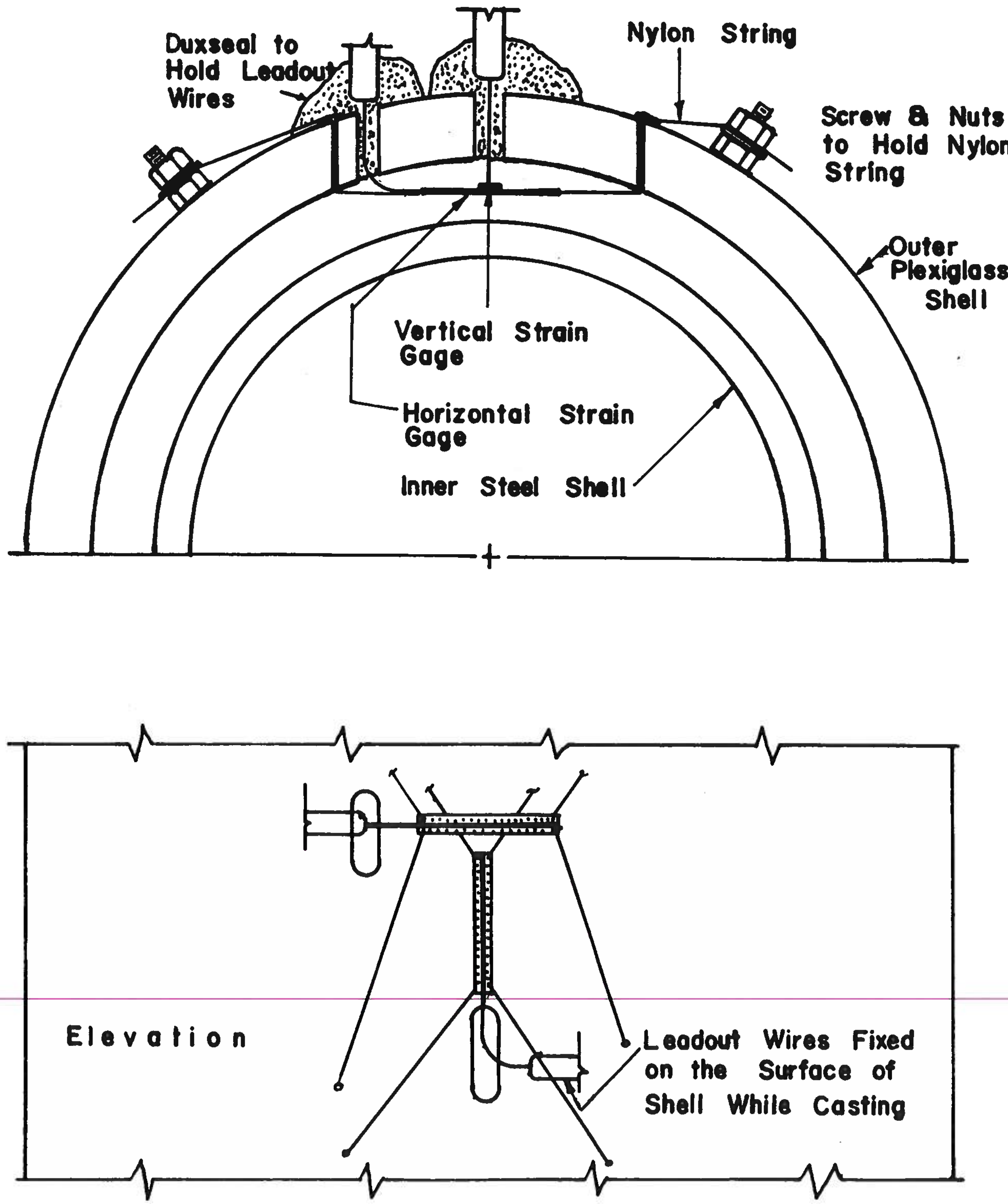

FIG. 6-a DETAILS OF POSITIONING EMBEDDED STRAIN GAGES IN CASTING MOLD FOR COMPRESSION SPECIMEN

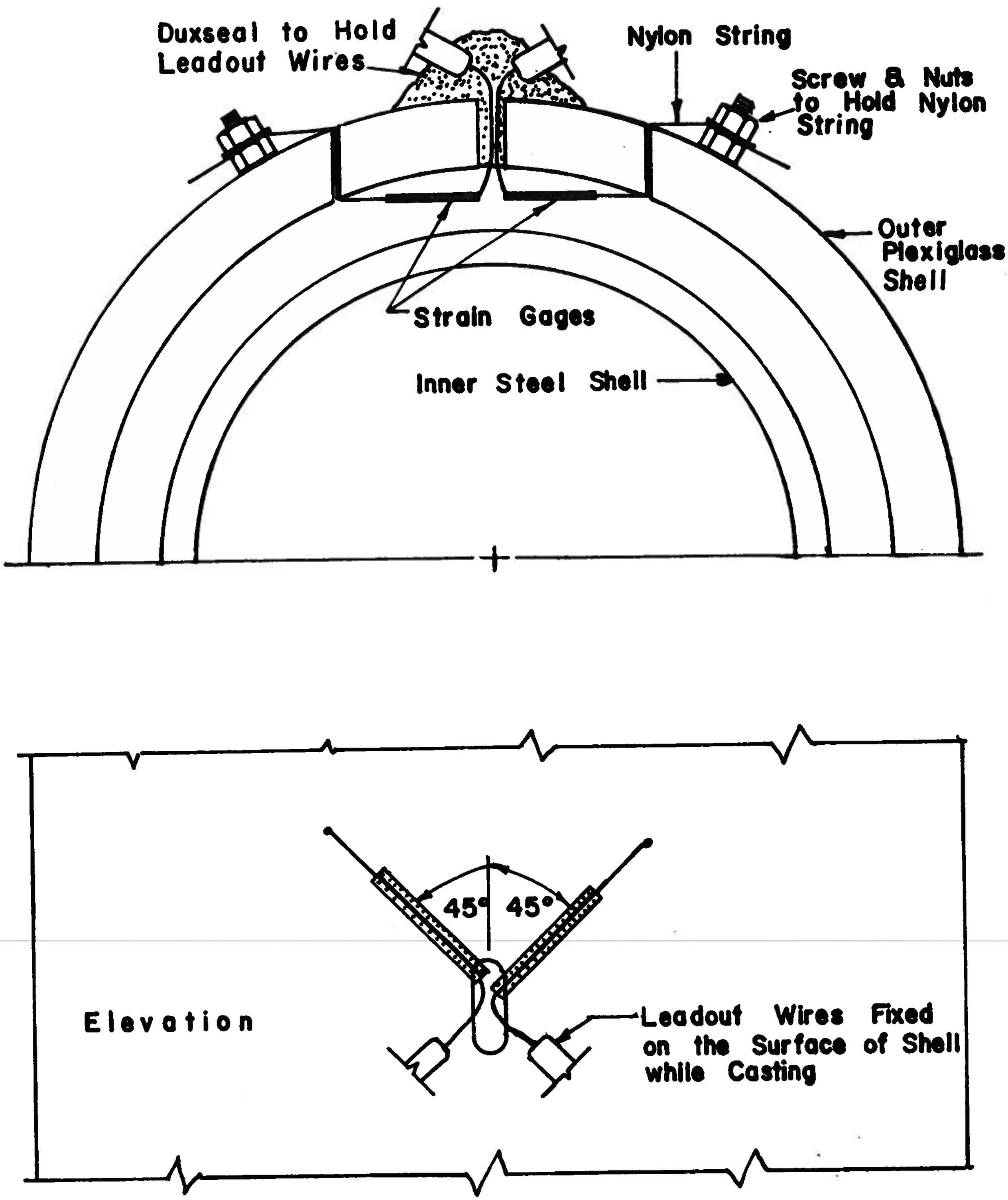

FIG. 6-b DETAILS OF POSITIONING EMBEDDED STRAIN GAGES IN CASTING MOLD FOR TORSION SPECIMEN

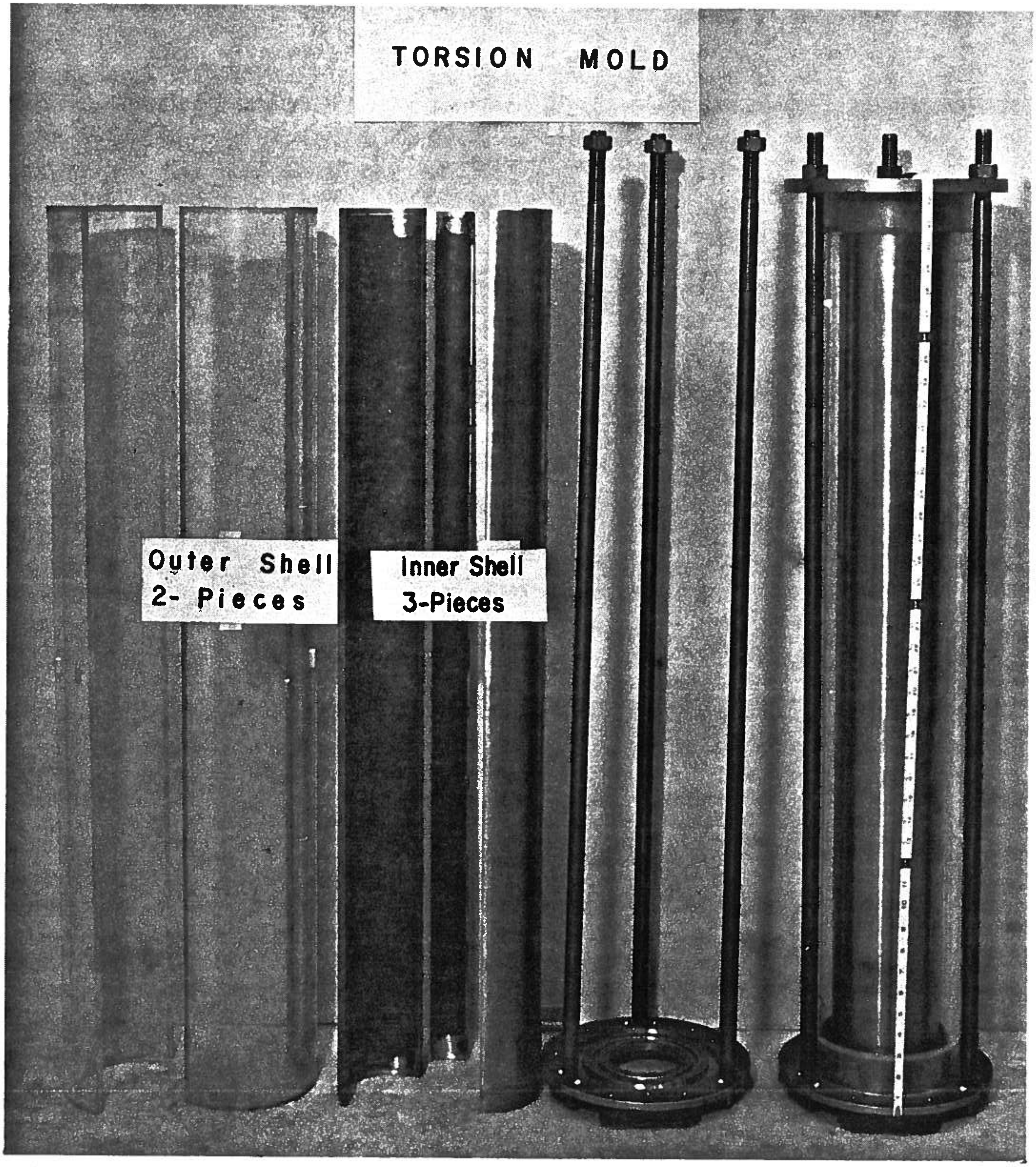

FIG. 7-a CASTING MOLD - TORSION SPECIMEN

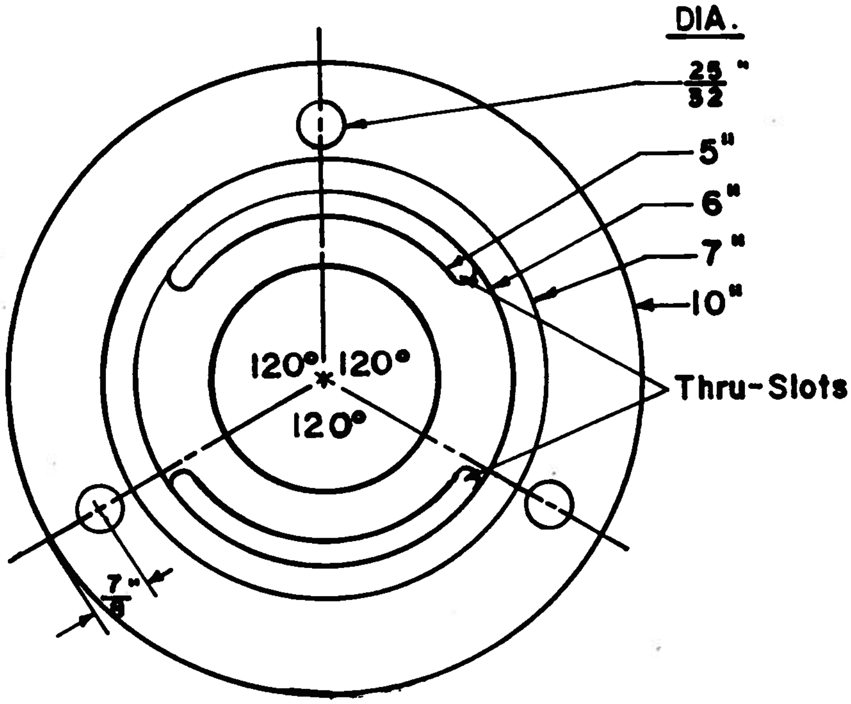

Top Flange

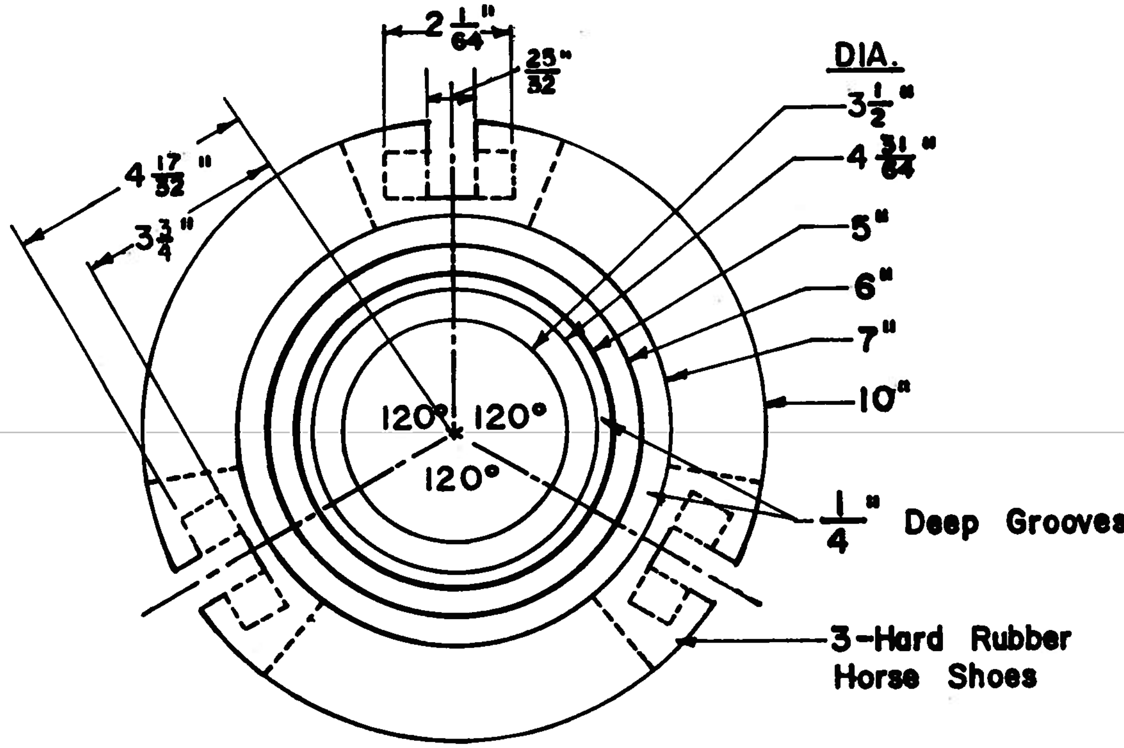

Bottom Flange

FIG. 7-b DETAILS OF TOP AND BOTTOM FLANGES OF CASTING MOLD

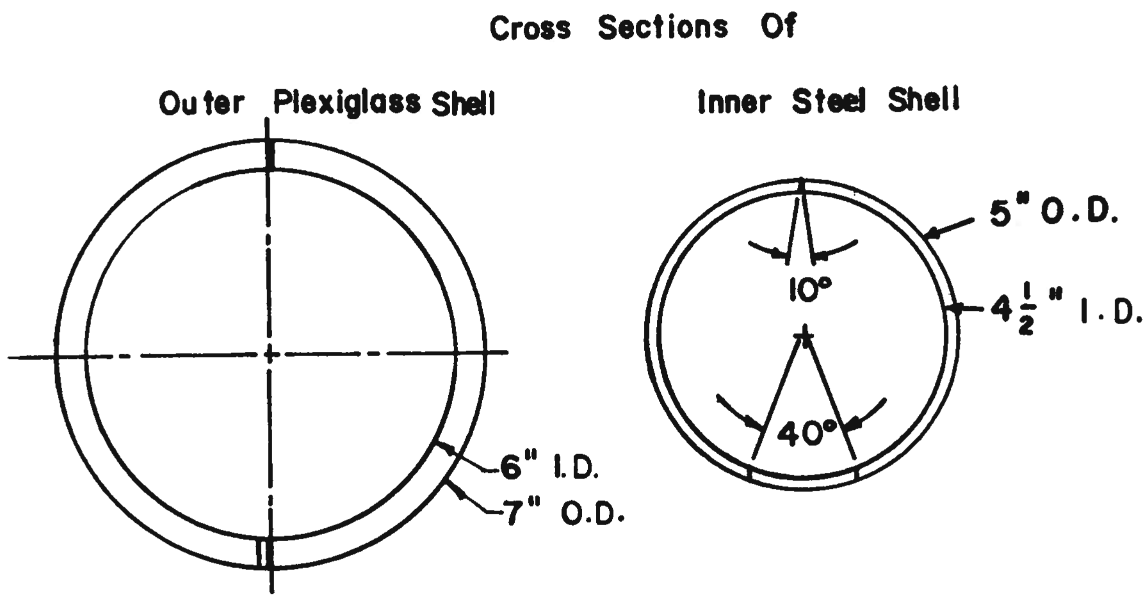

FIG. 7-c DETAILS OF INNER AND OUTER SHELLS OF CASTING MOLD

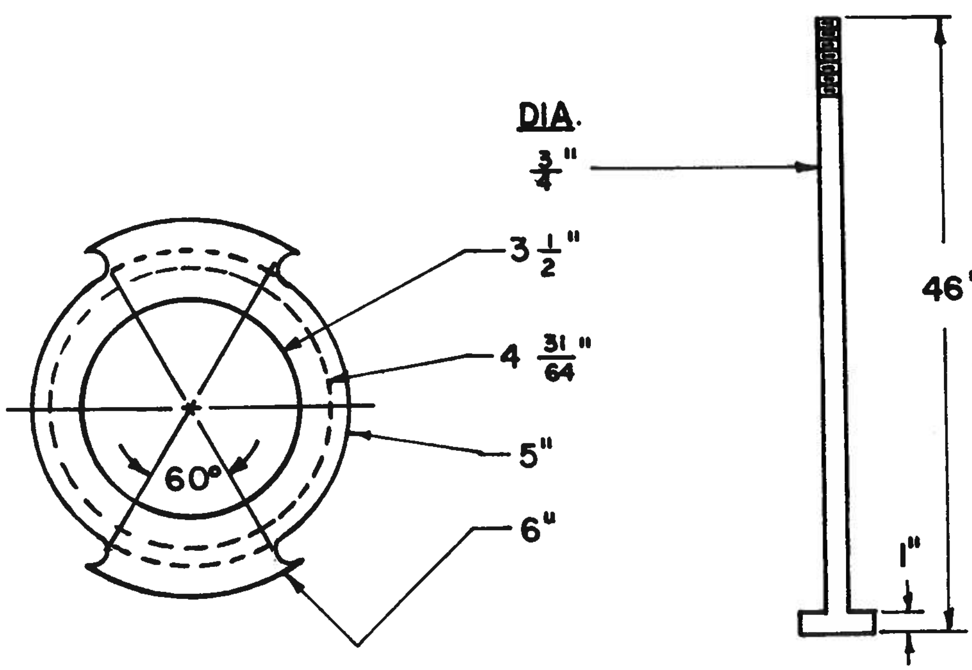

FIG. 7-d DETAILS OF UPPER HOLDING RING AND RESTRAINING RODS OF CASTING MOLD

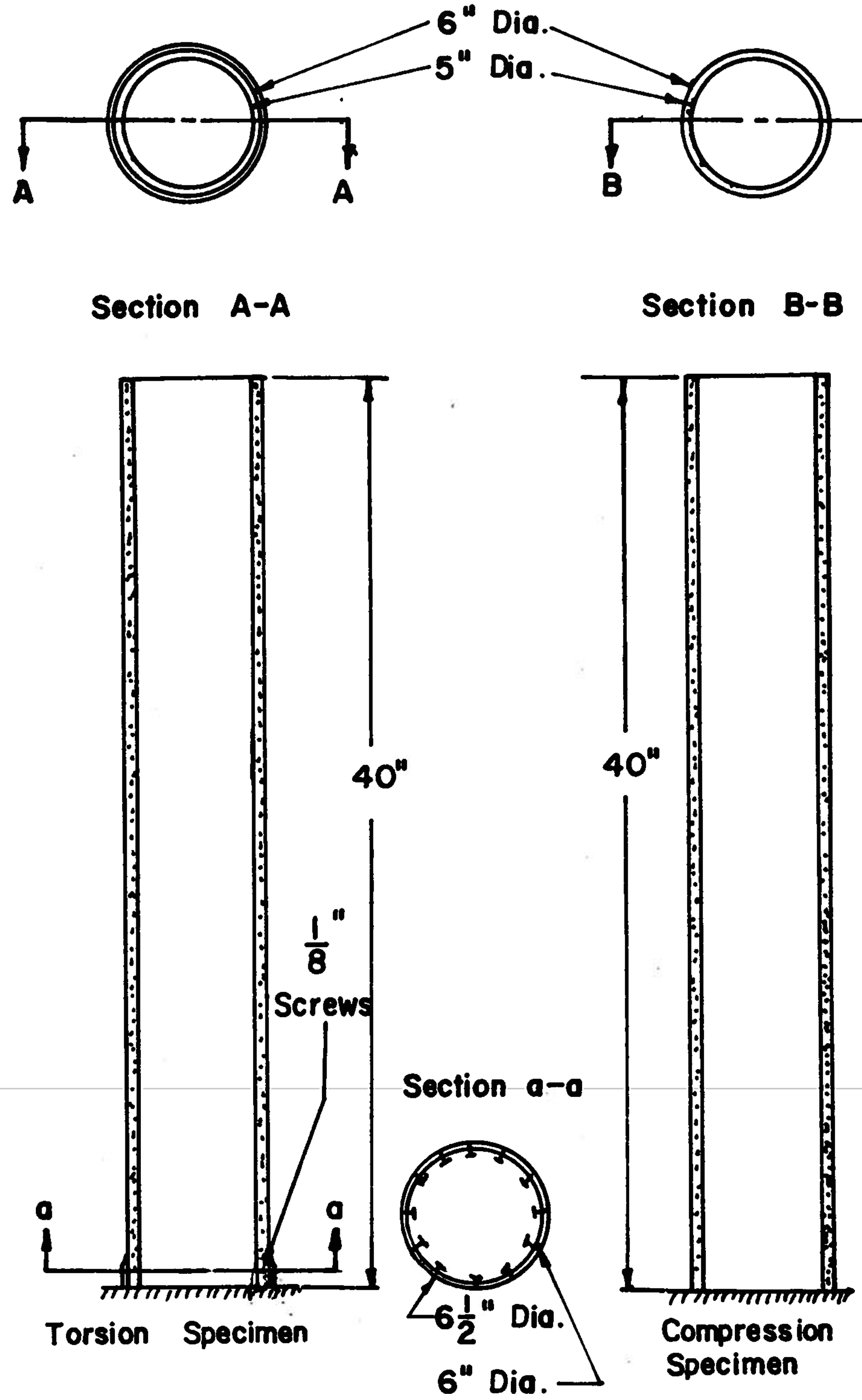

FIG. 7-e DETAILS OF SPECIMEN FABRICATION

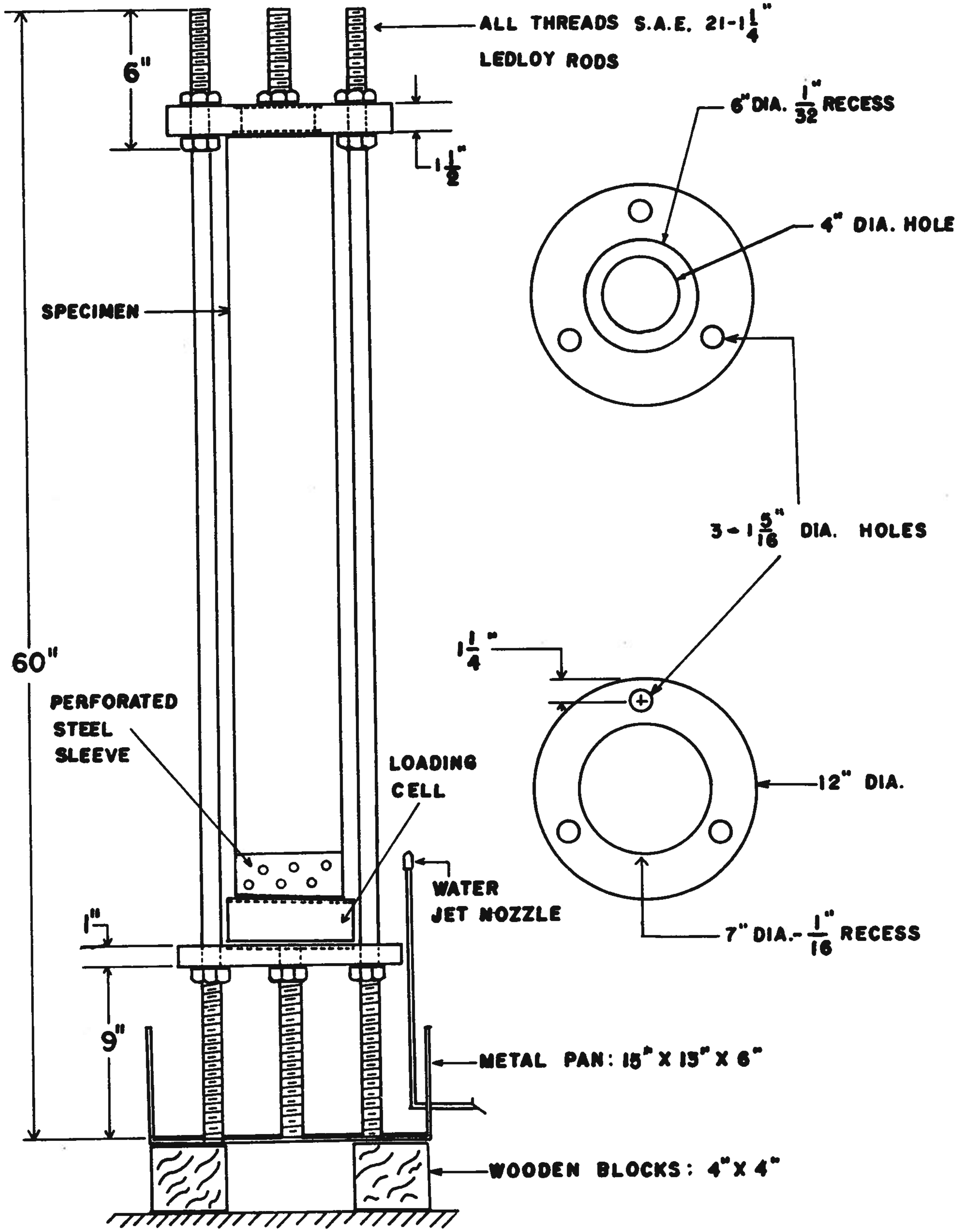

FIG. 8-a DETAILS OF COMPRESSION LOADING FRAME

FIG. 8-b POLYETHYLENE BAG ENCLOSURE OF A SPECIMEN SUBJECTED TO 100 PER CENT RELATIVE HUMIDITY

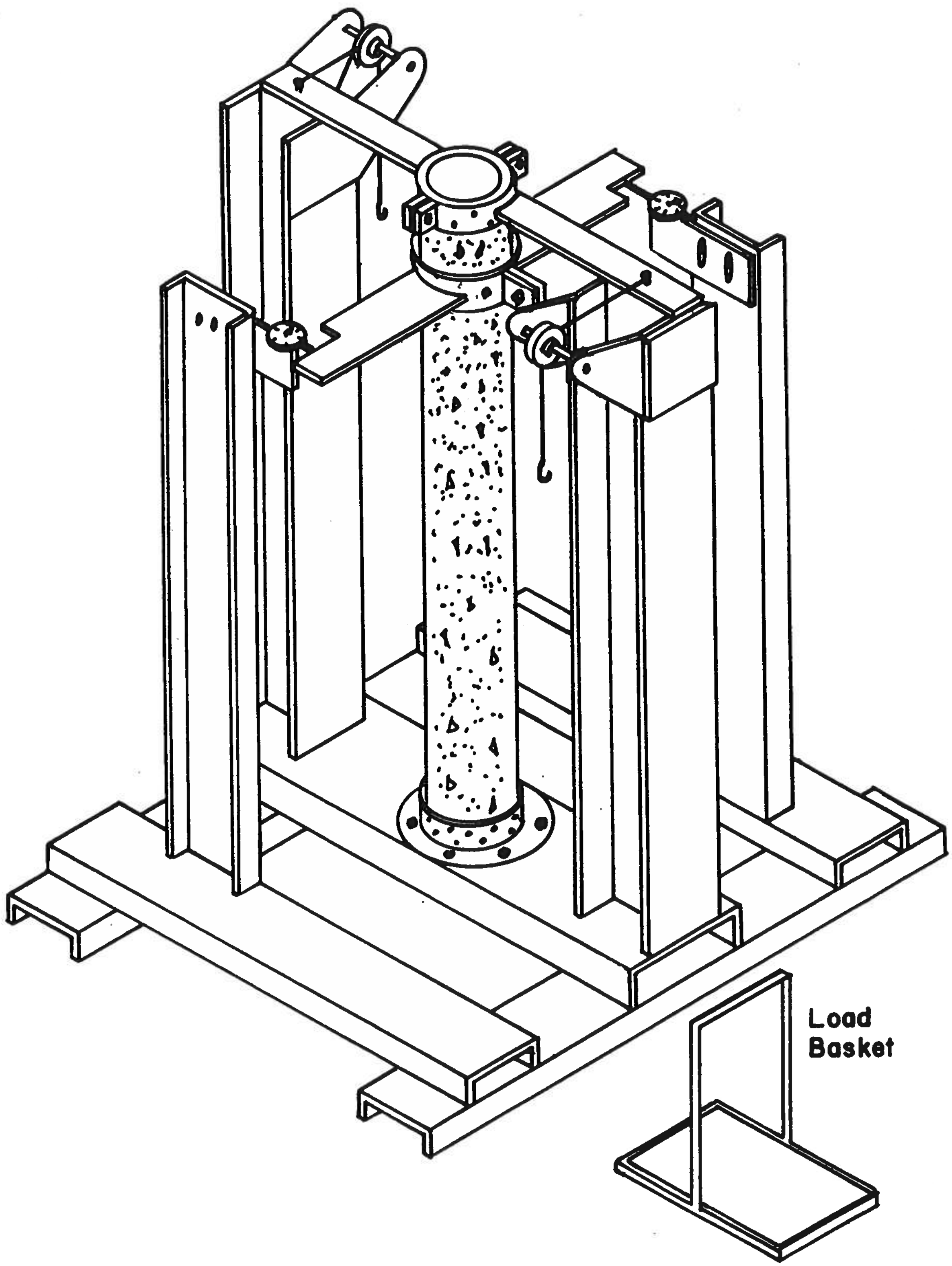

FIG. 9 TORSION LOADING APPARATUS

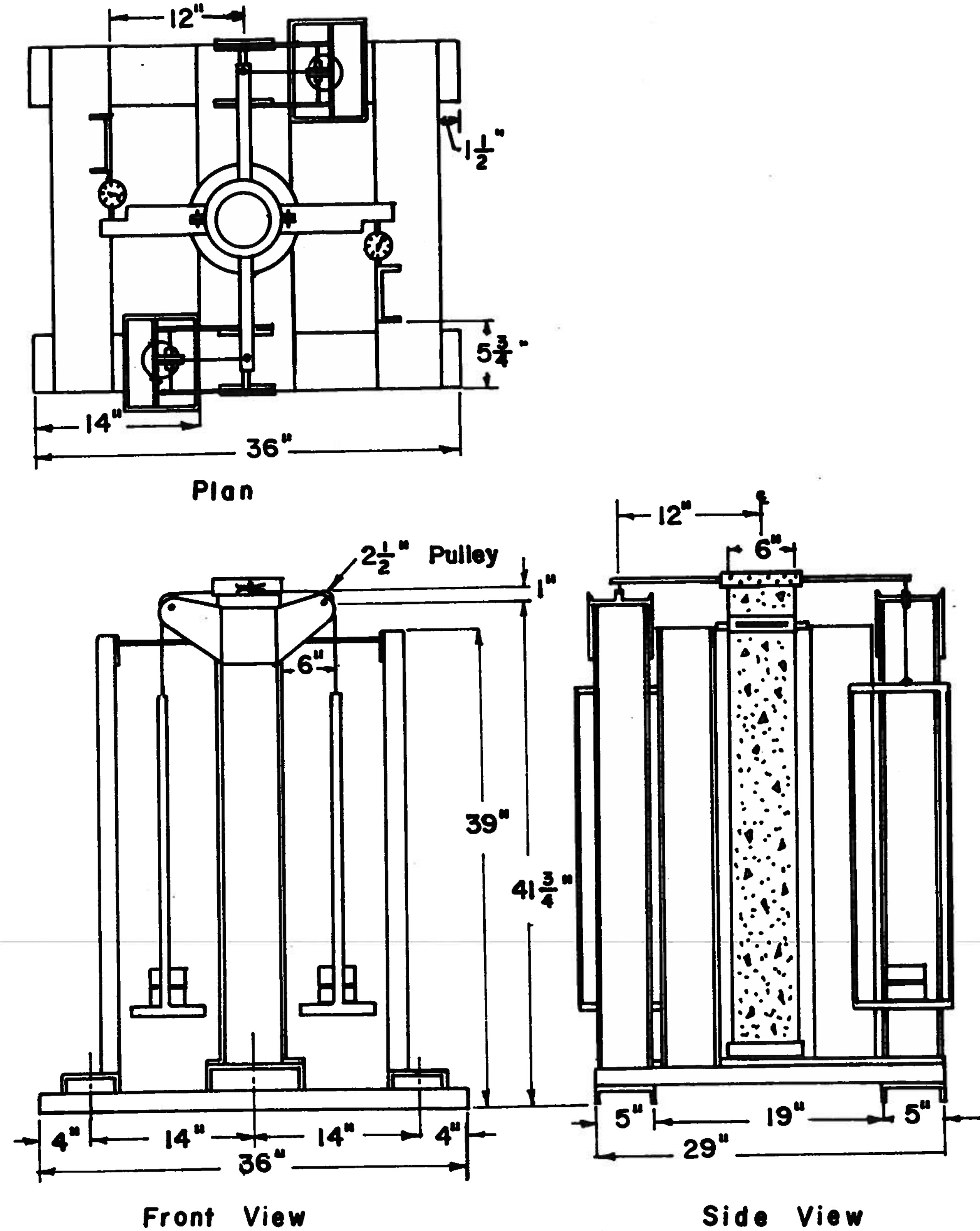

FIG. 10 PRINCIPAL DIMENSIONS OF TORSION LOADING APPARATUS

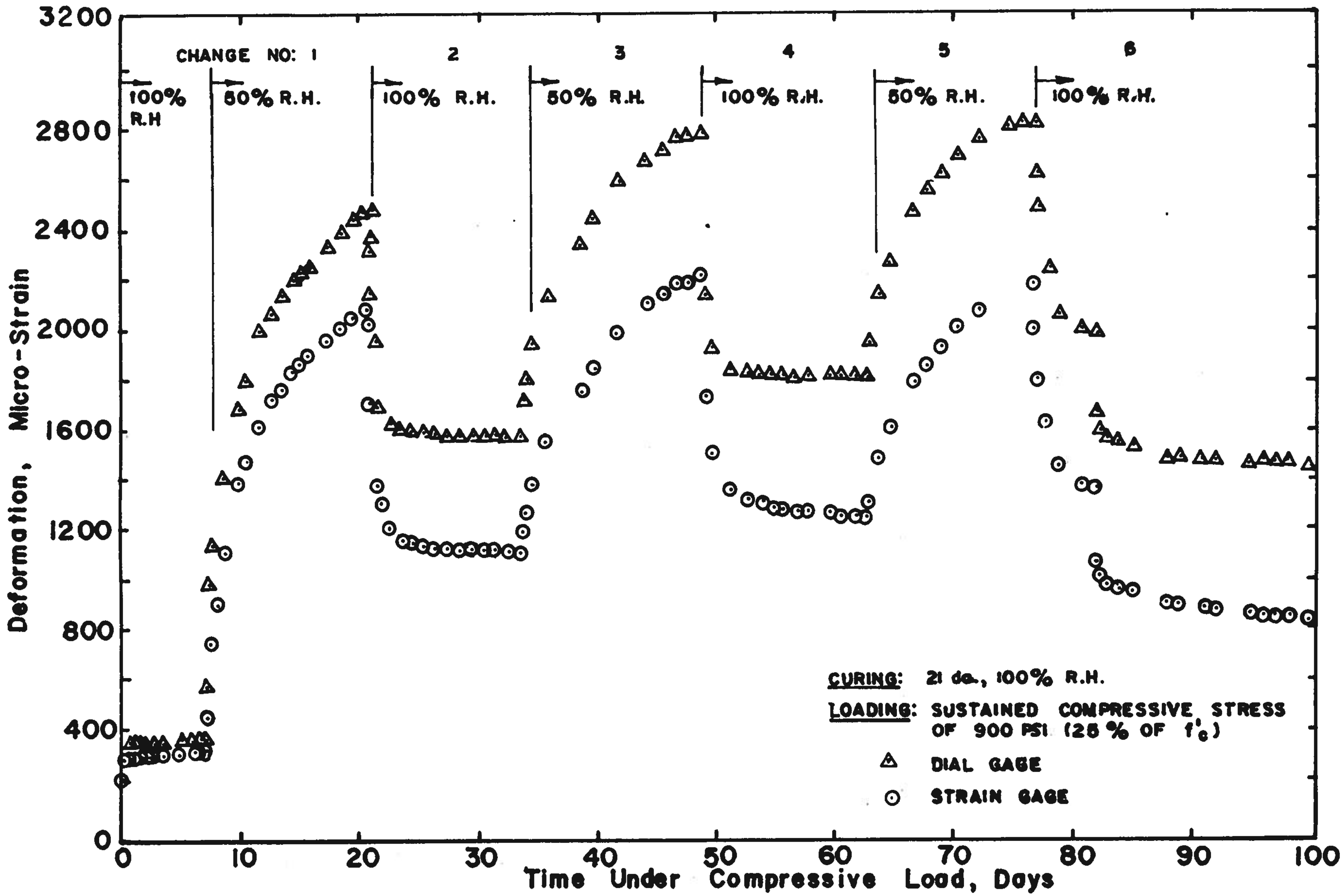

FIG. 11 EFFECT OF CYCLIC HUMIDITY ON SHRINKAGE AND CREEP OF A SPECIMEN UNDER SUSTAINED COMPRESSIVE LOADING

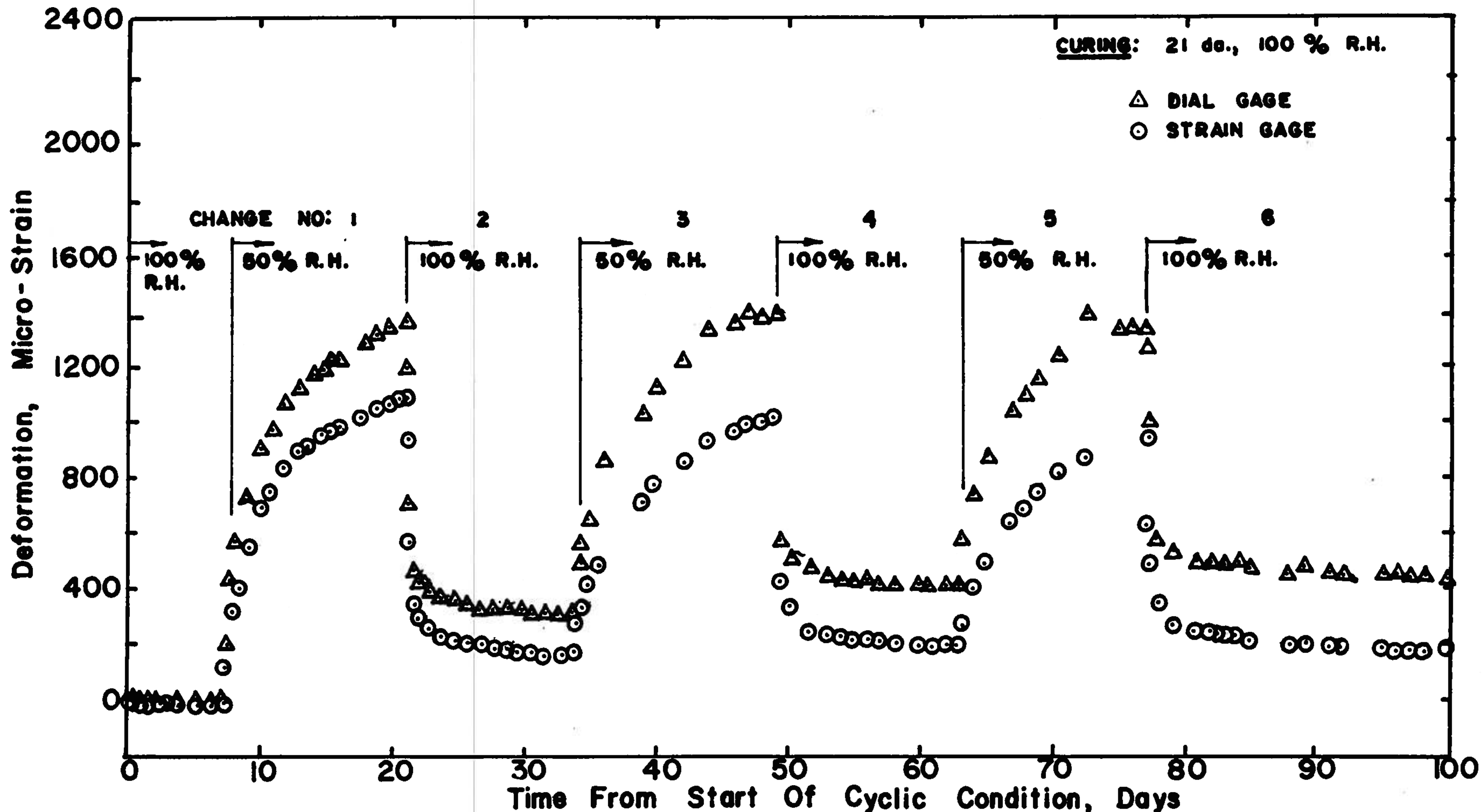

FIG. 12 SHRINKAGE AND SWELLING UNDER CYCLIC HUMIDITY

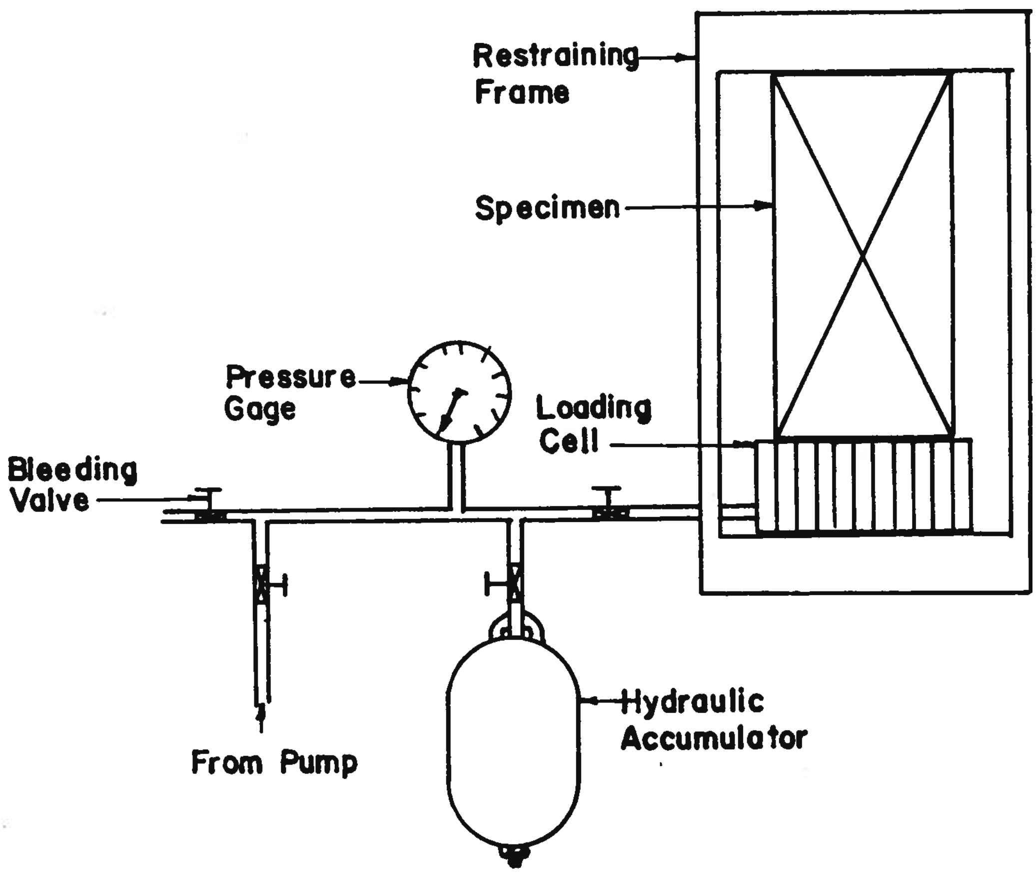

FIG. 13 SCHEMATIC REPRESENTATION OF HYDRAULIC LOADING SYSTEM FOR COMPRESSION SPECIMEN

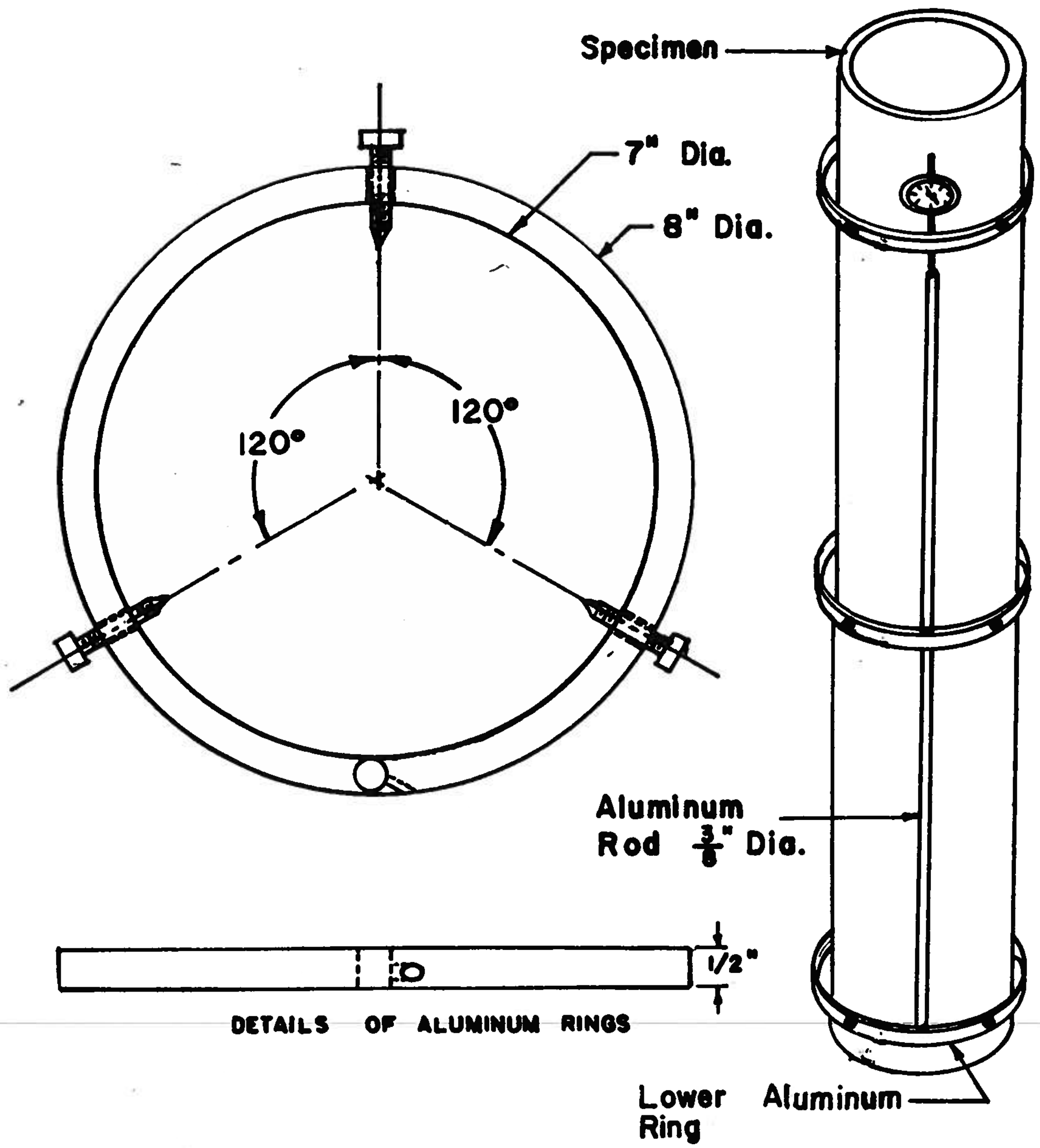

FIG. 14 DEVICE FOR MECHANICAL MEASUREMENT OF COMPRESIVE DEFORMATIONS

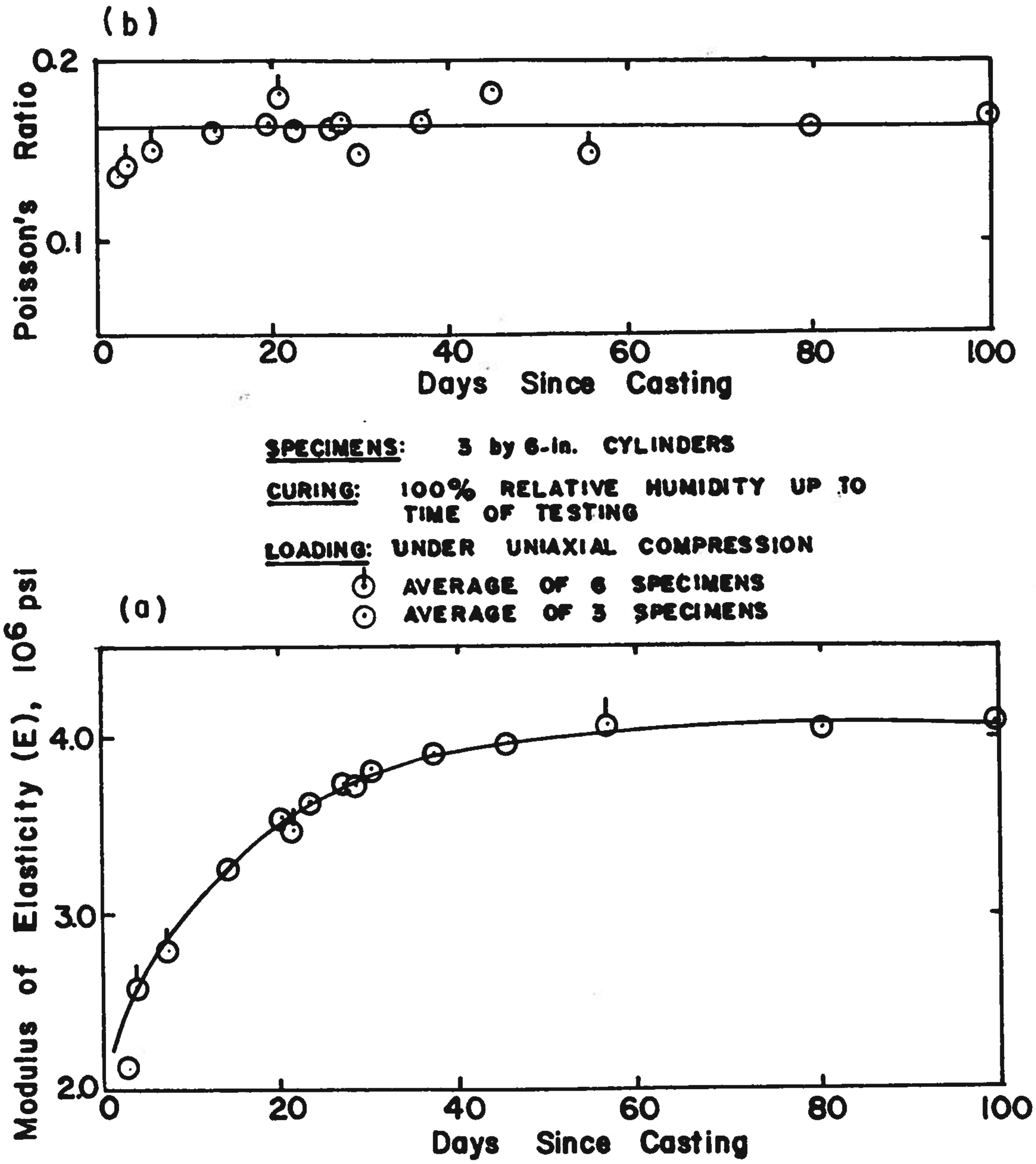

FIG. 15 EFFECT OF MATURITY ON THE MODULUS OF ELASTICITY (E) AND ON POISSON'S RATIO FOR 3 by 6 -in. CYLINDERS

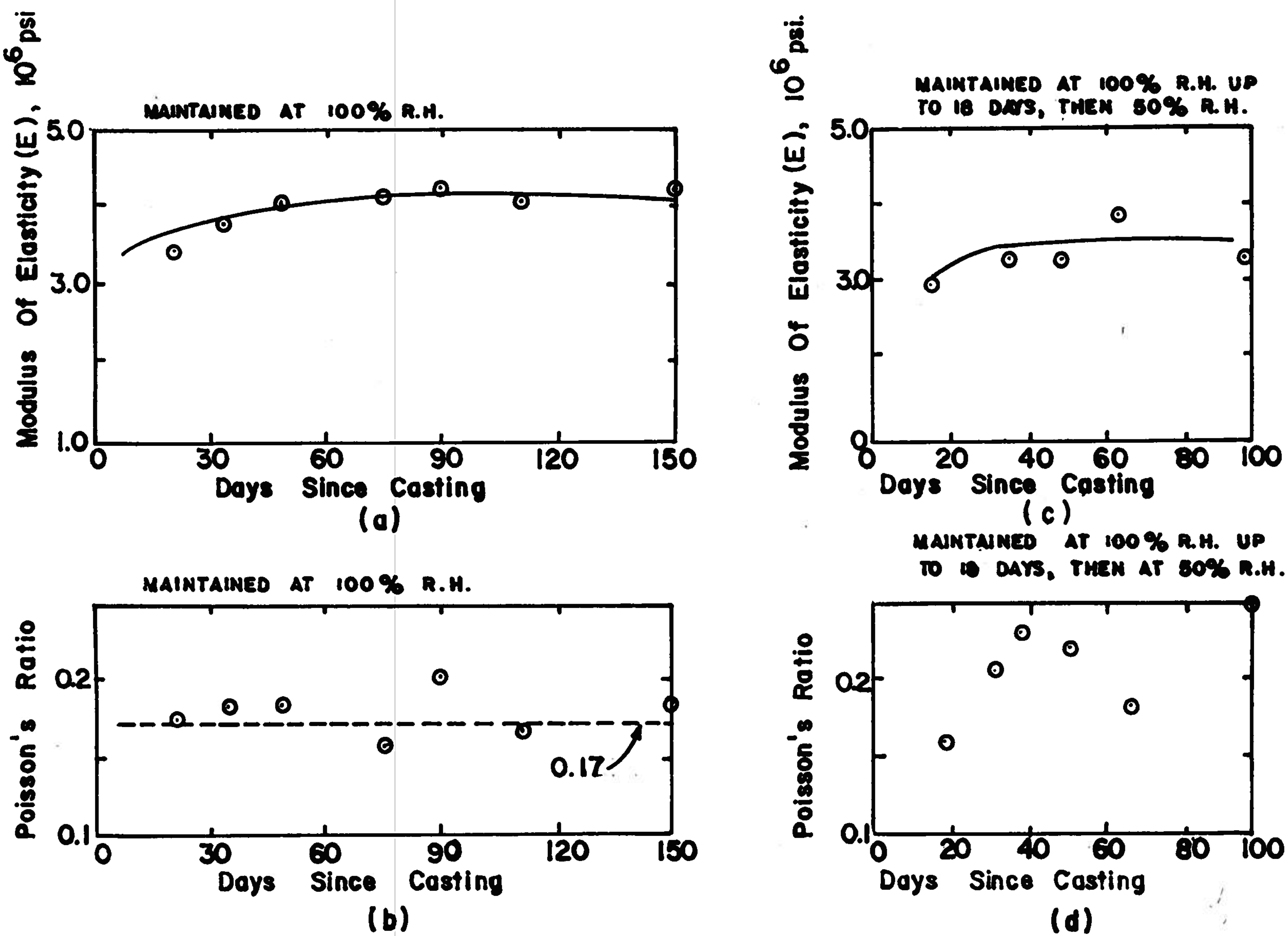

FIG. 16 EFFECT OF TIME ON MODULUS OF ELASTICITY (E) AND ON POISSON'S RATIO FOR HOLLOW CYLINDERS 5"-I.D., 6"-O.D. AND 40"-LONG. (Each point is an average of two or three tests)

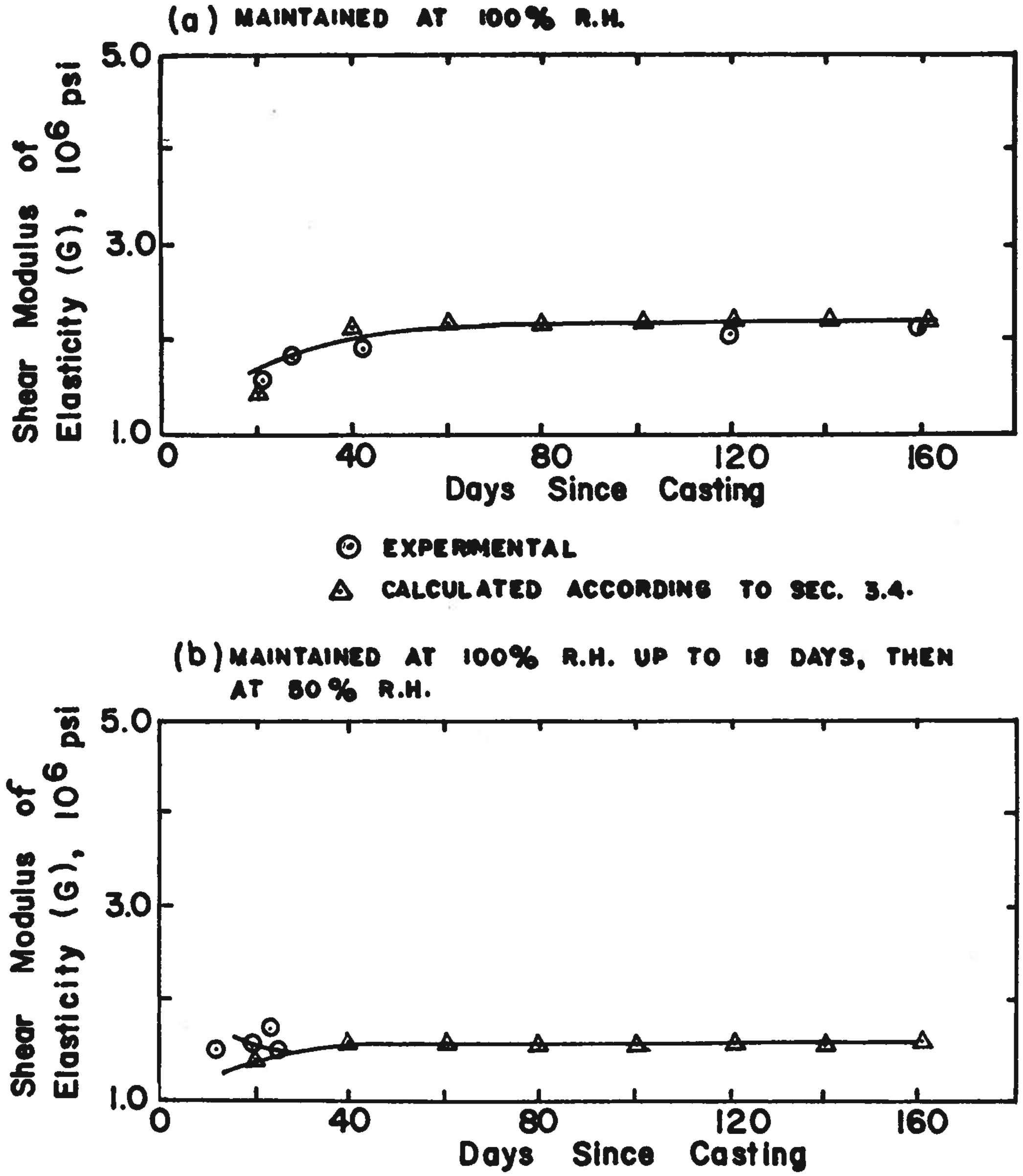

FIG. 17 EFFECT OF t_{eq} ON SHEAR MODULUS OF ELASTICITY (G) OBTAINED BY TORSION TESTS ON HOLLOW CYLINDERS, 5-in. I.D., 6-in. O.D. AND 40-in. LONG. (Each Point is an Average of Two or Three Tests)

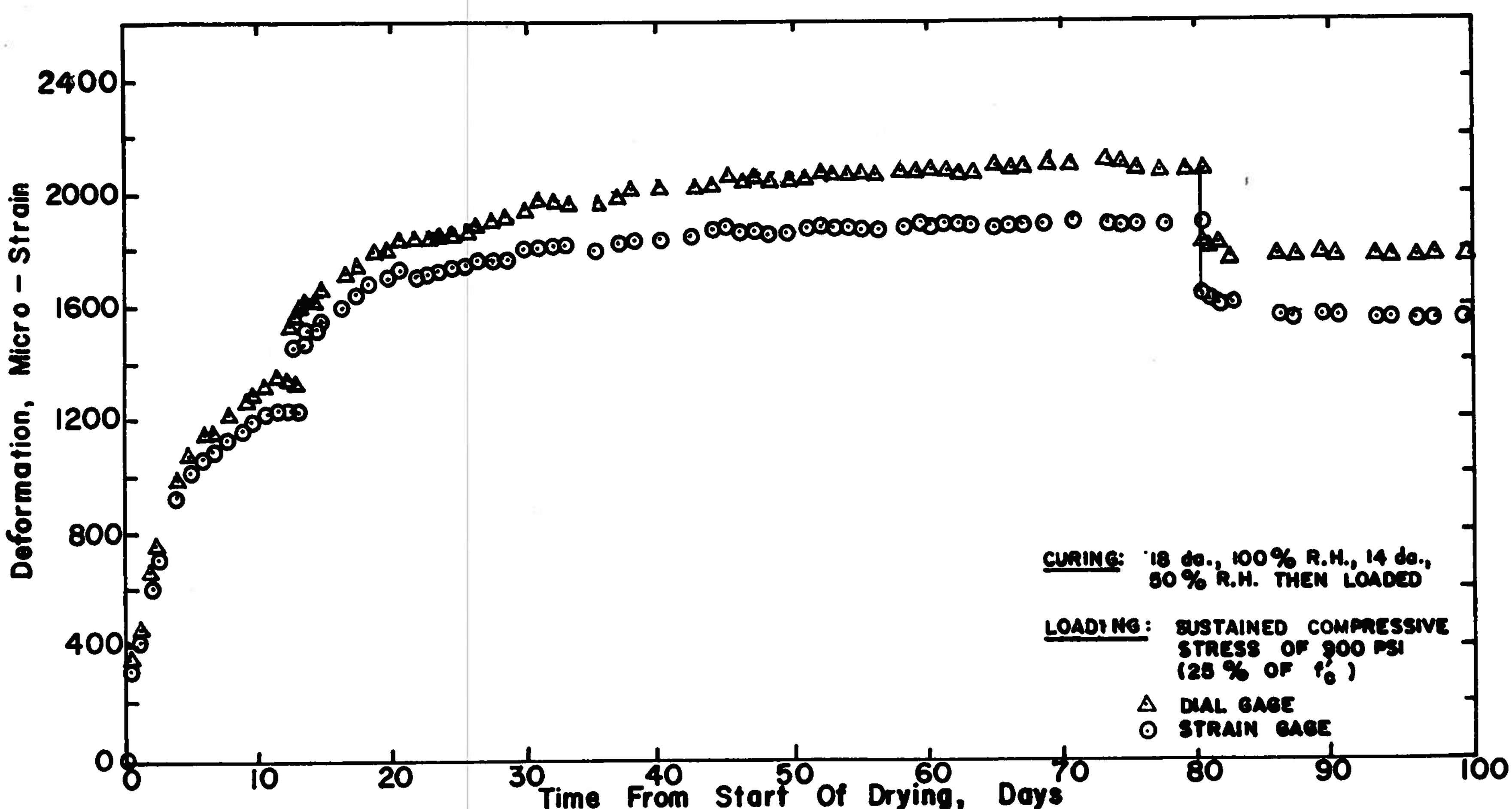

FIG. 18 SHRINKAGE AND CREEP UNDER 50 PER CENT RELATIVE HUMIDITY AND SUSTAINED COMPRESSIVE LOADING

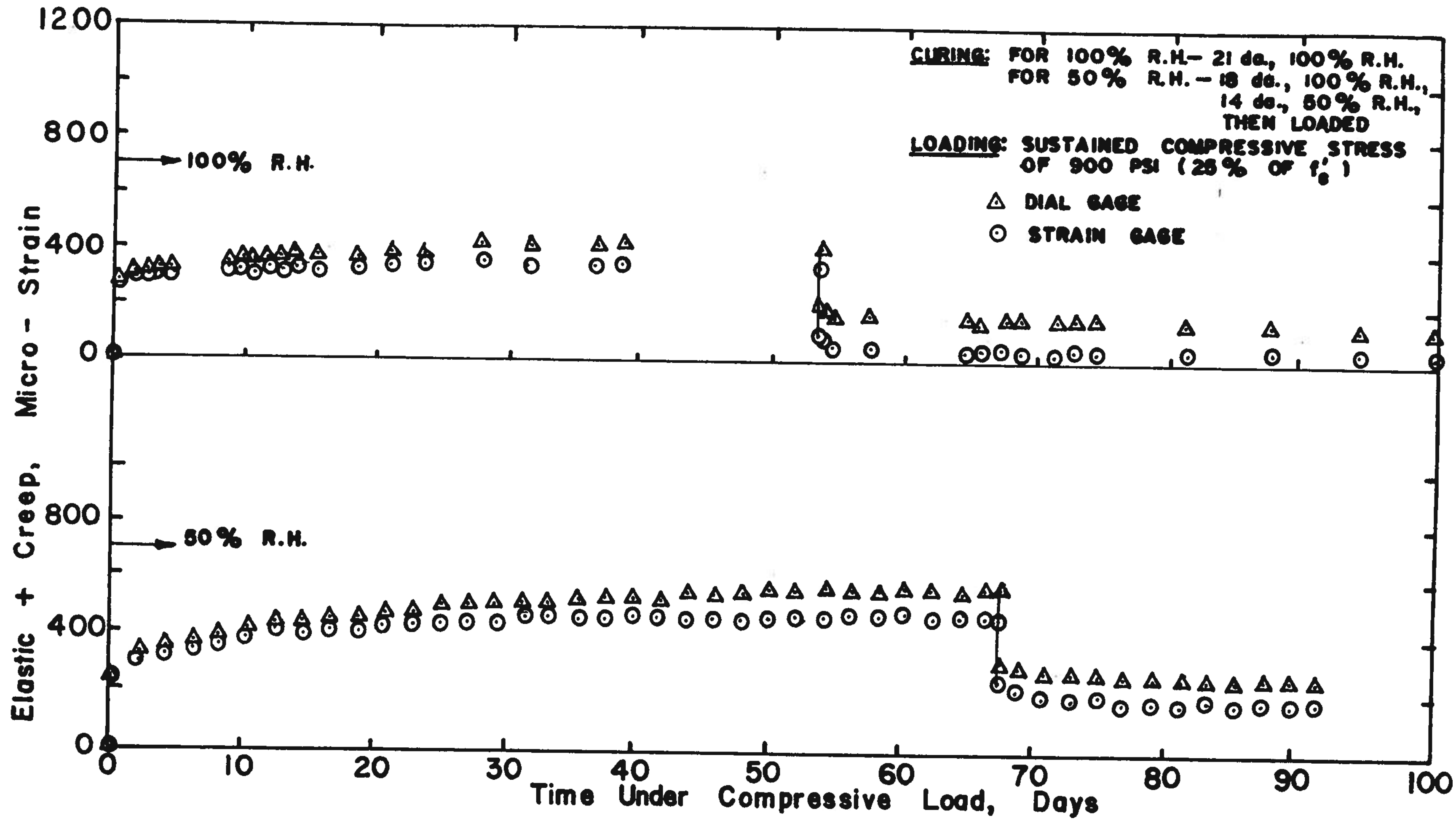

FIG. 19 EFFECT OF HUMIDITY AT TIME OF LOADING ON CREEP OF CONCRETE UNDER COMPRESSIVE LOADING

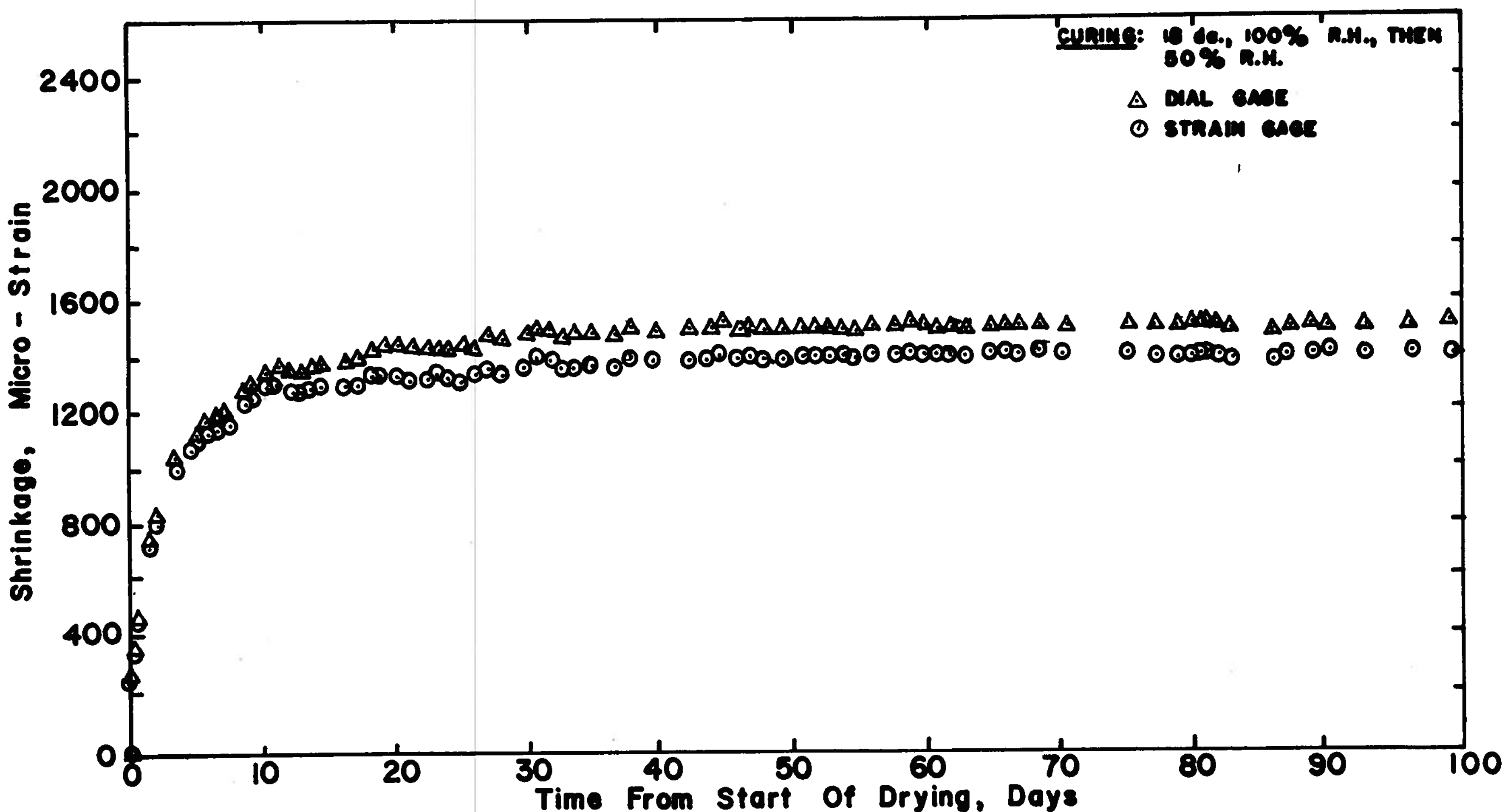

FIG. 20 SHRINKAGE AT CONSTANT 50 PER CENT RELATIVE HUMIDITY

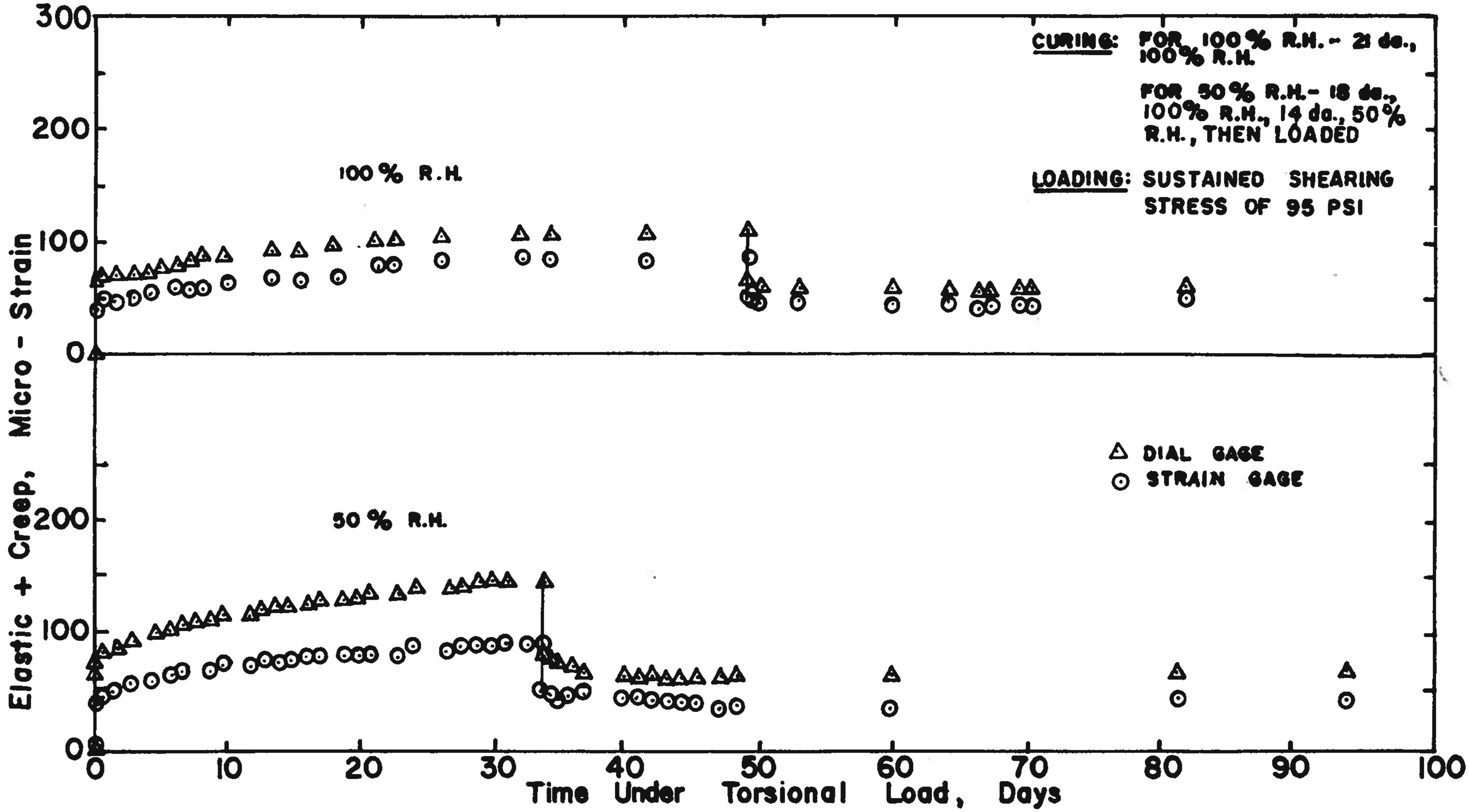

FIG. 21 EFFECT OF HUMIDITY AT TIME OF LOADING ON CREEP OF CONCRETE UNDER SUSTAINED TORSIONAL LOADING

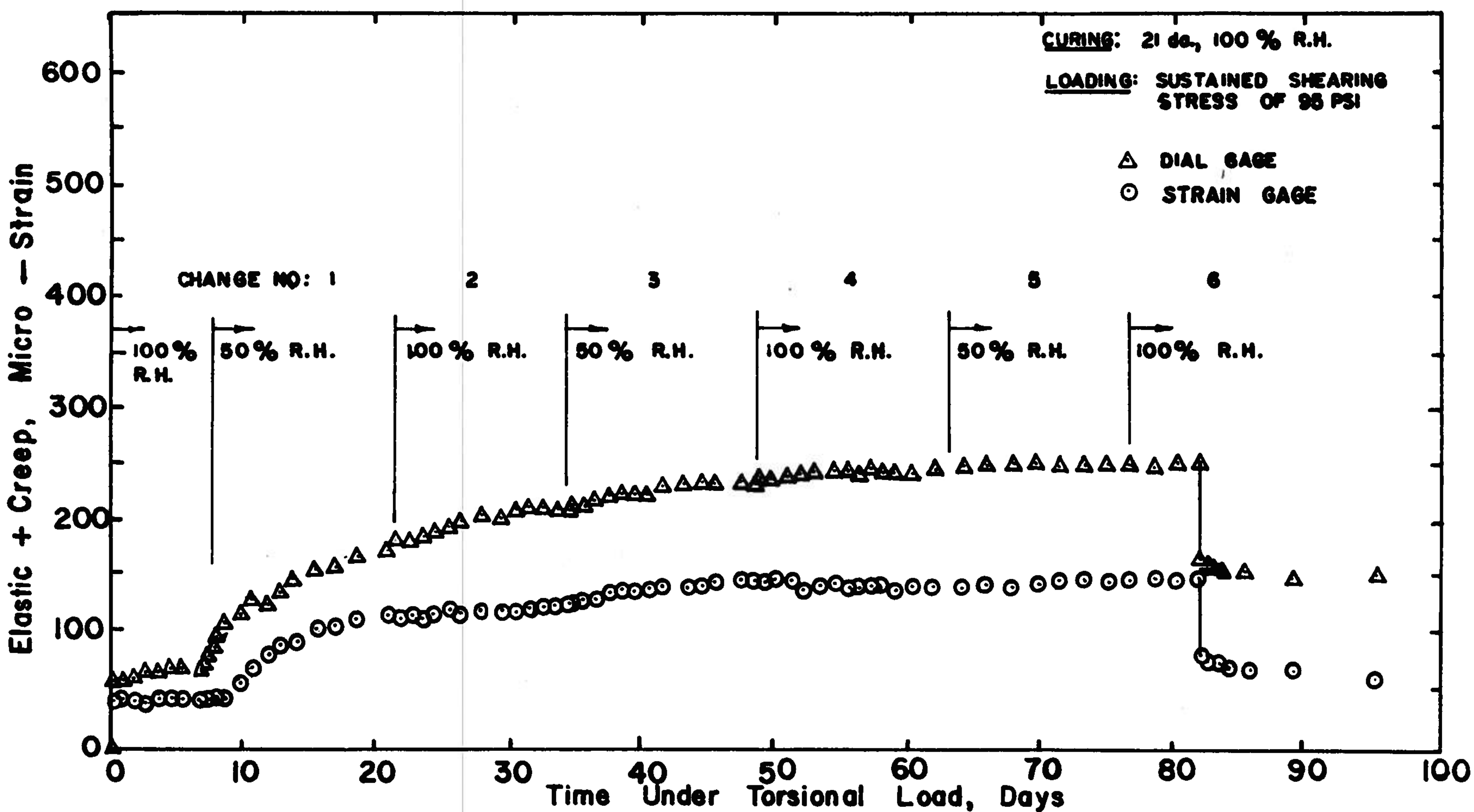

FIG. 22 EFFECT OF CYCLIC HUMIDITY ON CREEP OF CONCRETE UNDER SUSTAINED TORSIONAL LOADING

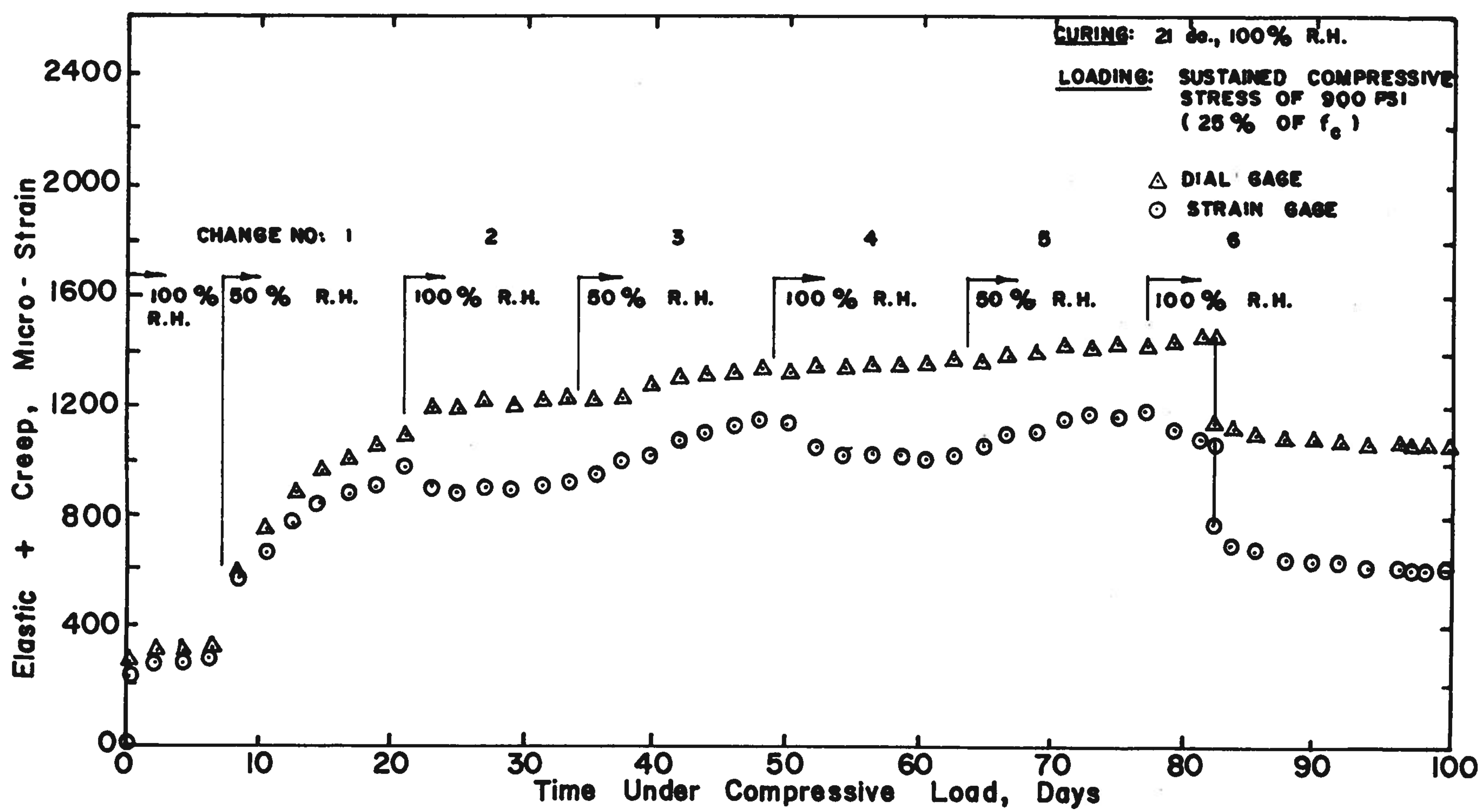

FIG. 23 EFFECT OF HUMIDITY ON CREEP OF CONCRETE UNDER SUSTAINED COMPRESSIVE LOADING

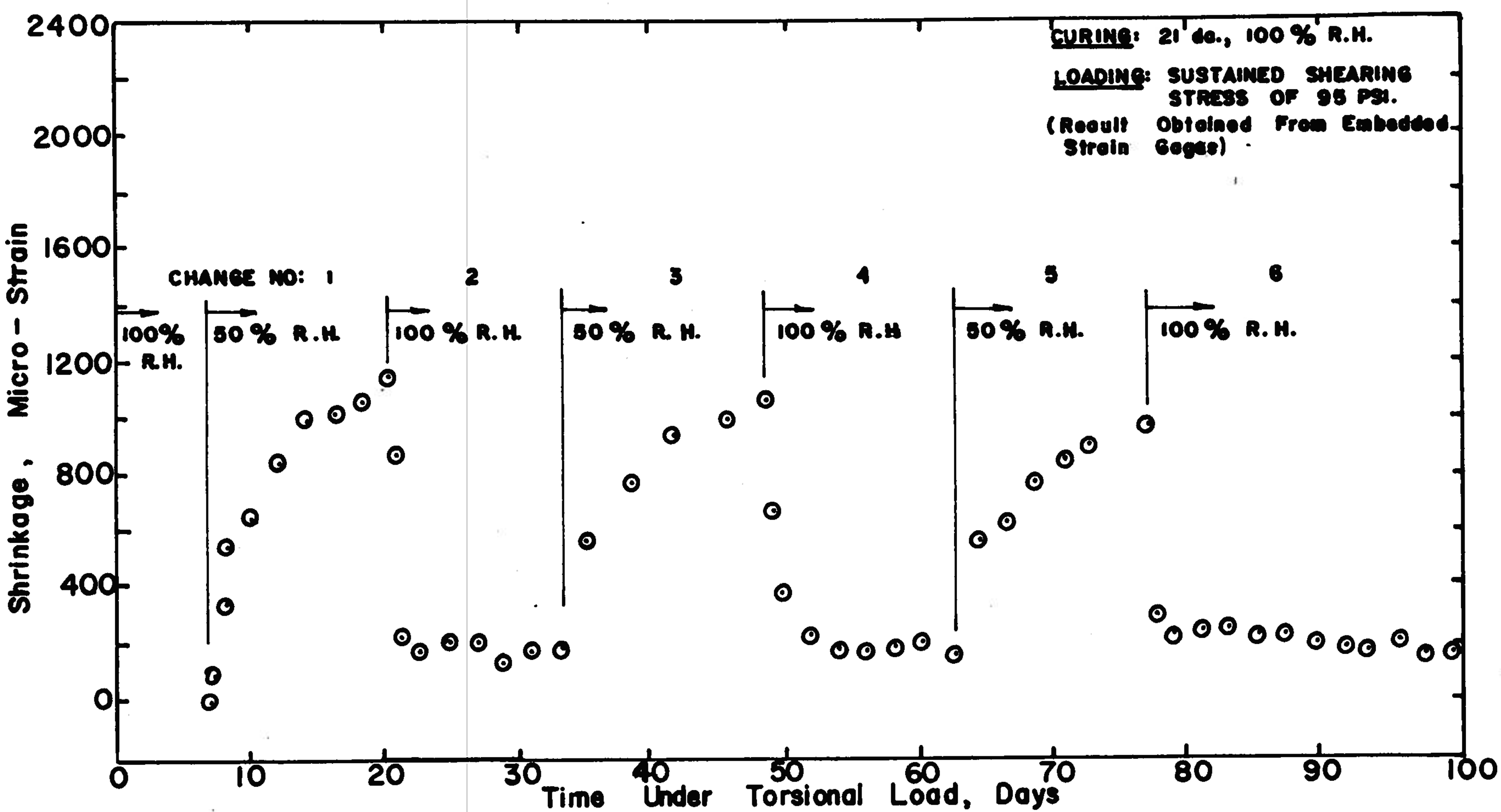

FIG. 24 CALCULATED SHRINKAGE, ε_s, FOR A DRYING SPECIMEN UNDER TORSIONAL SUSTAINED LOADING (Equation 2.6.4., Section 2.6.4)

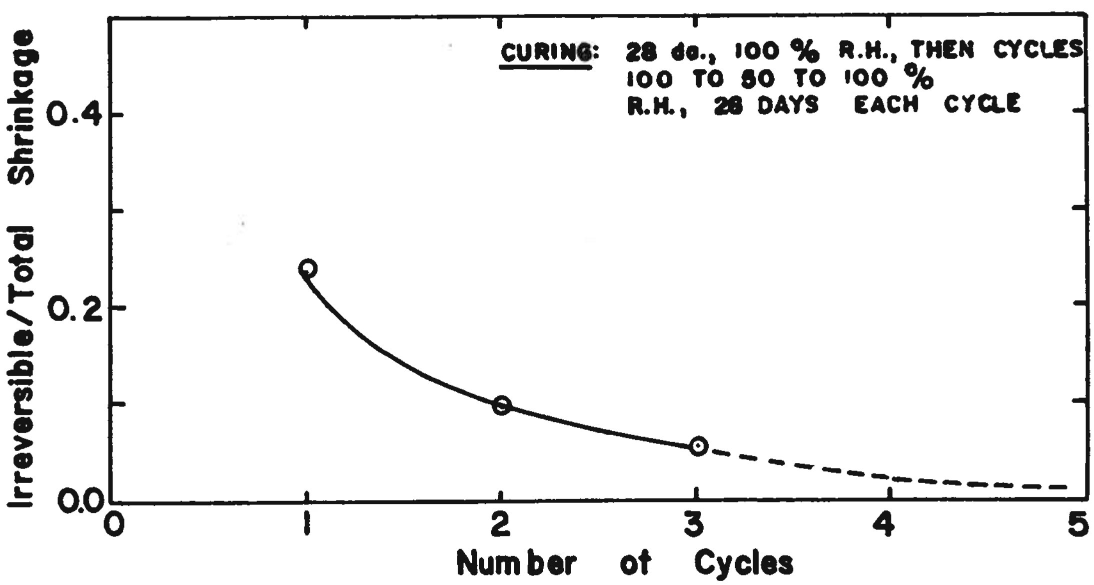

FIG. 25 EFFECT OF NUMBER OF HUMIDITY CYCLES ON IRREVERSIBLE SHRINKAGE

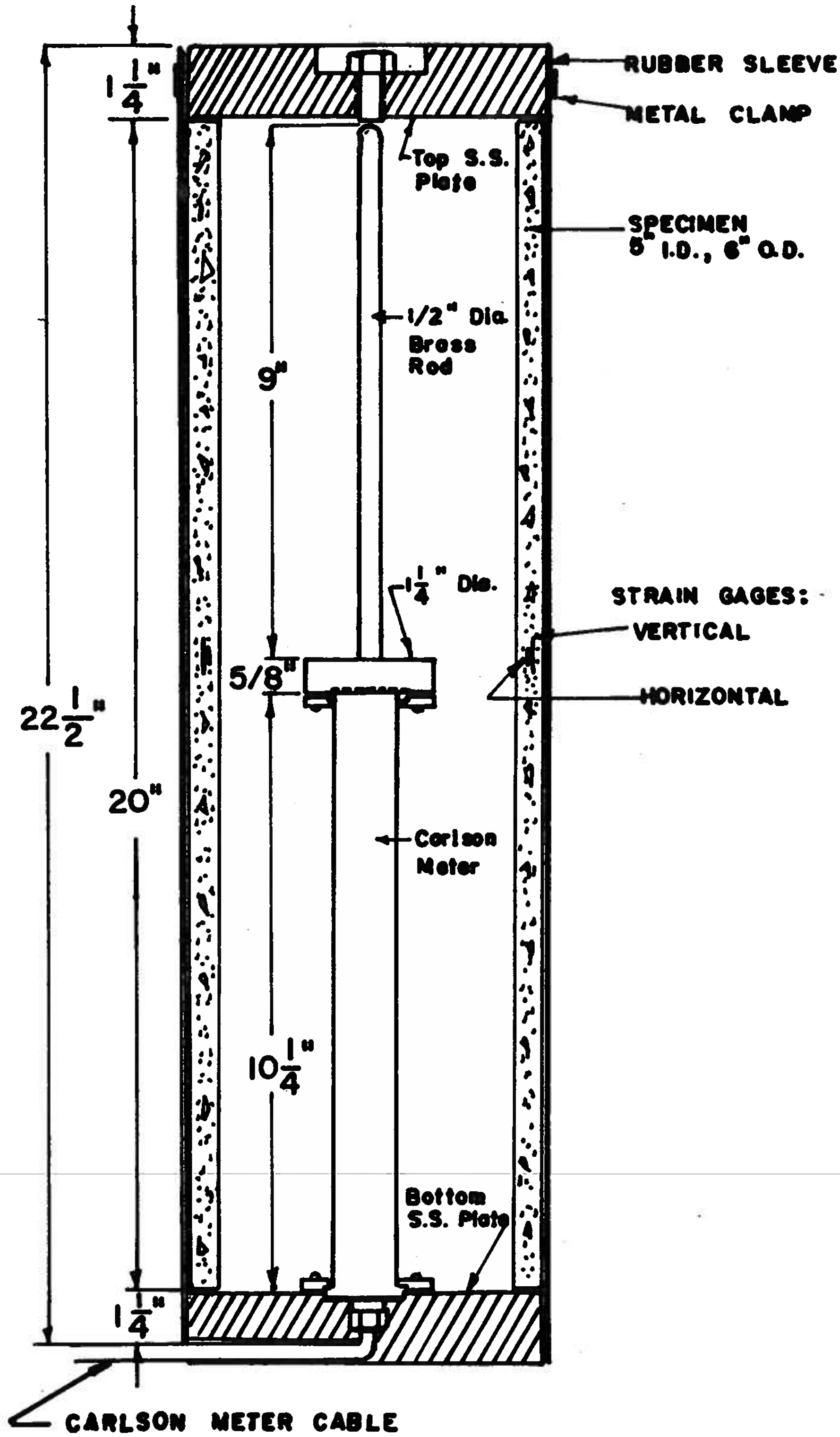

FIG. 26 DETAILS OF A BIAXIAL SPECIMEN WITH CARLSON METER

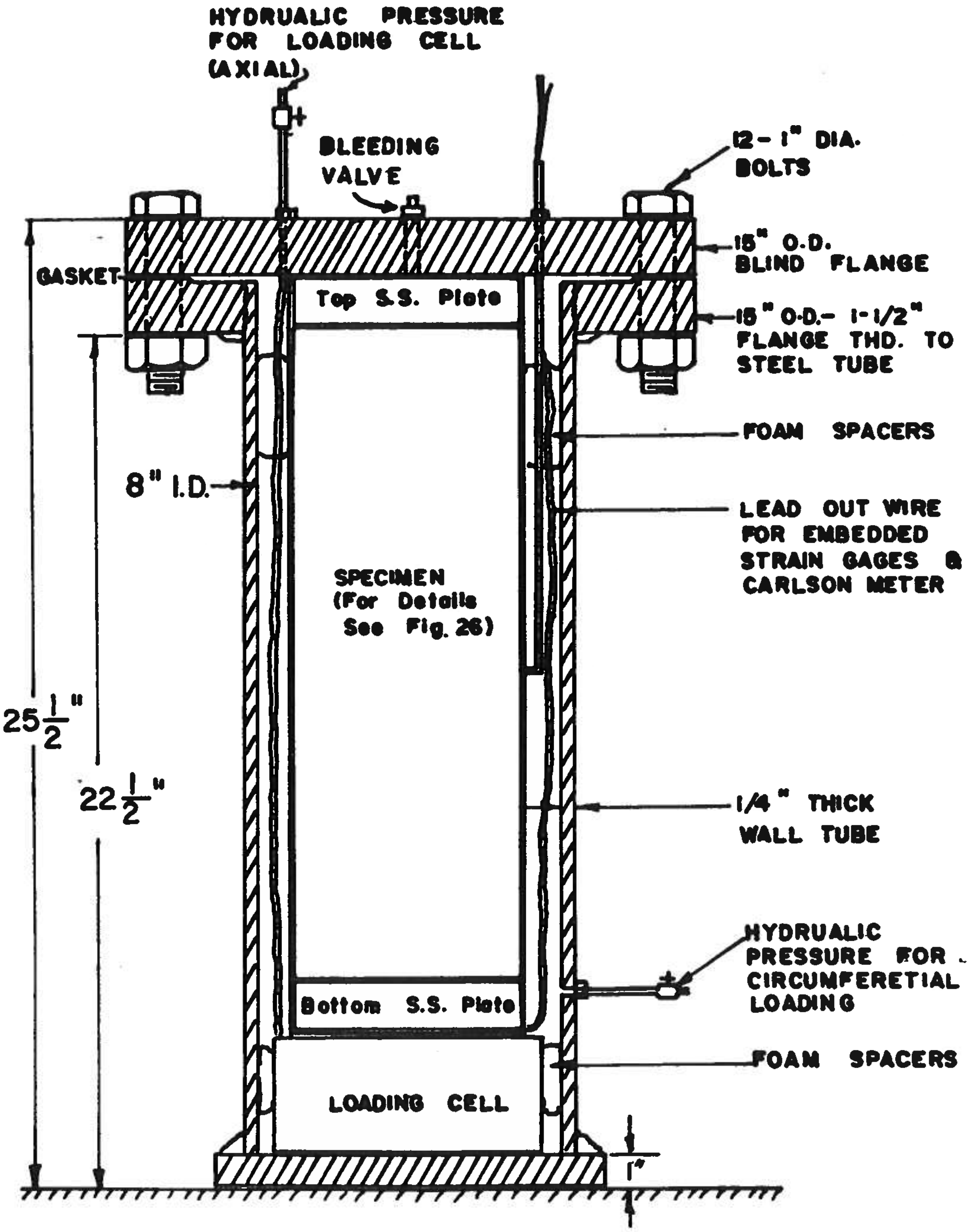

FIG. 27 DETAILS OF BIAXIAL LOADING VESSEL

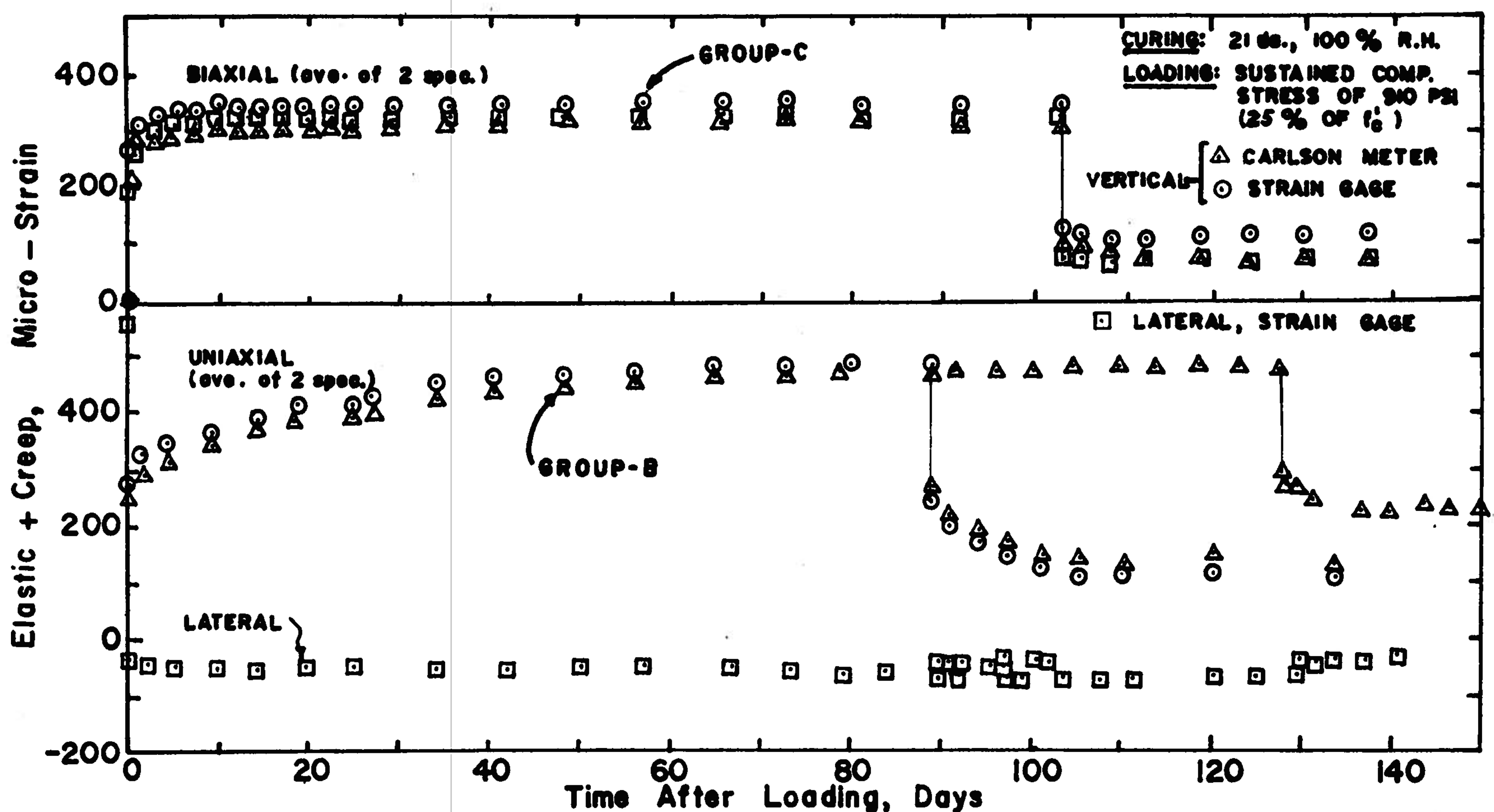

FIG. 28 CREEP OF SEALED CONCRETE SPECIMENS UNDER SUSTAINED UNIAXIAL AND BIAXIAL LOADING

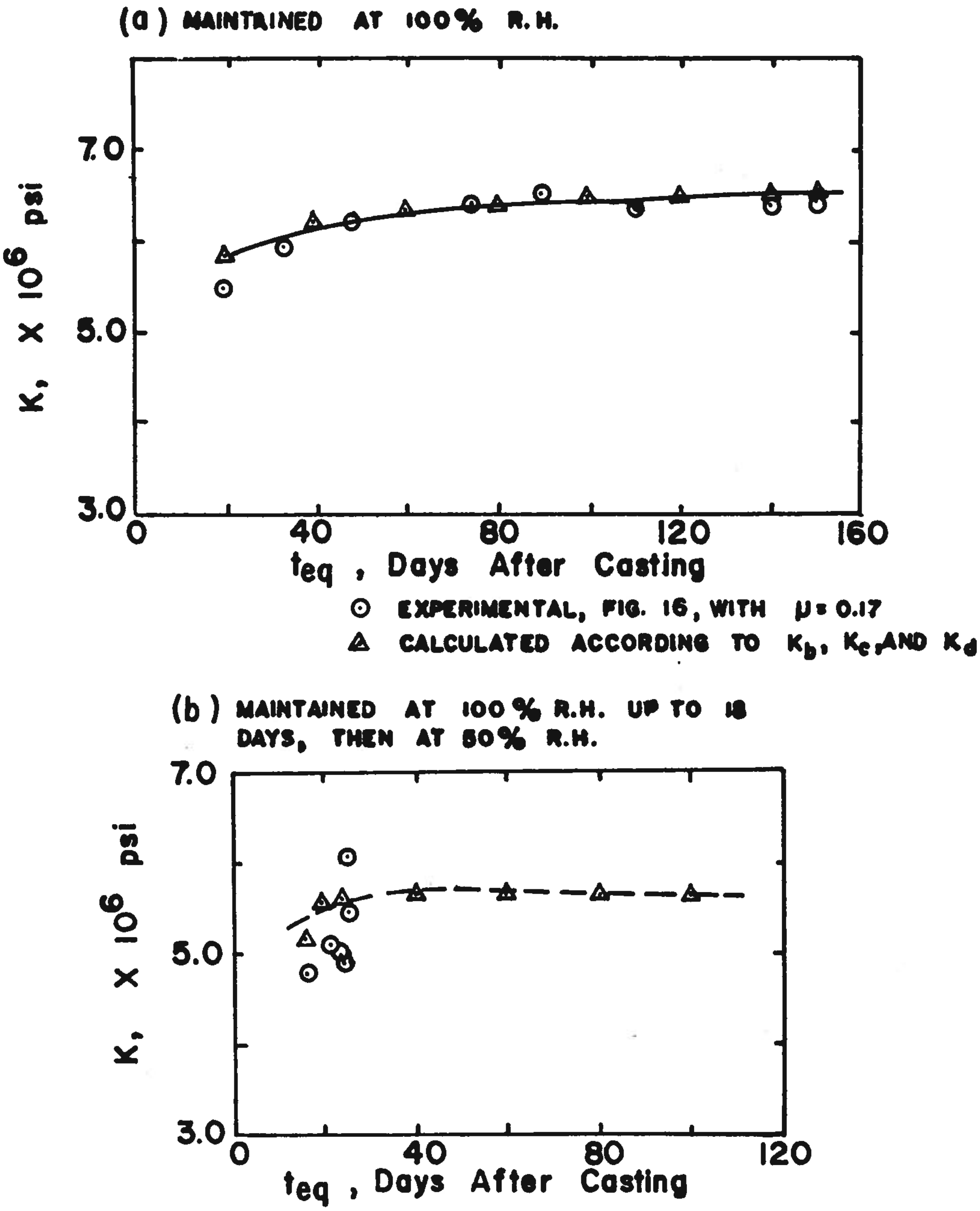

FIG. 29 EFFECT OF EQUIVALENT CURING TIME, t_{eq} AND HUMIDITY, h_{eq} ON BULK MODULS OF ELASTICITY, K. (Effect of h_s is neglected. t_{eq} is calculated using Equation 1.4.8)

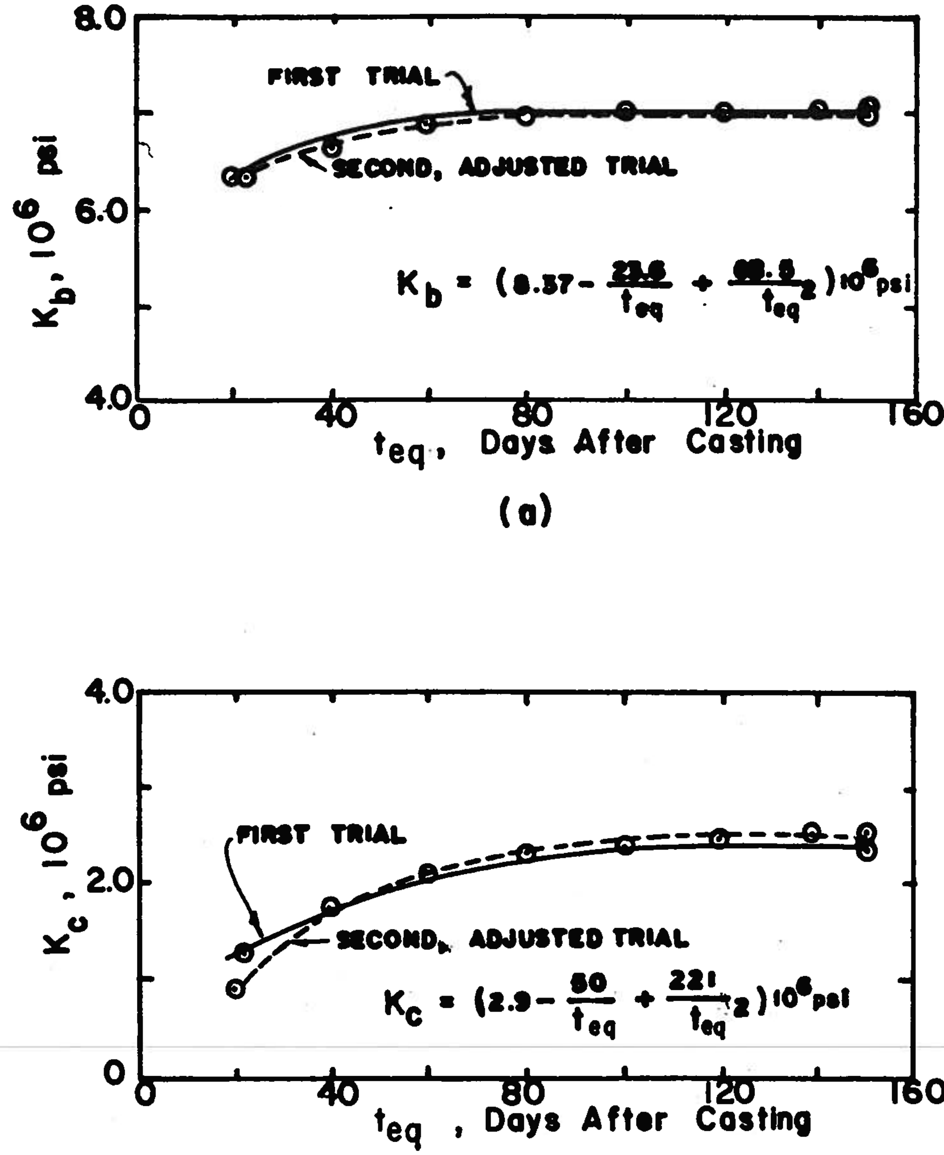

FIG. 30 EFFECT OF t_{eq} ON K_b AND K_c

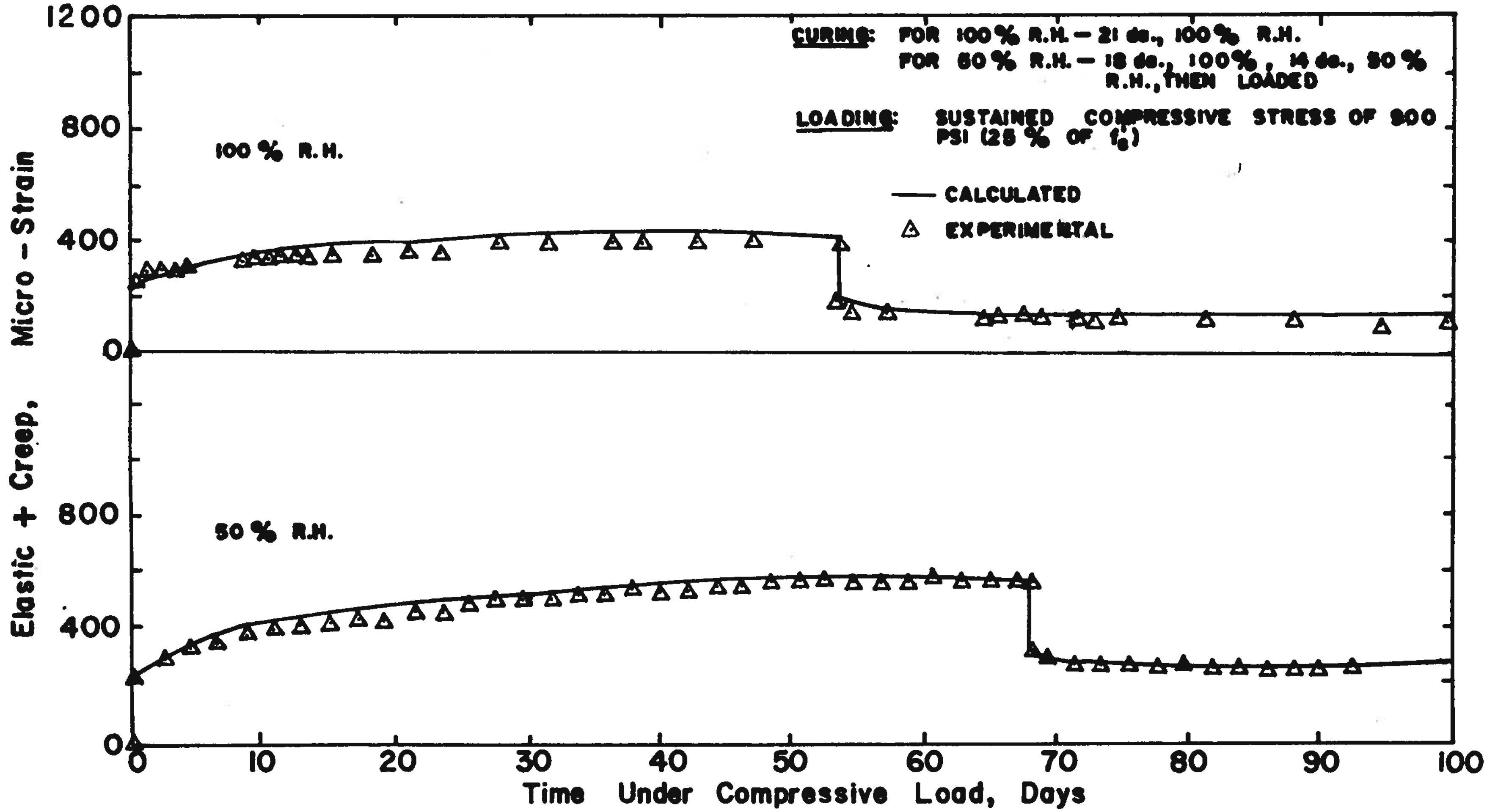

FIG. 31 COMPARISON BETWEEN CALCULATED AND EXPERIMENTAL CREEP DEFORMATIONS FOR A SPECIMEN UNDER COMPRESSIVE LOADING

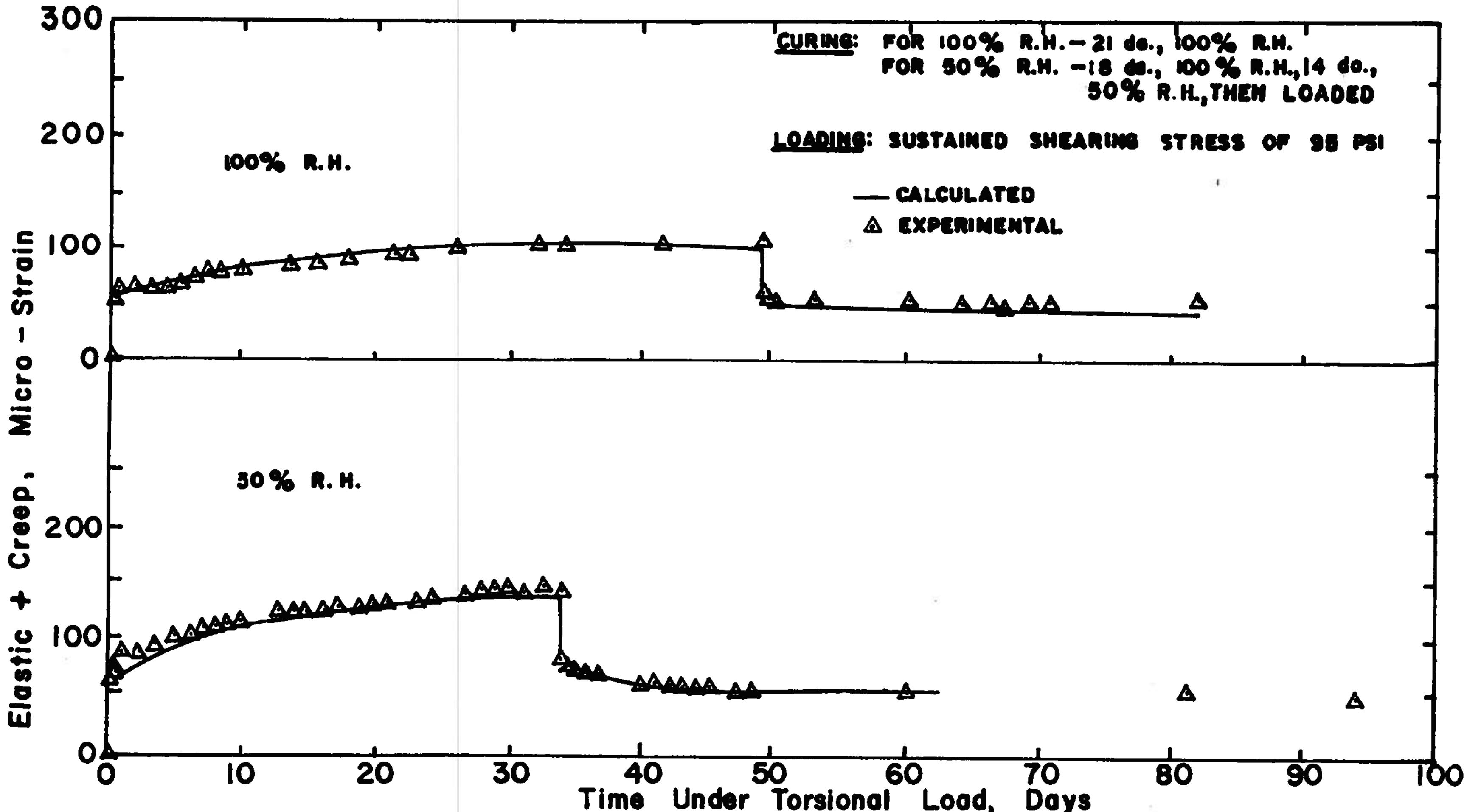

FIG. 32 COMPARISON BETWEEN CALCULATED AND EXPERIMENTAL CREEP DEFORMATIONS FOR A SPECIMEN UNDER TORSIONAL LOADING

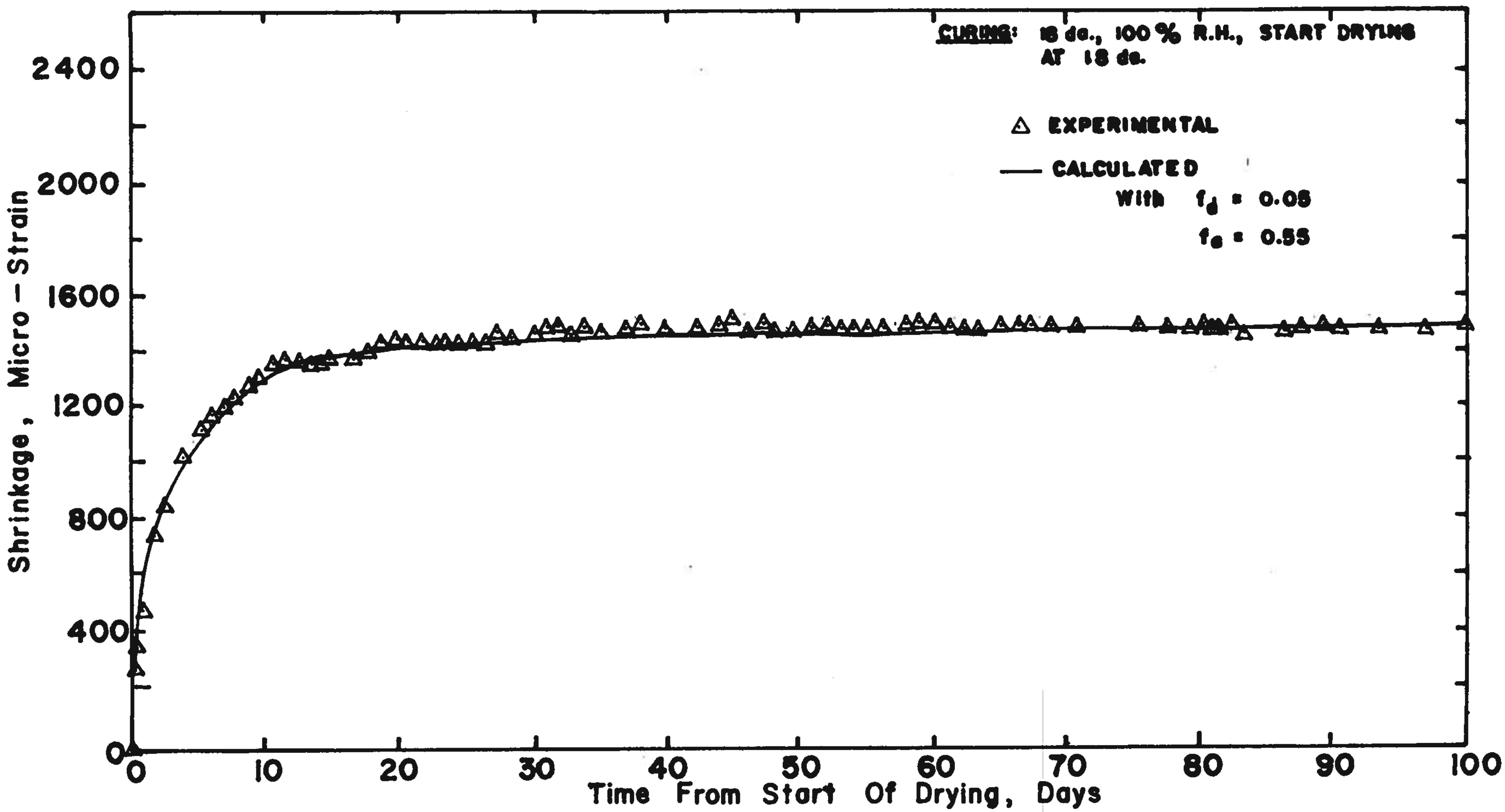

FIG. 33 CALCULATED SHRINKAGE FOR A SPECIMEN DRYING IN AN ENVIRONMENT OF CONSTANT 50 PER CENT RELATIVE HUMIDITY

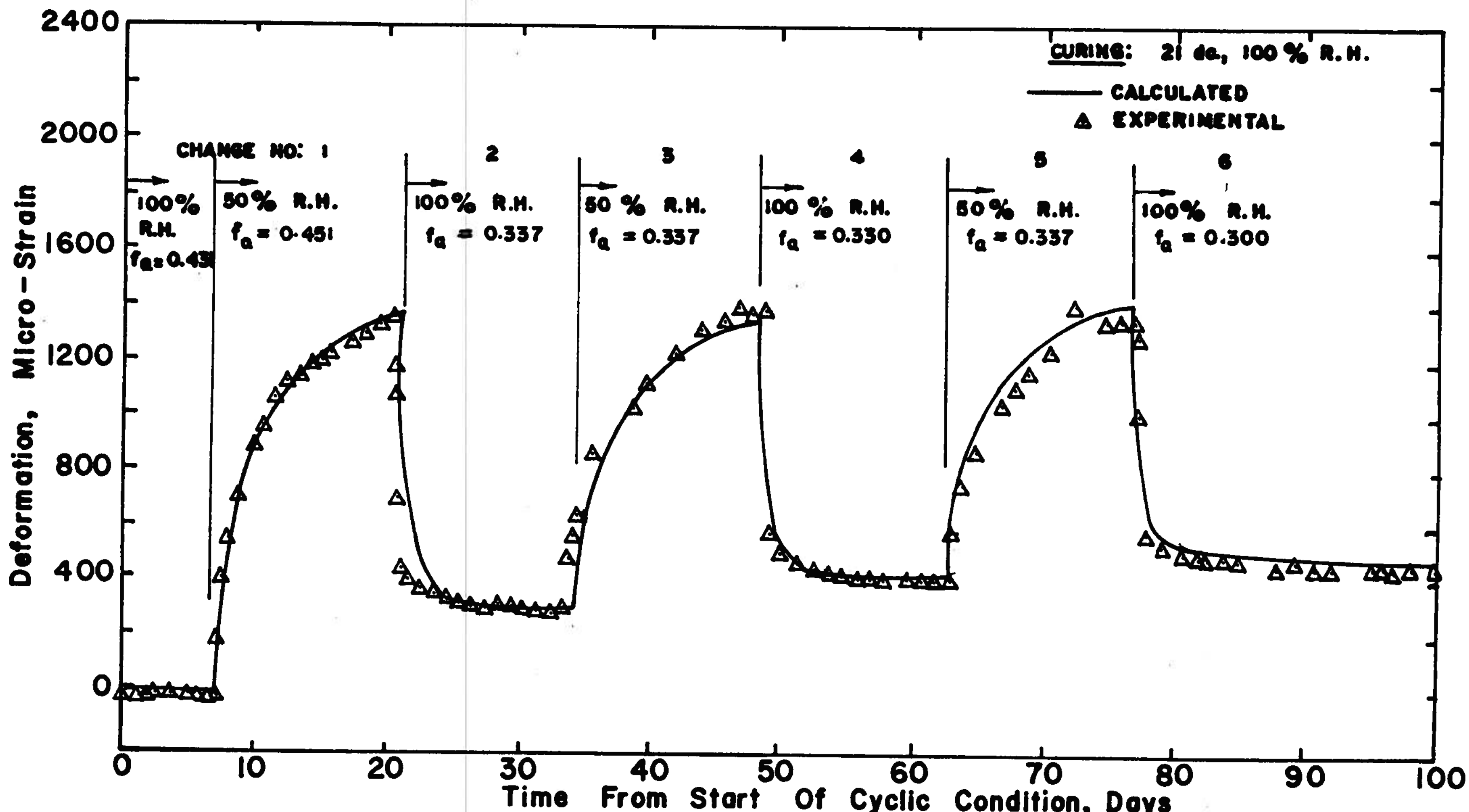

FIG. 34 COMPARISON BETWEEN CALCULATED AND EXPERIMENTAL VALUES OF DEFORMATION DUE TO CYCLIC HUMIDITY

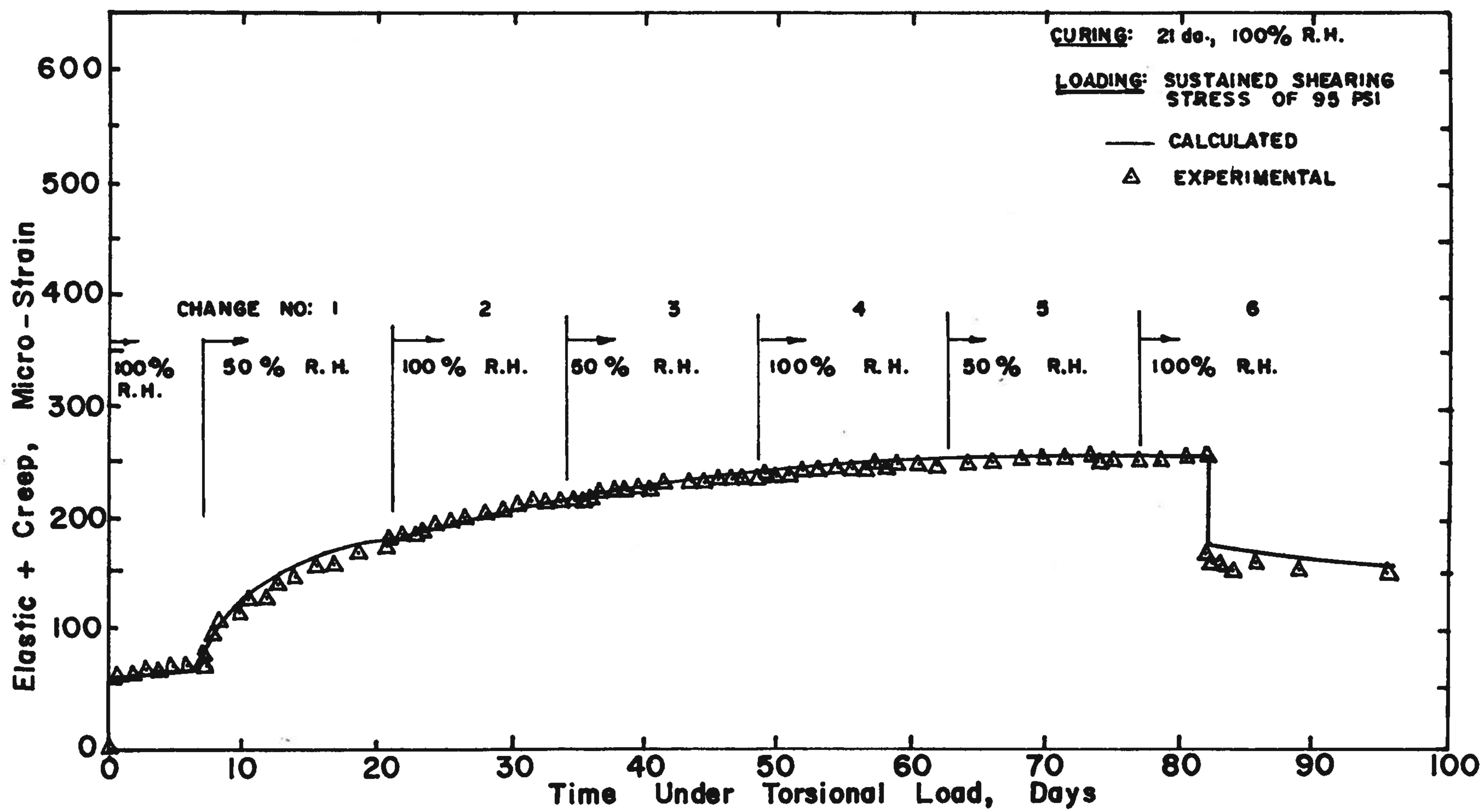

FIG. 35 COMPARISON BETWEEN CALCULATED AND EXPERIMENTAL VALUES OF TORSION CREEP UNDER CYCLIC HUMIDITY

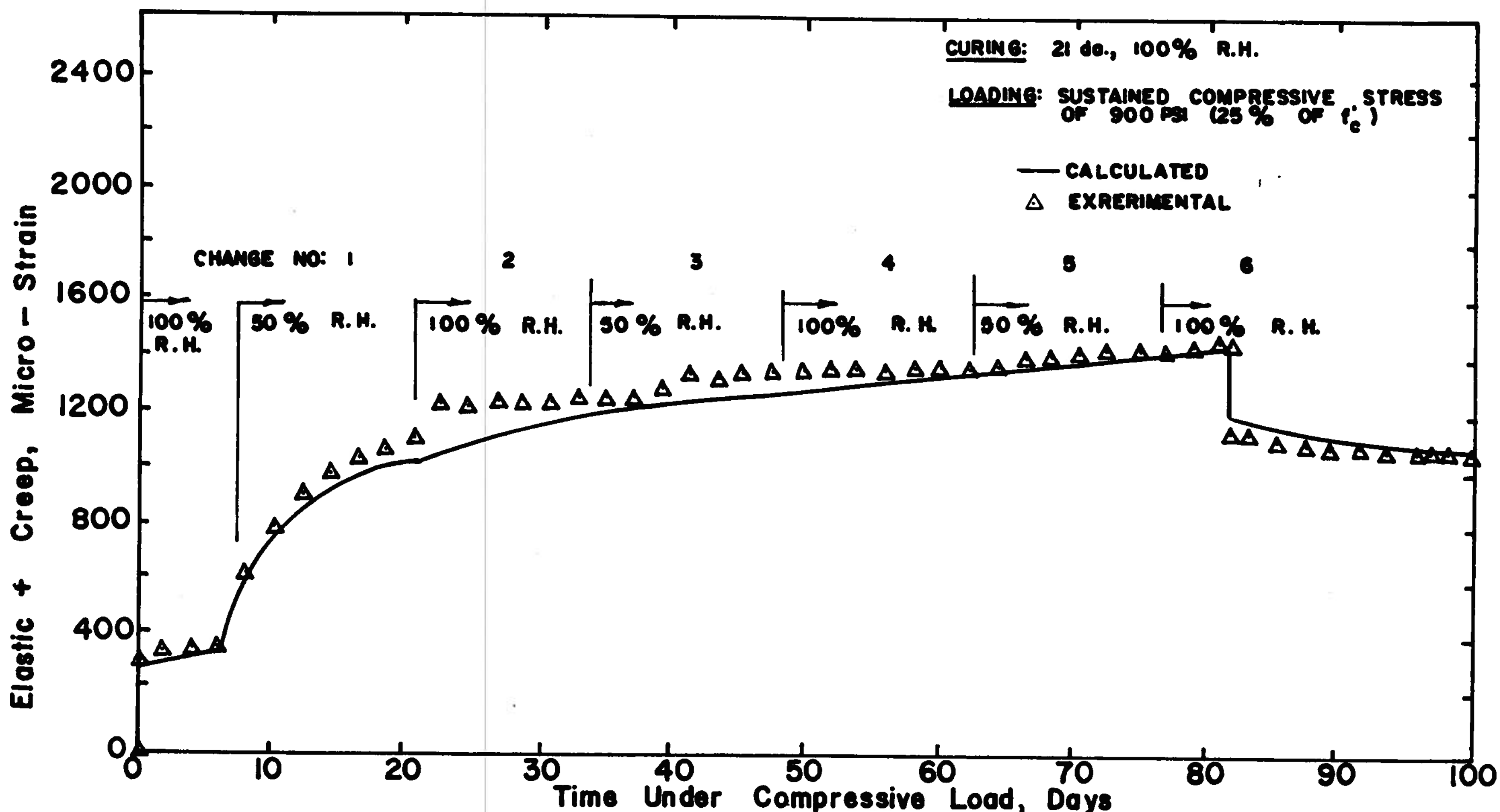

FIG. 36 COMPARISON BETWEEN CALCULATED AND EXPERIMENTAL VALUES OF COMPRESSION CREEP UNDER CYCLIC HUMIDITY

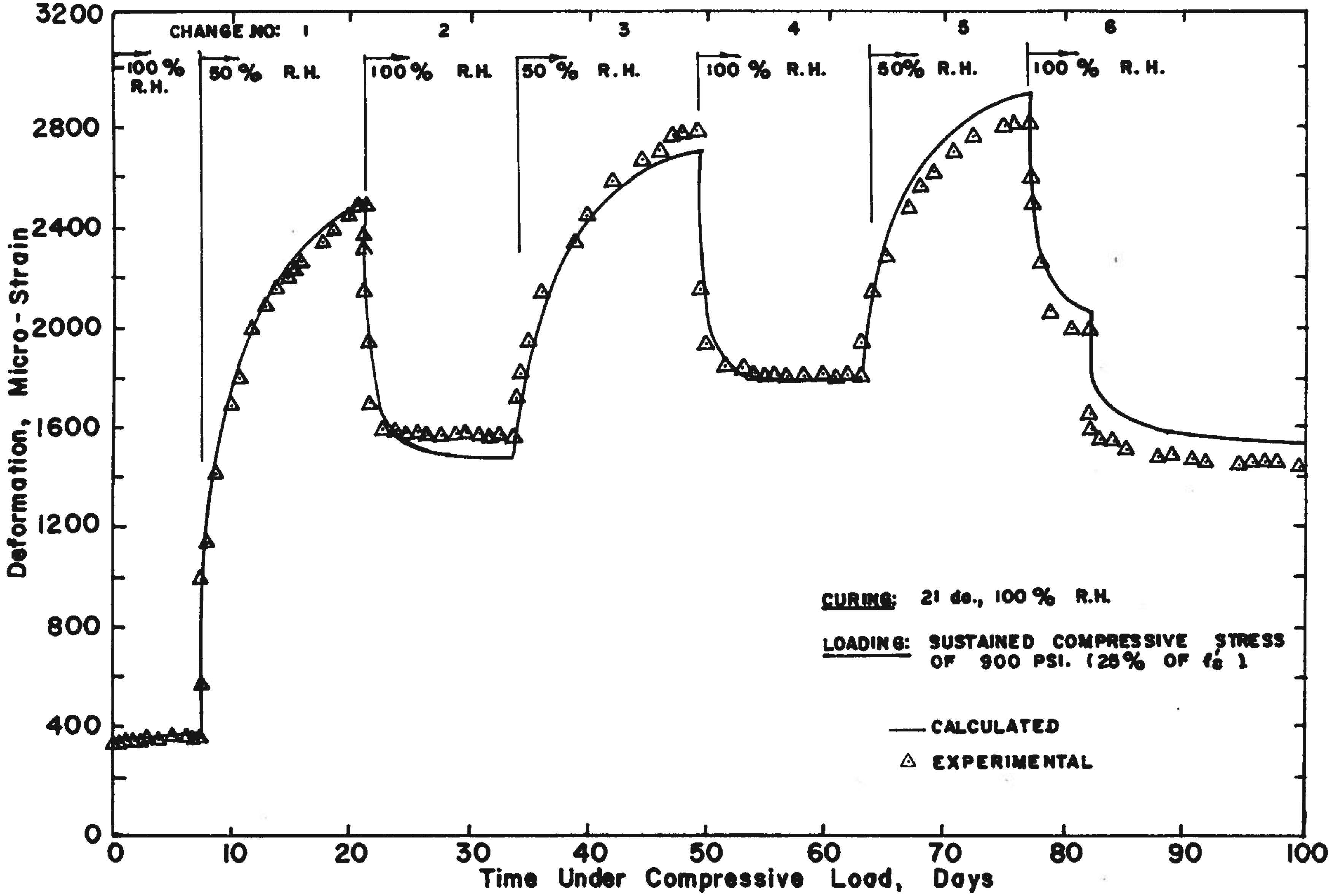

FIG. 37 COMPARISON BETWEEN CALCULATED AND EXPERIMENTAL VALUES FOR CREEP AND SHRINKAGE UNDER COMPRESSIVE LOADING AND CYCLIC HUMIDITY

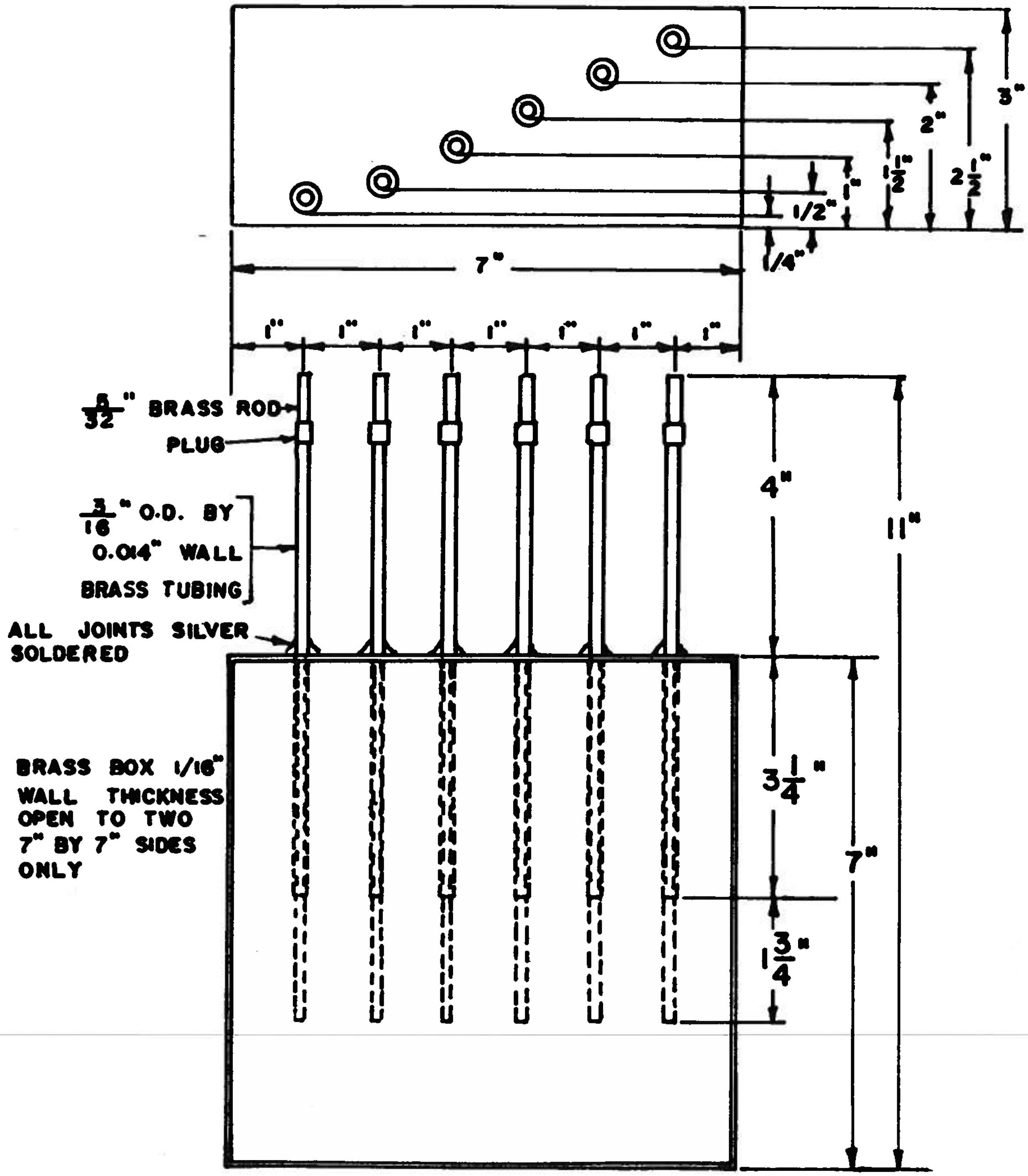

FIG. 38 PRINCIPAL DIMENSIONS OF BLOCK NO. I FOR MEASURING COEFFICIENT OF HYGRAL DIFFUSIVITY

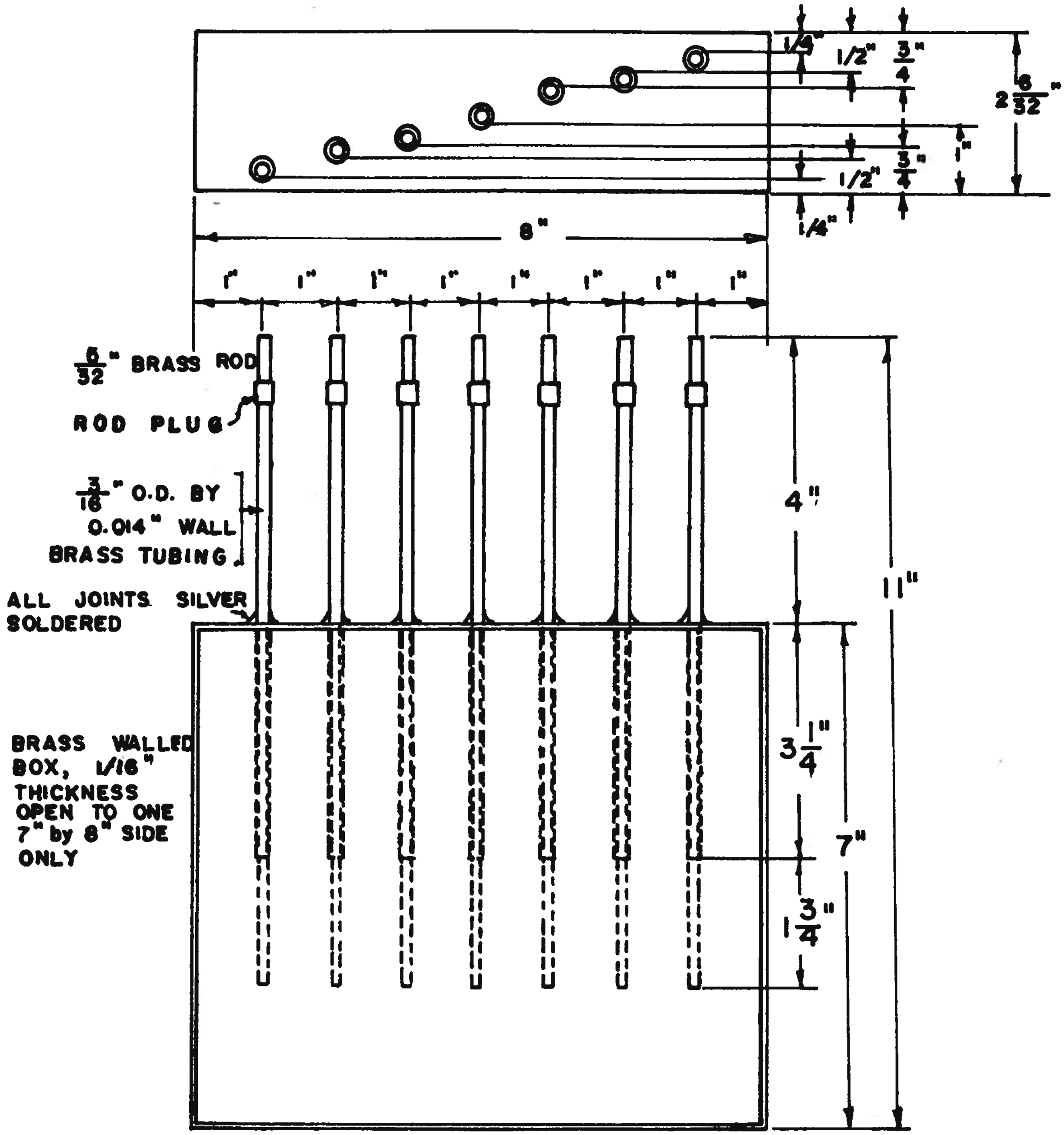

FIG. 39 PRINCIPAL DIMENSIONS OF BLOCK NO. 2 FOR MEASURING COEFFICIENT OF HYGRAL DIFFUSIVITY

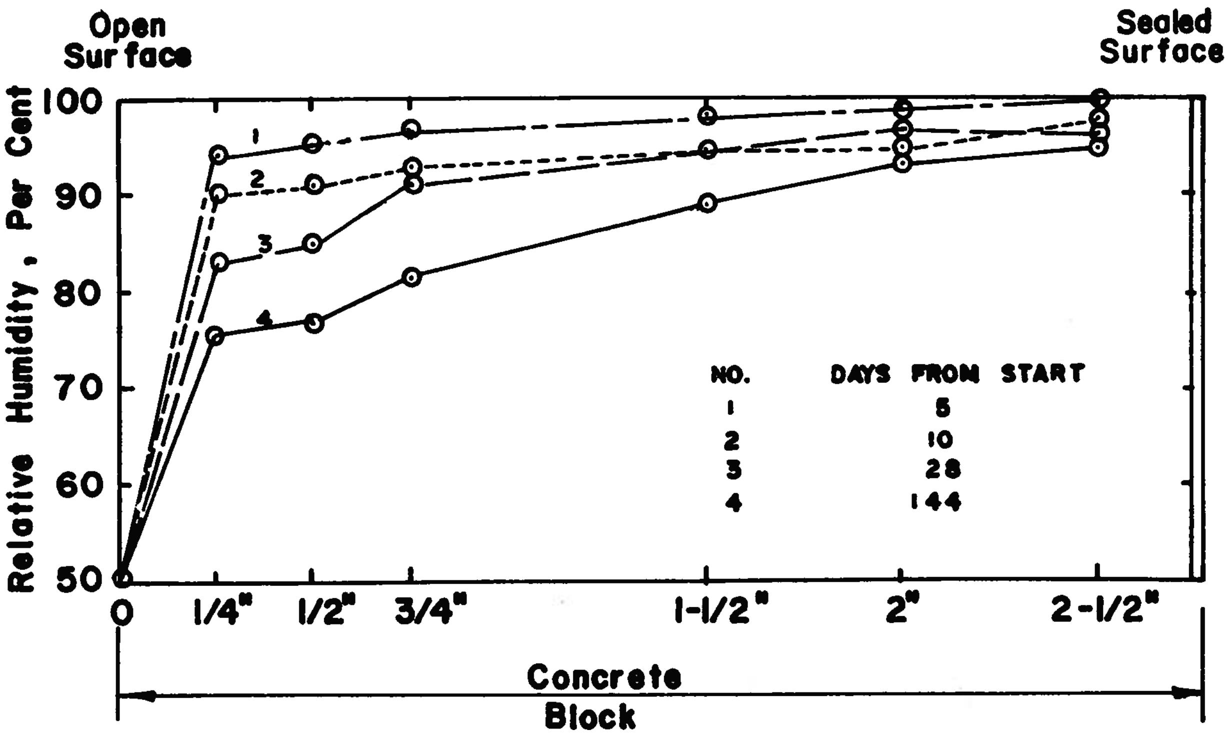

FIG. 40 DISTRIBUTION OF INTERNAL RELATIVE HUMIDITY OVER THICKNESS OF BLOCK NO. 1 OBTAINED AT DIFFERENT DRYING TIMES

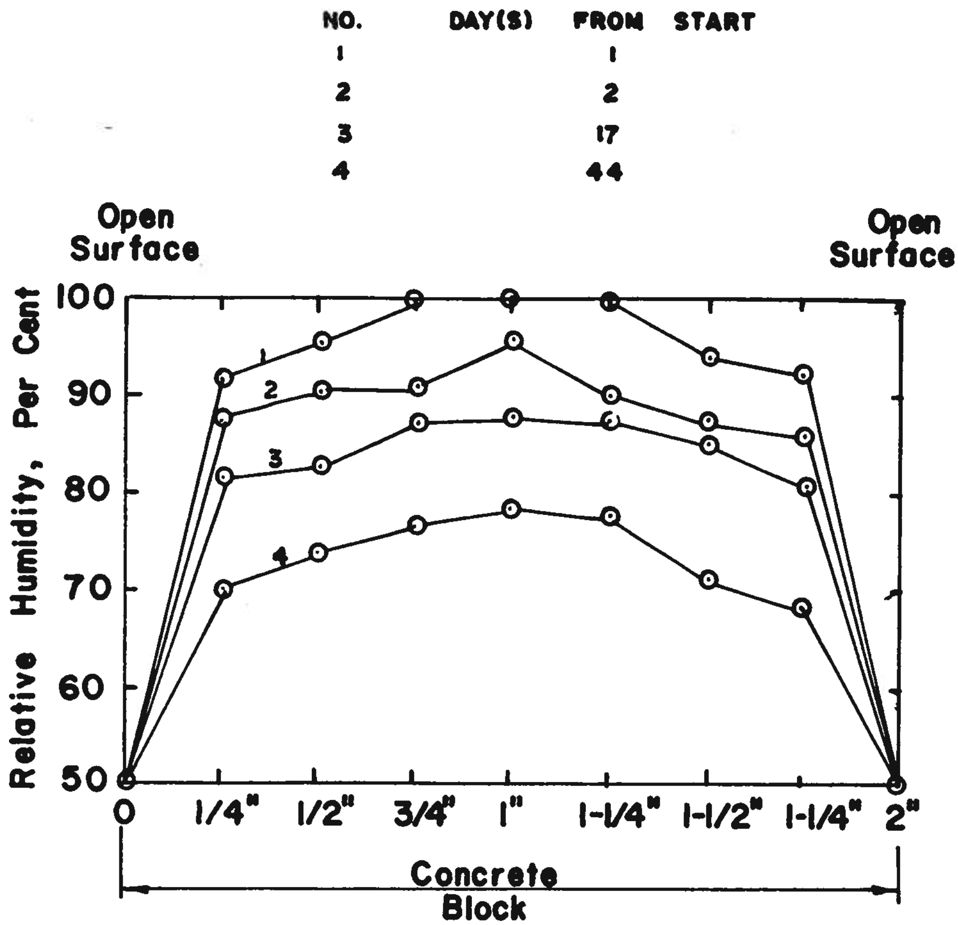

FIG. 41 DISTRIBUTION OF INTERNAL RELATIVE HUMIDITY OVER THICKNESS OF BLOCK NO. 2 OBTAINED AT DIFFERENT DRYING TIMES

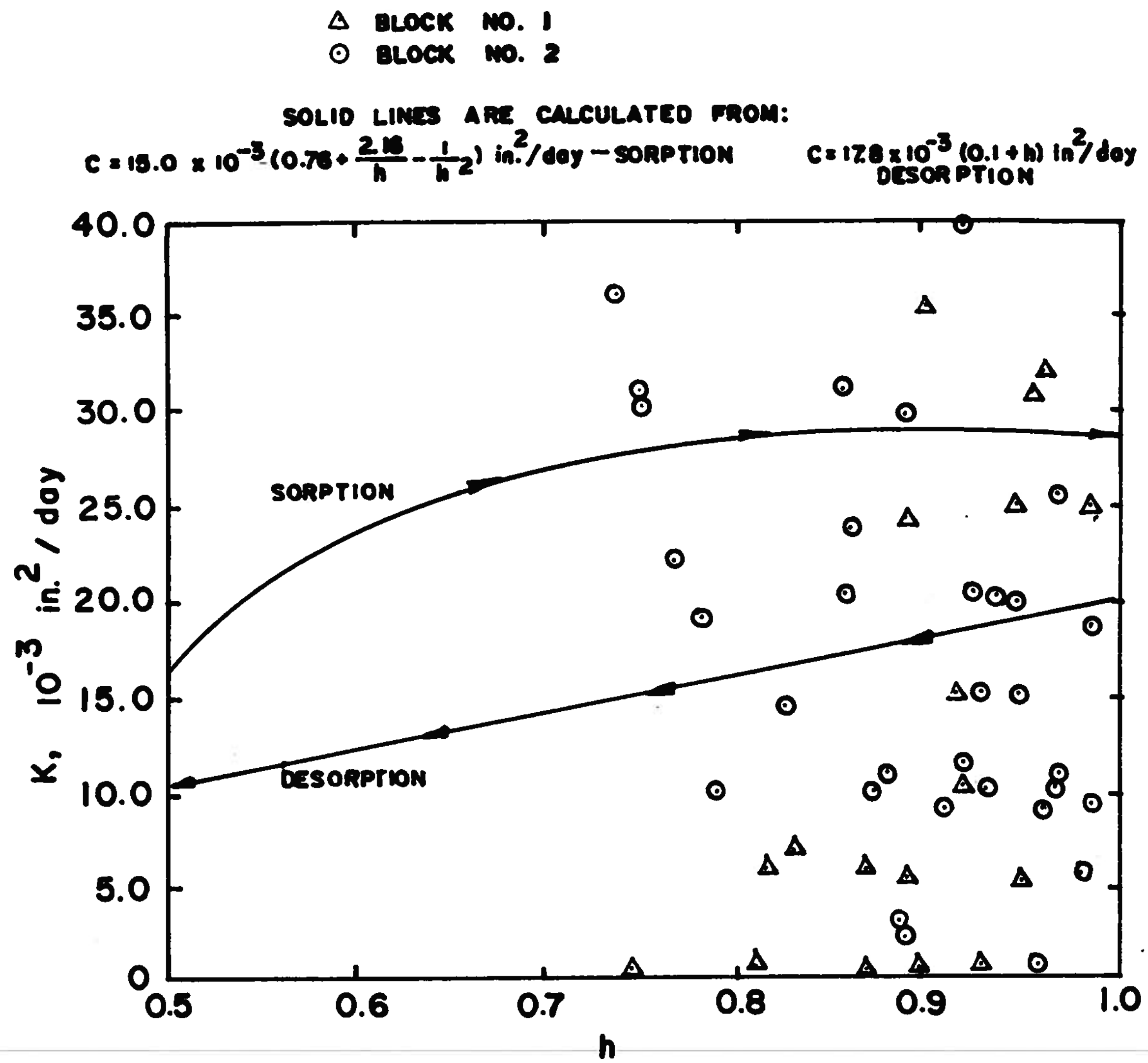

FIG. 42 EFFECT OF INTERNAL RELATIVE HUMIDITY ON COEFFICIENT OF HYGRAL DIFFUSIVITY "C"

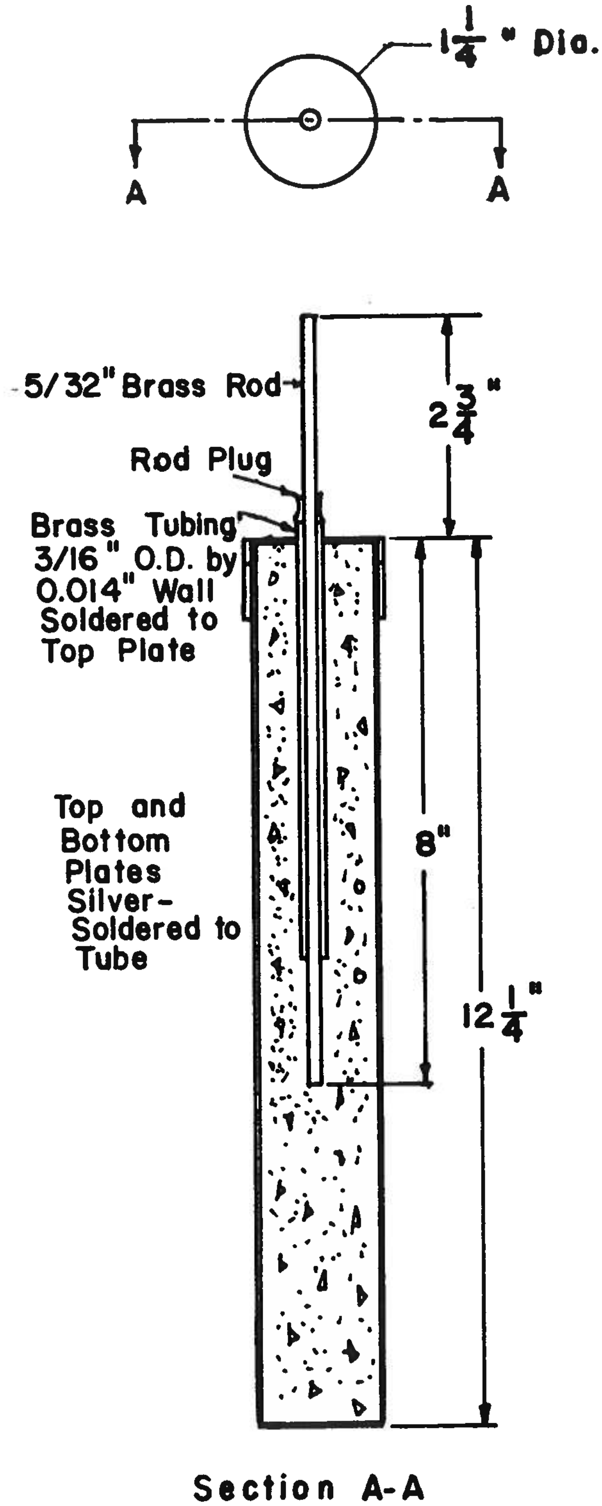

FIG. 43 DETAILS OF A SPECIMEN FOR SELF-DESICCATION TESTS

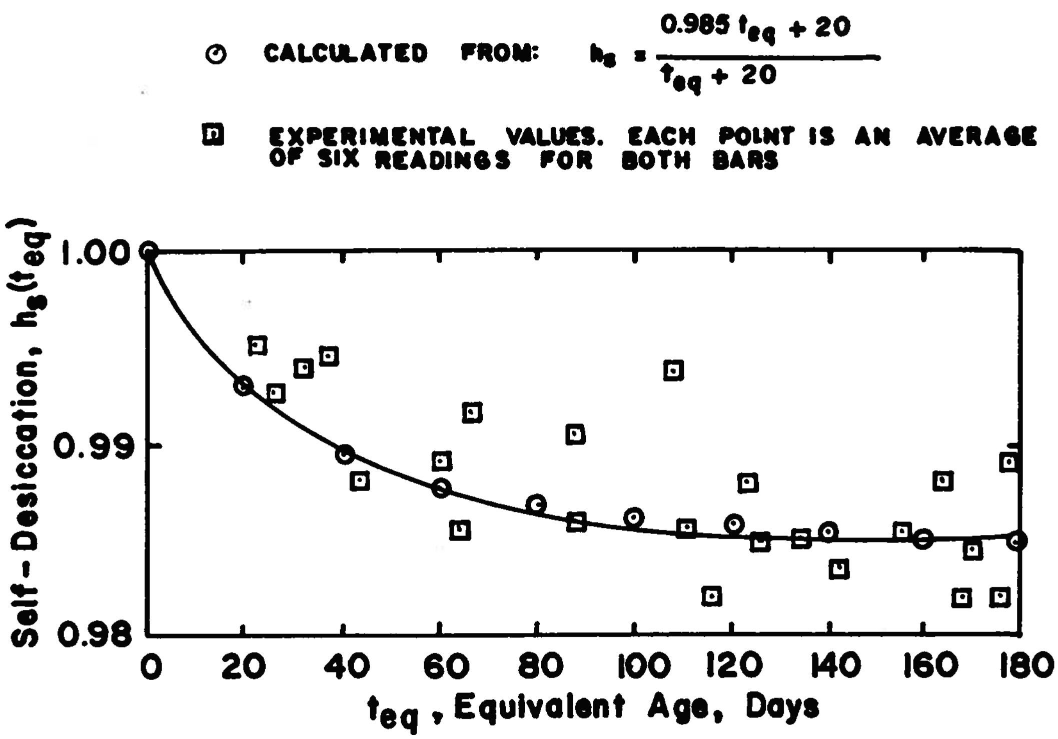

FIG. 44 EFFECT OF MATURITY ON SELF-DESICCATION OF MICROCONCRETE

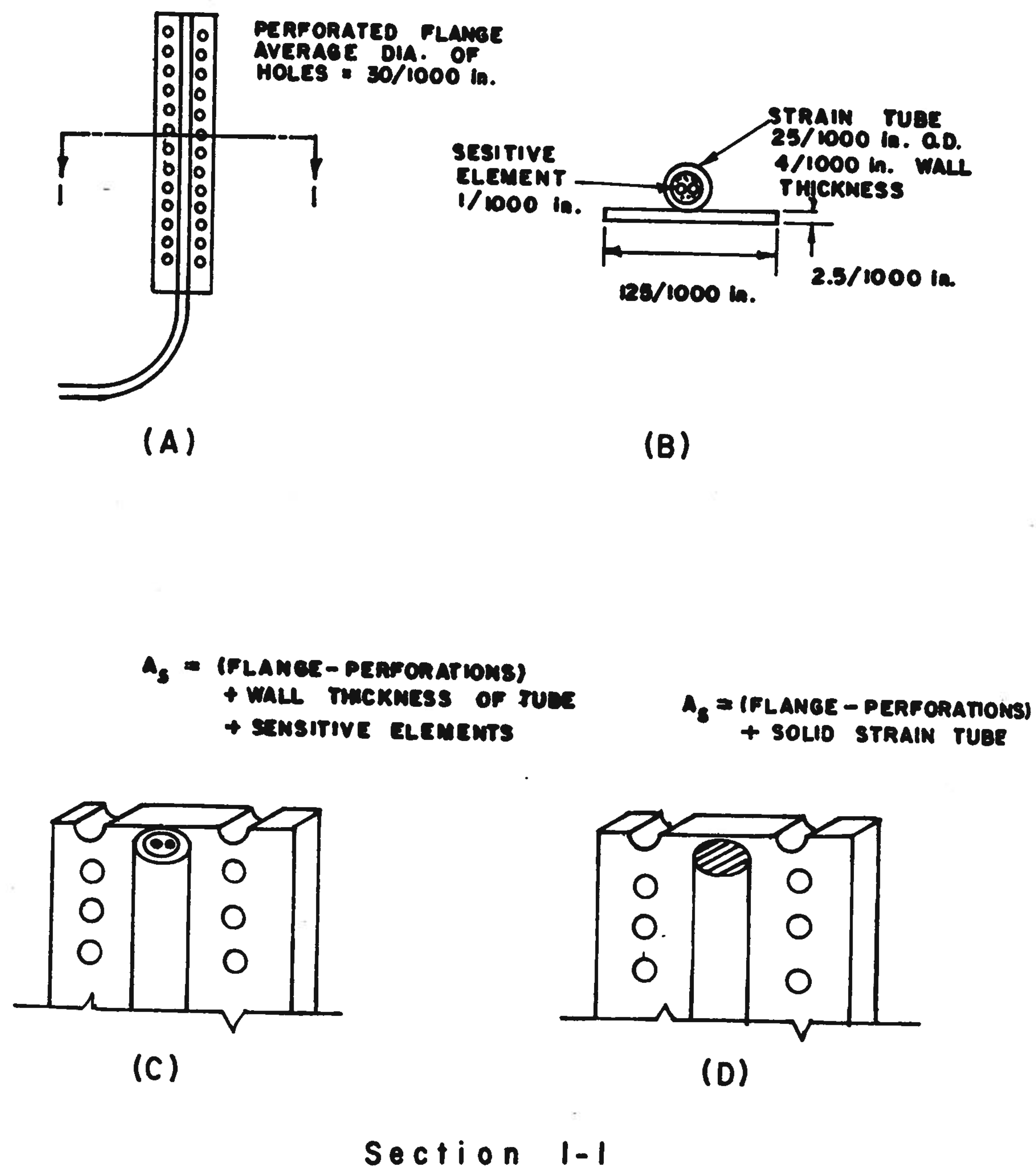

FIG. 45 DETAILS OF MICRODOT STRAIN GAGE WITH DIFFERENT DETAILS OF STRAIN TUBE

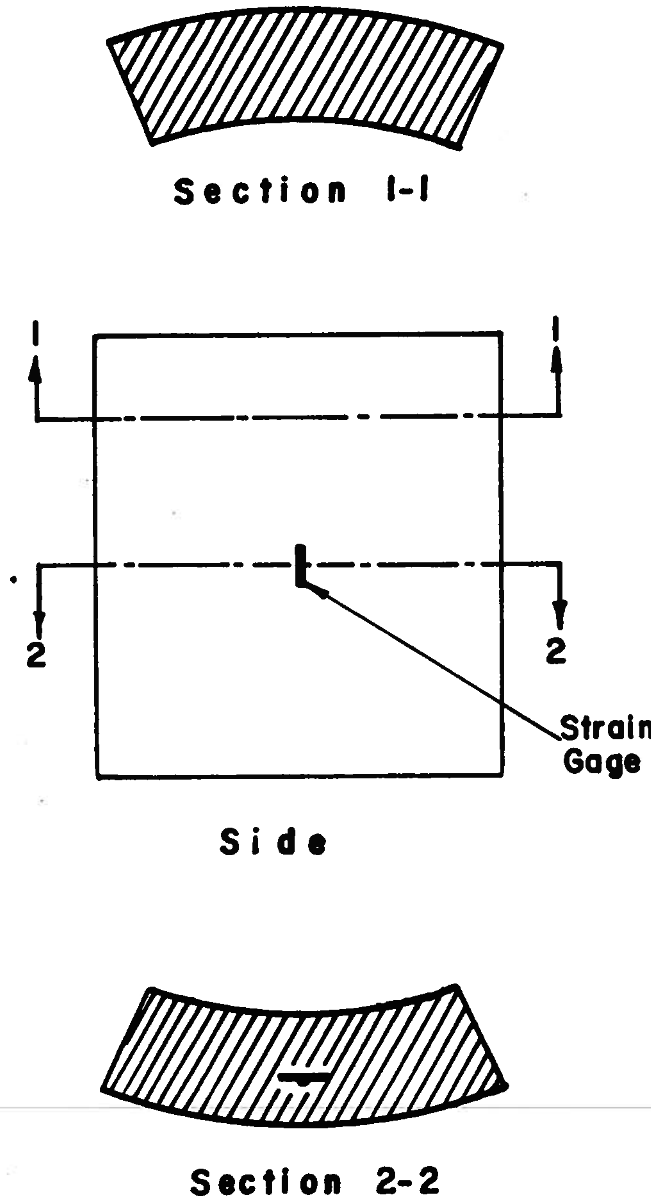

FIG. 46 CROSS-SECTION OF CONCRETE SPECIMEN WITH AND WITHOUT STRAIN GAGE

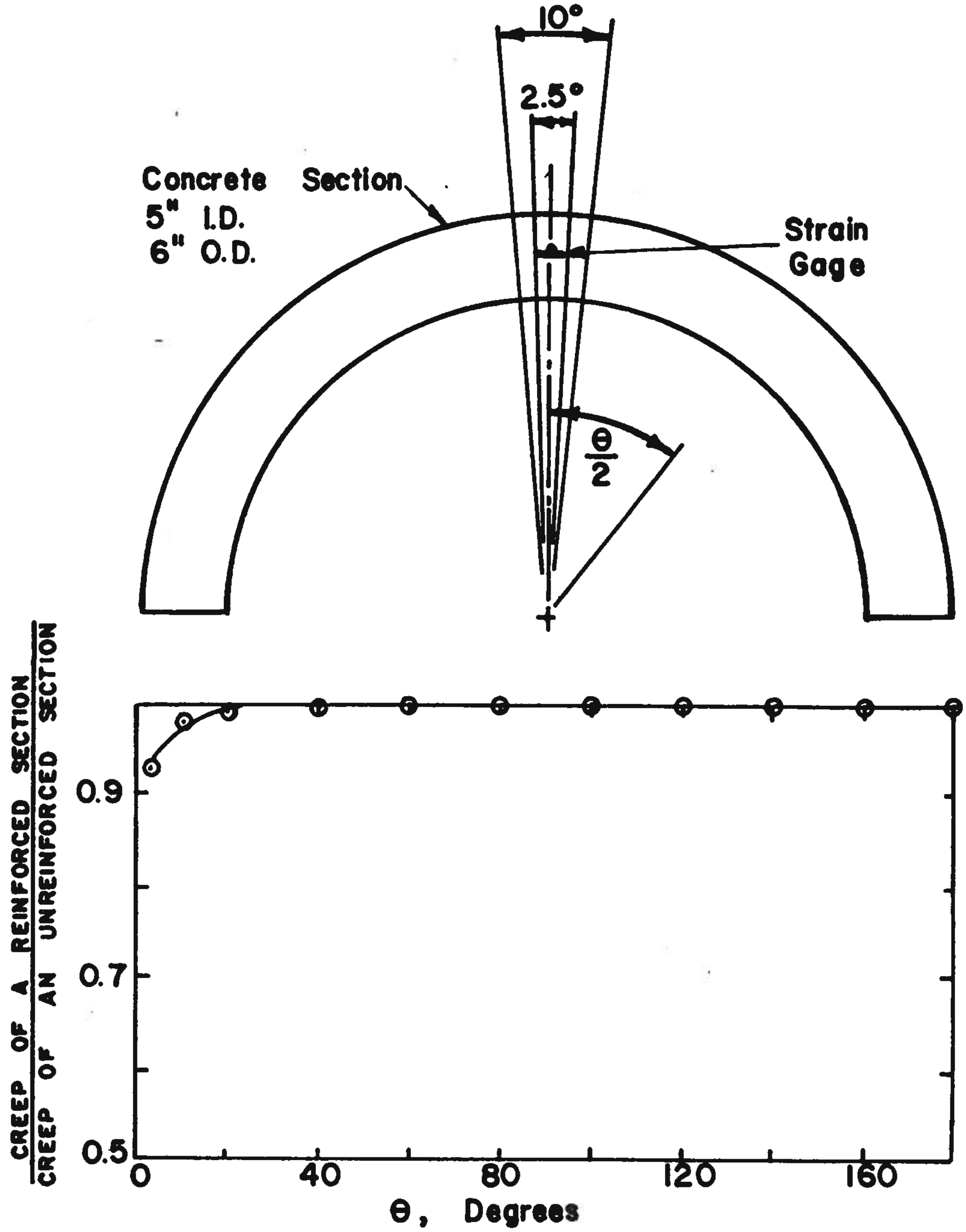

FIG. 47 EFFECT OF REINFORCEMENT, OFFERED BY STRAIN GAGE, ON CONCRETE DEFORMATIONS OF DIFFERENT SEGMENTS